CRYSTALLISATION OF

BARIUM CHROMATE

by

Efstratios Falangas

A Thesis submitted to the University of Aston in Birmingham

as a requirement for the Degree of Doctor of Philosophy

Department of Chemical Engineering

University of Aston in Birmingham

March 1980

CRYSTALLISATION OF BARIUM CHROMATE

E. FALANGAS PH.D. MARCH 1980

SUMMARY

In the present work the crystallisation of low solubility materials were studied, Barium chromate being chosen as a typical one.

The increase in solubility in acid solution was examined. Also the solubility of Barium chromate in the presence of other compounds (Urea, complexing agents) was studied.

Conditions of supersaturation were created by hydrolising Urea and thus neutralising the acid homogeneously.

The kinetics of Urea hydrolysis were examined and it was found that for conditions of excess Urea the model suggested in the literature was not strictly applicable. An alternative model was suggested by which the hydrolysis of Urea, for pH greater than 2.5, was zero order.

The crystallisation of Barium chromate was studied using a stirred vessel under a variety of conditions (baffles, initial concentration of materials etc.) It was found that the crystals grew to about 20 μm (equivalent spherical radius). It was found that the process obeys an empirical equation of the form:

$$\frac{dL}{dt} = 2.1 \times 10^{-3} L^{-1.5} pH^{0.03} R^{1.2} \left(\frac{C-C_s}{C_s}\right)^{0.83}$$

where L = mass mean radius (μm), R = agitation (rpm), $\frac{C-C_s}{C_s}$ = driving force

This led to the suggestion of a model of growth applicable to conditions of low supersaturation used and a theoretical equation was obtained of the form :

$$\frac{dL}{dt} = Km_2 L^{a-2} pH^{b} R^{f} \left(\frac{C-C_s}{C_s}\right)^{n}$$

The epitaxial growth was also studied of Barium chromate crystals on Tungsten particles in a fluidised bed crystalliser. Epitaxial growth in a stirred vessel was unsuccessful. The shape of the crystals produced was influenced by the source of the metal particles possibly due to the various impurities present.

Keywords

Barium chromate
Tungsten
Solubility
Crystallisation
Epitaxy

ACKNOWLEDGEMENTS

The author would like to express his sincere thanks to the following :-

The University of Aston in Birmingham.

The Ministry of Defence for sponsoring the project.

TABLE OF CONTENTS

LIST OF TABLES

LIST OF TABLES (CONTINUED)

LIST OF DIAGRAMS

LIST OF DIAGRAMS (CONTINUED) Page

Page

LIST OF GRAPHS

LIST OF GRAPHS (CONTINUED)

LIST OF GRAPHS (CONTINUED)

LIST OF GRAPHS (CONTINUED) Page

LIST OF GRAPHS (CONTINUED)

LIST OF PHOTOGRAPHS

CHAPTER 1

INTRODUCTION

It has been found that with certain compositions of delay fuses, non-reproducible burning rates occur. This has been thought to be due to non-uniform mixing of the reactants and/or variation of size distribution of the product (R.1.1.).

The composition of a fuse is usually a simple binary one of a fuel, typically Tungsten powder, and an oxidant, typically Barium chromate. As typical materials, Tungsten and Barium chromate only are considered in this work.

The project is a continuation of the work of Skander (R.3.1.) and investigates:

(i) the parameters affecting the crystallisation process of Barium chromate,

(ii) the suitability of different crystallisers for "large" scale production of Barium chromate crystals, and

(iii) the growth of Barium chromate crystals on metal (Tungsten) nuclei.

Incidental to this work, the kinetics of the hydrolysis of Urea were studied and also the influence of the presence of the Chlorochromate ion in acid solution of Barium chromate.

The above objectives have been mathematically formulated to either physical parameters which control the process or to suitable mathematical expressions which permit their computation. Diagram D.1.1. is the proposed flow diagram of the research.

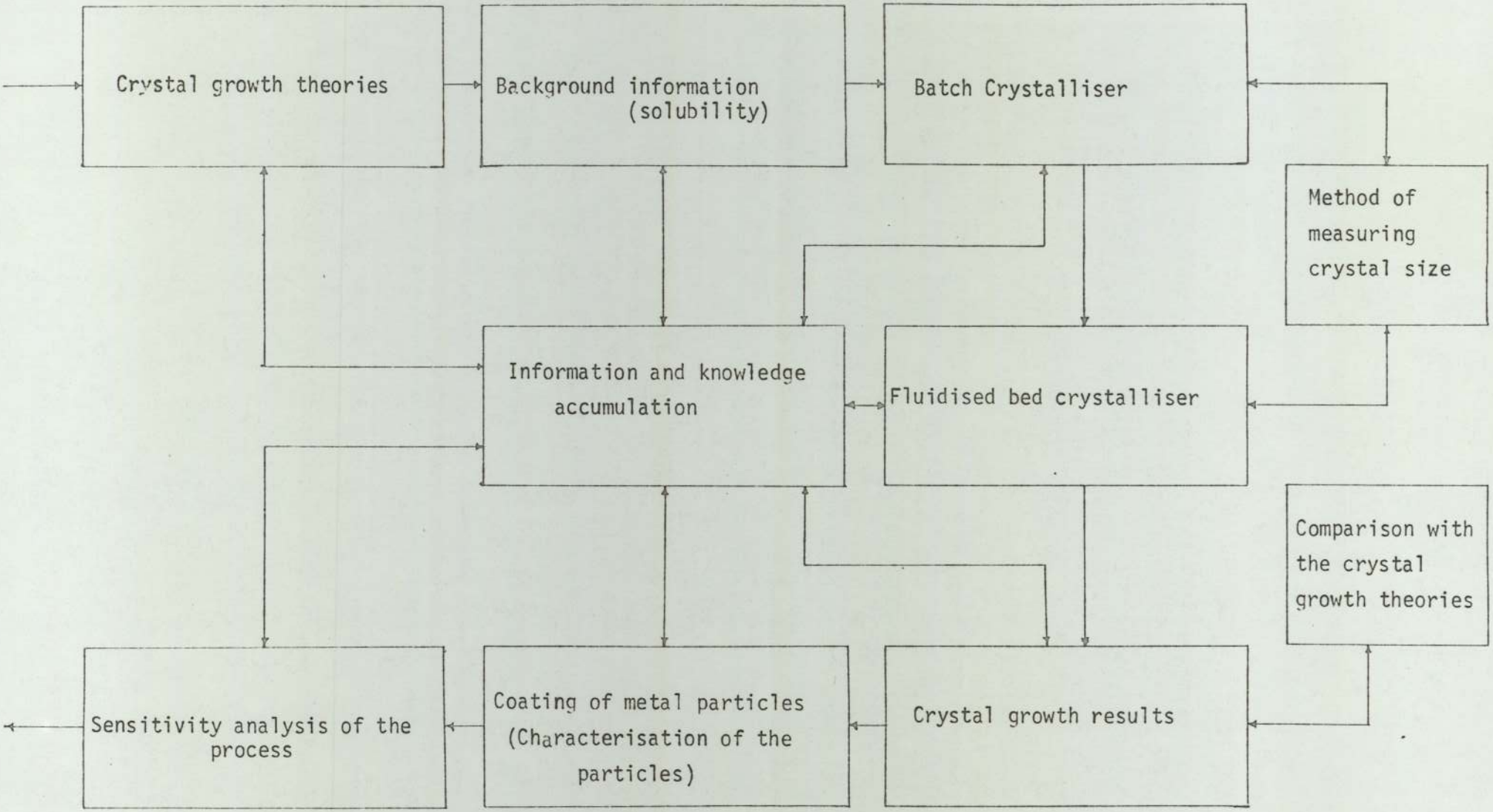

D.1.1. Logical flow diagram of the various stages of the project

CHAPTER 2

CRYSTALLISATION

2.1 Background information (R.2.1.), (R.2.2.), (R.2.3.)

2.1.1 Crystal morphology (R.2.3.)

A crystal comprises a rigid lattice of molecules, atoms or ions, the interlocation and dependence of which are characteristic of the substance. Crystals, however, grow under constraints and these result in deformities and stresses to such an extent that no two crystals are structurally identical. Under ideal conditions the crystals of a substance are similar and consist of symmetrical parts: symmetrical either about a point or an axis or a plane or any combination.

This results in seven basic "unit cell" structures of which Barium chromate is rhombohedral and Tungsten metal is (body centred) cubic.

2.1.2 Crystal habits (R.2.3.)

The deformities of the crystals are of paramount importance since they affect the physical properties of the product. Interpenetration, parallel growth, elongation, dendride formation are some. Although the effects of these deformities are often clearly observable from their effect on the crystal growth rate, they cannot at the moment be predicted and therefore the crystallisation process remains something of an art.

2.1.3 Crystallisation from solution

The crystallisation process consists of two stages which may sometimes proceed simultaneously.

The first stage is the formation of small particles or nuclei from the supersaturated solution.

The second is the growth of the nuclei in the supersaturated solution. If the number of the nuclei can be controlled, the size of the crystals formed can be regulated (R.2.1.).

A precondition for crystallisation from solution is the generation of a supersaturated state. This is usually presented in a solubility-supersolubility diagram (figure D.2.1.). In this figure, the concentration of the material is plotted against some property which controls the solubility.

$$C = f(Y)$$

C is the concentration

Y is usually temperature but it can also be pH etc.

The supersaturation curve is in fact a region with no exactly defined position, whereas the solubility curve is the locus of a phase transition. The width of the metastable zone is dependent on the conditions, e.g. agitation, history of solution, etc.(R.2.9.).

Since the kinetics of crystal nucleation and growth depend on the degree of supersaturation, knowledge of the solubility is all important. Several ways are used to express supersaturation (R.2.3.):

(i) the concentration difference $\Delta C' = C - C_s$ $(C > C_s)$ E.2.1.

(ii) the supersaturation ratio $S = C/C_s$ E.2.2.

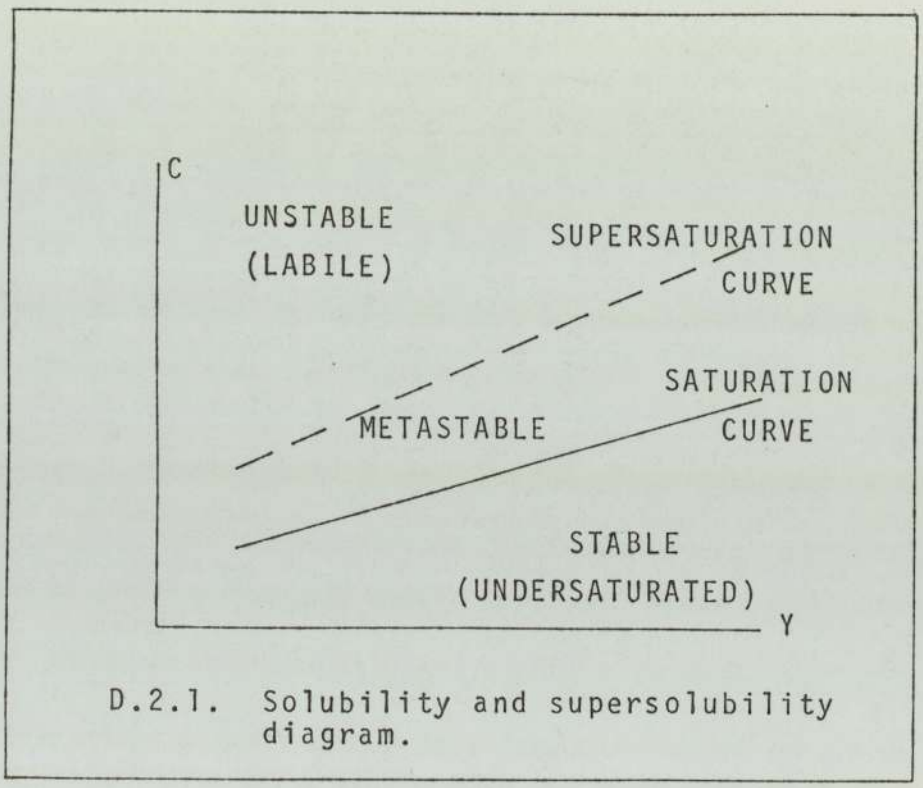

D.2.1. Solubility and supersolubility diagram.

(iii) the relative supersaturation $\Delta C = \frac{\Delta C'}{C} = S - 1$ E.2.3.

2.2 Theoretical aspects of the crystallisation process

Crystallisation is a complex process which involves at least two and possibly three loosely connected processes (R.2.2.); these are nucleation (the formation of embryos on which crystals could be built), the actual growth of the crystals and the "ripening" of the suspension.

2.2.1 Nucleation

Nucleation involves the activation of small particles. Under conditions of supersaturation there is a continuous formation and disintegration of agglomerates of particles. The groups formed become stable only after attaining a certain size determined by the solubility of the system and by the level of supersaturation. Nucleation is basically a stochastic process but which has parameters affected by the external conditions.

Two main types of nucleation are distinguished (R.2.3.) as shown in Diagram D.2.2. .

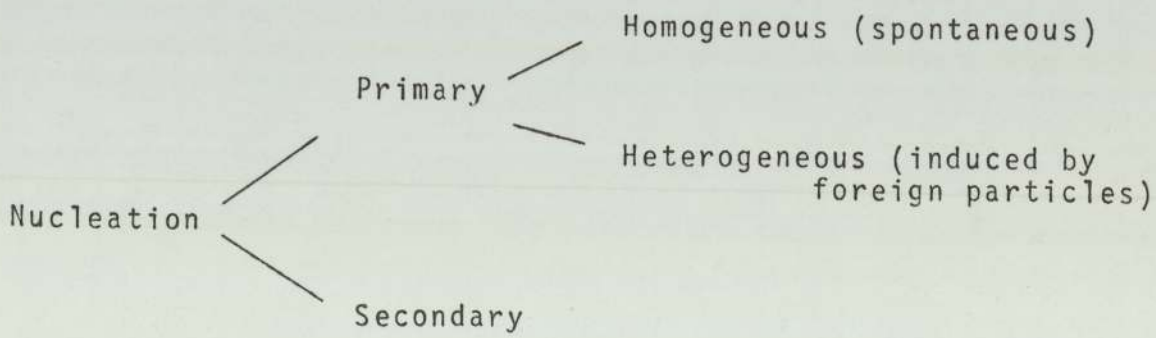

D.2.2. Types of nucleation

2.2.1.1. Primary Nucleation

(i) Homogeneous

The formation of crystal nuclei from embryos is something that cannot be experimentally studied, and all theories suggest a molecular addition process to a chain or cluster already existing. Statistically, when particles collide at a high rate, they stay together for a short time interval. Further collisions increase the size of the clusters until eventually it attains a critical size beyond which the cluster is stable. At this point perhaps re-orientation of the molecules occurs and thus the crystal lattice is obtained.

As expected from such a statistical approach (R.2.9) the probability of nucleation yields an equation of the form:

$$\frac{dN}{dt} = k_{N_1} \exp\left(-\frac{\Delta G}{RT}\right) \qquad \text{E.2.4.}$$

N is the number of nuclei per unit volume formed at time t.

k_{N_1} is a constant of nucleation at temperature T.

ΔG is the free energy of formation of a critical nucleus.

On the basis of the above statistical assumptions, Becker and Döring (R.2.4) suggested the following equation:

$$\frac{dN}{dt} = k_{N_2} \exp\left(-K_T/\ln^2 S\right) \qquad \text{E.2.5.}$$

K_T is a constant at a given temperature

S is the supersaturation ratio.

However, not all nuclei formed evolve into crystals and therefore Nyvlt (R.2.9.) suggested that only crystals above a certain size d_c are considered and therefore the possibility of the latter disappearing is minimal.

The total weight $w = N a_1 \rho \frac{d_c^3}{8}$ E.2.6.

ρ is the density

a_1 is the shape factor

The use of these equations however is subject to the accuracy of the values of the concentration at saturation and super-saturation conditions.

(ii) Heterogeneous

It is impossible to make a clear distinction between homogeneous and heterogeneous nucleation since even in the most carefully prepared solutions there are foreign particles (dust, impurities, etc.) which may act as nuclei (R.2.3.). The presence of these solid impurities usually act as accelerators to nucleation. In the extreme case, in epitaxial crystallisation, this is intentional and nuclei are formed and grow on a carefully chosen substrate.

The free energy of formation of the critical nuclei for heterogeneous nucleation ΔG^* is related to the free energy of formation of the critical nucleus for homogeneous nucleation ΔG^*_H (Eq. E.2.4.) by:

$$\Delta G^*_H = K_H \Delta G^* \qquad \text{E.2.7.}$$

K_H is a constant depending on the angle of contact between the crystalline deposit and the foreign solid surface Θ:

$$K_H = \frac{(2 + \cos \Theta)(1 - \cos \Theta)^2}{4} \qquad \text{E.2.8.}$$

when $\Theta = 2\Pi$	$K_H = 1$	and $\Delta G_H^* = \Delta G^*$	homogeneous nucleation
$\Theta = 0$	$K_H = 0$	and $\Delta G^*_H = 0$	spontaneous nucleation
$0 < \Theta < 2\Pi$	$0 < K_H < 1$	$\Delta G^*_H < \Delta G^*$	the impurity acts as an accelerator.

2.2.1.2. Secondary Nucleation

Secondary nucleation occurs when crystals are introduced intoa supersaturated solution which is in the metastable state (R.2.9.).

Strickland-Constable and Mason (R.2.17) distinguish four types of secondary nucleation:

(i) "Initial breeding" which occurred when a seed crystal yielded a shower of small crystals, which were originally attached to it, after immersion in a supersaturated solution.

(ii) "True breeding" which resulted from broken portions of a dendrite or needle-like growth of the original seed.

(iii) "Splinter breeding" which occurred when a needle broke off a mother crystal accompanied by a shower of smaller crystals.

(iv) "Attrition breeding" which is the result of agitation. (R.2.18.).

In all types of secondary nucleation, the rate of formation on new nuclei is a function of the super-saturation (R.2.30.). The recent papers of Nienow (R.2.18.), Ramshaw (R.2.19.) and Bujak (R.2.20.) competently review secondary nucleation.

2.2.1.3. Factors influencing nucleation

The factors influencing the rate of nucleation assume importance even if the crystal growth is not dependent on it (R.2.9.). The final size of the crystals will depend on their number, the higher the population the smaller their size for a given total weight (Equation E.2.6.).

(i) The effect of temperature

Thermodynamically, the higher the internal energy of the system, the higher is the probability of two or more molecules to collide (Equation E.2.4.). Furthermore, many semi-theoretical correlations have been suggested. Srikantan (R.2.21.) proposes that the rate of nucleation is directly proportional to the temperature coefficient of the viscosity.

(ii) The effect of the "history" of the solution

Nyvlt (R.2.9.) suggests that a long preheating time results in the widening of the metastable zone. This increase is dependent on both the time and the degree of overheating.

(iii) The effect of stirring

Mullin and Raven (R.3.25.) have found that an increase in the intensity of agitation does not always lead to an increase in nucleation. They suggest that gentle agitation causes nucleation in solutions that are otherwise stable and vigorous agitation considerably enhances nucleation, but the transition between the two is not continuous (R.2.3.). Other authors, (R.2.19.), (R.2.20.) and (R.2.29.) also acknowledge the existence of a transition state but suggest only empirical correlations relating the rate of nucleation and agitation.

Experimentally, (R.2.3.) a local maximum and minimum is found. (Diagram D.2.3.).

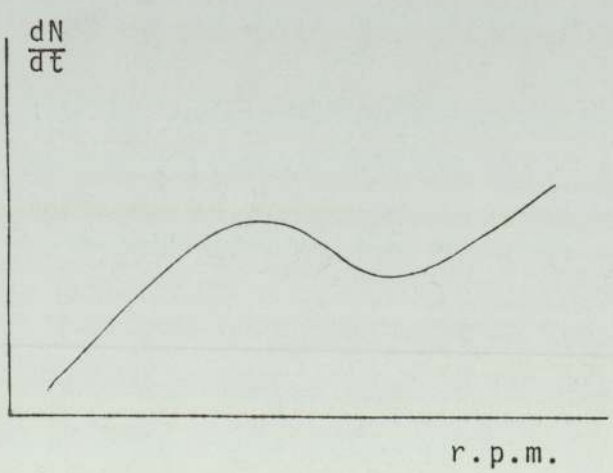

D.2.3. Diagram showing the effect of agitation on the nucleation rate

(iv) The effect of impurities

The presence of impurities in a system greatly affects the rate of nucleation (R.2.3.). The inhibiting effect has been related to the nature of the molecules of the impurity (R.2.27.). However, a "threshold" effect often appears above which the concentration of the impurity actually weakens the inhibiting effect (R.2.3.), (R.2.28.).

2.2.2. Crystal growth

Many theories of crystal growth exist, all subject to individual interpretation. Some are more popular than others not so much on their theoretical merits but because they can describe experimental results. Indeed, in the crystallisation process the theories are developed so as to "fit" the results. This lack of a coherent theory leaves individual researchers to subjectively choose one which would present their results in an understandable form. Hence a claimed mechanism is usually based simply on which model empirically best fits the experimental data (R.2.12.), (R.2.13.), (R.2.15.),(R.2.16.).

The transition of a molecule from solution into the lattice of a crystal involves three main steps and the various theories are concerned on the assumptions that one or more of these steps is the limiting factor of the process. These are:

(i) Transport of the molecule or agglomerate of molecules from the solution to the crystal surface

(ii) Adsorption on the surface

(iii) Orientation and integration into the lattice.

2.2.2.1. Bulk diffusion controlled mass transfer model

The main assumption of this model is that the rate of incorporating the molecules into the crystal lattice is very fast compared with the rate of transport through the solution. This model is sometimes called the "film" model because it assumes that the crystal is surrounded by a stagnant film of thickness δ through which the solute has to diffuse (R.2.10.). The growth of the crystal is then:

$$\frac{dL}{dt} = Kg \quad f(C)^n \qquad \text{E.2.9.}$$

$\frac{dL}{dt}$ is the linear growth rate of the crystal

f(C) is a function of the driving force

Kg is a constant which depends on the diffusivity D and the thickness of the stagnant layer δ,

n is a constant

$$Kg = D/\delta \; . \qquad \text{E.2.10.}$$

However δ and D depend on the geometry of the crystal, the fluid dynamics and the physical properties of the system.

and $$f(C) = \frac{C-C_s}{C_s} \qquad \text{E.2.11.}$$

for moderate supersaturations.

C is the concentration of the solute

C_s is the concentration of the solute at saturation.

The model suffers from the assumption that the concentration of the solution next to the crystal surface does not exceed the solution value (R.2.9.),(R.2.3.).

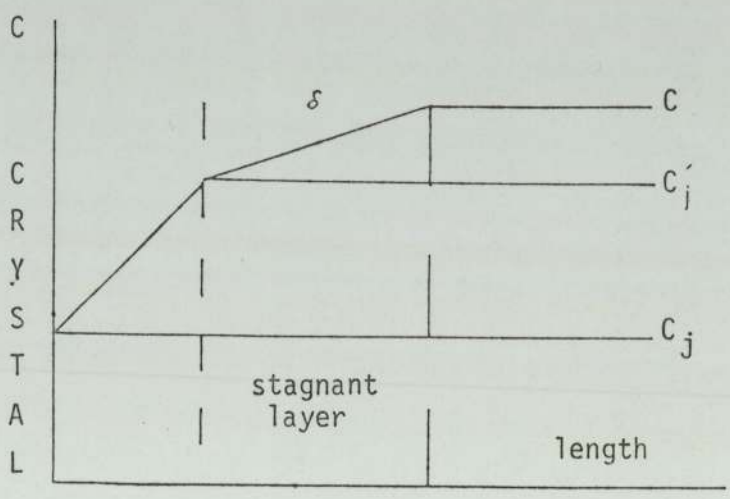

D.2.4.Concentration driving forces on crystallisation from solution

C_j' is the solute concentration at the solution crystal interface

C_j is the solute concentration at the crystal surface.

The value of Kg is correlated with the other physical parameters by the modified Ranz and Marshall equation :

$$Sh = 2.0 + 0.6 \sqrt{Re.Sc.} \qquad E.2.12.$$

(R.2.15)

Sh is the Sherwood's number, $Sh = Kgd/_D$ E.2.13.

Re is the Reynold's number, $Re = V\rho\, d/\mu$ E.2.14.

Sc is the Schmitt number, $Sc = \mu/_{D\,\rho}$ E.2.15.

Kg is the mass transfer coefficient (m/s)

d is the characteristic length of the crystal (m)

V is the relative velocity between the crystals and the solute (m/s)

μ is the viscosity of the solution (Kg/ms)

At very low velocities only the first term of the right hand side of equation E.2.12 is important and therefore

$$Kg = 2.0\ D/_d \qquad E.2.16.$$

At high velocities only the second term is important and therefore

$$Kg = 0.6\ \frac{D}{d}\sqrt{Re\ Sc} \qquad E.2.17.$$

This model is usually used when the crystals grow from very low concentrations of ionic solutions and it may therefore apply to Barium Chromate crystallisation.

2.2.2.2. <u>The surface diffusion model</u>

This model is closely associated with Burton, Cabrera

and Frank (R.2.22.) who suggested that the growth of the crystals is due to spirals which self-perpe tuate avoiding both the edges and the spirals of the other faces. The spirals originate from dislocations which are very common. Indeed, no crystal exists which does not have some form of deformity. According to this model, the molecules are easily adsorbed on the surface of the crystal and the limiting factor is their placement into the lattice. The growth of the crystal face is determined by the velocity of the spiral steps (R.2.10.):

$$\frac{V_{Rd}}{V_{\infty}} = 1 - \frac{Rd^{*}}{Rd} \qquad \text{E.2.18.}$$

V_{Rd} is the velocity of the curved step of Rd = radius of curvature

V_{∞} is the velocity of a straight step of radius = ∞

Rd^{*} is the radius of a critical size two dimensional radius.

The main disadvantages of this theory is that it relies on parameters which are difficult to measure. It also assumes that the resistance to the adsorption of molecules onto the crystal surface from solution is negligible.

2.2.2.3. Two-dimensional nucleation growth models

These models assume that the growth of the crystal is due to the birth and addition into the crystal lattice of a critical sized nucleus. Ohara (R.2.10.) suggests that this results in three main models.

(i) Mononuclear addition

By this is meant that one nucleus is born and grows to cover the whole surface of the crystal face before the next nucleus forms.

(ii) Polynuclear addition

According to this model a number of nuclei are added at a time. The velocity of spreading is zero in this case, and the crystal grows only by accumulating enough nuclei to cover all its surface.

iii) Birth and spread model

In this case, nuclei are formed and spread continuously but the amount of spread is limited by the neighbouring nuclei.

2.2.3.4. Probalistic models

The extensive use of computers by many workers in recent years has given rise to many probalistic models. The argument behind these models is that both nucleation and growth are stochastic processes, possibly statistically controlled.

The main disadvantage of these models lies in the mathematical techniques used, which have progressed very little compared with the enormous progress the computers have made in the last decades.

2.2.2.5. Factors influencing the crystal growth rate

(i) Crystal size

Probably all crystal growth models depend on the size of the crystals (R.2.3.). However, not all substances exhibit a size effect and for crystals of about 10 μm or over the effect can be related to the relative velocity of the solution in bulk diffusion controlled growth. Usually the effect of the size is included in the value of the constants (Equation E.2.19.).

$$\therefore \quad \frac{dG}{dt} = Ks\ L^{a}\ f(C)^{n}. \qquad \text{E.2.19.}$$

(ii) Agitation

The intensity of stirring is a measure of the relative velocity between the crystals and the liquid (R.2.4.). As the stirring increases, access to fresh supersaturated solution is increased. Furthermore, the diffusion layer is decreased in thickness (Equation E.2.11.).If the solution velocity is sufficiently high, the overall growth rate should be determined by the rate of integration of the solute molecules into the crystal lattice. If a crystal is grown in a stagnant solution then the rate of the diffusion step will be at a minimum (R.2.3.), (R.2.26.).

For diffusion mass transfer rates the growth can be related to the relative velocity in the solution by equation E.2.12..

(iii) Temperature

In the crystallisation process it is the nucleation which is affected by the temperature rather than the crystal growth. However, the constant of equation E.2.9 can be related to the temperature by the usual Arrhenious activation energy type of relation (R.2.9.):

$$\frac{d(\ln Kg)}{dT} = \frac{Eg}{RT^2} \qquad \text{E.2.20.}$$

T is the temperature
Eg is the activation energy of the growth process

(iv) Impurities

Impurities when present, almost always affect the crystal growth. The effect is largely dependent on the concentration. They act by slowing the growth rate of the crystal faces, often by different amounts. This results in crystal deformities and habit modification (R.2.3.) and in the limit a trace of an impurity may completely inhibit growth altogether.

2.2.3. Epitaxial growth

Epitaxial growth occurs when the crystal lattice is built on a substrate. Epitaxy is favoured by a small mismatch of the lattices (<5%) (R.2.30.) although larger mismatches do not exclude epitaxial growth. Strickland-Constable (R.2.30.) suggests that epitaxy is explained by a number of dislocations accommodating the lattice dislocation in the interface. Buckley (R.2.31.) in his book competently reviews epitaxial growth and gives a large number of examples (Appendix 3, p179)

2.3. Particle size distributions

The analysis of the size distribution of the product crystals, provides the criterion of growth and its accurate study is necessary in determining the parameters affecting the process.

There are many methods available for analysing particle size distributions (R.2.32.) and in Table T.2.1. five different methods are compared.

Method	Size for greatest accuracy	Measured quantity	Simplicity	Cost	Comments
Sieves	Not below 100 μm	second largest dimension	simple and quick	very cheap	large amounts of material needed
Coulter-Counter	Most accurate 10-100 μm	volume	simple and quick	cheap if a machine available	small amounts analysed
Microscopy and/or photography	$<10\mu m$	projected area	not simple rather slow	expensive	very small amounts analysed
Sedimentation	1-50 μm	surface area	simple and quick	very cheap	small amounts analysed
elutriation	1-50 μm	surface area	simple and quick	cheap	difficult to separate a sample to very fine divisions large amounts of material required

Table T.2.1. Comparison of alternative methods for analysing size distribution.

Considering that about 5 g of $BaCrO_4$ were produced (or less) in each test (R.2.32.) and that a large number of samples (≃100) would have to be analysed, the Coulter-Counter and the sedimentation methods are the most suitable, for the present work.

Furthermore, the difference in the measuring quantity (volume and surface area) would give a direct value for the sphericity of the particles.

2.4. Mathematical fuctions suitable for describing distributions

The most frequently used distributions in the crystallisation process are (R.2.33.) :

(i) Normal

(ii) log-Normal

(iii) Gamma

2.4.1. The Normal distribution

The Normal distribution is perhaps the most widely known (R.2.33.), (R.2.34.). It can be represented by an equation of the form

$$f(d_i) = \frac{1}{\sigma\sqrt{2\pi}} \exp\left(\frac{-(d_i - \bar{d})^2}{2\sigma^2}\right) \qquad \text{E.2.21.}$$

$f(d_i)$ is the property of the distribution, (weight, population)

d_i is the equivalent diameter of the particles at i

$\bar{d}$ is the mass mean of the d_i values

σ is the standard deviation of the distribution.

2.4.2. The log-Normal distribution

The log-Normal distribution (R.2.34.) although more difficult to manipulate, combines the easily understood properties of mean and standard deviation with a skewed shape.

2.4.3. The Gamma distribution

The Gamma distribution has gained popularity recently because its parameters directly control the shape of the curve (R.2.34.), (R.2.35.).

Table T.2.2. compares the three distributions (R.2.34).

	Normal	log-Normal	Gamma
parameters	2	2	2
easily identifiable variables	Yes	Yes	Yes
operational within limits	Yes	Yes	lower limit
shape	symmetrical	skewed	skewed

Table T.2.2. Comparing mathematical distributions suitable for describing crystal distribution.

Although a mathematical distribution can adequately describe the size of the crystals at any moment, for crystal growth studies, one parameter is usually required which

would describe the distribution as a whole. (R.2.34.).

Such parameters are:

(i) The arithmetic or length mean $L_{a_1} \equiv \frac{1}{N} \sum_{i=1}^{N} n_i \frac{d}{2}_i$ E.2.22.

L_{a_1} divides the distribution into equal numbers.

(ii) The area mean $L_{ar}^2 = \frac{1}{N} \sum_{i=1}^{N} n_i \frac{d}{2}_i^2$ E.2.23.

The area mean divides the distribution into equal areas.

(iii) The volume or mass mean

$$L_m^3 = \frac{1}{N} \sum_{i=1}^{N} n_i \frac{d}{2}_i^3 \qquad \text{E.2.24.}$$

The mass mean divides the distribution into equal masses.

(iv) The mode, which is the most probable size of the distribution.

The other parameters of the distribution, variance and skewness, can also be used to examine whether secondary nucleation occurs and at what stage, or whether a certain fraction of the crystals grow faster.

CHAPTER 3

BARIUM CHROMATE

3.1 Properties of Barium chromate

The properties of $BaCrO_4$ will be examined with respect to the operating conditions of the crystallisation process which are:

Temperature = $100^{o}C$

Pressure: 1 Atm

Chemical Environment : acidic solutions.

3.1.1 Morphology of $BaCrO_4$

Barium chromate has an orthorombic crystalline structure of lattice dimensions

$x = 5.526$ Å

$y = 7.337$ Å

$z = 9.103$ Å (R.3.2.) , (R.3.9.)

The coefficients of thermal expansion for the lattice co-ordinates are (K^{-1})

$\alpha_x = 3.38 \times 10^{-5}$

$\alpha_y = 2.04$

$\alpha_z = 1.65$ (R.3.4.)

Diagram D.3.1. presents a scale drawing of a $BaCrO_4$ crystal showing only the {111} faces based on the above lattice dimensions. The sphericity of the crystal is 0.81.

3.1.2 Physical Properties

$BaCrO_4$ has a molecular weight of 253.33 (R.3.5.)
Its density is given as 4.498 g /cm^3 (4498kg /m^3) and the surface energy as 12 J/m^2 (R.3.5.).

(i) Clinographic projection

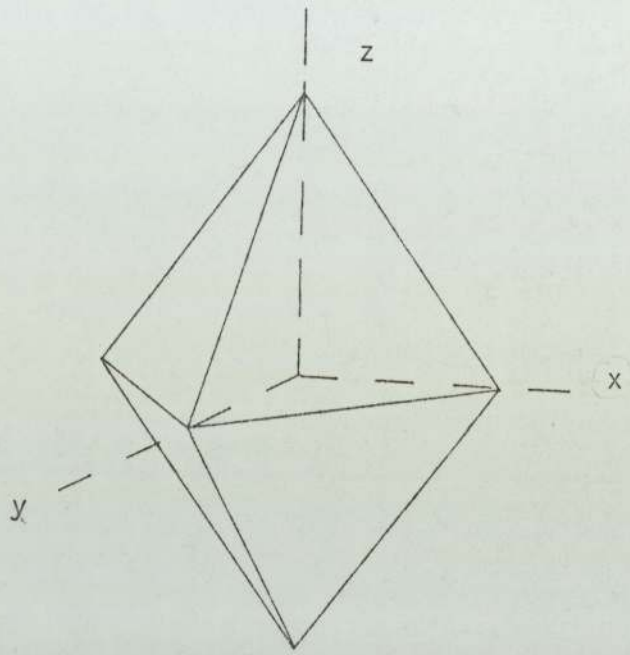

(ii) Side view

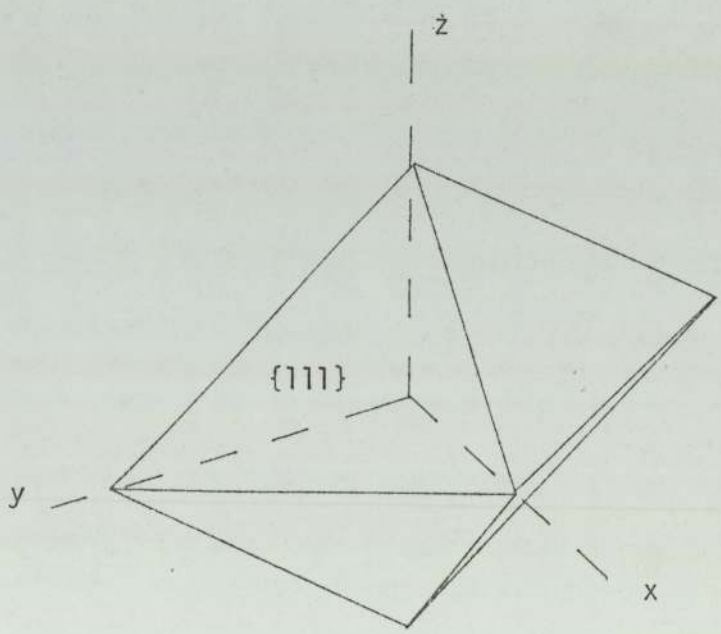

D.3.1. Scale drawing of a $BaCrO_4$ crystal showing the {111} faces. In (ii) the crystal is lying on the parallel $\{\bar{1}\bar{1}\bar{1}\}$ face and thus shows the true face shape.

The solubility product is given by various authors (R.3.1.) as $1.3 \times 10^{-10} \pm 0.3 \times 10^{-10} (mol/dm^3)^2$

The heat of crystallisation is -6.4 kcal/mol (exothermic) at 25^oC (297 K) and pH = 7 (R.3.3.).

3.1.3 Biological properties

$BaCrO_4$ is very poisonous (R.3.6) and carcinogenic (R.3.11) Although long periods of inhaling $BaCrO_4$ vapour produced no lung cancer, in solution it produces skin cancers to about 27% of the cases tested (R.3.11) reaching up to 70% under certain conditions.

3.1.4 Chemical properties

$BaCrO_4$ is a yellow precipitate and it can be produced by mixing solutions of the more soluble salts (R.3.10) for example:

$$BaCl_2 + K_2CrO_4 \rightleftharpoons BaCrO_{4\downarrow} + 2KCl \qquad E.3.1$$

$Ba(NO_3)_2$ is also used and so are other alkali-chromates.

Other methods of production involve the addition of alkali to an acidic solution of $BaCrO_4$ when the salt precipitates as a fine powder. The use of Urea to produce alkali homogeneously by hydrolysis as well as similar processes, are covered extensively by Skander (R.3.1).

The salt, $BaCrO_4$, is almost insoluble in water but its solubility increases rapidly with acidity. In acid solution the following equilibria may exist (R.3.6.).

$$BaCrO_4 \rightleftharpoons Ba^{++} + CrO_4^{--} \qquad \text{E.3.2.}$$

$$CrO_4^{--} + H^+ \rightleftharpoons HCrO_4^- \qquad \text{E.3.3.}$$

$$HCrO_4^- + H^+ \rightleftharpoons H_2CrO_4 \qquad \text{E.3.4.}$$

$$2HCrO_4^- \rightleftharpoons Cr_2O_7^{--} + H_2O \qquad \text{E.3.5.}$$

The position of the equilibrium depends both on the pH and Cr(VI) concentration (R.3.7.) , (R.3.8.). The equilibria are however, labile and on adding cations which form insoluble Chromates, the Chromate, and not the Dichromate is rapidly precipitated. Furthermore, the equilibrium species depend on the nature of the acid used and only in HNO_3 and $HClO_4$ are the equilibria as given above. In HCl the Chlorochromate ion forms and a Sulphate complex in H_2SO_4:

$$HCrO_4^- + H^+ + Cl^- \rightleftharpoons CrO_3Cl^- + H_2O \qquad \text{E.3.6.}$$

$$HCrO_4^- + HSO_4^- \rightleftharpoons CrO_3(OSO_3)^{2-} + H_2O \qquad \text{E.3.7.}$$

The $Cr_2O_7^{--}$ ion which forms in acidic solutions is a strong oxidising agent while the CrO_4^{--} which exists in basic solutions is not (R.3.3).

$$Cr_2O_7^{--} + 14\ H^+ + 6\ e \rightleftharpoons 2Cr^{3+} + 7\ H_2O$$

$$E^o = 1.33V \qquad \text{E.3.8.}$$

$$CrO_4^{--} + 4\ H_2O + 3\ e \rightleftharpoons Cr(OH)_3 + 5\ OH^-$$

$$E^o = -0.13V \qquad \text{E.3.9.}$$

$BaCrO_4$ decomposes and loses Oxygen at very high temperature, but at ambient temperatures, it is fairly unreactive. The only major reactions which it undergoes are those associated

with the H^+ ion and which have been described above.

Barium chromate was obtained from two sources:

(i) Hopkin and Williams

Specification : Assay 99.0% min.

Maximum limit of impurities per cent Cl = 0.001

SO_4 = 0.02

Na = 0.01

K = 0.01.

(ii) B.D.H. Chemicals Ltd.

Assay (iodometric) not less than 98%.

Maximum limit of impurities Cl = 0.005%

SO_4 = 0.1% .

3.2 The solubility of $BaCrO_4$ in acidic solutions

The solubility of $BaCrO_4$ is dependent on the pH, the acid used and the temperature. In general it can be said that the total solubility S_t is the sum of the concentrations of the ions formed. The solubility with respect to Cr(VI) is given by equation E.3.10. in which the final term is only present when the acid used is HCl.

$$S_t = [H_2CrO_4]+[HCrO_4^-]+[CrO_4^{--}]+2[Cr_2O_7^{--}]+ \ldots [CrO_3Cl^-] \quad \text{E.3.10.}$$

The solubility with respect to Barium is given by:

$$S_t = [Ba^{++}] + [\text{Ba. Anion}] \quad \text{E.3.11.}$$

(Anion $\neq CrO_4^{--}$), S_t is mole $/dm^3$

The high concentration of the H^+ ion however, does not favour the formation of the Ba^{++} anion salt and therefore the Barium is stored in solution mainly as Ba^{++}. The Cr(VI) complexes however, are favoured by the acidic conditions and thus most of the Cr(VI) is stored in these forms. Although a great number of possible ions exist, their concentration is negligible and we need only be concerned with $HCrO_4^-$, CrO_4^{--}, $Cr_2O_7^{--}$ and $Cr_2O_3Cl^-$ (R.3.1.).

Actually the concentration of CrO_4^{--} is very small, and because of this it is the controlling factor in the crystallisation of Barium chromate.

3.2.1 The CrO_3Cl^- ion

The CrO_3Cl^- ion exists in solutions of $BaCrO_4$ in HCl. It is formed by equation E.3.6 as defined in section 3.1.4. and the value of the equilibrium constant K_{Cl} is given by:

$$K_{Cl} = \frac{[CrO_3Cl^-]}{[Cl^-]\ [H^+]\ [HCrO_4^-]} \qquad \text{E.3.12.}$$

Its presence should increase the total solubility of $BaCrO_4$ (equation E.3.10) and thus the concentration is calculable by comparing the total solubility of Barium chromate in HCl and HNO_3 solutions.

However, the error associated with the curves on graphs G.3.10.to G.3.12. is larger than the error of those on graphs G.3.2. to G.3.4. and so the evaluated value of the CrO_3Cl^- concentration is not very accurate. (Chapter 9).

The value of K_{Cl} is given as 10 at room temperature and moderate acidities (R.3.1.) although somewhat higher values are given by other workers (R.3.7).

3.2.2. The $Cr_2O_7^{--}$ ion

The $Cr_2O_7^{--}$ the Dichromate ion is favoured by high H^+ ion concentration and high Cr(VI) concentrations. It is formed by equation E.3.13.

$$Kd = \frac{[Cr_2O_7^{--}]}{[HCrO_4^-]^2} \qquad \text{E.3.13.}$$

The value of Kd is given as 35 at room temperature (R.3.1.). Other workers (R.3.7.) and (R.3.19.) to (R.3.25.) suggest similar values.

In very acidic solutions (pH~1) the concentration of the $Cr_2O_7^{=}$ is about 20% of the total Cr $\underline{|VI|}$ concentration but it falls rapidly as pH increases (R.3.13.).

3.2.3 The $HCrO_4^-$ ion

This ion is perhaps the most important ion in solution. It constitutes 95% of the total Cr(VI) concentration at pH=4 but its concentration falls at higher and lower acidities (R.3.1).

It is formed by equation E.3.3. or E.3.4. and the value of the equilibrium constant, Ka, is given by:

$$Ka = \frac{[H^+]\ [HCrO_4^-]}{[H_2CrO_4]} \qquad \text{E.3.14.}$$

In the literature Ka is quoted as Ka = 0.18 (R.3.25) although others (R.3.24) suggest slightly higher values.

3.2.4 The CrO_4^{--} ion

The concentration of the Chromate ion is related directly to the crystal growth, since only Cr(VI) in the form of CrO_4^{--} is directly available for crystallisation. It is formed as described by equation E3.3. and the value of the equilibrium constant Kc is given as $\sim 2.5 \times 10^{-7}$ although some of the earlier works suggest somewhat higher values (R.3.19.) to (R.3.25.). It is defined by :

$$Kc = \frac{[CrO_4^{--}]\ [H^+]}{[HCrO_4^-]} \qquad \text{E.3.15.}$$

In very concentrated acid solutions the concentration of CrO_4^{--} is very small; for example,

at pH = 1 it is 2 p.p.m. of total Cr(VI),
at pH = 2 it increases to 0.3% (3000 p.p.m.) and in neutral solution it is 75% of the total Cr(VI) (R.3.1.).

The concentration of the CrO_4^{--} ion can be estimated from equation E.3.15.. The uncertainty however, in calculating $HCrO_4^-$ produces suspect values for the driving force.

The driving force for crystal growth of ionic materials has been shown (R.2.25.), (R.2.26.) and (R.2.27.) to be :

$$\text{driving force} = \ln \left(\frac{[CrO_4^{--}]\,[Ba^{++}]}{[CrO_4^{--}]_s [Ba^{++}]_s} \right) \qquad \text{E.3.16.}$$

or

$$\text{driving force} = \ln \left(\frac{C_c \cdot C}{C_{cs} \cdot C_s} \right) \qquad \text{E.3.16.a.}$$

However the concentration of the CrO_4^{--} ion can be related to the total Cr(VI) concentration (R.3.1.) by:

$$C_c = \alpha C^m \qquad \text{E.3.17.}$$

and

$$C_{cs} = \alpha C_s^m \qquad \text{E.3.18.}$$

Graph G.3.1. presents this relationship and a portion of the solubility curve. For modest supersaturation ($S < 1.5$) in the region of interest ($2 < pH < 4$) the value of m and α can be assumed constant.

This assumption enables us to evaluate the driving force in terms of the total Cr(VI) concentration at saturation and supersaturation conditions (Section 6.3.2.).

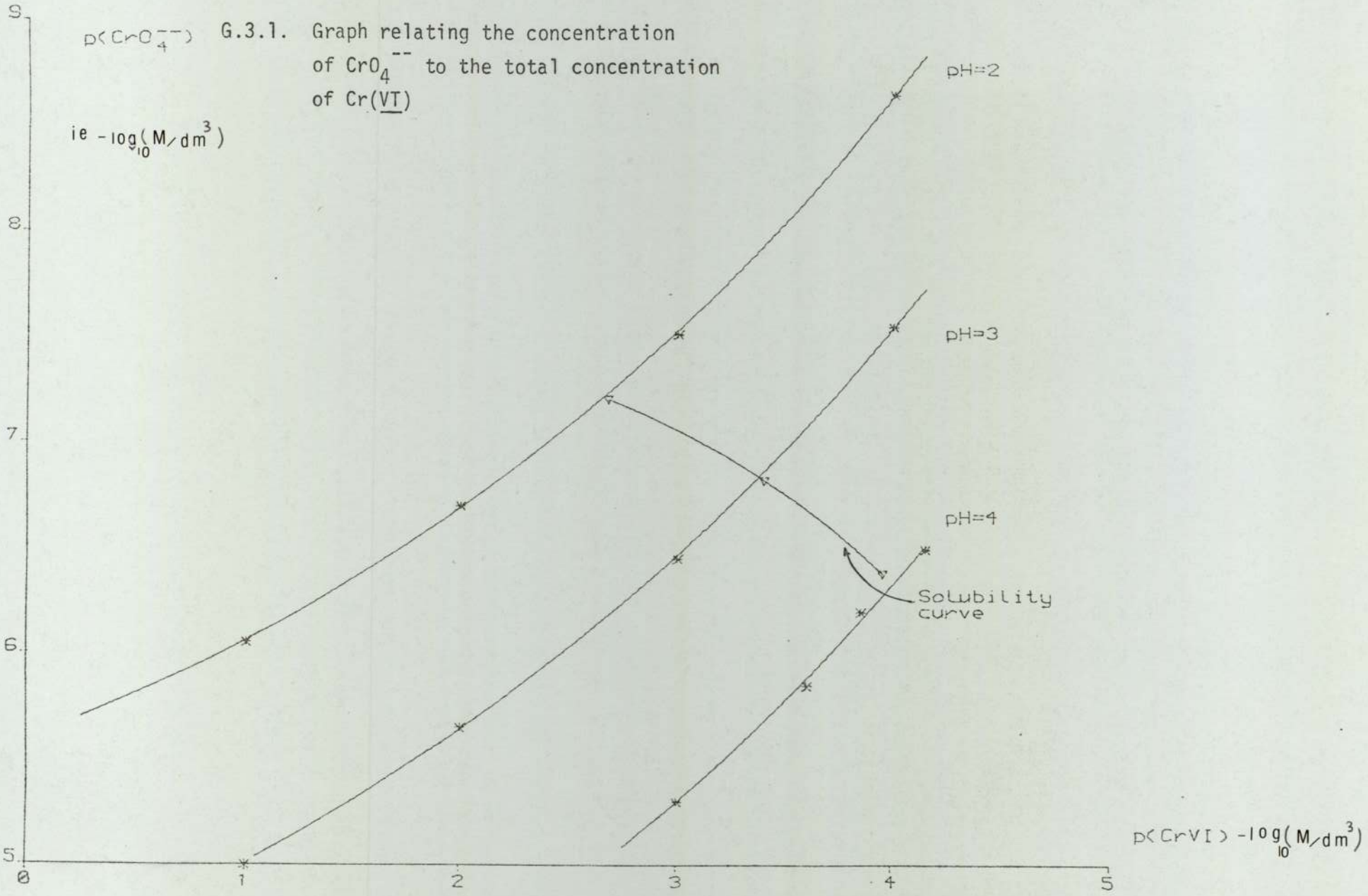
p(CrO4--)
ie -log10(M/dm3)
G.3.1. Graph relating the concentration of CrO4-- to the total concentration of Cr(VI)
pH=2
pH=3
pH=4
Solubility curve
9
8
7
6
5
0
1
2
3
4
5
p(CrVI) -log10(M/dm3)

3.3 Measurement of the solubility of Barium chromate

There are many methods for measuring the solubility of a compound and they can be broadly classified into two categories: those involving the analysis of a sample of the equilibrium saturated solution and those on which the measurements are made on the bulk of the solution.

Skander (R.3.1) gives a detailed account of the methods available. Three methods are used in this work:

3.3.1. Residue weight

By this method a sample of a saturated solution is withdrawn and placed in a shallow basin. The sample is allowed to evaporate and the solids left are weighed.

3.3.2. Ultra-violet spectrophotometry (Appendix 8)

This method makes use of the Beer and Lambert law which states that the absorptive capacity of the solute in a solution is directly proportional to the concentration of the solute (Beer's law) and that each layer of equal thickness of an absorbing medium absorbs an equal fraction of the radiant energy that transverses it (Lambert's law). The above laws hold true only when monochromatic radiation is provided and When the physical and chemical state of the solute does not change with concentration. If these assumptions are valid then the absorbance of a solute (number of absorbing molecules of the solute) relative to the absorbance

of the solvent is proportional to the concentration, and therefore the fraction of the radiant energy transmitted by a given thickness of the absorbing medium is independent of the intensity of the incident radiation, provided that the radiation does not alter the physical or chemical state of the medium (R.3.12.).

No evidence that the radiation does alter the physical or chemical state of the Barium chromate solution has been found (R.3.1.). However, the equilibrium equations E.3.2. to E.3.8. are subject to the total concentration of the Cr(VT) and indirectly to the pH of the solution. In such cases the laws of Beer and Lambert are combined to give the Beer-Lambert law which states that the total absorbance of a solution in which an equilibrium exists is the sum of the (individual absorbances) x (molar absorptivity of the components).

or $$AB = \sum_{i=1}^{n_T} \varepsilon_i C_i \qquad \text{E.3.19.}$$

where AB is the total absorbance

n_T is the total number of species in the solution

ε_i is the molar absorptivity of species i

C_i is the concentration of specie i.

3.3.3. Atomic absorption/emission (Appendix 9)

When atoms or ions are in the maximum state of "excitement" electromagnetic radiation is absorbed/emitted. The method makes use of this by exciting the ions in the solution with an acetylene flame (R.3.17) (Appendix 9, P 222)

3.4. The effect of complexing agents on the solubility

In recent decades the application and use of complexing agents has grown enormously. The purpose of the complexing agent is to preferentially keep the metal ions (if there are more than one type) in solution, bonded to electron donor groups, and thus increasing the overall solubility (R.3.14). The choice of the complexing agent is important since the metal ion would have to compete with H^+ of the solution for the electron donor groups. The more basic the metal ions the greater is the affinity for Oxygen electron donor groups than for Nitrogen ones. In general, the following order exists with respect to affinity (R.3.15) for most metal ions:

$$\underset{\uparrow}{-O^-} > \underset{\uparrow}{-O^-} > COO^- > R_2N- O- > \quad \diagdown\!\!\diagup C = O$$

(Alkyl) (Aromatic)

For many transition metals the order is

$$\underset{\uparrow}{-O^-} > -NH_2 > -N = N- > -COO^- > -O- > \quad \diagdown\!\!\diagup C = O$$

(Enolic)

The presence of the Sulphur and Phosphorous molecules in the donor group or in adjacent positions gives increased affinity for the heavier metals.

On the basis of the above, five complexing agents were tried in an attempt to increase the $BaCrO_4$ solubility. Their choice was primarily based on their capacity to preferentially

complex the Barium ion (Ba^{++}) but not to reduce the Cr(VT) into a lower state which would upset the equilibrium balance of the Cr(VT) (equations E.3.2. to E.3.6.) and yet to cover a wide range of electron donor group types (R.3.16).

The five complexing agents chosen were :

(i) E.D.T.A.

(ii) Citric acid

(iii) Nitrite-triacetic acid

(iv) Sodium oxalate

(v) Tri-sodium orthophosphate.

For other reasons, the effect of Acetic and Formic acids on the solubility were also tested and thus seven types of complexing agents were tested altogether.

The main disadvantage of the complexing agents is that they tended to buffer the pH of the solution and thus actually decreased the total amount of Barium chromate which could be dissolved. It was found that the solubility of Barium chromate is far more sensitive to the pH of the solution than to any complexing agent. A further consideration was the possible interference with the crystal growth mechanism which the agents might cause and hence this approach was abandoned.

3.5. Solubility data

3.5.1. Solubility in Nitric acid

Graphs G.3.2., G.3.3. and G.3.4. present the data obtained at 35°C, 52°C and 65°C respectively. The samples were collected from reactors 1, 2, 3 and 4 and analysed in the ultraviolet spectrophotometer (Chapter 7). The scatter of the data points, especially at the higher temperatures, suggests that these reactors are not suitable for measuring the solubility of Barium chromate. However, a large number of data points were obtained and a statistical analysis was possible by the least squares method and straight lines fitted relating the pC_s ($-\log_{10}C_s$) with the pH.

3.5.2. Solubility in Hydrochloric acid

Graph G.3.5. to G.3.8. present the data obtained at 35°C, 52°C, 65°C and 100°C respectively. Reactors 1, 2 and 3 were used for the lower temperature, while reactor No. 5 for the 100°C. The samples were analysed in the ultraviolet spectrophotometer and plotted as pC_s vs pH. Straight lines were fitted to the data using the least squares method.

3.5.3. Solubility in Urea/Hydrochloric acid

Graphs G.3.9. to G.3.12. present the data obtained at 21°C, 52°C, 65°C and 90°C respectively. Reactor 5 was used and the samples were collected and analysed as described in Chapter 7. The data points were again correlated by the method of least squares to give the best straight line relating pC_s to pH.

Data points were also collected at 100°C but because of the hydrolysis of Urea, equilibrium conditions were never reached due to the rapid change of pH and therefore these data were ignored.

G.3.2. Graph relating the solubility of Barium Chromate with pH

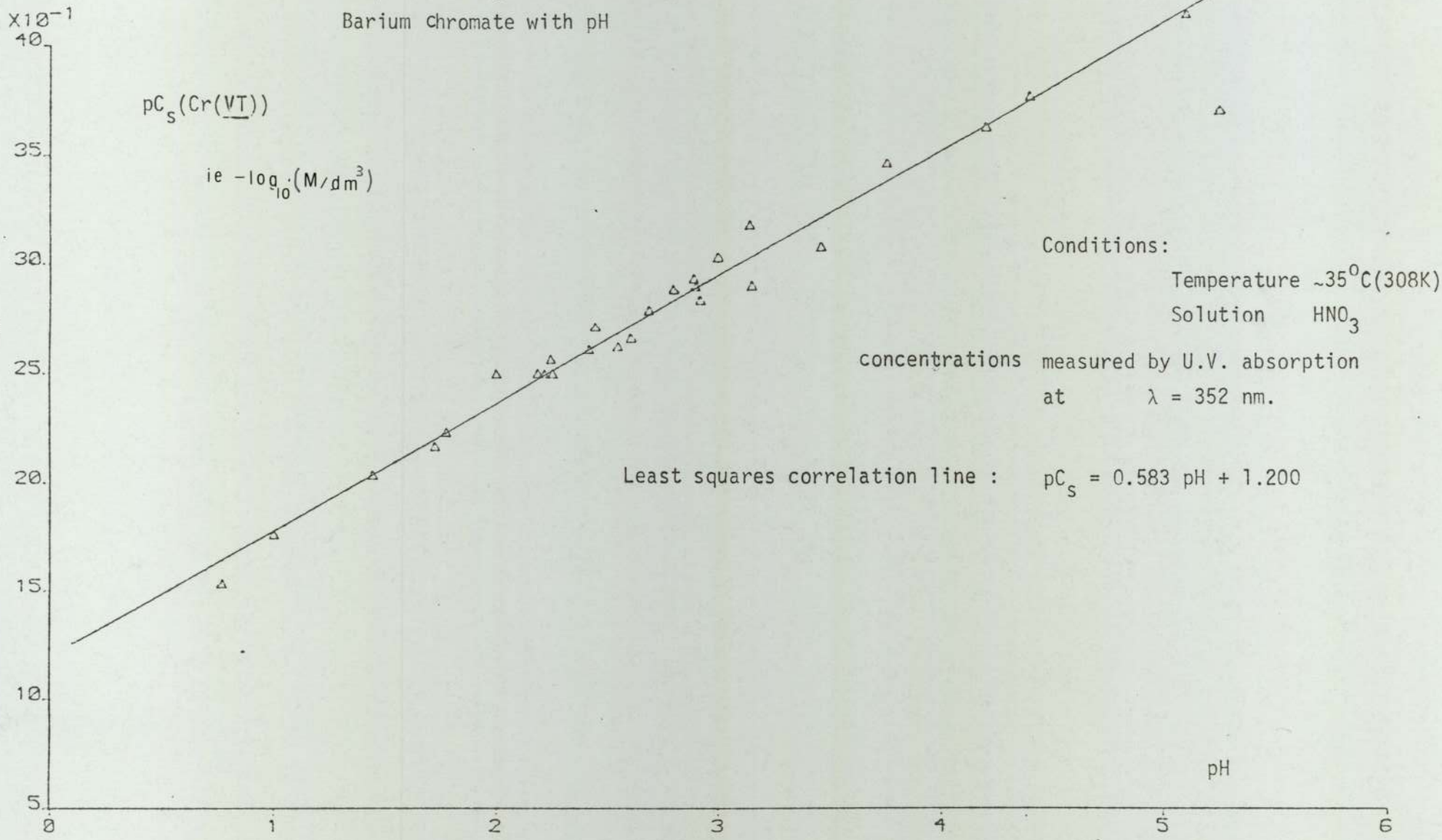

Conditions:

Temperature ~35°C(308K)

Solution HNO_3

concentrations measured by U.V. absorption at λ = 352 nm.

Least squares correlation line : $pC_S = 0.583\ pH + 1.200$

G.3.3. Graph relating the solubility of Barium chromate with pH

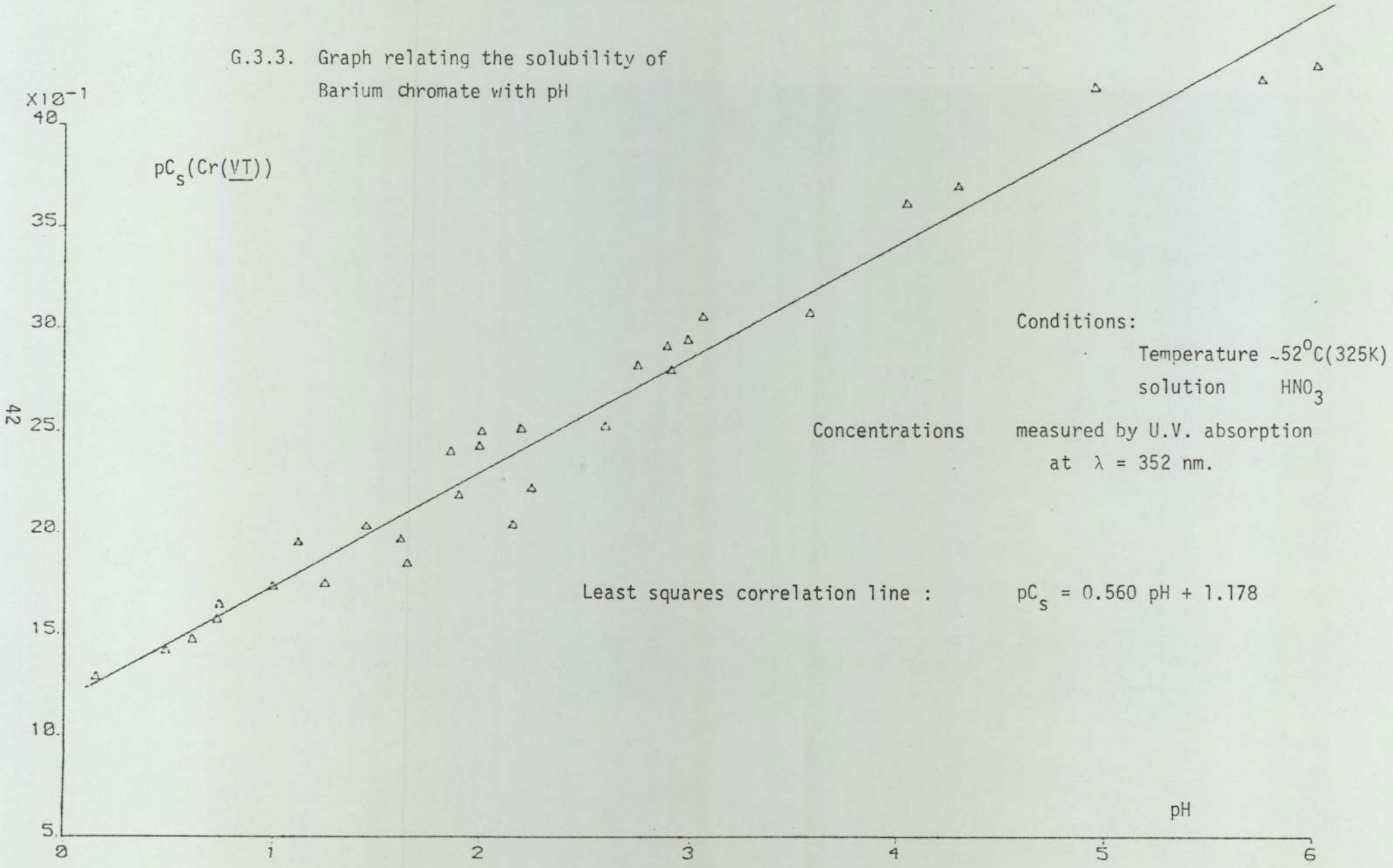

Conditions:

Temperature ~52°C(325K)

solution HNO_3

Concentrations measured by U.V. absorption at λ = 352 nm.

Least squares correlation line : $pC_s = 0.560\ pH + 1.178$

G.3.4 Graph relating the solubility of Barium chromate with pH

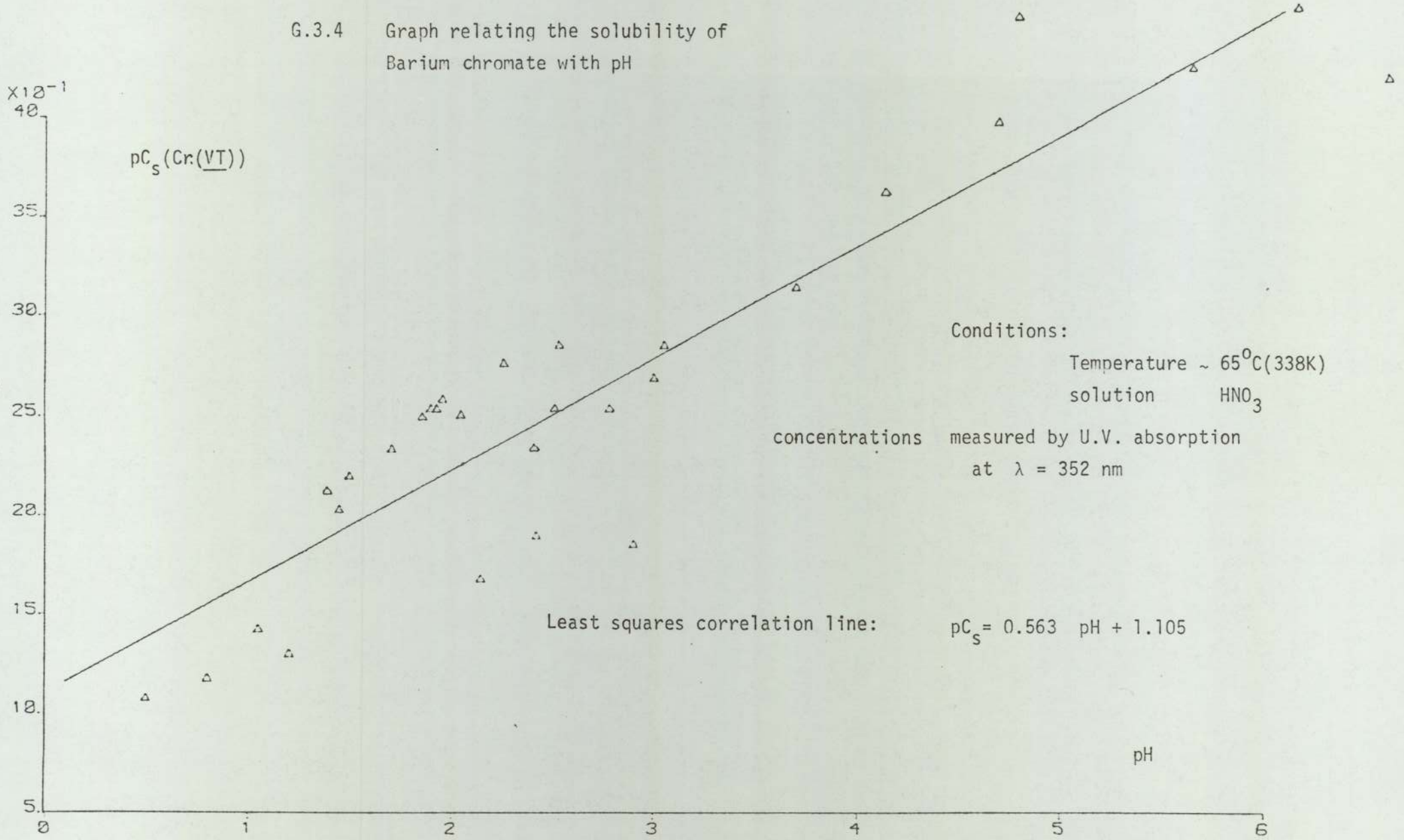

G.3.5. Graph relating the solubility of Barium Chromate with pH

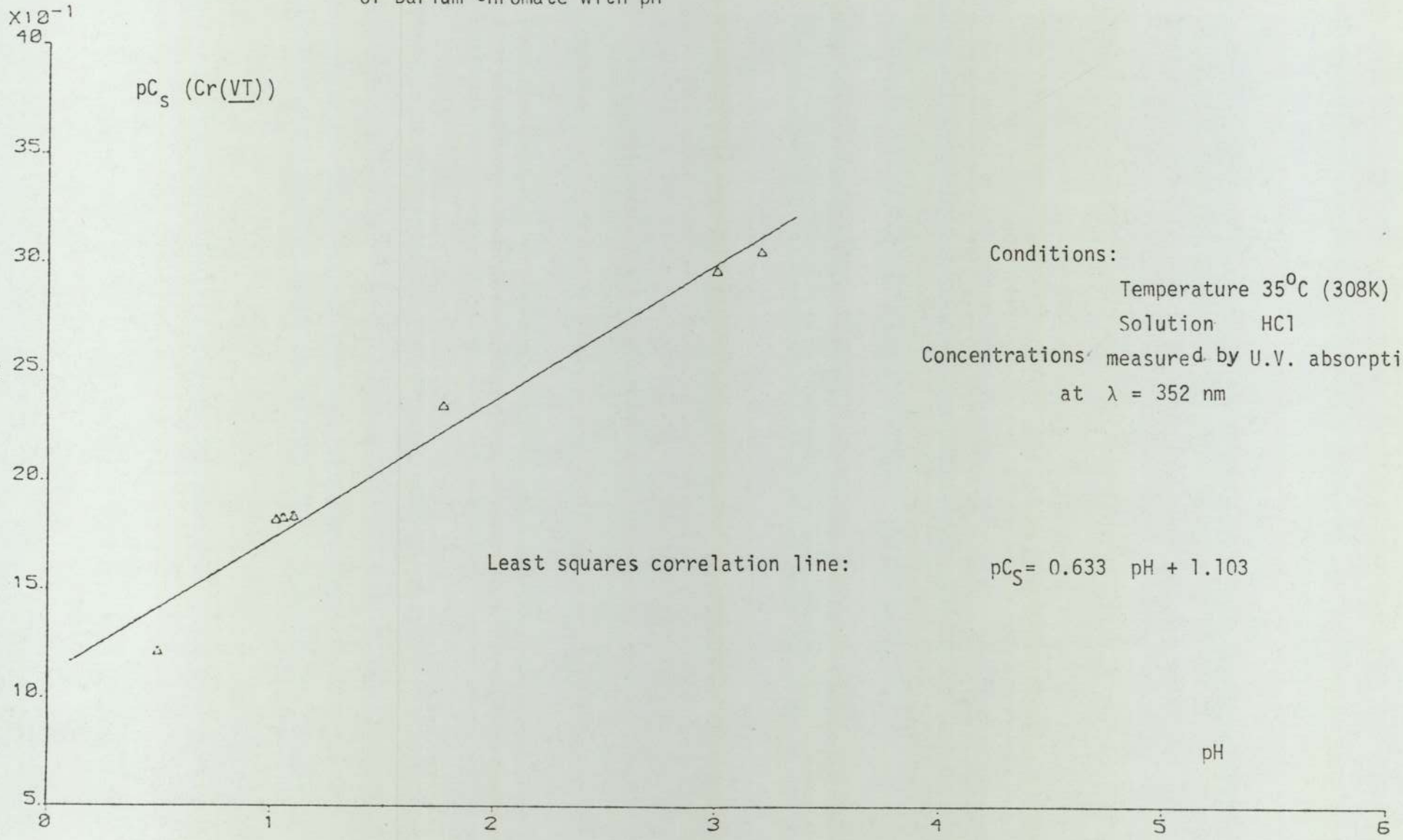

Conditions:

Temperature 35°C (308K)

Solution HCl

Concentrations measured by U.V. absorption at λ = 352 nm

Least squares correlation line: $pC_S = 0.633\ pH + 1.103$

G.3.6. Graph relating the solubility of Barium Chromate with pH

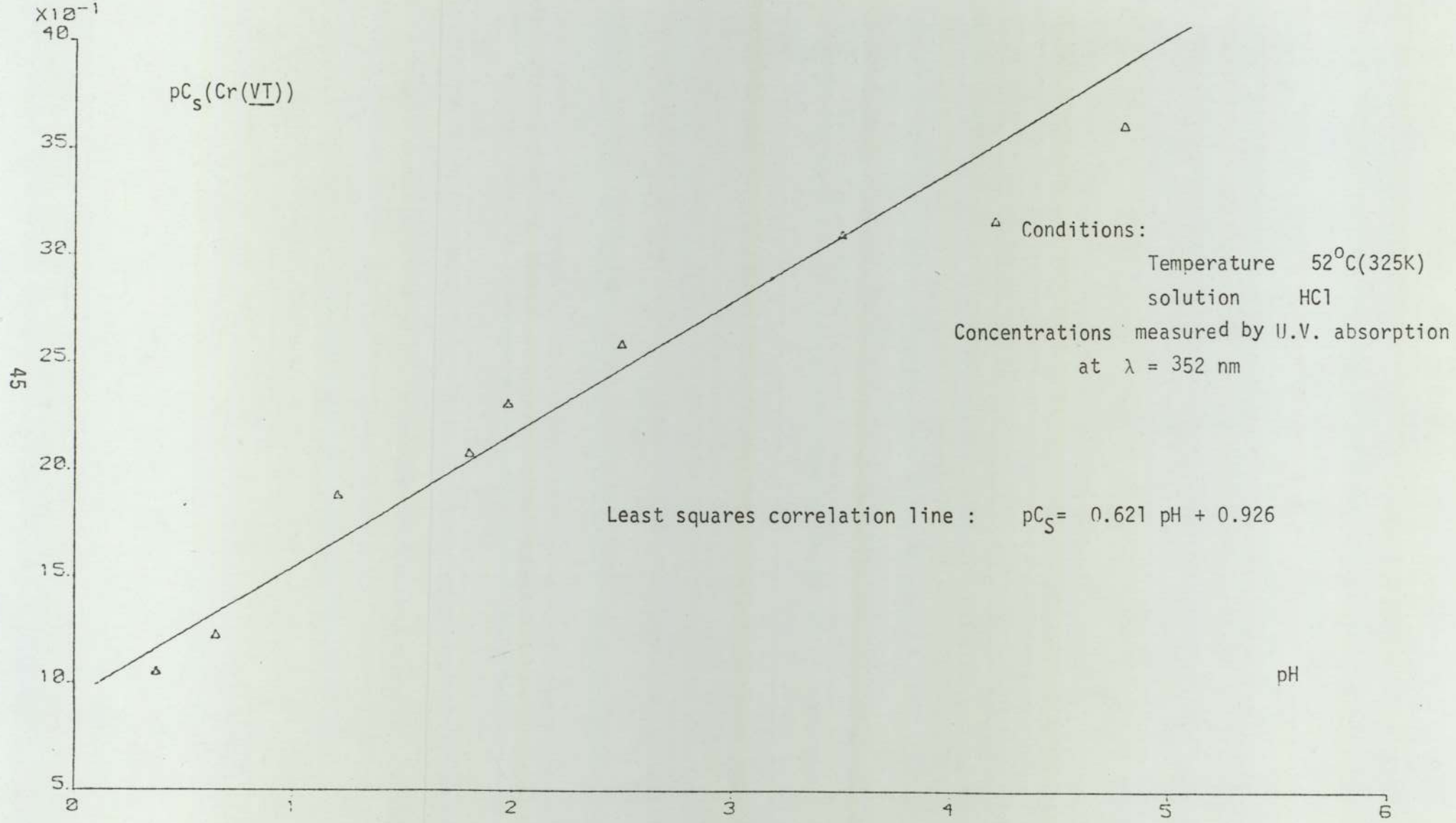

G.3.7. Graph relating the solubility of Barium Chromate with pH

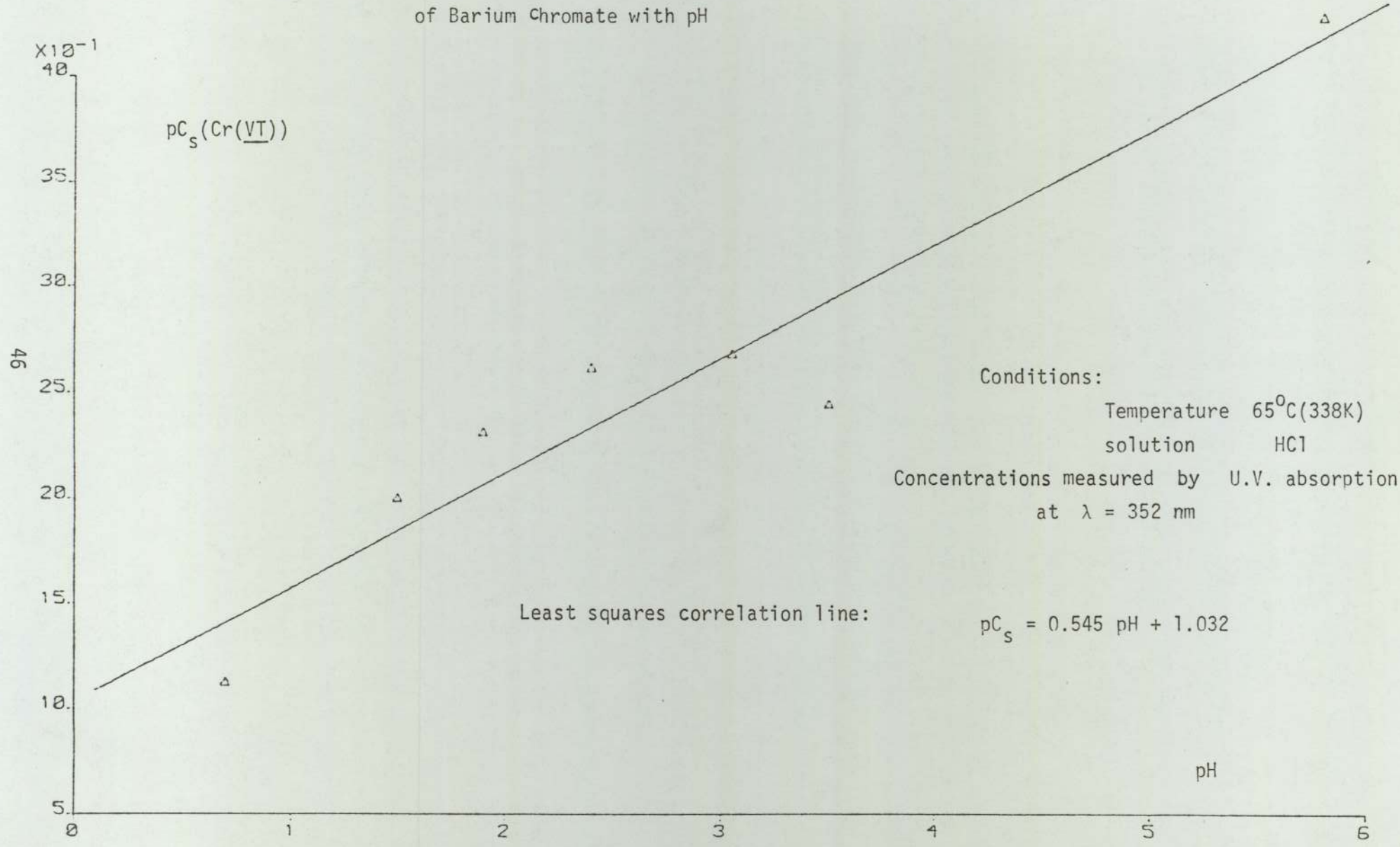

Conditions:

Temperature 65°C(338K)

solution HCl

Concentrations measured by U.V. absorption at λ = 352 nm

Least squares correlation line:

$pC_s = 0.545\ pH + 1.032$

G.3.8. Graph relating the solubility of Barium chromate with pH

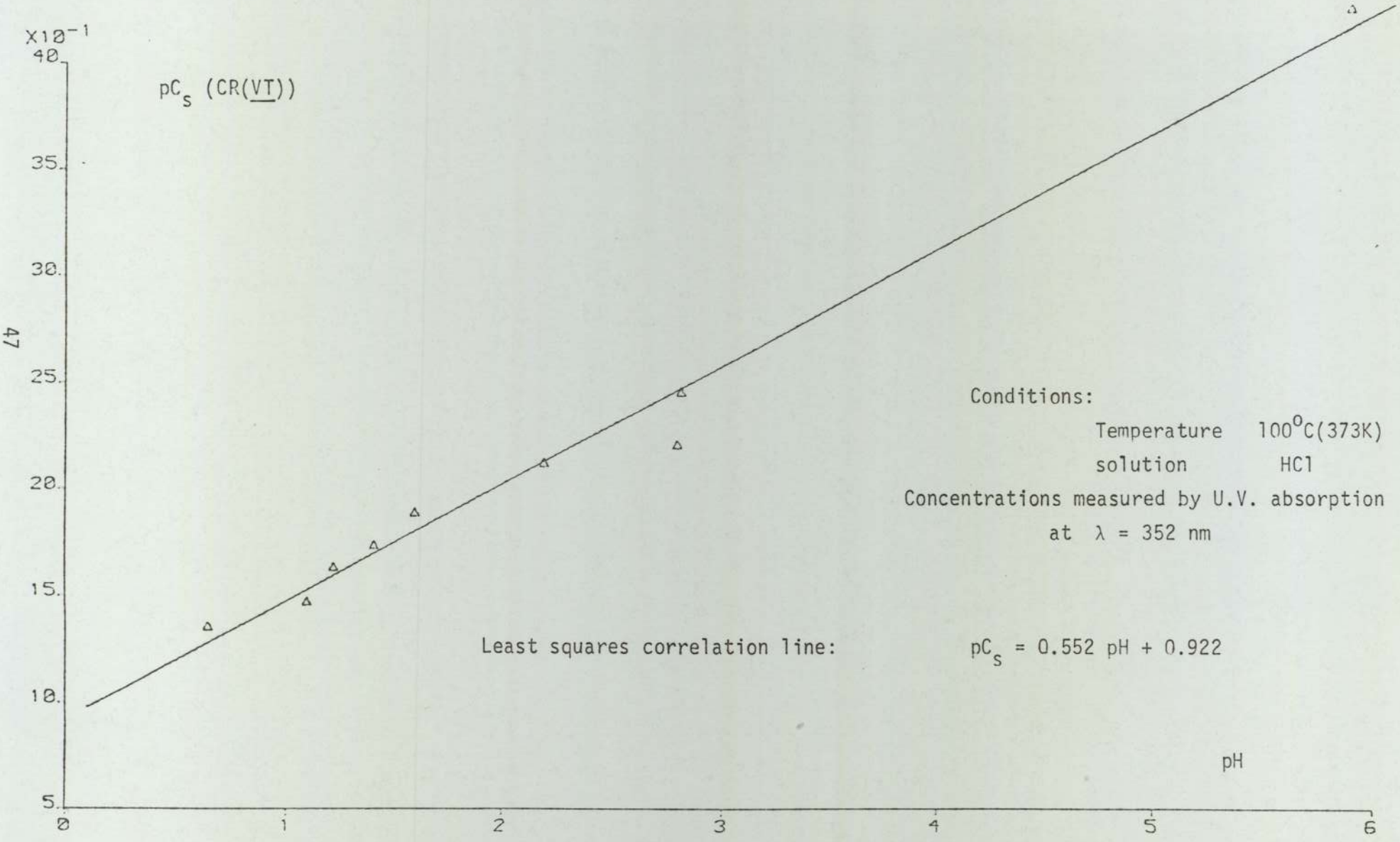

Conditions:

Temperature $100^{o}C(373K)$

solution HCl

Concentrations measured by U.V. absorption at λ = 352 nm

Least squares correlation line: $pC_s = 0.552\ pH + 0.922$

G.3.9. Graph relating the solubility of Barium Chromate with pH

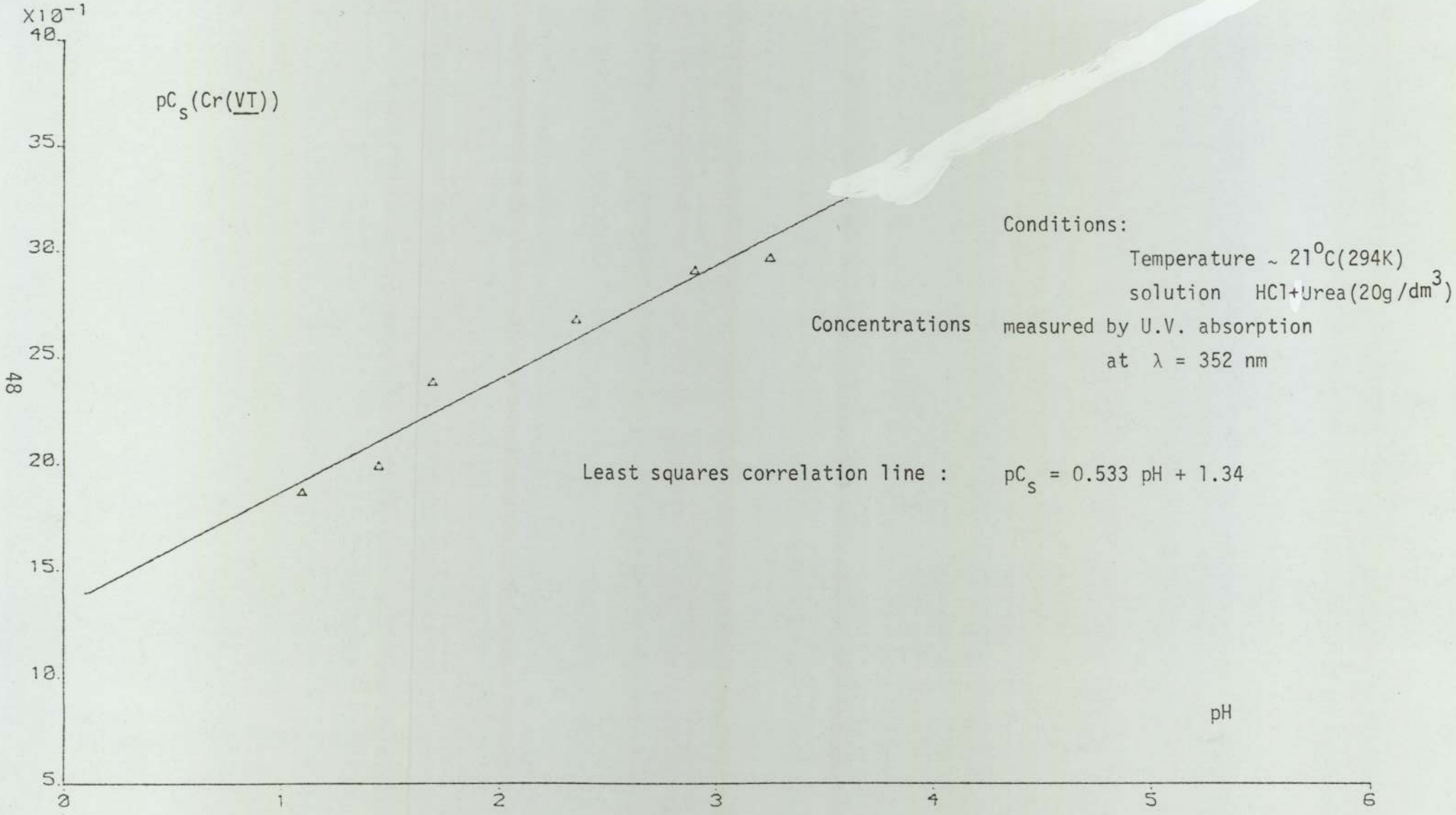

Conditions:

Temperature ~ 21°C(294K)

solution HCl+Urea(20g/dm³)

Concentrations measured by U.V. absorption at λ = 352 nm

Least squares correlation line : $pC_s = 0.533\ pH + 1.34$

G.3.10. Graph relating the solubility of Barium chromate with pH

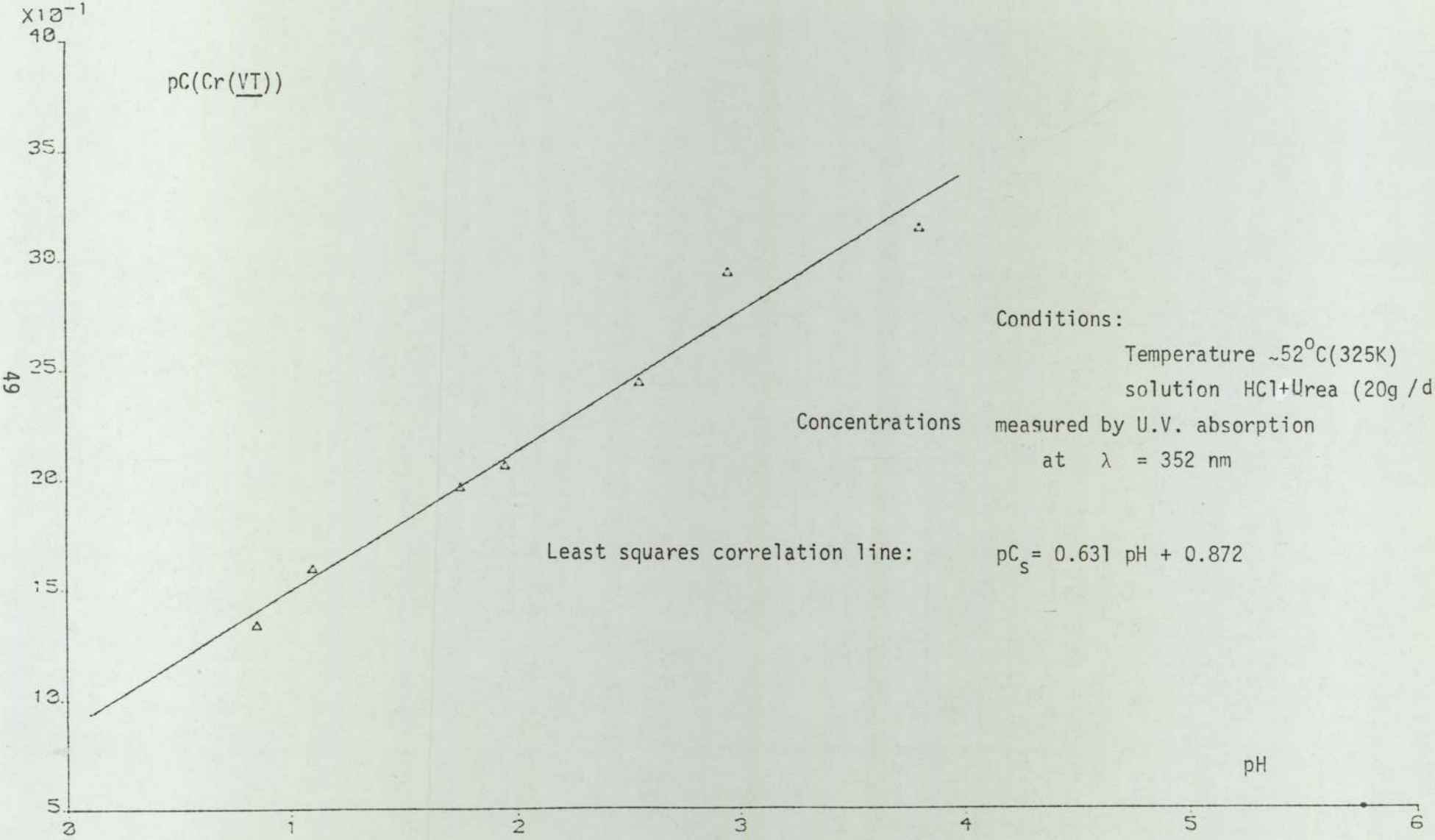

Conditions:

Temperature ~52°C(325K)

solution HCl+Urea (20g /dm^3)

Concentrations measured by U.V. absorption at λ = 352 nm

Least squares correlation line: $pC_s = 0.631\ pH + 0.872$

G.3.11. Graph relating the solubility of Barium Chromate with pH

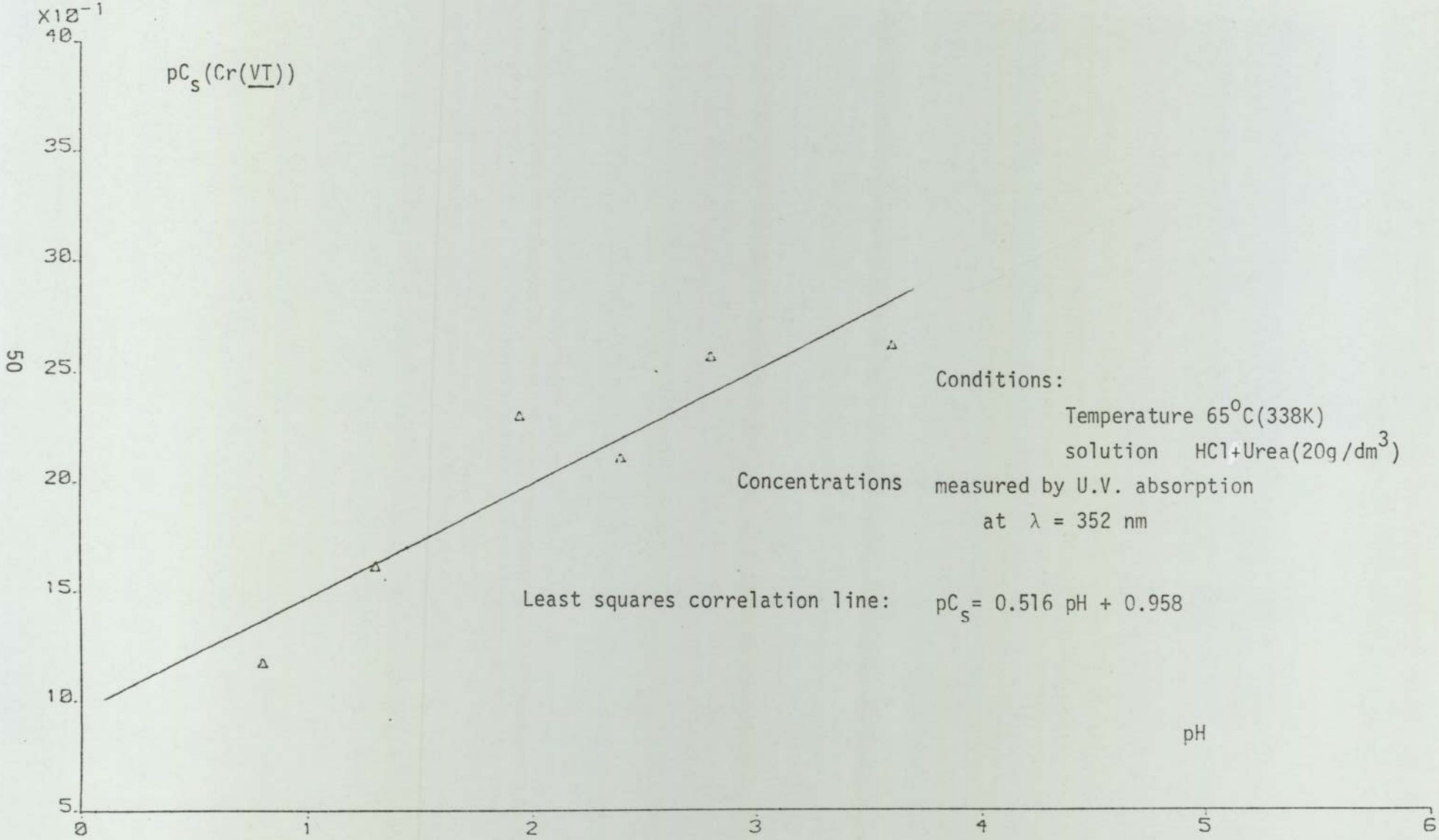

Conditions:

Temperature 65°C(338K)

solution HCl+Urea(20g/dm³)

measured by U.V. absorption

at λ = 352 nm

Concentrations

Least squares correlation line: $pC_s = 0.516\ pH + 0.958$

G.3.12. Graph relating the solubility of Barium Chromate with pH

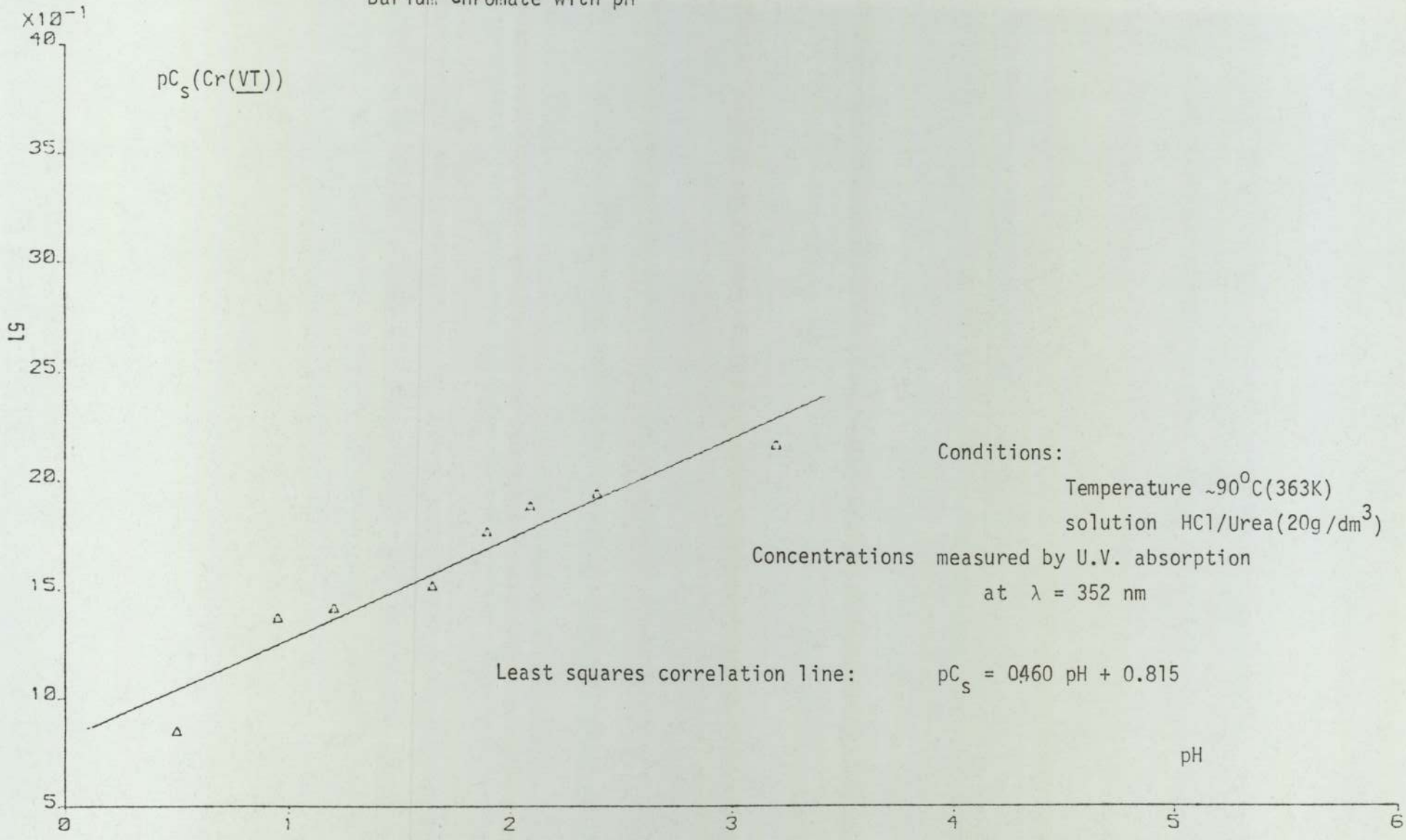

Conditions:

Temperature ~90°C(363K)

solution HCl/Urea(20g/dm^3)

Concentrations measured by U.V. absorption at λ = 352 nm

Least squares correlation line: $pC_s = 0.460\ pH + 0.815$

3.6. Discussion

The data obtained were taken from different types of reactors and they were analysed by different techniques; This should be noted when they are compared.

3.6.1. The residue weight method for measuring the solubility of Barium chromate

The main advantages of this method are simplicity and speed. However, it produces fairly accurate results only for low pH values (<3). Greater confidence can be placed on the results obtained at higher acidities (pH<1) but at this range the linear relationship between pC_s and pH possibly fails.

3.6.2. The Ultraviolet spectrophotometry method

Theoretically this is a very accurate method for measuring the concentration of a solute in solution. (as little as 10^{-4} g/dm^3 of solute can be detected)(R.3.12.). In practice, the inaccuracies of the sampling techniques limit the usefulness of the method.

3.6.3. The Atomic absorption/emission method

The accuracy of this method is very high (R.3.17.) and as little as 10^{-6} g/dm^3 of solute can be detected. The inaccuracies of the sampling technique however reduce the accuracy. Furthermore, the results obtained by this method are ignored because of a suspected fault in the electronics of the instrument (Appendix 9).

3.6.4. The use of the complexing agents for increasing the solubility of Barium chromate

The use of complexing agents are quite inappropriate for the following reasons:

(i) it buffers the pH, and thus reduces the amount of Barium chromate which could be dissolved due to a drop in pH without a sufficiently compensating increase due to complexing the Ba^{++},

(ii) it affects the quality of the crystals in the crystallisation of Barium chromate (Chapter 6),

(iii) irreversible reactions may take place which either change the complexing agents themselves or reduce the Cr(VI) to a lower oxidation state.

3.6.5. The effect of pH on the solubility

All workers on the subject agree that the solubility of Barium chromate is very sensitive to pH although the values of C_s which they suggest at specific acidities tend to vary. Skander (R.3.1.) has reviewed the published data and has suggested possible reasons for the discrepancy. The results of the present work agree with those found by Skander at low temperature (~35°C), the difference being about 5%. However, at higher temperatures somewhat lower solubilities were found than those by Skander. Although the effect of the acidity on the C_s is not linear, a straight line can be fitted relating pC_s with pH. This enabled speedy computation of the concentration at saturated conditions for various values of pH. These relationships are included in the graphs G.3.2 to G.3.12.

3.6.6. The effect of the temperature on the solubility

The solubility of a solute is usually related to the temperature by the Clasius – Clapeyron equation (R.3.2):

$$C_s = Co \quad \exp\left(-\frac{\Lambda}{n_T K_T \quad T}\right) \qquad \text{E. 3.20.}$$

C_s is the concentration of the solute at saturation

T is the temperature

n_T is the number of ions formed from 1 molecule of solute

Λ is the enthalpy of the phase change

Co and K_T are constants

For dilute solutions this can be simplified to:

$$pC_s = K_{To}\left(\frac{1}{T}\right) - \text{constant} \qquad \text{E. 3.21.}$$

where K_{T_o} is a new constant.

Graphs G. 3.13. to G.3.15. present pC_s vs. temperature for selected pH values (2, 3 and 4), and a statistical treatment using the least squares method enables extrapolation to 100°C, the operating temperature of the crystallisation.

The equations relating the pC_s with $\frac{1}{T}$ are included in the graphs G.3.13. to G.3.15. for selected pH values.

The value of K_{To} varies with pH and tends to decrease as acidity increases, the reason possibly being the variation of the constants n_T, K_T and Λ with pH.

Although there are also theoretical reasons (R.3.2 .) for suggesting that the curves presented in graphs G.3.13. to G. 3.15. should pass through the same point, no further

extrapolation is attempted at this stage because of the experimental errors involved (Chapter 9).

3.6.7. The concentration of the CrO_3Cl^- ion

In section 3.2.1. it was suggested that the formation of the Chlorochromate ion would result in an increase in the solubility of Barium chromate. This increase would be detectable if the solubilities in Nitric and Hydrochloric acids were compared (R.3.6.) and (R.3.7.).

From Graphs G.3.13. and G.3.14. it is estimated that the percentage concentration of the Chlorochromate ion at pH = 2 changes from 4% to 12% of the total $Cr[VI]$ concentration as the temperature increases from 35 to 100°C, assuming that the solubility change is due entirely to the formation of this ion. This finding is in agreement with the model suggested by Skander (R.3.1.).

3.6.8. The effect of Urea on the solubility

In the literature (R.3.13.) it is suggested that the Urea increases the dialectric constant of the solution and thus the solubility of ionic compounds. In this experimental work it was found that Urea increases considerably the solubility of $BaCrO_4$, especially at higher temperatures. By comparing graphs G.3.14. and G.3.15. it is seen that at 35°C the increase is about 20% and 120% at 100°C (for pH=2).

G.3.13. Graph relating the concentration of $BaCrO_4$ with temperature at specific pH values in HNO_3 solutions

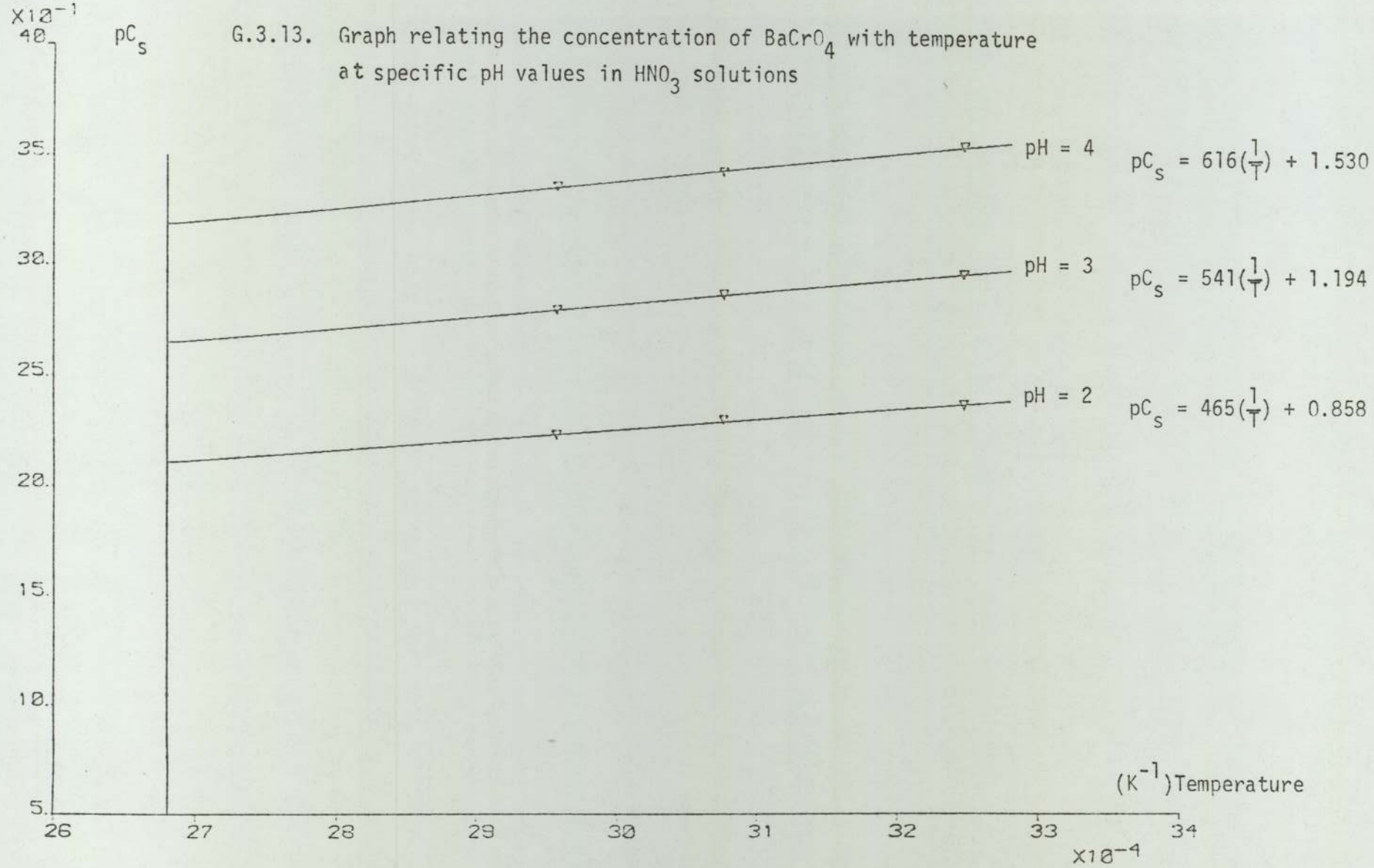

G.3.14. Graph relating the concentration of $BaCrO_4$ with temperature at specific pH values in HCl solutions

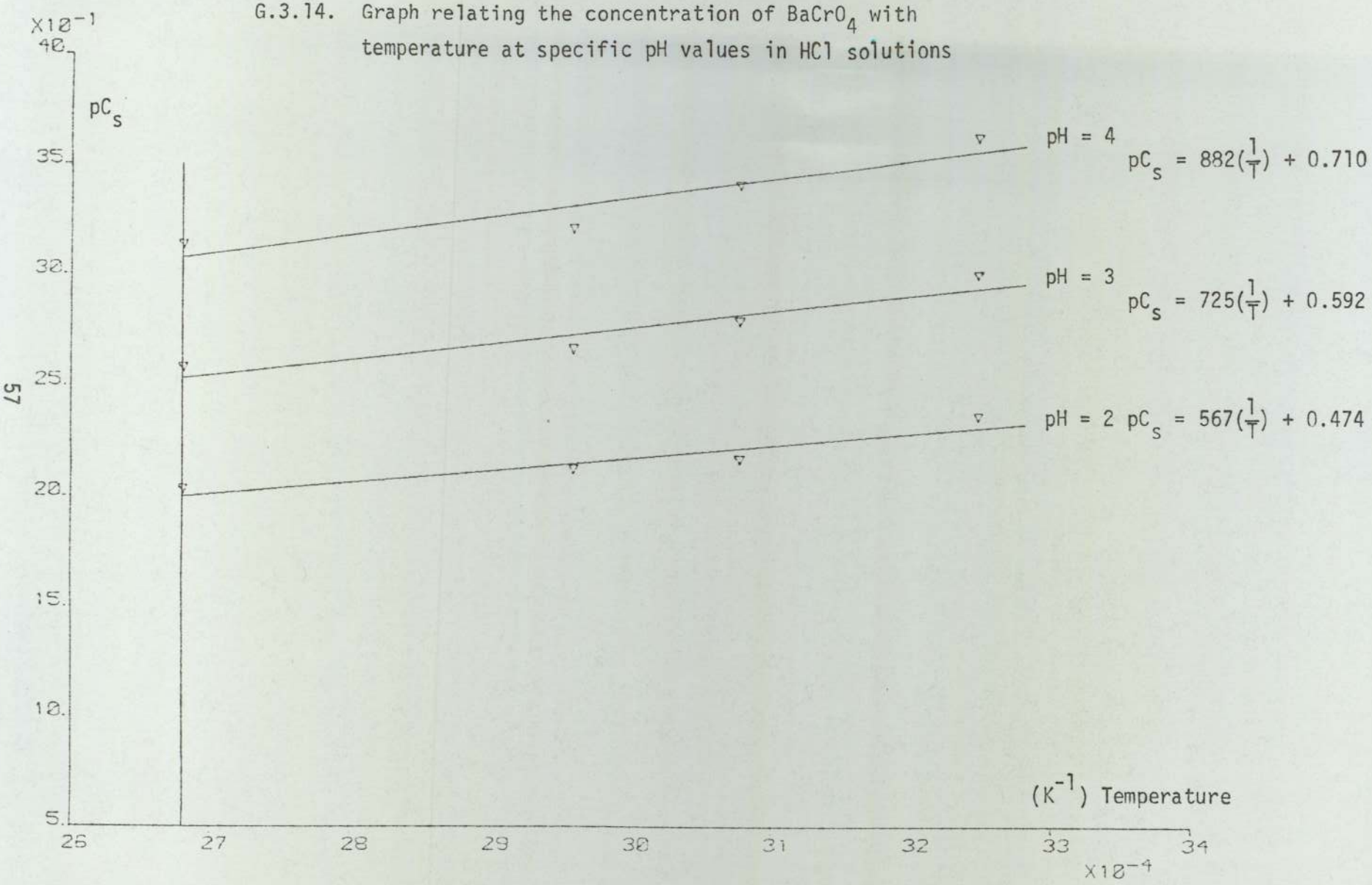

G.3.15. Graph relating the concentration of $BaCrO_4$ with temperature at specific pH values in HCl/Urea solution

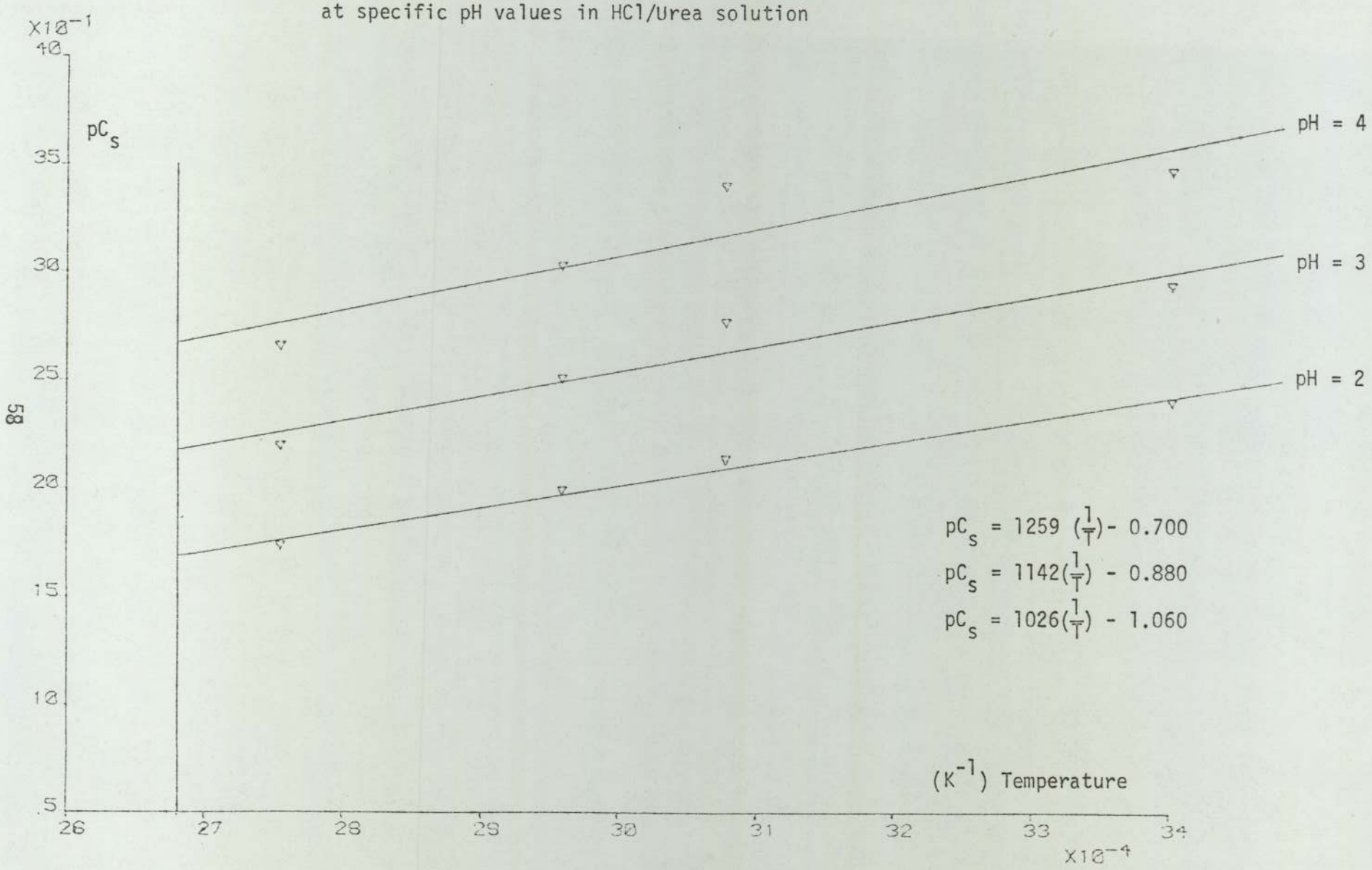

CHAPTER 4

TUNGSTEN

Tungsten is the metal on which it is desired to grow Barium chromate crystals. Although extensive work has been published on the coating of Tungsten with various metals and compounds by adsorption at high temperature, alloy formation at melt and electrolysis under high potential difference, in the present work we are only concerned with growth from solution of Barium chromate crystals on Tungsten nuclei at about 100°C.

4.1. Properties of Tungsten

4.1.1. Physical properties

The atomic number of Tungsten is 74 and its atomic weight is 183.86 (R.4.1.) The density of the metal is usually taken to be between 18.7 and 19.3 g/cm^3 at 20°C and 1Atm. The density of the powder is 19.2 g/cm^3 (R.4.2.) The densities of its oxides are much lower at between 14 g/cm^3 for W_3O and 7.3 g/cm^3 for WO_3.

The melting point is 3400°C (R.4.2.).

4.1.2. Chemical properties

Tungsten is resistent to most chemicals. In air it is stable up to 500°C and oxidation begins only above this temperature. The first oxide layer is black, but as further oxidation occurs and its thickness increases, the colour goes through the range of the spectrum (R.4.3.). Towards certain acids Tungsten is unreactive. At higher temperatures however, and in mixtures of concentrated acids, Tungsten powder dissolves completely (R.4.1.) , (R.4.7.).

Table T.4.1. summarises the degree of attack and as it can be seen, HNO_3 produces the greatest attack, especially in combination with the Halide acids.

T^oC	HCl	H_2SO_4	H_3PO_4	HNO_3	HNO_3+HCl	HNO_3+HF
20	-	-	-	slight oxidation	dissolves	
100	slight	slight	slight	oxidation	dissolves	dissolves

Table T.4.1. Attack on Tungsten in an acidic environment (R.4.7.).

4.1.3. Structural properties

Tungsten has a body centred cubic crystal structure of type A2 with two atoms per cell in positions 0,0,0 and $\frac{1}{2},\frac{1}{2},\frac{1}{2}$. The lattice constant $\alpha_o = 3.165$ Å at 20^oC (R.4.4.)
The shortest interatomic distance (corner to centre atom) is 2.741 Å at 25^oC.

However, when the metal is prepared by the electrolysis of fused Tungstates a meta-stable b-form of body centred lattice is produced, having $\alpha_o = 5.083$ Å.

On heating to 700^oC the ß-form reverts to the α-form. It has been suggested that the ß-form is in fact a sub-oxide (possibly W_3O).

When epitaxial growth is attempted the lattice mismatch should be less than 20% (R.A3.1.) Although the Tungsten inter-atomic distances are much smaller than those of Barium Chromate (Chapter 3), if alternate Tungsten atoms (α-lattice) are considered, then the lattice mismatch is less than 2%

(Appendix 3, p 179)

4.2. Tungsten powder

Two types of Tungsten powder were available:

(i) from Hopkin and Williams nominal size 1 μm of bimodal distribution with peaks at 2 and 8 μm diameter as measured by the Andreasen sedimentometer and the distribution is shown in graph G.4.1., and

(ii) from New Metals nominal size 0.4 m of about 2μm diameter as measured by the Andreasen sedimentometer and by 'stereo' photography, as shown in graph G.4.2. and photograph F.6.6..

Grinding of the first sample to produce a more uniform sized product (10 minutes in a micromill) had no significant effect on the distribution and thus it was concluded that the large particles were not agglomerates as had been originally assumed.

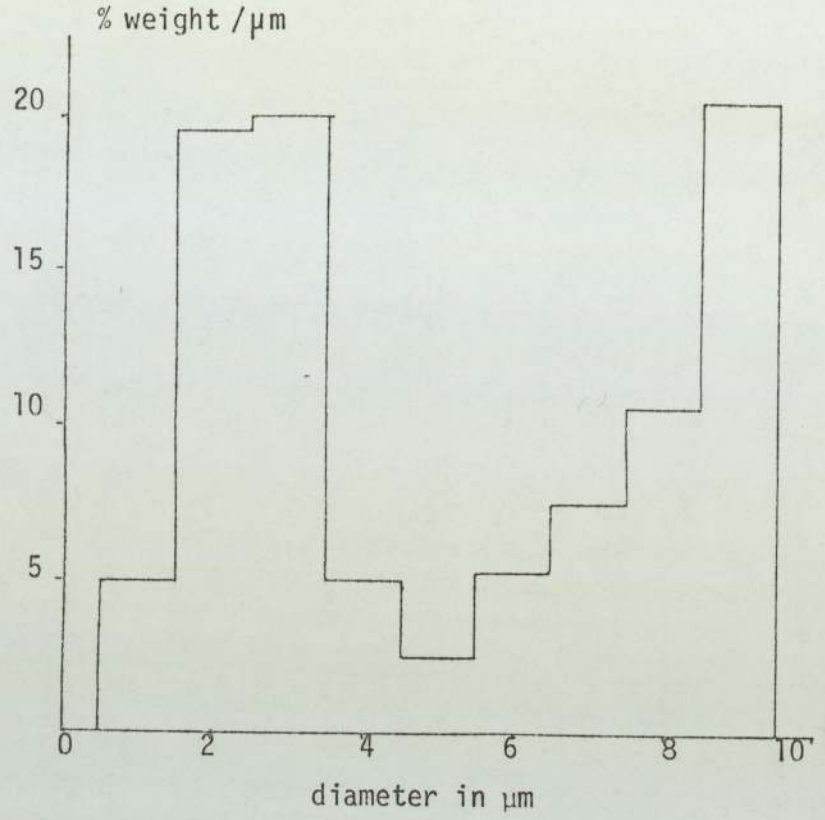

G.4.1. Size distribution of Tungsten type (i)

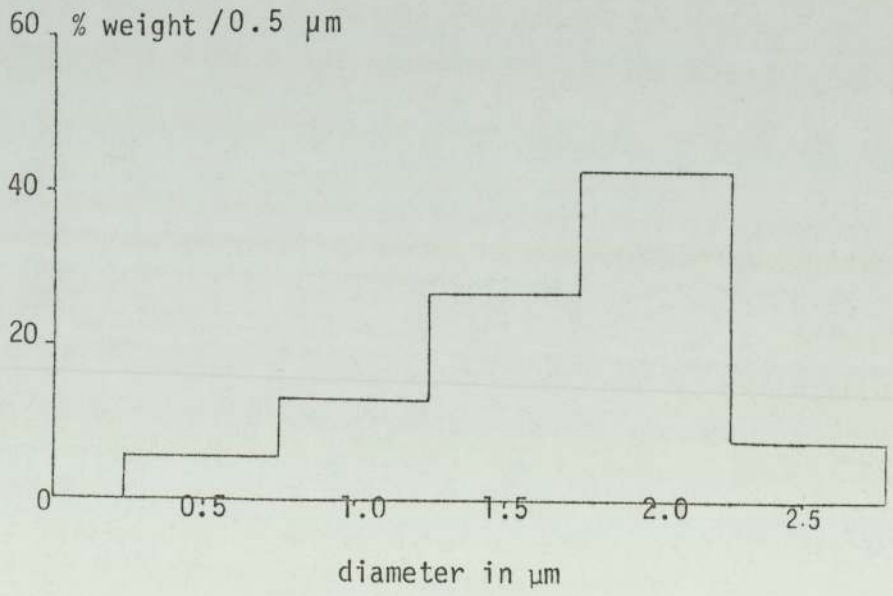

G.4.2. Size distribution of Tungsten type (ii)

CHAPTER 5

THE HYDROLYSIS OF UREA IN ACID SOLUTIONS

Urea hydrolyses in acidic solutions to produce ammonia and carbon dioxide. The rate of the reaction increases rapidly above 95°C (R.3.1.). Since the reaction is of a strong acid with a moderately strong alkali, the pH change of the solution can be used to follow the progress of the reaction.

5.1. Literature survey

Early work (R.5.1.) on the hydrolysis reaction suggests that the process occurs in two steps:

$$CO(NH_2)_2 \underset{K2}{\overset{K1}{\rightleftharpoons}} N H_4^+ + OCN^- \qquad \text{E.5.1.}$$

$$OCN^- + H_3O^+ \xrightarrow{K_3} NH_3 + CO_2 \qquad \text{E.5.2.}$$

It was further suggested that the reaction E.5.2. was very fast and for pH < 5 the process may be simplified to:

$$\frac{dC_u}{dt} = -K_1 C_u \qquad \text{E.5.3.}$$

The value of K_1 changes with acidity and temperature and at a given temperature (100°C) it is claimed to be constant for pH < 1.5 or pH > 5 (R.5.1.).

Table T.5.1. lists and evaluates critically the work that has been done on the subject.

Author	Year/Method used	Model suggested	Comments
Warner et al. (R.5.1.)	1942/Xanthydrol	$\frac{dC_u}{dt} = -C_u K_1$	HCl was used for the evaluation of K_1 for pH < 1.5 while Citric and Acetic for 2<pH< 5. The values obtained therefore are not comparable.(Moderate Urea concentrations 0.01M to 0.005M, 100°C).
Kucheryavyi et al. (R.5.2.)	1968/diaelectric properties of urea	as above	The value of K_1 at 100°C is found by extrapolating from lower temperatures. (High Urea concentrations up to 10M and low acidities pH~7.
Welles et al. (R.5.3.)	1971/specific conductivity	as above	as above.
Shaw et al. (R.5.4.)	1955/photoelectric calorimetry	as above	Values of K_1 were calculated for conditions comparable with the present work but were only concerned with very long intervals and thus the calculated values for K_1 refer to the tail end of the hydrolysis curves (graphs G.5.1. et seq .). (Urea concentrations 0.005 to 1.5M, pH<2).

T. 5.1. Table listing the word done on the hydrolysis of Urea

Although the methods of measuring the concentration of Urea differ considerably, the model suggested or accepted by all workers is that developed by Warner et al. (R.5.1.).

The present experimental work, which is concerned with excess Urea hydrolysing in acid solutions, is not fully explained by such a model.

5.2. Experimental work

Experiments were carried out in a 1 litre stirred vessel (described in Chapter 7, reactor 5) and the pH of the solution, measured by a pH meter, was used to follow the progress of the hydrolysis (Equations E.5.1. and E.5.2.). Solutions of various acid strength and Urea concentration were used. Tests in weak acids (Citric, Formic) were also carried out. Finally, tests in mixtures of strong and weak acids were carried out, including Barium chromate (the salt of a weak acid).

Excess of Urea ensured that its total concentration did not change in the region of the experimental measurements. (0.1.N. acid is neutralised by 0.05M Urea). The temperature was kept constant at about 100°C and the speed of the stirrer at about 550 rpm. The results obtained were found to be very reproducable. The standard conditions were chosen as:

0.3 M of Urea (20g)
0.06M of HNO_3
Temperature ~100°C
Agitation ~550 rpm
Total volume of solution 1dm.

Curve 3 of graph G.5.1. represents a hydrolysis carried out starting with these standard conditions.

5.3. Analysis of the results

The hydrolysis rate of Urea and thus the rate of change of pH, (Equations E.5.1. and E.5.2.) in solutions of strong acids is different from that in weak ones. In fact, the pH time curve for the rate of hydrolysis for the first case strongly resembles a strong acid, weak base titration curve (possibly HNO_3 vs. NH_4^+) and the results are in graphs G.5.1. and G.5.2. For the second case, graphs G.5.5. to G.5.7. show the effect of a weak acid on the hydrolysis rate of Urea. It is worth noting however, that the pH does not move to the alkali region but tends to level out at pH 6. Because of the marked differences between the two cases the results are analysed in two parts.

5.3.1. Hydrolysis in strong acid

The curves in graphs G.5.1. and G.5.2. represent the hydrolysis of Urea in HNO_3 solutions. The different initial pH (graph G.5.1.) is attributed to the Urea which is a weak base, while the levelling of the pH curves is due to the hydrolysis rate becoming negligible and possibly the formation of NH_4NO_3 which is a salt of strong acid.

The model suggested by Warner et al. (R.5.1.) produces equation E.5.3. which when integrated gives:

$$\ln \frac{Cu}{Co} = -K_1 t \qquad \text{E.5.4.}$$

where Co is the initial concentration of Urea.

In graph G.5.3. this model is tested by plotting $\ln \frac{Cu}{Co}$ versus t. The data are obtained from graph G.5.1. curves 1 to 5 pH=2. However for pH>2.5 the curves (graphs G.5.1. and G.5.2.) adopt the same "shape" and thus the model fails.

In graph G.5.4. an alternative model is examined for the hydrolysis of Urea in strong acids. Equation E.5.3. is rewritten as:

$$\ln \frac{dCu}{dt} = -\ln K_1 + n_U \ln Cu \qquad E.5.5.$$

and $\ln \frac{dCu}{dt}$ is plotted versus lnCu. The slope of the straight line is n_U .Curves 1 to 5 from graph G.5.1. are used again for pH=2.5.

Graph G.5.4. produces an almost horizontal line and thus $n_U \sim 0$. The model will be examined in the subsequent sections.

5.3.2. Hydrolysis in weak acids and also in mixtures of strong and weak acids

Graph G.5.5. presents the hydrolysis of Urea in a mixture of Formic and Nitric acid and Barium chromate ($2X10^{-2}$ mole/dm^3).

Graph G.5.6. presents the hydrolysis of Urea in a mixture of Formic and Nitric acids only. Graph G.5.7. presents the hydrolysis of Urea in Citric acid only. The concentrations of the Citric acid were particularly important. Warner et al (R.5.1.) used 0.25 M Citric acid to test the suggested model.

G.5.1. Hydrolysis of Urea in acid solution

Curve of PH of the solution as a Function of time showing the effect of the initial Urea concentration

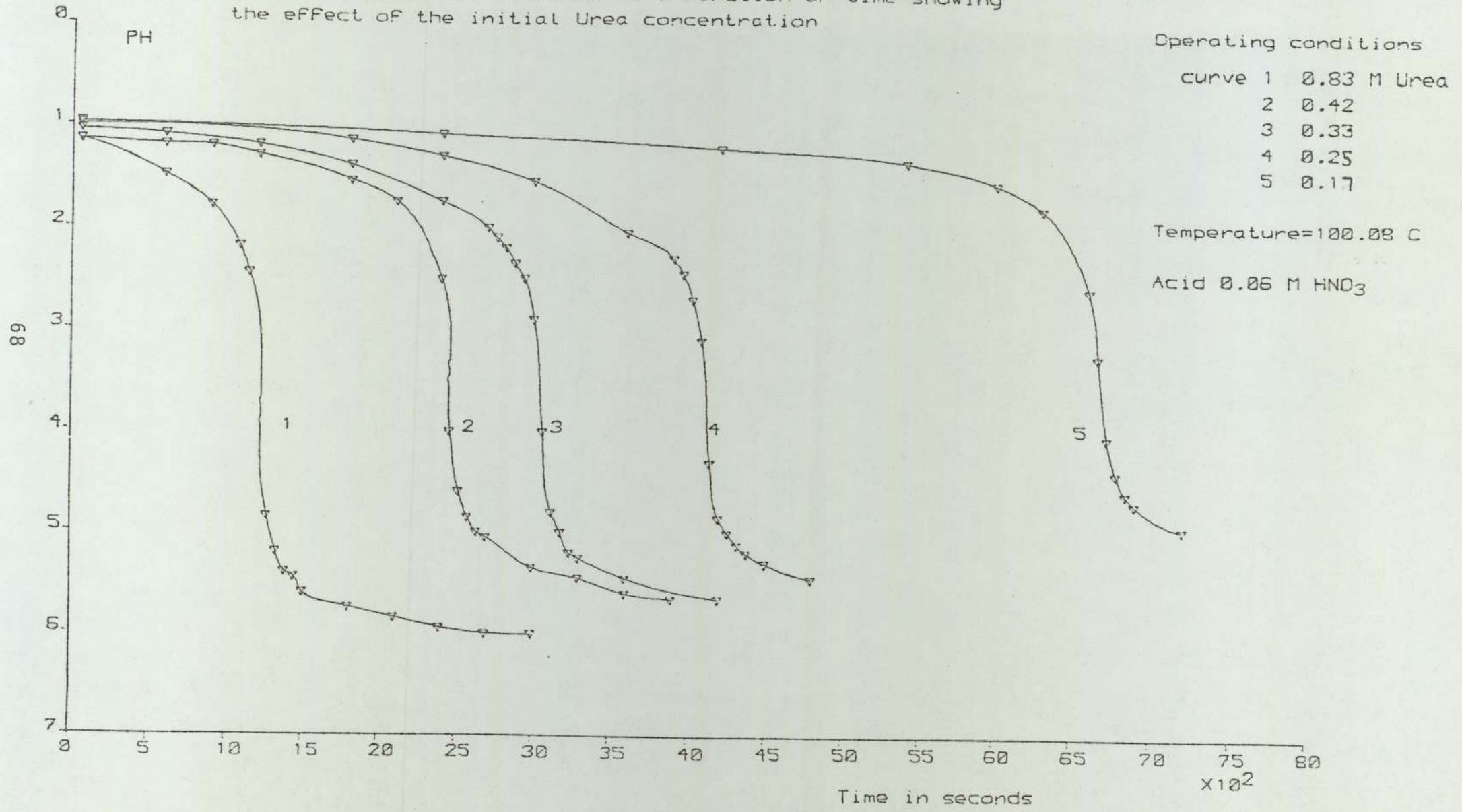

Operating conditions

curve 1 0.83 M Urea
2 0.42
3 0.33
4 0.25
5 0.17

Temperature=100.08 C

Acid 0.06 M HNO_3

G.5.2. Hydrolysis of Urea in acid solution
Curve of PH of the solution as a function of time showing the effect of the initial Acid concentration

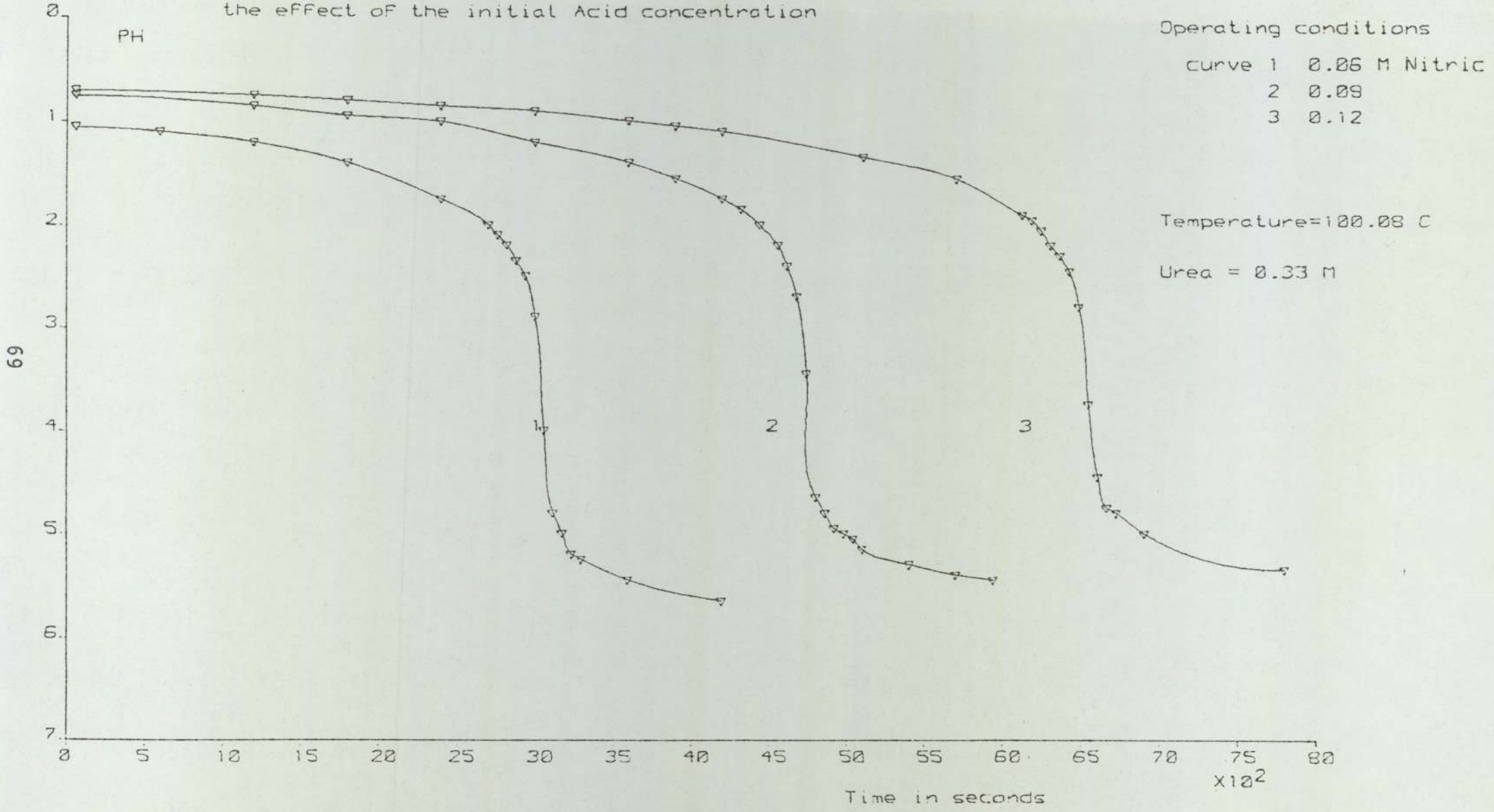

G.5.3. Plot of $\ln Cu/_{Co}$ versus time according to the Warner (R.5.1.) model

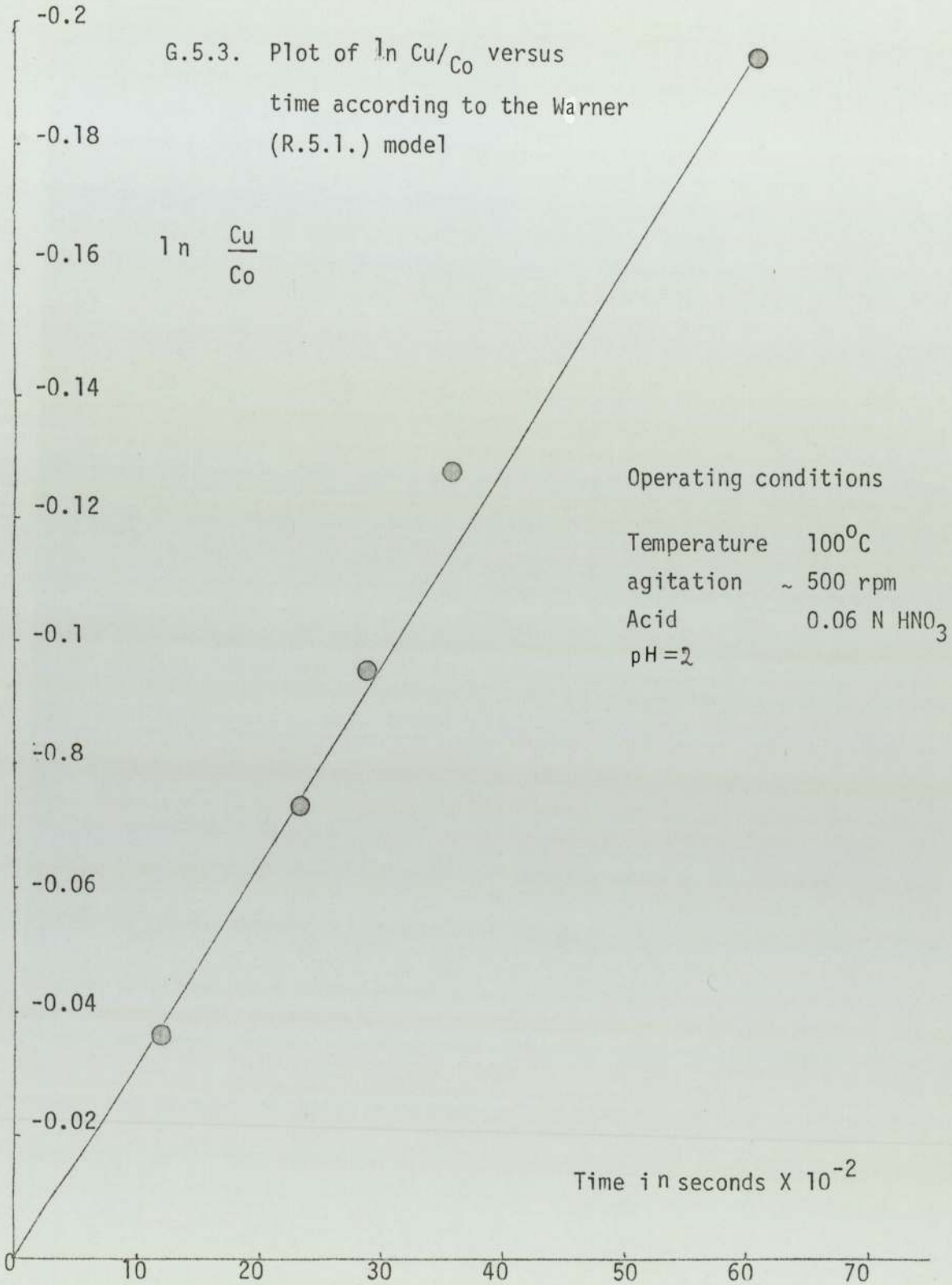

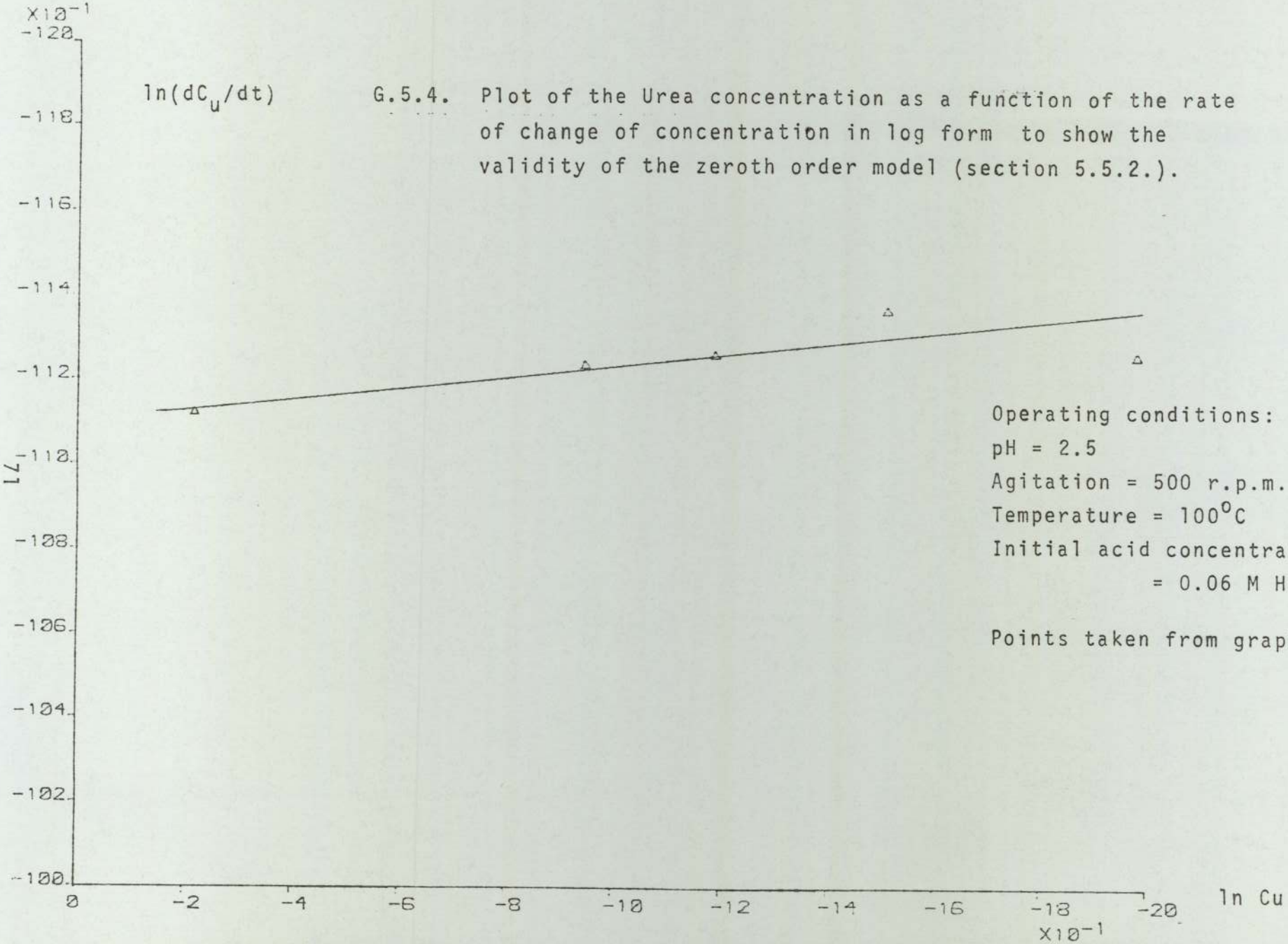

G.5.4. Plot of the Urea concentration as a function of the rate of change of concentration in log form to show the validity of the zeroth order model (section 5.5.2.).

Operating conditions:
pH = 2.5
Agitation = 500 r.p.m.
Temperature = 100°C
Initial acid concentration
= 0.06 M HNO_3.

Points taken from graph G.5.1.

G.5.5. Hydrolysis of Urea in acid solution

Curve of PH of the solution as a function of time showing the effect of the initial Acid concentration

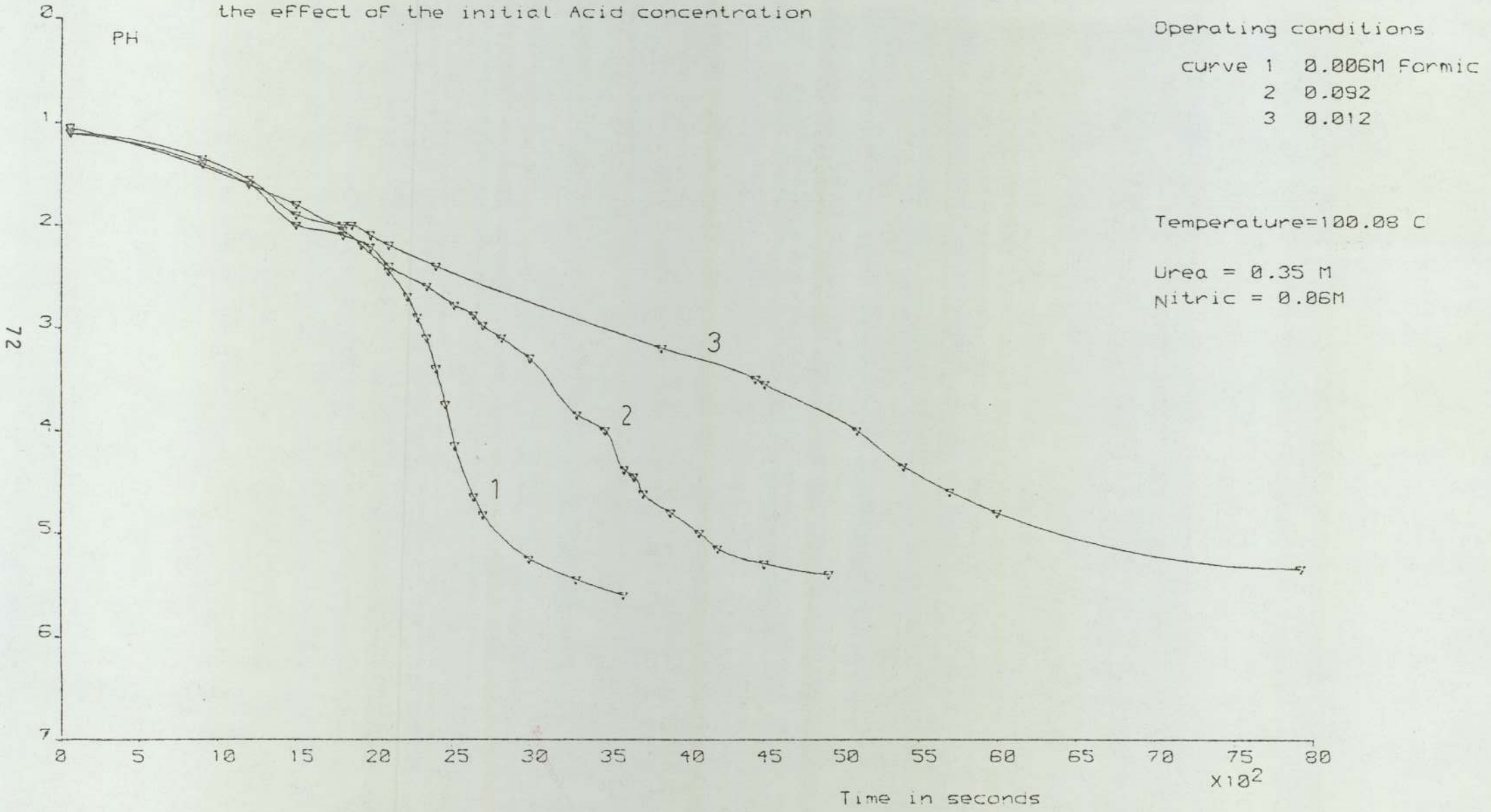

G.5.6. Hydrolysis of Urea in acid solution

Curve of PH of the solution as a function of time showing the effect of the initial Acid concentration

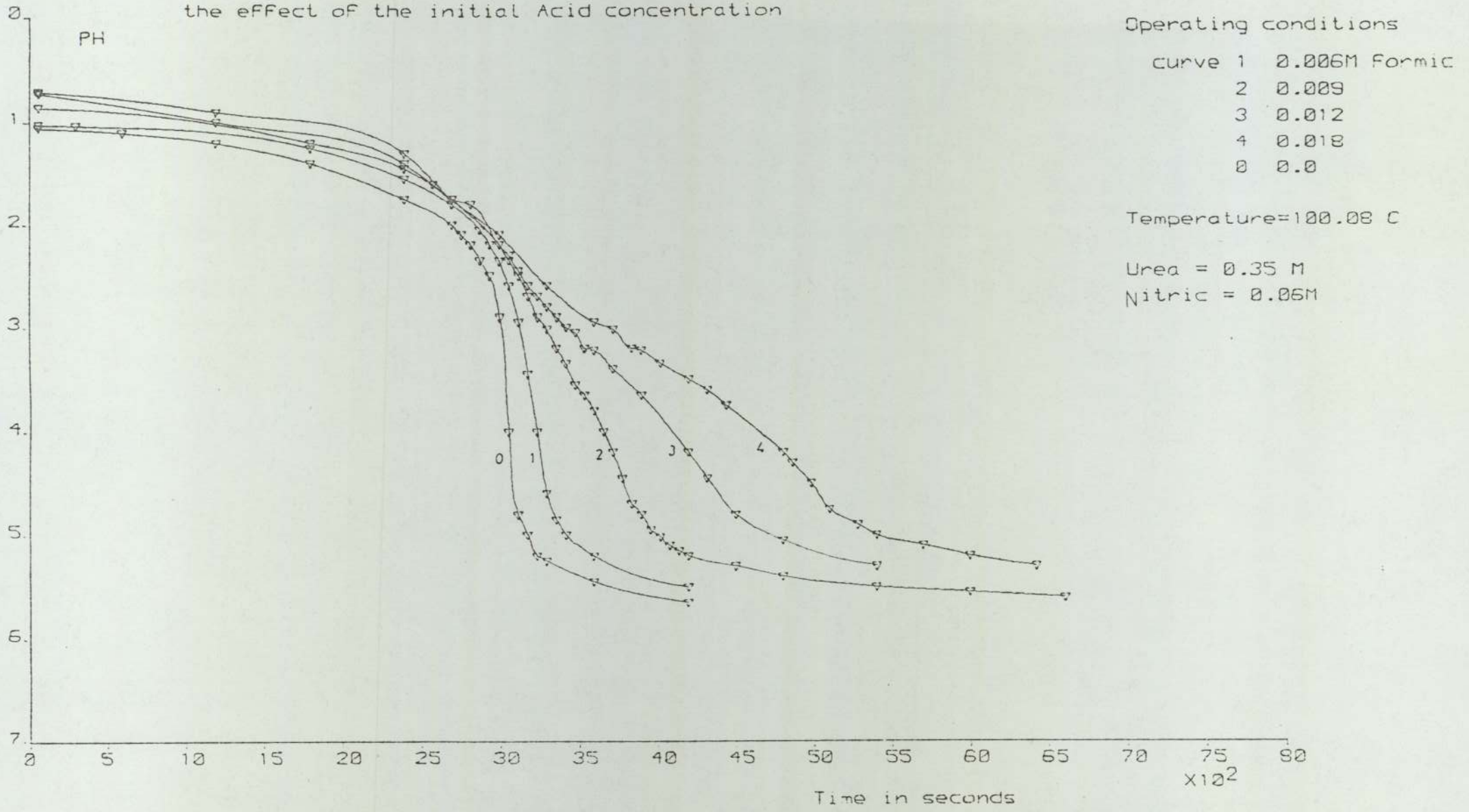

Operating conditions

curve 1 0.006M Formic
2 0.009
3 0.012
4 0.018
0 0.0

Temperature=100.08 C

Urea = 0.35 M
Nitric = 0.06M

G.5.7. Hydrolysis of Urea in acid solution
Curve of PH of the solution as a function of time showing the effect of the initial Acid concentration

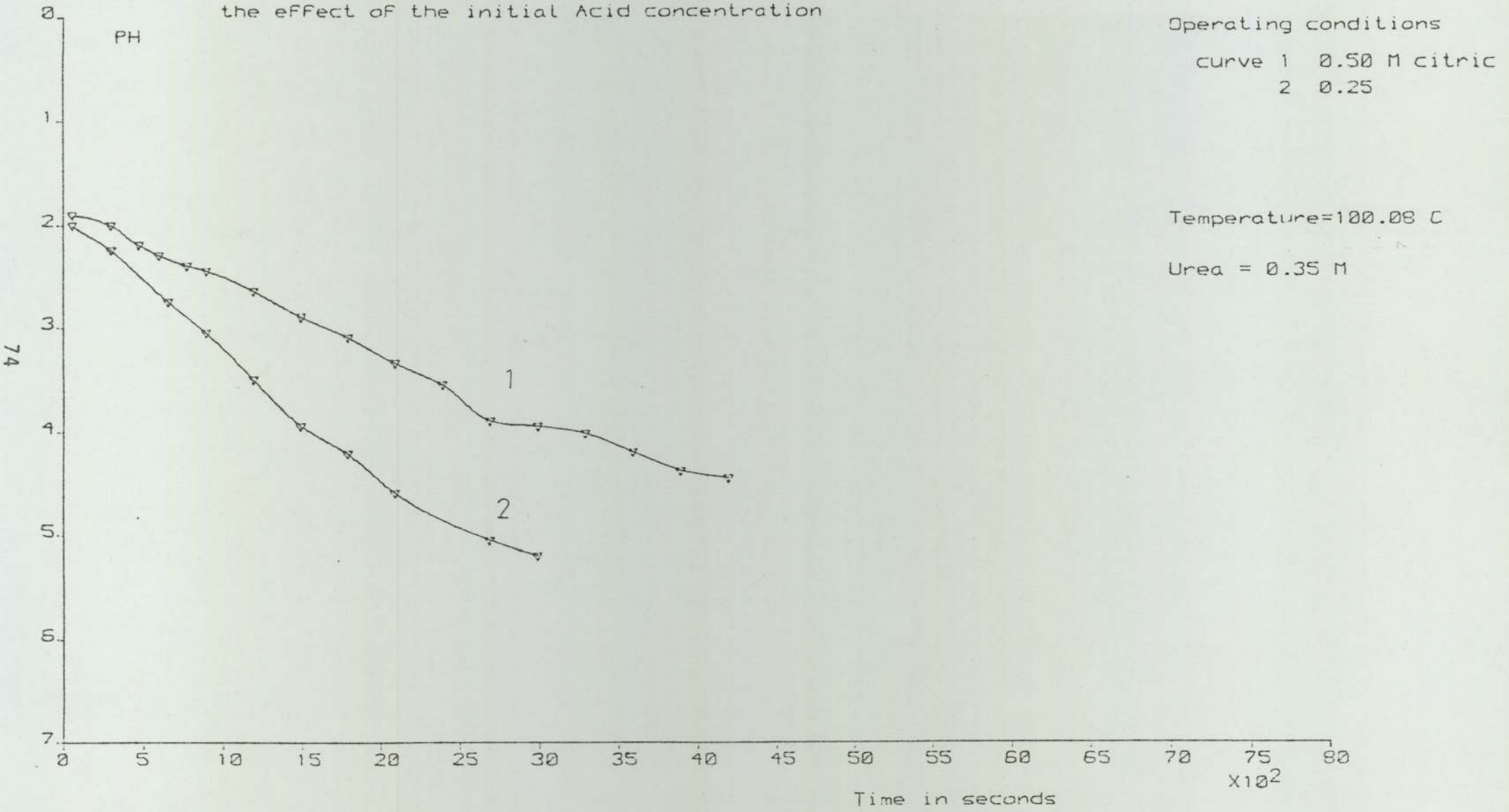

However, a weak acid whenever present tends to buffer the acidity of the solution and thus the pH change measured cannot be directly related to the consumption of Urea.

5.4. Critical evaluation of the model

The model suggested by Warner et al (R.5.1.) is applicable for the region pH <2 but it fails for pH>2.5, since the slope of the curves 1 to 5 and 1 to 3 in graphs G.5.1. and G.5.2. are constant for a given pH greater than 2.5.It therefore appears that at this region the hydrolysis becomes independent of the Urea concentration.

5.5. Alternative models

Many alternative models have been considered to describe the behaviour of the hydrolysis of Urea in strong solutions. Of these, the "active Urea concentration" and the "zeroth order" ones are described below.

5.5.1. The active Urea concentration model

By this model equation E.5.3. is modified to the form described by:

$$\frac{dCu}{dt} = K_1 \, Cu^* \qquad \text{E.5.6.}$$

where

Cu, t, and K_1 are defined as before and,

Cu* is the concentration of Urea available for hydrolysis.

The model implies that not all the Urea is available for hydrolysis, but part of it stored in an equilibrium form.

A possible equilibrium suggested is:

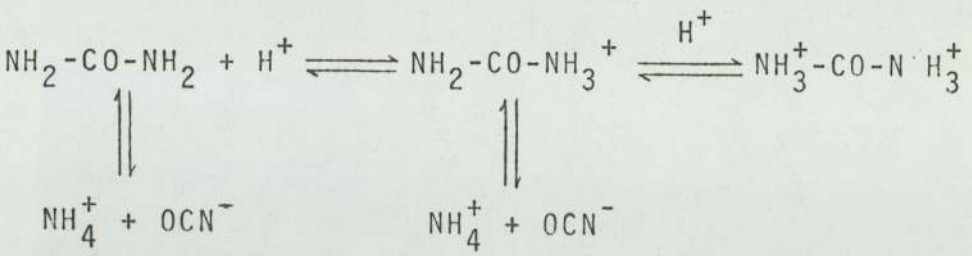

The value of Cu* is therefore (possibly) dependent on the pH of the solution, the total Urea concentration and the temperature.

5.5.2. The zeroth order model

According to the model the rate of hydrolysis of Urea is independent of the Urea concentration and only a function of the pH. To examine the validity of such a model equation E.5.3. is rewritten as:

$$\frac{dCu}{dt} = -K_{m_1} Cu^{m_1} \qquad \text{E.5.7.}$$

where m is the order of the reaction.

In graph G.5.4. $\ln(\frac{d\ Cu}{dt})$ is plotted versus ln Cu and the value of K_{m_1} and m are estimated to be :

$$K_{m_1} = -1.5 \times 10^{-5} \pm 0.8 \times 10^{-5}$$

$$m_1 = 0.12 \pm 0.07$$

for pH = 2.5 .

The minus sign of the K_{m_1} is an indication of the "destruction" of Urea, in accordance with equation E.5.3. Because the value of m_1 is very small equation E.5.7. can be rewritten as

$$\frac{dCu}{dt} = -K_m \qquad \text{E.5.8.}$$

valid for any given pH >2.5.

5.6. Conclusions on the hydrolysis of Urea

Table T.5.1. compares the values of the constant K_1 computed from this work with those evaluated by Warner et al. (R.5.1.) and it can be seen that as the concentration of the weak acids increases the value of K_1 decreases, while the concentration of the strong acid as indicated by the pH value had the opposite effect, unlike Warner et al. (R.5.1.) who suggest that the K_1 value is constant for pH>1.5.

pH	$K_1 \times 10^5$ sec^{-1}								
	Warner (R.5.1.)	Present work							
		HNO_3	Citric		Formic/Nitric/$BaCrO_4$		Formic/Nitric		Nitric/$BaCrO_4$
		0.06 M	0.25	0.5	0.06/0.06/0.02	0.12/0.06/0.02	0.06/0.06	0.18/0.06	0.06/0.02
1.0	4.2	4.5							
1.5	3.5	3.6							
2.0	3.5		9	5	4.1	1.3	5.7	4.3	4.5
2.5	3.5		2.5	2	2.1	0.53	5.3	1.7	1.2
3.0	3.5		1.5	0.9	1.1	0.2	2.5	0.4	0.08

T. 5.2. Comparison of K_1 values with those evaluated by Warner (R.5.1.)

CHAPTER 6

RESULTS

6.1. The results obtained for the crystallisation of Barium Chromate

In the previous chapters, the various theories of crystal growth were considered as well as the other factors concerning the process of crystallisation in general and of Barium chromate in particular. The solubility of Barium chromate in acid solutions was examined and certain assumptions were made which would simplify the calculations and thus improve the accuracy of the driving force calculation . The hydrolysis of Urea, the pivot of of the pH change, was studied under a number of conditions. The nature and behaviour of the Tungsten powder in acidic environment was also considered, since any conclusions on the crystal growth of Barium chromate should be seen in the context of the epitaxial coating of the metal particles. The experimental data obtained are presented in this chapter in graphical form because of their bulk. The conclusions however are explicitly presented and explained. These conclusions are used to formulate the controlling parameters and to consider an alternative growth rate model.. The epitaxial coating of the metal particles is considered also.

The parameters which were investigated were:

(i) agitation ,

(ii) initial Barium chromate/acid concentration ,

(iii) the presence of weak acids ,

(iv) annealing time ,

(v) the initial Urea concentration and

(vi) the presence of baffles in the crystalliser.

These results were obtained by both the "freezing" and the "sampling" methods (Chapter 7).

The epitaxial growth of Barium Chromate on Tungsten particles was also studied (the tables of the results are included in Appendix A.6.)(p 200).

The standard conditions were taken as:

Agitation = 800 rpm

Initial Barium Chromate concentration = 5 g /dm^3 ($\sim 2 \times 10^{-2}$ M)

Initial Urea concentration = 20g /dm^3 (0.33 M)

Initial Acid concentration = 0.06M HCl

Temperature $100^{o}C$ (373 K)

1dm^3 solution (spherical crystalliser without baffles)

Zero time is taken as the beginning of nucleation for the crystallisation process under the standard conditions.

The following definition of symbols is used:

L_i = the characteristic length of a particle, equal to the radius of an equivalent sphere of the same mass.(volume diameter /2)

t = time of crystallisation (s)

R = agitation (rpm)

pH = the final pH of the solution.

wt = weight of the crystals formed (g)

L, $\bar{L}$, Lj mean value of L_{ij} (mass basis)

σ^2 = variance

sk = skewness

N = total population in the crystalliser (of crystals).

6.2. Distribution of samples

As it was stated earlier, (Chapter 2), the size distribution of the crystals on both a number and a mass basis, can indicate whether secondary nucleation(or attrition)occurs. From the Coulter¬Counter (Appendix 1) such a distribution can be obtained, while the Andreasen sedimentometer(Appendix 2) can be used to evaluate the shape factor of the crystals when used in conjunction with the Coulter data.

6.2.1. Result obtained by the Coulter-Counter

All the samples obtained were analysed by the Coulter-Counter. The results were then fed into programme EF17 (Appendix 4) which drew the distribution histograms and calculated the mass mean, the mode, the variance and the skewness, all on a mass basis. The correction factor, which adjusts the results to give a mass balance P_{cj} (Appendix 1) was also calculated. Output OUT.G.1. is a typical one for Barium chromate crystals. Graph G.6.1. represents these data graphically. In the first part (G.6.1.a.) of the graph the population is plotted against size both before and after the correction by P_{cj} (Appendix 1.). In the G.6.1.b. the mass fraction is plotted against size and in G6.1.c. the cumulative weight is plotted against size (the Andreasen sedimentation results are also included).

6.2.2. Results obtained from the Andreasen sedimentometer

The results obtained by the Andreasen sedimentometer were used to evaluate the shape factor of the crystals as well as to check whether the two methods produced similar

answers. However, the apparatus proved unsuitable for the upper range of the distribution (L_i >20μm) possibly because the particles were too heavy, even when viscous solutions of Water and Glycerol were used (Appendix 2). The apparatus also proved insensitive for the lower range of the distribution (L_i< 10 μm) possibly because of the small masses involved. For the region around the mass mean however (10 < L_i< 20 μm) the reproducibility was found to be within ± 1.5 μm and thus a statistical comparison with the mean value obtained from the Coulter-Counter was possible (graph G.6.1.c).

6.2.3. Discussion on the distributions obtained

In graphs G.6.2. and G.6.3. a selection of the distributions obtained are presented, chosen to cover the time range. In them the mass fraction is plotted against diameter ($2L_i$). These distributions refer to results obtained by the "freezing" method. Similar distributions were obtained also by the "sampling" method. The histograms presented in graphs G.6.2. and G.6.3. are not representative but rather a selection of all types of distributions encountered. It should be noted however that the number of crystals increases from 1 to 5 X 10^7(dm^{-3}), from 0-300s (for the standard conditions).

Both methods, the "sampling" and the "freezing" produced similar results (graphs G.6.5. and G.6.6.) although the former method gave poor mass balances. A possible

explanation to this is a separating effect occurring in the sampling probe. The choice of the mass mean (Section 6.3.) as the parameter which would describe the process appears not to be very critical since for small times ($t < 300$ s) the mass mean and number mean are very close together ($\sim \pm 2$ μm). For higher times (> 300 s), although the difference becomes more significant, the driving force is not accurately known and thus no overall growth correlation can be usefully attempted in this region.

As seen below, the sphericity of the crystals as calculated by $(La/_{Lc})^2$ (Appendix 2) appears to be somewhat high; but the agreement with the value calculated from the crystal shape is reasonable when considering the error in the Andreasen diameter to be ± 3μm.

For the tests shown in graph G.6.1.c.

Mass mean obtained by the Coulter-Counter, $2L_c = 37.66$ μm.

Mass mean obtained by the Andreasen sedimentometer, $2La = 35 + 3$ μm (from graph G.6.1.c.).

From Appendix 2, sphericity = $(\frac{La}{Lc})^2 = 0.86 \pm 0.08$ μm

Theoretical sphericity of a {III} crystal is 0.813 evaluated from the dimensions given in Chapter 3, the crystal habit being shown in figure D.1.3..

G.6.1. Graph presenting the population and mass distributions obtained by the Coulter-Counter analysis

a)

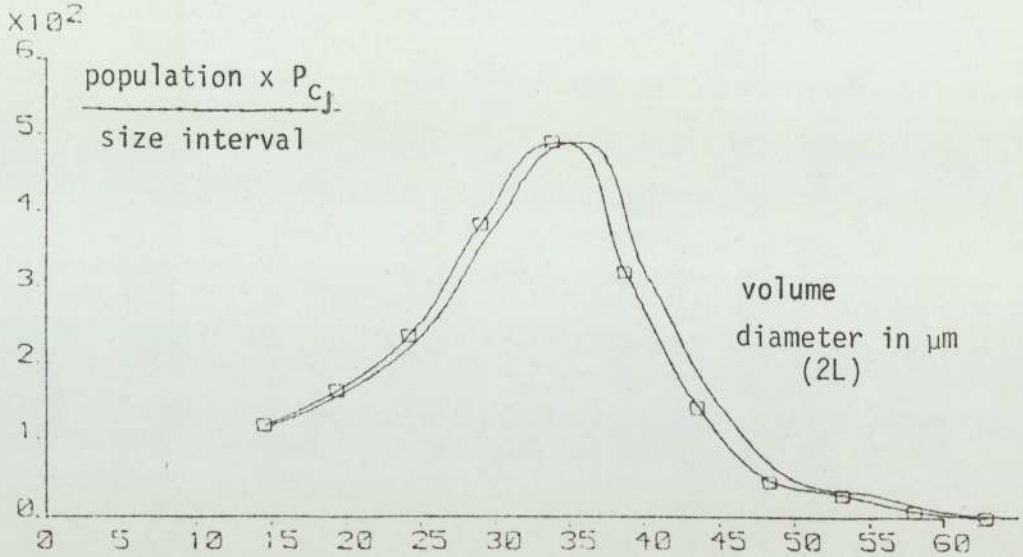

b)

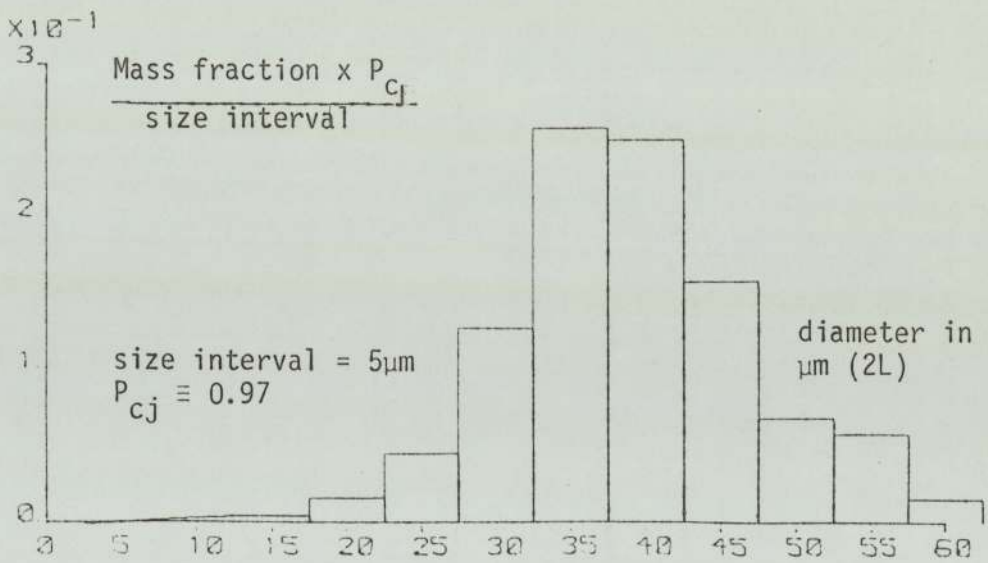

c)

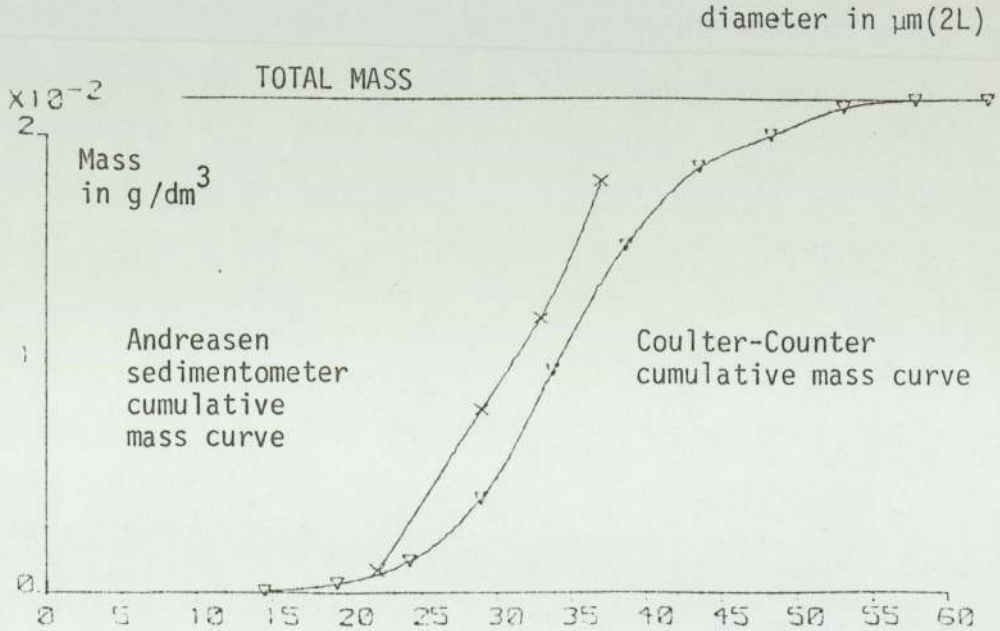

OUTPUT OUT.6.1. FIRST INTERATION

Sample number 4th June 1979 B

VALUES OF N		AVERAGE	DIFFERENCE	MASS	MASSFR	DIAMETER
1900.00	1903.00	1927.70				
			113.6	0.0001	0.005	15.00
1777.00	1792.00	1809.09				
			164.2	0.0004	0.016	20.00
1606.00	1639.00	1644.80				
			234.7	0.0011	0.045	25.00
1397.00	1385.00	1410.17				
			382.2	0.0030	0.127	30.00
1018.00	1010.00	1027.97				
			490.7	0.0062	0.258	35.00
536.00	524.00	537.30				
			318.8	0.0060	0.251	40.00
216.00	215.00	218.47				
			140.5	0.0035	0.157	45.00
76.00	80.00	78.00				
			44.0	0.0016	0.068	50.00
37.00	31.00	34.00				
			28.0	0.0014	0.057	55.00
5.00	7.00	6.00				
			6.0	0.0004	0.016	60.00
0.00	0.00	0.00				
			0.0	0.0000	0.000	65.00

NUMBER IS 1

TOTAL MASS IS 0.0239 GRAMMES

THE MASS MEAN DIAMETER IS 38.96 MICRON

INITIAL WEIGHT IS 0.0216

PEJ IS 1.00

VARIANCE IS 6.7652

SKEWNESS IS -1.5215

G.6.2. Graph presenting a selection of crystal distributions at selected times obtained by the "freezing" method.

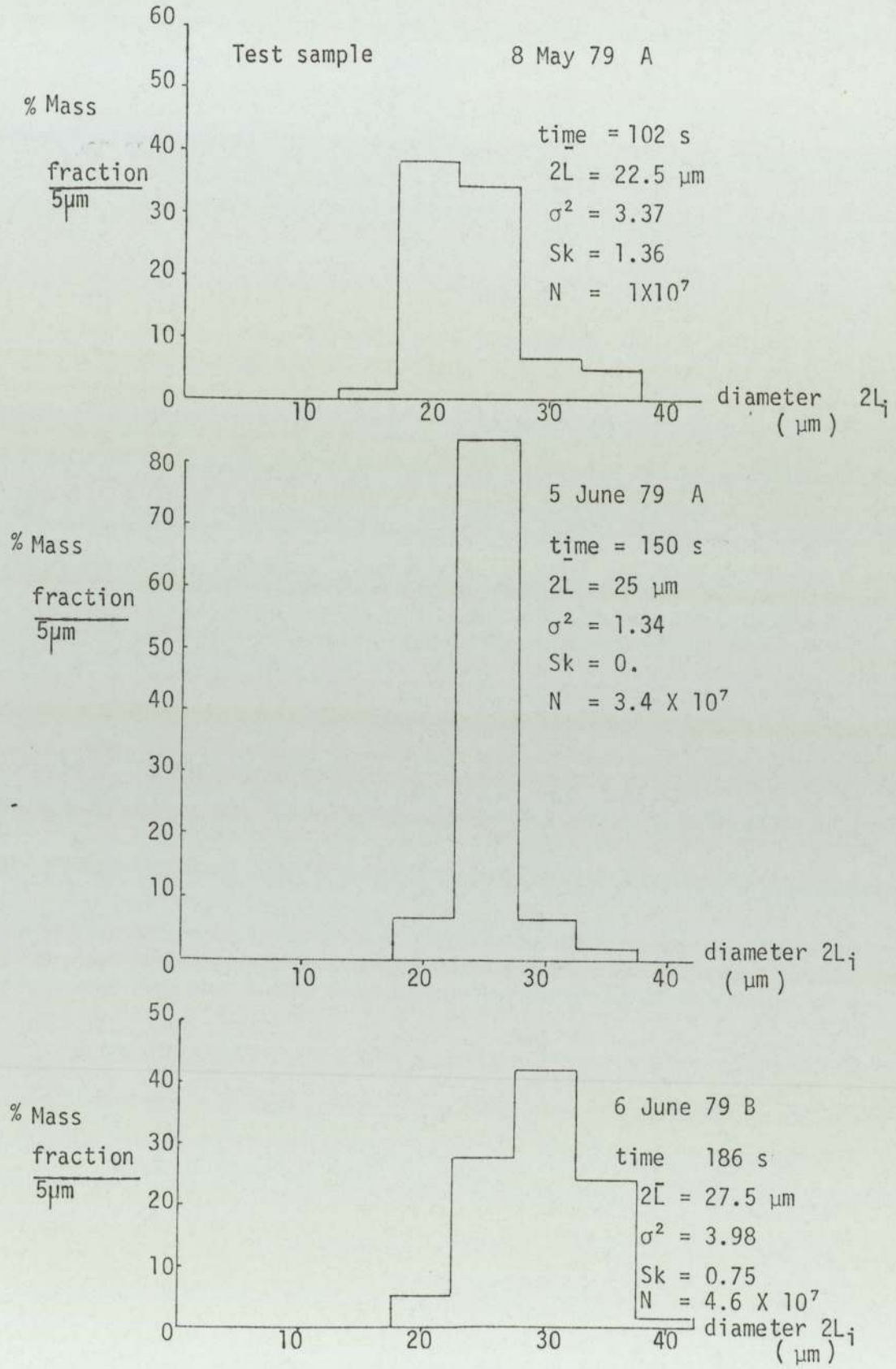

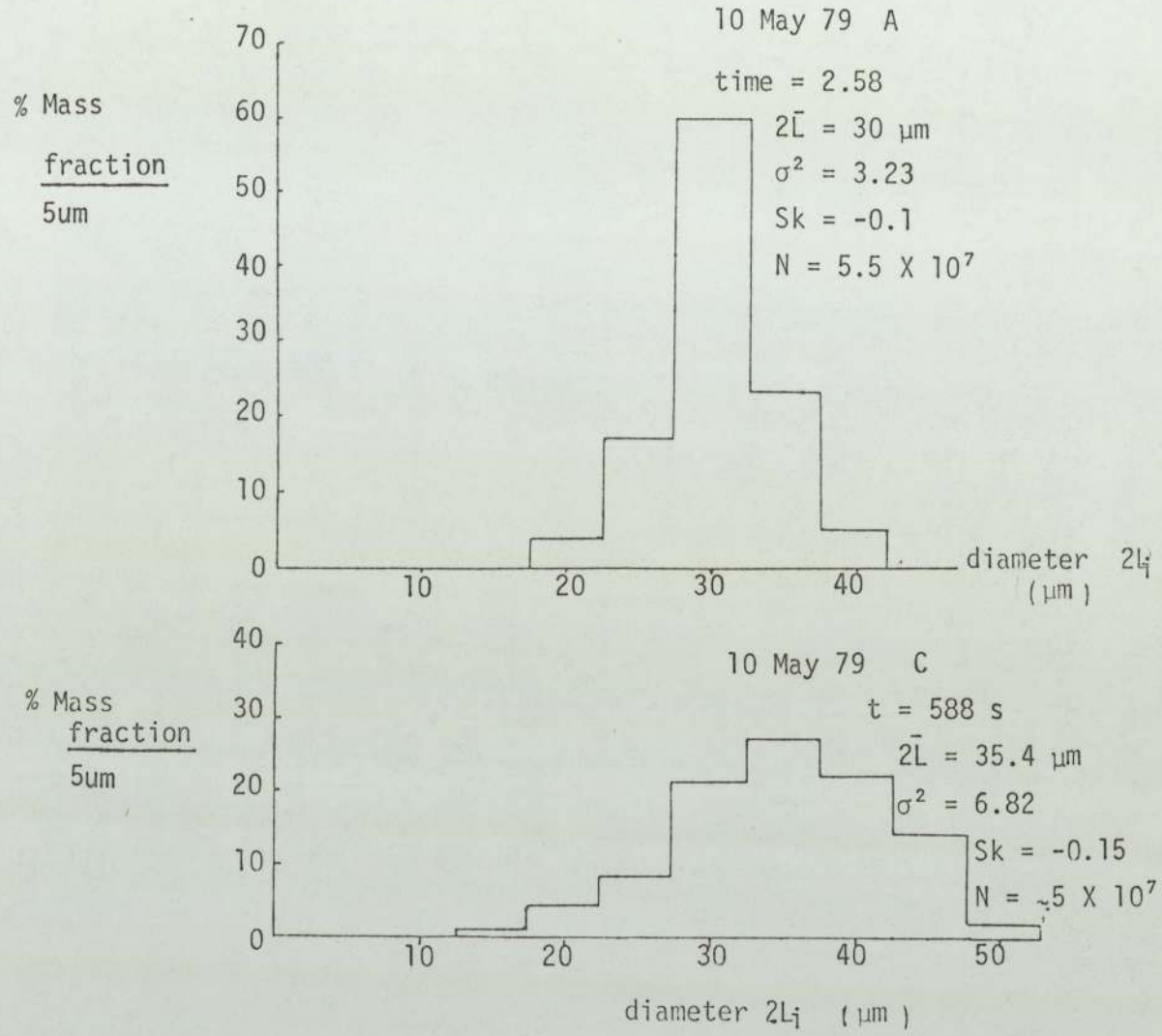

G.6.3. Graph presenting a selection of crystal distributions at selected times obtained by the "freezing" method.

6.3. Crystal growth

As described previously (Chapter 2) the mass transfer rate equation can be written in the form:

$$\frac{dL}{dt} = Kg\left(\frac{C-C_s}{C_s}\right)^n \qquad \text{E.6.1.}$$

where

Kg is the growth constant in μm/s

(Kg is not a true constant, but a function of the other controlling parameters, agitation, pH etc.).

$\frac{dL}{dt}$ is the linear growth rate of the mass mean size (μm/s)

The length mean and the area mean (Chapter 2) are often used as the parameters to characterise a distribution.

Equation E.6.1. can be rewritten empirically as:

$$\frac{dL}{dt} = K\ L^a\ pH^b\ R^f\left(\frac{C-C_s}{C_s}\right)^n \qquad \text{E.6.2.}$$

where

K is the new constant and

L is the mean characteristic radius

In order to evaluate a, b, f and n, equation E.6.2. is rewritten as

$$\log_{10}\left(\frac{dL}{dt}\right) = \log_{10}K + a\log_{10}L + b\log_{10}pH + f\log_{10}R + n\log_{10}\left(\frac{C-C_s}{C_s}\right) \qquad \text{E.6.3.}$$

which is an equation of the form:

$$Y = A_1 + A_2X_1 + A_3X_2 + \ldots\ldots\ldots + A_nX_{n-1} \qquad \text{E.6.4.}$$

By applying the least squares method for the values of Y vs. X's the coefficients A_1 to A_n can be evaluated.

6.3.1. Linear growth rate as a function of time

The term $\frac{dL}{dt}$ in equation E.6.2. represents the linear growth of a mean size particle with time. On graphs G.6.6. and G.6.5. the mass mean characteristic length (L, μm) is plotted vs. time in the slope of the curves at any given time is the term $\frac{dL}{dt}$. To aid computation a curve is fitted, using the least squares method to each set of data, of the form:

$$\frac{L}{L_\infty} = 1 - \exp f(t\text{-}to) \qquad \text{E.6.5.}$$

where $f(t\text{-}to) = B_1 + B_2(t\text{-}to) + B_3(t\text{-}to)^2 + \ldots$ E.6.6.

L_∞ is the final mean radial size of the crystals (μm)

to is the time at which nucleation occurred(s). Zero time is taken as the nucleation of the standard conditions (section 6.3.3.1.) and therefore by definition to=0 for this case.

A three term approximation was found to be sufficient to describe the data. In table T.6.1. the B coefficients are tabulated for each curve.

Because of the relative simplicity of equation E.6.5. the differential $\frac{dL}{dt}$ can be evaluated both numerically and analytically.

Analytically $$\frac{dL}{dt} = -L_\infty f'(t - to)\exp(f(t-to)) \quad \text{E.6.7.}$$

at $t = t_j$

Numerically $$\frac{dL}{dt} = \frac{L_{j+1} - L_{j-1}}{t_{j+1} - t_{j-1}} \quad \text{E.6.8.}$$

For small increments of time ($t_{j+1} - t_j \ll 10$ seconds) the two methods yield answers to within 2%. Programme EF20 and its modified version EF21 perform both the curve fitting and the differentiation (Appendix 7, p210)

6.3.2. Evaluation of the driving force

The driving force as defined in equation E.2.3. is a function of the saturated and supersaturated concentration of the Chromate ion (CrO_4^{--}).

$$\text{driving force} \propto \frac{[CrO_4^{--}] - [CrO_4^{--}]_s}{[CrO_4^{--}]_s} \quad \text{E.6.9.}$$

's denotes supersaturation. However the driving force can also be expressed in terms of the total Cr(VI) concentration (section 3.2.4.).

$$\text{Driving force} \propto \ln\left(\frac{C^m C}{C_s{}^m C_s}\right) \quad \text{E.6.10.}$$

$$\text{Driving force} \propto (m+1)\ln\left(1+\frac{C-C_s}{C_s}\right) \approx (m+1)\left(\frac{C-C_s}{C_s}\right) \quad \text{E.6.11.}$$

Equation E.6.11. is in fact Equation E.2.3. (the proportionality constant m+1 can be absorbed in the constant of the overall growth correlation).

Therefore driving force = $\frac{C-C_s}{C_s}$ E.6.12.

At constant temperature (100°C) C_s is a function of pH and in effect of time.

C also can be expressed in terms of the independent variable (t) (section 6.3.2.1.).

6.3.2.1. Evaluation of the supersaturation curve (operating line)

Although, as it was stated earlier (Chapter 2) the supersolubility region has no distinct boundaries, a curve can be drawn, because of the high reproducibility of the process, which would describe the path taken for a given set of initial conditions. The operating line was estimated by measuring the weight of the crystals produced at given times.

Amount held in solution =(Initial weight)-(weight of crystals) E.6.13.

The weight of the crystals collected at different times is plotted versus time on graph G.6.4. (data taken from the freezing tests). It can be seen that within experimental scatter the supersaturation at a given time is independent of the agitation and thus a common operating as well as equilibrium line can be assumed. A common operating line can also be assumed for the cases of the varied initial Barium chromate concentration. (e.g. the 10g case can be seen as starting at zero time with five grammes in solution and 5 g as crystals) (section 6.3.3.i.).

The polynomial E.6.14. was fitted to the operating data,

$$pC = D_1 + D_2t + D_3t^2 + D_4t^3 \qquad E.6.14.$$

A four term approximation was found to be sufficient to describe the data. The coefficients D_n are presented in table T.6.2. and on graph G.6.7. the operating line is shown as function of time.

6.3.2.2. Evaluation of the solubility curve (equilibrium line)

The curve is drawn by measuring both the solubility of Barium chromate in HCl/Urea mixture under conditions of saturation (chapter 3) and the rate of hydrolysis of Urea in acid (chapter 5). Thus the saturated concentration C_s can be expressed in terms of the independent variable (t).

A fourth order polynomial was fitted using the least squares method of the form:

$$pC_s = D_1 + D_2t + D_3t^2 + D_4t^3 \qquad E.6.15.$$

The coefficients D_n are presented in table T.6.2. and on graph G.6.7. the equilibrium line is shown graphically.

Curve/ symbol	L_∞ (μm)	to (s)	B_1 X10·2	B_2 X10·4	B_3 X10·8	R (rpm)	Initial $BaCrO_4$ concentration (g/dm^3)
1 Δ	19.0	0	-0.972	0.132	-1.18	800	5 standard conditions
2 ∇	15.54	170	-1.82	0.522	-0.721	800	4
3 +	13.3	230	-2.88	0.871	-11.0	800	3
4 X	11.35	270	-3.82	1.42	-30.5	800	2
5 □	24.0	-280	-0.453	0.0407	0.398	800	10
6 ∇	13.9	0	-1.14	0.24	-2.73	400	5
7 +	10.54	0	-1.18	0.43	-5.45	200	5

Table T.6.1. Table presenting the coefficients of the fitted curves in graphs G.6.6. and G.6.5.

	Equilibrium line	Operating line
$D_1 \times 10^{-1}$	0.1853	0.1698
$D_2 \times 10^{3}$	0.6056	0.4045
$D_3 \times 10^{5}$	-0.1545	0.1052
$D_4 \times 10^{7}$	0.1996	0.1679

Table T.6.2. Comparing the coefficients of the polynomials used to approximate the equilibrium and operating lines.

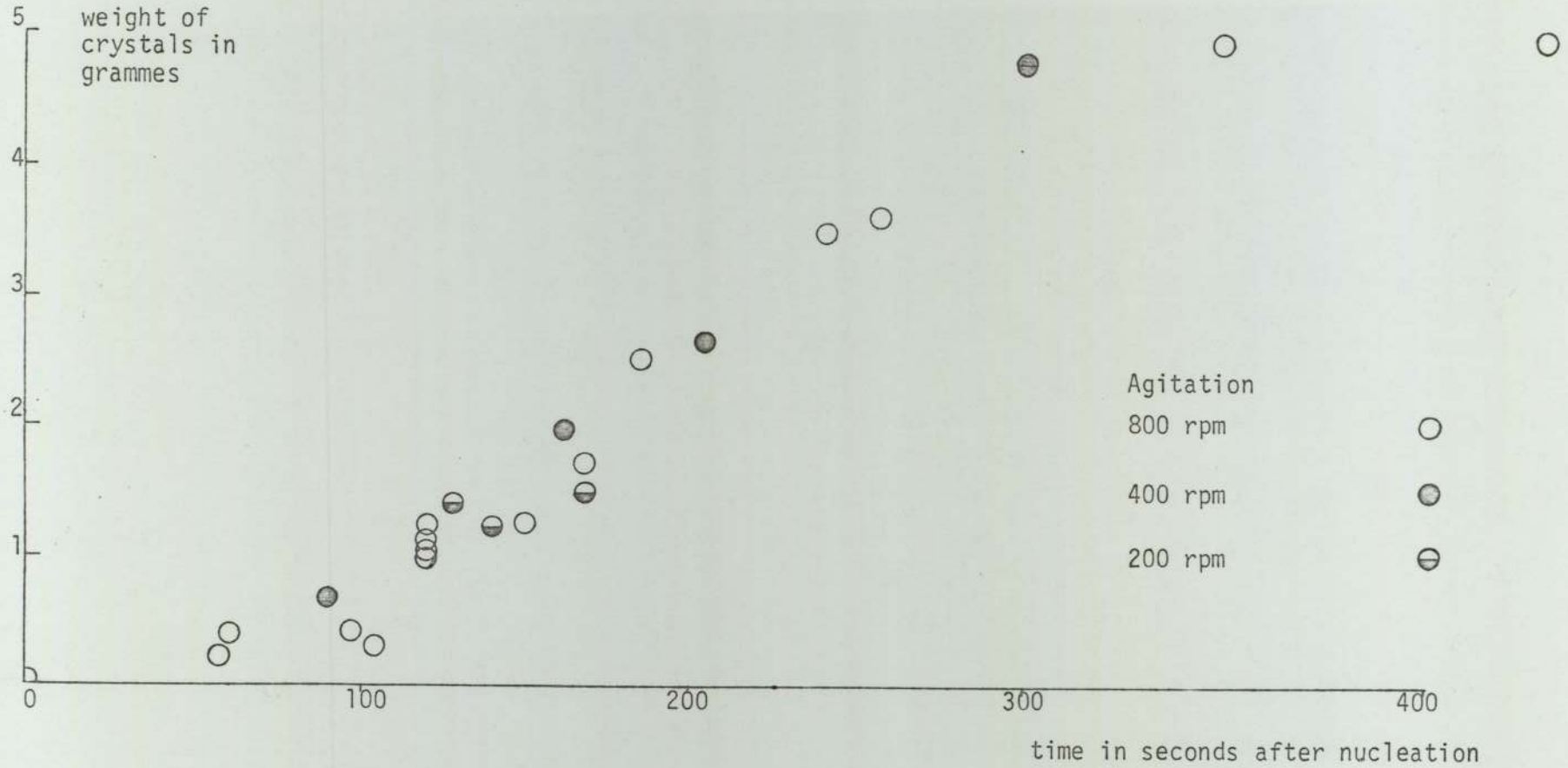

G.6.4. Weight of crystals produced by the $1\,dm^3$ batch crystalliser (No.5.) "Freezing" method
Initial weight of $BaCrO_4$ 5 g
Initial weight of Urea 20g
Initial acid strength 0.06 M HCl

Temperature = $100^{o}C$

G.6.5. Graph presenting the linear growth of the mass mean crystal size showing the effect of the initial Barium chromate concentration.

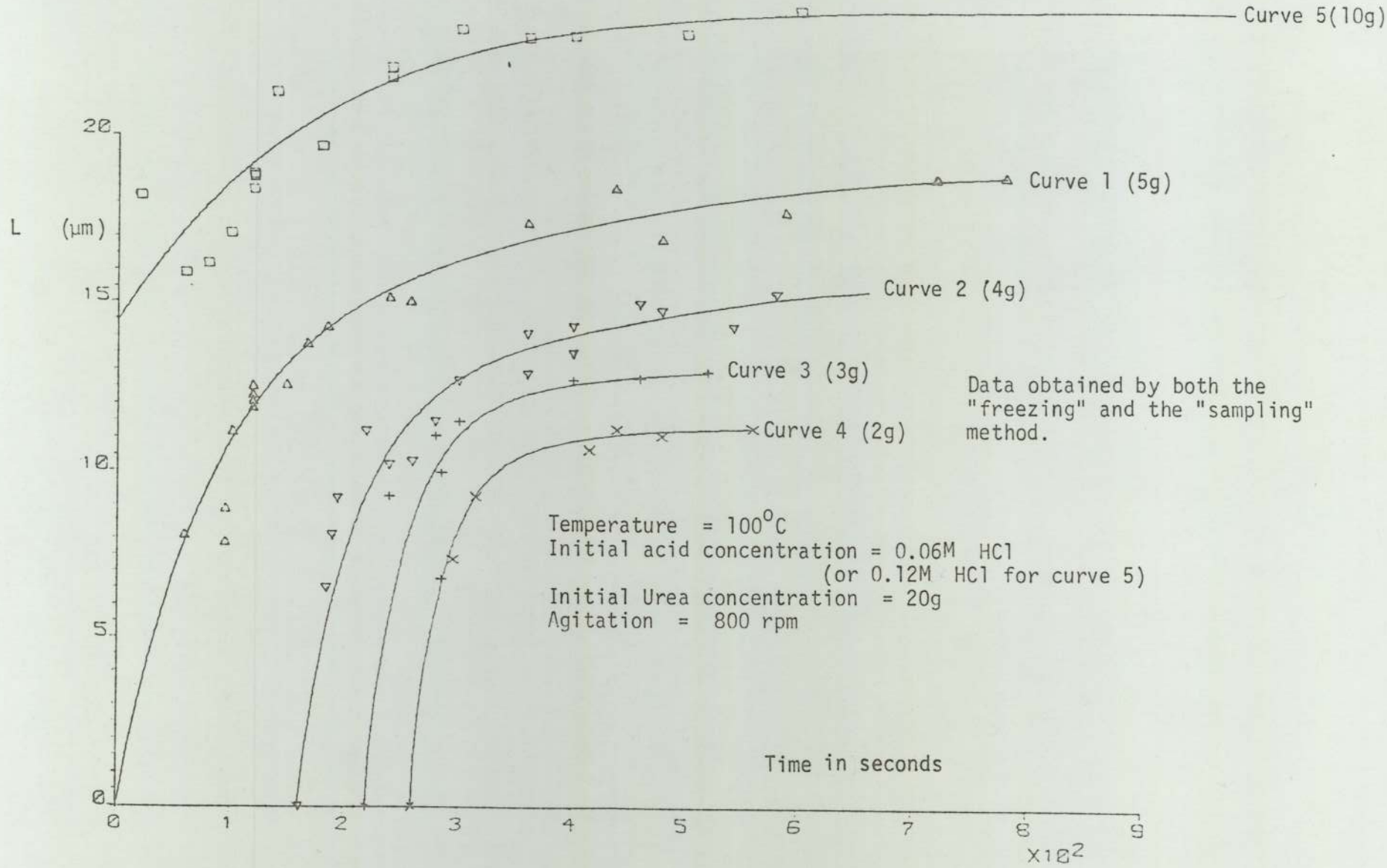

G.6. 6. Graph presenting the linear growth of the mass mean (L) with time showing the effect of agitation

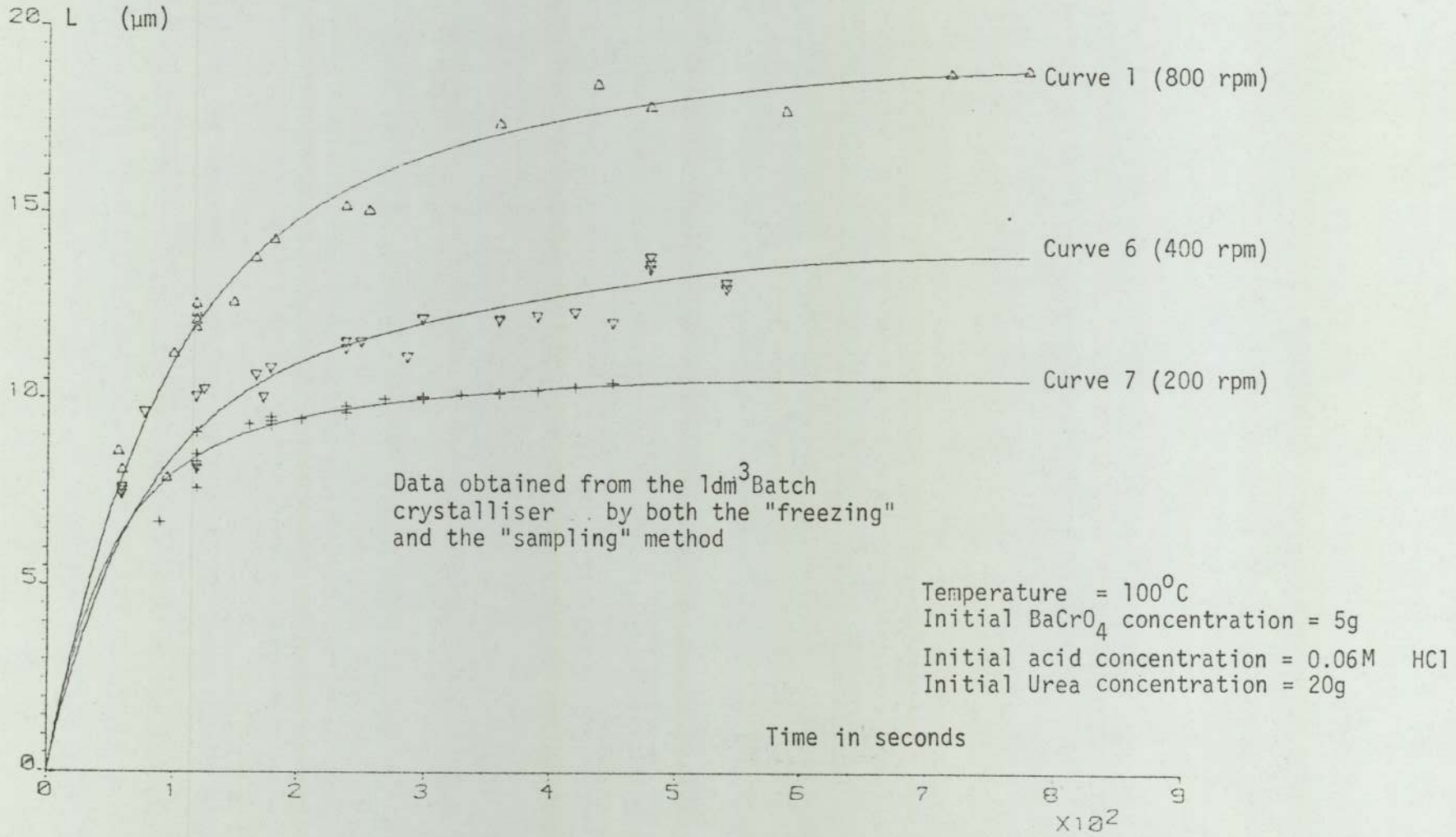

G.6.7. Graph presenting the parameters of the driving force as functions of time

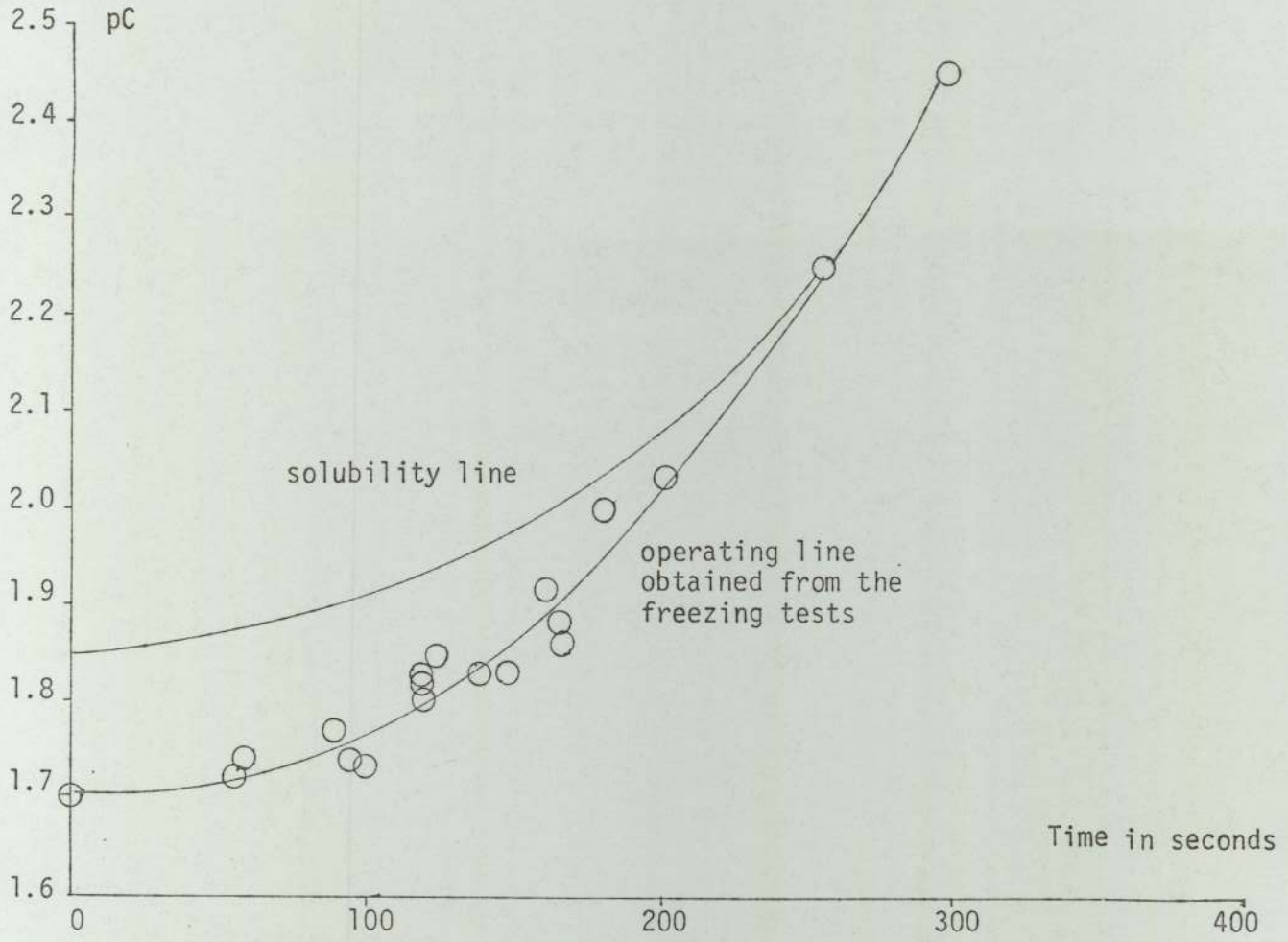

6.3.3. Treatment of data for use in an overall growth correlation

It is essential, in a correlation obtained by regression analysis, that all the independent parameters to be examined are not only equally and fairly represented but also that they are cross-related among themselves. Failure of the above conditions would lead to a "false" correlation. In order to make the available data suitable for mathematical treatment the following steps were taken:

(i) Time was chosen as the independent variable and all the other parameters (pH, L, driving force, etc.) were related to it with either an empirical or physical correlation.
These correlations gave "smoothed" relationships and so avoided the perpetuating errors due to random variations (graphs G.6.4. to G.6.7.).

(ii) Using these correlations, the values of the parameters were evaluated at specific (and equal) time intervals (20 s). Thus not only computational convenience was ensured (because of the equal intervals) but also both regions of fast and slow growth ($t<200$ s and $t>200$s respectively) were equally represented. (Graphs G.6.6. and G.6.5.). In the former region data had been determined by obtaining more values of pH, L etc. of lesser certainty (because of the rapid change with time) while in the latter, by fewer points of these parameters of greater certainty.

(iii) The driving force of the non-standard cases was expressed in terms of the standard one. The 10g case (say) was considered as a standard one starting at zero time but having 5g of seeds already in suspension. This is represented in diagram D.6.1. which assumes that the curves coincide and that a common driving force can be taken for all the cases. Experimental evidence (tables T.A6.2. and T.A6.4.)suggested that such an assumption was valid for the cases of different speeds of agitation (graph G.6.4.) as well as for the cases of varied initial Barium chromate concentration. Later it was found that this assumption was not strictly valid, the curves (as shown in diagram D.6.1.) differed slightly (within the experimental error). The 10g case differed from the standard one by about 10% (graph G.6.9.). This is possibly due to the effect of the population on the level of supersaturation and therefore on the driving force (section 6.3.5.).

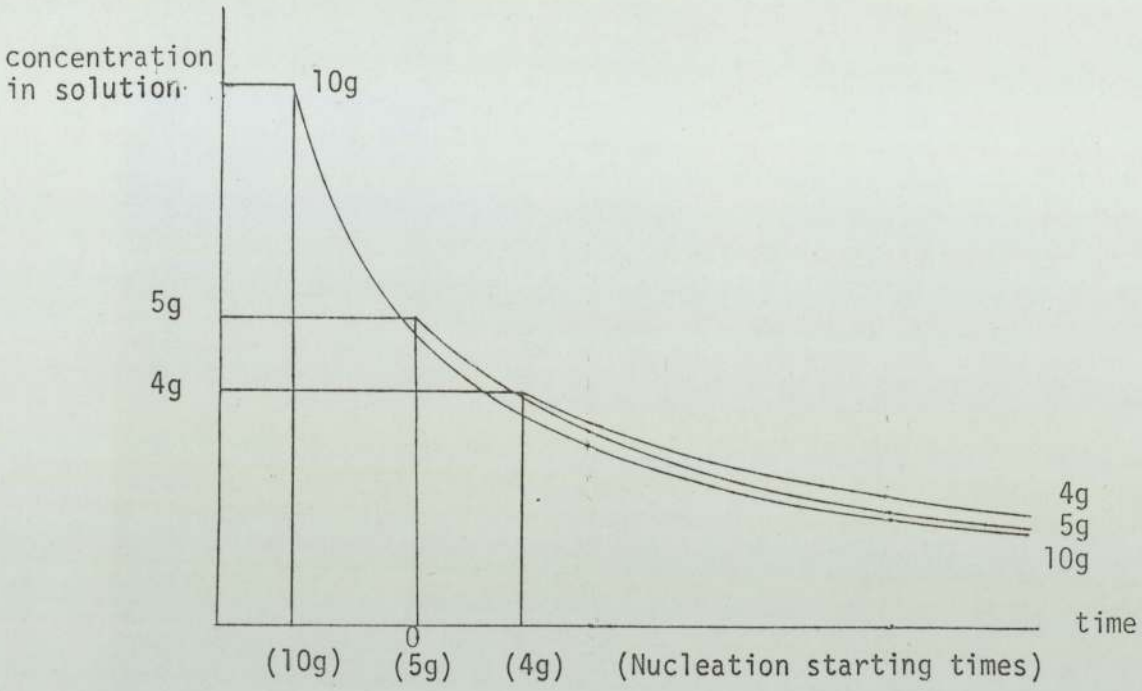

Diagram D.6.1. representing the non-standard cases expressed in terms of the standard one

(iv) Although each curve (graphs G.6.6. and G.6.5., curves 1,2,5,6 and 7) was obtained by an average of 25 points (by both the "freezing" and the "sampling" method) only 14 points were chosen to represent each curve (15 equal time intervals from t=0 to 300s) except for curve No. 2 (graph G.6.5.) for which 6 points were taken (t=180 to 300s). The limit set by t<300s is that for longer times, the driving force is not accurately known and thus no attempt can be made to correlate that region. Indeed, as it can be seen from graphs G.6.6. and G.6.5. very little growth occurs after 300 seconds. A total of 62 points taken as described

above were considered sufficient to represent all parameters fairly and were thus fed into programmes EF22 and EF23 (Appendix 12.) which evaluated the exponents given in equation E.6.2. (p 235)

6.3.4. Evaluation of an overall growth correlation

The overall growth correlation (equation E.6.2.) can be found using programme EF22 (Appendix 12) which performs the regression analysis and calculates the exponents a, b, f and n as well as the coefficient K by the least squares method. It also evaluates the standard deviations. Thus equation E.6.2. has the form:

$$\frac{dL}{dt} = 2.1 \times 10^{-3} \; L^{-1.5} \; pH^{0.03} \; R^{1.2} \left(\frac{C-C_s}{C_s}\right)^{0.83} \qquad \text{E.6.16.}$$

$K = 2.1 \pm 0.22 \times 10^{-3}$

$a = -1.5 \pm 0.13$ (μm)

$b = 0.03 \pm 0.02$

$f = 1.2 \pm 0.1$ (rpm)

$n = 0.83 \pm 0.15$

By re-evaluating the exponents, omitting the pH term the value of the constant changes to :

$K = 2 \pm 0.23 \times 10^{-3}$

Similar results are also obtained using an optimisation method (dichotomy). Programme EF23 (Appendix12) performs this optimisation and calculates the values of the exponents to be:

$K = 2.3 \times 10^{-3}$

$a = -1.4$ (μm)

$b = 0.03$

$f = 1.1$ (rpm)

$n = 0.98$

It can be seen that the values obtained by the optimisation method lie within the 95% confidence limits of the values evaluated by performing the regression analysis.

To examine the closeness of fit of the correlation, the values of $\frac{dL}{dt}$ calculated from the experimental data (curves 1 to 7 on graphs G.6.6. and G.6.5.) are plotted versus time on graphs G.6.8. and G.6.9. together with values of $\frac{dL}{dt}$ obtained from equation E.6.16. .

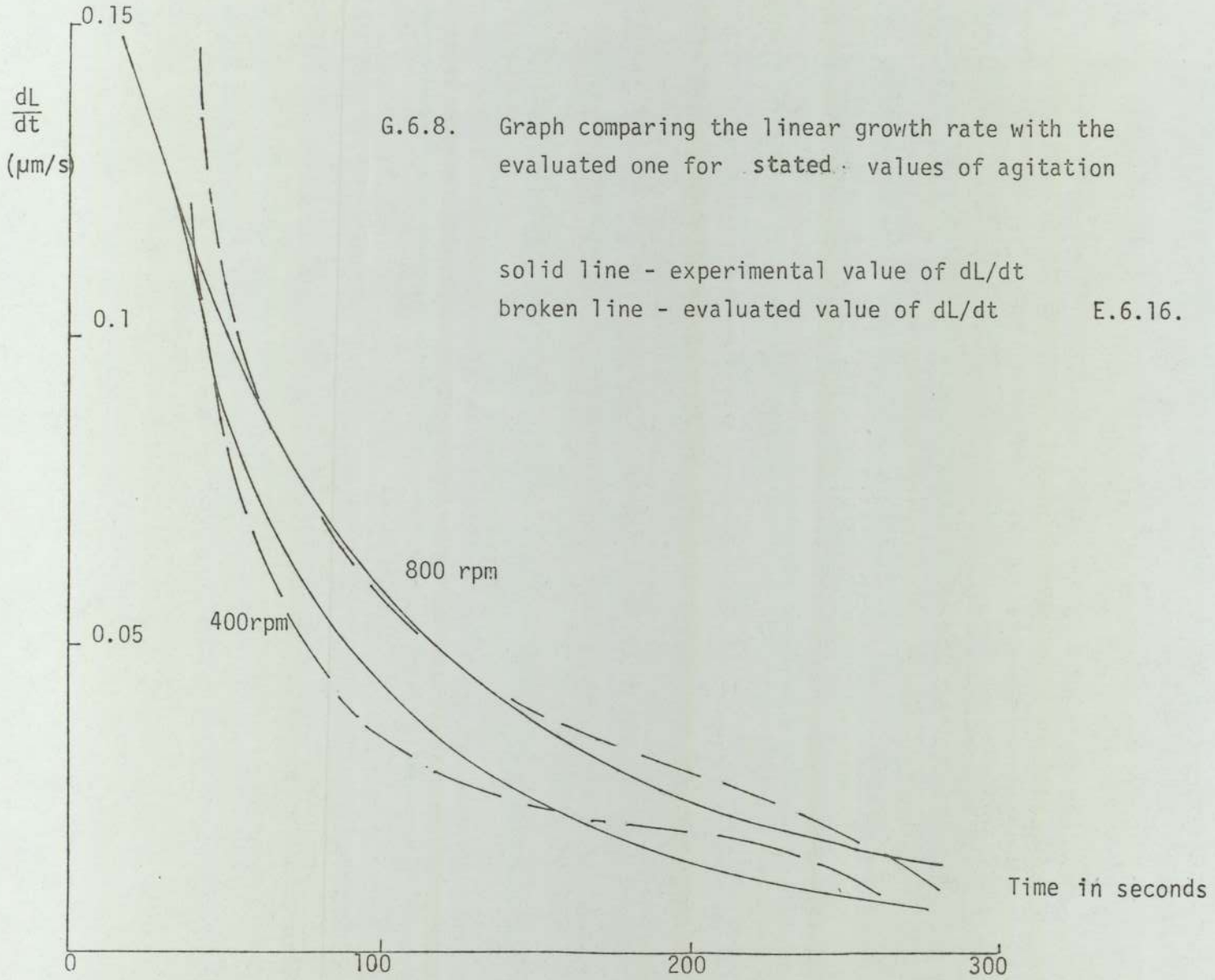

G.6.8. Graph comparing the linear growth rate with the evaluated one for stated values of agitation

solid line - experimental value of dL/dt
broken line - evaluated value of dL/dt E.6.16.

G.6.9. Graph comparing the linear growth rate with the evaluated one for stated initial Barium chromate concentration.

solid line - experimental value of dL/dt

broken line - evaluated value of dL/dt

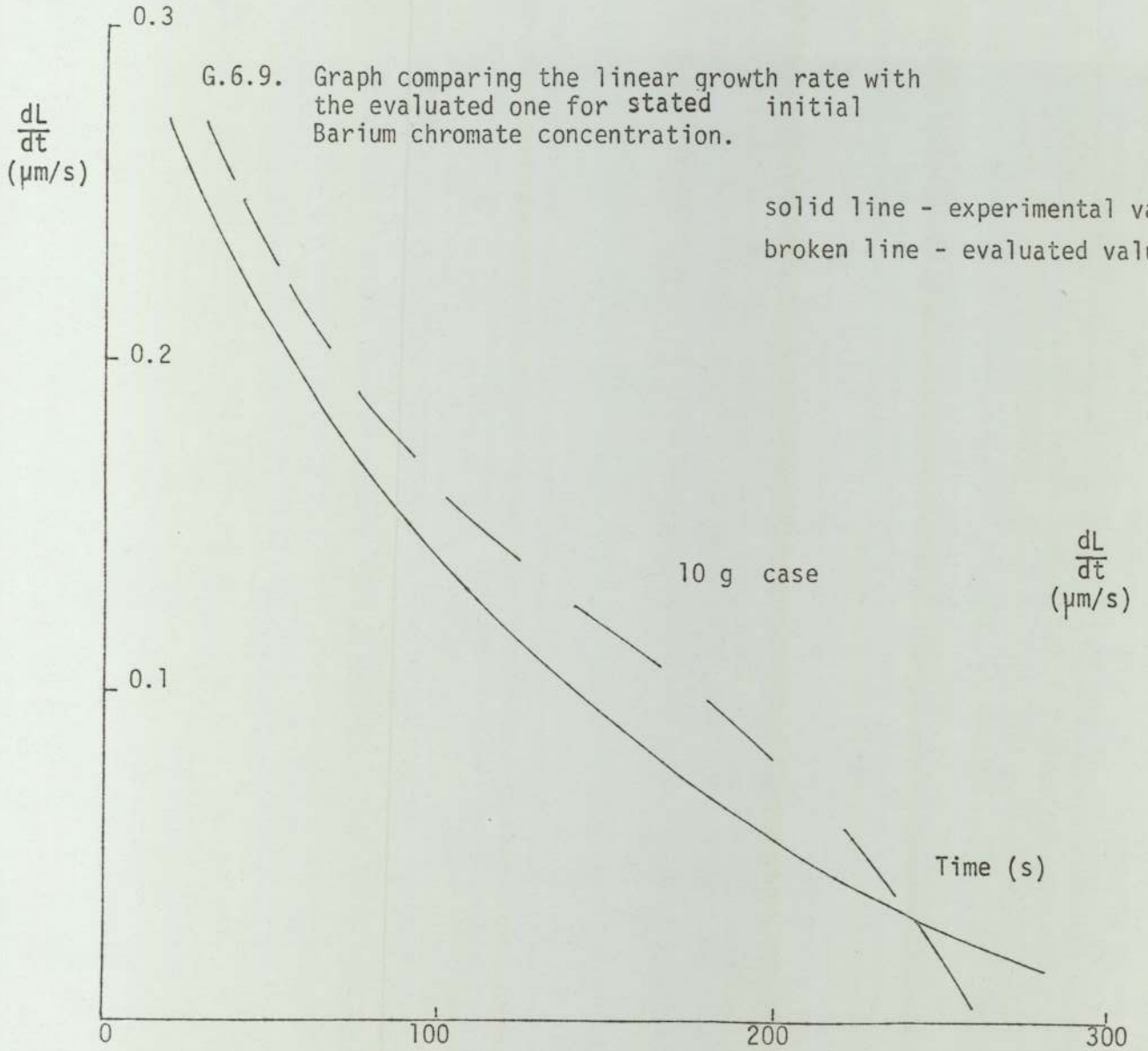

G.6.10. Graph comparing the linear growth rate with the evaluated one for stated initial Barium chromate concentration.

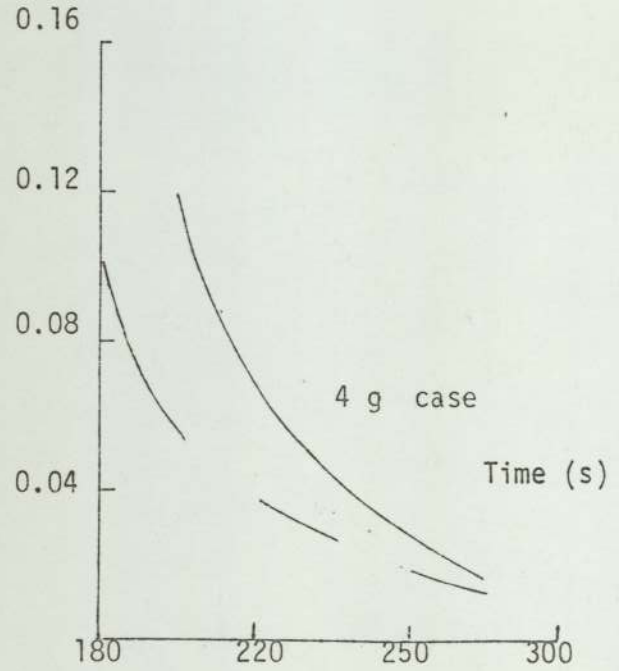

6.3.5. Discussion on the correlation obtained

The obtained correlation fits the data poorly for times $t < 60s$ and $t > 280$ s . A possible reason may be that for $t < 60s$ a transient state exists between the formation of the first nuclei and the actual growth of the crystals (5g,4g) while for $t > 280s$ the driving force is very small and swamped by experimental error (graph G.6.6. and G.6.7.). Other observations that can be made are:

(i) The existence of an "inflection" point in the curve obtained by equation E.6.2., typical of a three term approximation (L, R, $\frac{C-C_s}{C_s}$).

(ii) The existence of the agitation term and its exponent (equation E.6.2.) is an indication of the dependence of the crystal growth of Barium Chromate on agitation. The agitation term is expressed in r.p.m. although it can be related to the other parameters of the system. Other workers (R.6.1. and R.6.2.) have tried to relate the agitation to the Reynold's number and the various characteristics of the system (size and shape of vessel, type of blade, etc.). However, such correlations are applicable only to one system and for this reason no attempt is made in this work to express R in anything else.

(iii) The closeness of fit of the correlation for the case of 400 r.p.m. is less than that of the standard conditions. A possible explanation is

that as the agitation decreases, less fresh material reaches each particle and thus the stationary particle model begins to fail as the particles compete for fresh solution (section 6.3.5.).

(iv) The exponent of the pH term is very small (0.03 ± 0.02) and it seems that pH does not affect the crystal growth, under these conditions.

(v) From graph G.6.9. it is seen that the value $\frac{dL}{dt}$ obtained from the correlation is higher than the experimental one of the 10g case, while lower for the 4g one. This suggests that the earlier made assumption about a common operating line is possibly not valid. The difference of the value of $\frac{dL}{dt}$ appears to be constant (~ 10%) for the 10g case and since the exponent of the driving force n is ~1, the driving force which is the parameter known with least certainty appears to be about 10% higher than it actually was.

Therefore, a correction can be applied

$$\left(\frac{C-C_s}{C_s}\right)_{corrected} = X \left(\frac{C-C_s}{C_s}\right)_{calculated} \qquad \text{E.6.}$$

X is a correction factor which can either be taken as constant ~ 0.9 or as function of time.

(vi) The exponent of the term which involves the characteristic length (L) is negative and this indicates that the smaller particles grow faster

than the bigger ones. Furthermore, the distributions obtained in section 6.2. have no "tails" from the origin after a certain time, although the population appears to increase (section 6.4.) and this also suggests that the smaller particles grow much faster than the bigger ones. This led to the suggestion of an alternative model of crystal growth (section 8.2.).

(vii) Equation E.6.2. can be modified to the form:

$$\frac{dm}{dt} = K L^a R^f \left(\frac{C-C_s}{C_s}\right)^n \qquad \text{E.6.17.}$$

where

$\frac{dm}{dt}$ is the mass growth of the mean particle

$\frac{dm}{dt}$ is proportional to $L^2 \frac{dL}{dt}$

$a = 0.5 \pm 0.04$ (μm)

$f = 1.2 \pm 0.1$ (rpm)

$n = 0.83 \pm 0.15$

6.3.6. The effect of other parameters on crystal growth

(i) Initial Urea concentration (Table T.A6.5.).

Tests with varied amounts of Urea produced crystals of the same characteristic length (for a given time) as those obtained from the standard conditions. Because of this it appears that the Urea concentration does not affect the crystal growth. This is in agreement with the conclusions drawn in chapter 5 by which the rate of hydrolysis of Urea is independent of the initial Urea concentration (pH > 2.5).

(ii) Annealing time (Table T.A6.3.).

Tests with varied annealing times also produced crystals of the same characteristic length (L) as those obtained from the standard conditions. Therefore it can be said that annealing time does not affect the crystallisation of Barium chromate crystals.

(iii) The presence of weak acids (Table T.A6.6.).

Three weak acids were tested :

a) Acetic

b) Formic

c) Citric

All three affected the crystal habit, resulting in "flake" type crystals, in the case of Acetic acid to equant crystals of "uneven" surface in the case of Formic. These results are difficult

to quantify and thus only stereoscan photographs are shown F.6.2. and F.6.3. for qualitative comparison with the theoretical shape of the crystals (chapter 3) and also with the actual crystals produced (photograph F.6.1.).

(iv) The presence of baffles in reactor No. 5.(Table T.A6.3.)

The presence of baffles in reactor No. 5. appeared to have no effect for the speed of agitation of 800 r.p.m., since the crystals produced were of the same characteristic length (L) with those obtained from the standard conditions.

6.3.7. Epitaxial growth studies in reactor No. 5.(Table T.A6.6.).

Attempts were made to coat various amounts of Tungsten particles at agitation speeds sufficiently high to suspend them, however the crystals produced were not growing on the metal particles. The product consisted of Tungsten particles and Barium chromate crystals, which segregated when agitation stopped because of their marked difference in density. The reason for the failure has possibly been that the agitation was very intense and owing to hydrodynamic drag the weakly attached crystals (because of only one line matching at crystal lattice) were detached from the metal particles.

6.4. Nucleation

6.4.1. The Effect of nucleation on the process

As it was stated earlier (Chapter 2), secondary nucleation is a function of the supersaturation. Usually the assumption made that the population does not change with time is not valid but in practice the effect on growth rate calculations which neglect it is negligible. (8.2.).The present method of evaluating distributions on a number basis, using a Coulter-Counter (Appendix 1) enables evaluation of the population. In graph G.6.13. the total population is plotted against time for the standard conditions.

The results appear to be scattered, the reason being that an error in the characteristic length (L) is magnified to L_c^3 in the population since:

$$N_j = M_{j/Kp}\, L_j^3 \qquad \text{E.6.18.}$$

M_j is the total mass

N_j is the total population

L_j is the mass mean radius at time t=j

Kp is a constant

Strickland-Constable (R.2.30.) suggested that secondary nucleation from all sources including attrition depends on the level of supersaturation. However (from graph G.6.13) it appears that the population could be represented by a logistic type curve. Thus by comparison to biological systems, the rate of increase of the population is subject to a stochastic process (a function of the number of particles already existing) and the driving force.

The rate of increase of population is dependent on both the driving force and the population. E.6.19.

The final population was found to be about 5×10^7 dm^{-3} particles after 300s (for the standard conditions), graph G.6.13..

Now

Volume of solution = 10^{15} μm^3

Volume of solution/particle = 10^{15} $\mu m^3 / 5 \times 10^7$ particles

$\therefore$ spherical controlling volume of radius = 170μm is allocated per particle.

6.4.2. The effect of the initial Barium chromate concentration

On graph G.6.11. the initial Barium chromate concentration is plotted against the population. It appears that as the initial concentration increases the population decreases until an initial mass of about 5g is exceeded. After that it appears to remain constant. This is possibly due to the rate of change of pH: the pH changes very slowly with time at first while later the rate of change is much faster (chapter 5). As a result the supersaturation conditions are reached slowly for the 5 and 10g cases encouraging a few seeds only to form, while with increasing suddenness for the smaller initial concentrations encouraging more seed to form.

6.4.3. The effect of agitation

On graph G.6.12. the agitation expressed as r.p.m. is plotted versus population. It appears that the agitation has an inverse effect on nucleation. This is in agreement with the evidence provided in the literature (chapter 2). A possible explanation of what physically happens is that as agitation decreases the rate of local supersaturation increases since the freshly released material from solution is not immediately adsorbed by the crystals.

6.4.5. The effect of other parameters

(i) Initial Urea concentration

Because the initial Urea concentration does not affect the crystal growth, it can be concluded that it does not affect the nucleation either. (Section 6.3.6.).

(ii) Annealing time

For the above stated reason it appears that annealing time does not affect the nucleation.

(iii) The presence of baffles in reactor No. 5 also has no effect.

(iv) The presence of weak acids.

Because all the weak acids tested tended to change the crystal habit resulting in "flake" or "equant" type crystals (section 6.3.6.) no conclusions can be drawn about the effect of the weak acids on the nucleation.

G.6.11. Graph relating the total population versus the initial concentration of $BaCrO_4$ (Batch crystalliser No. 5.)

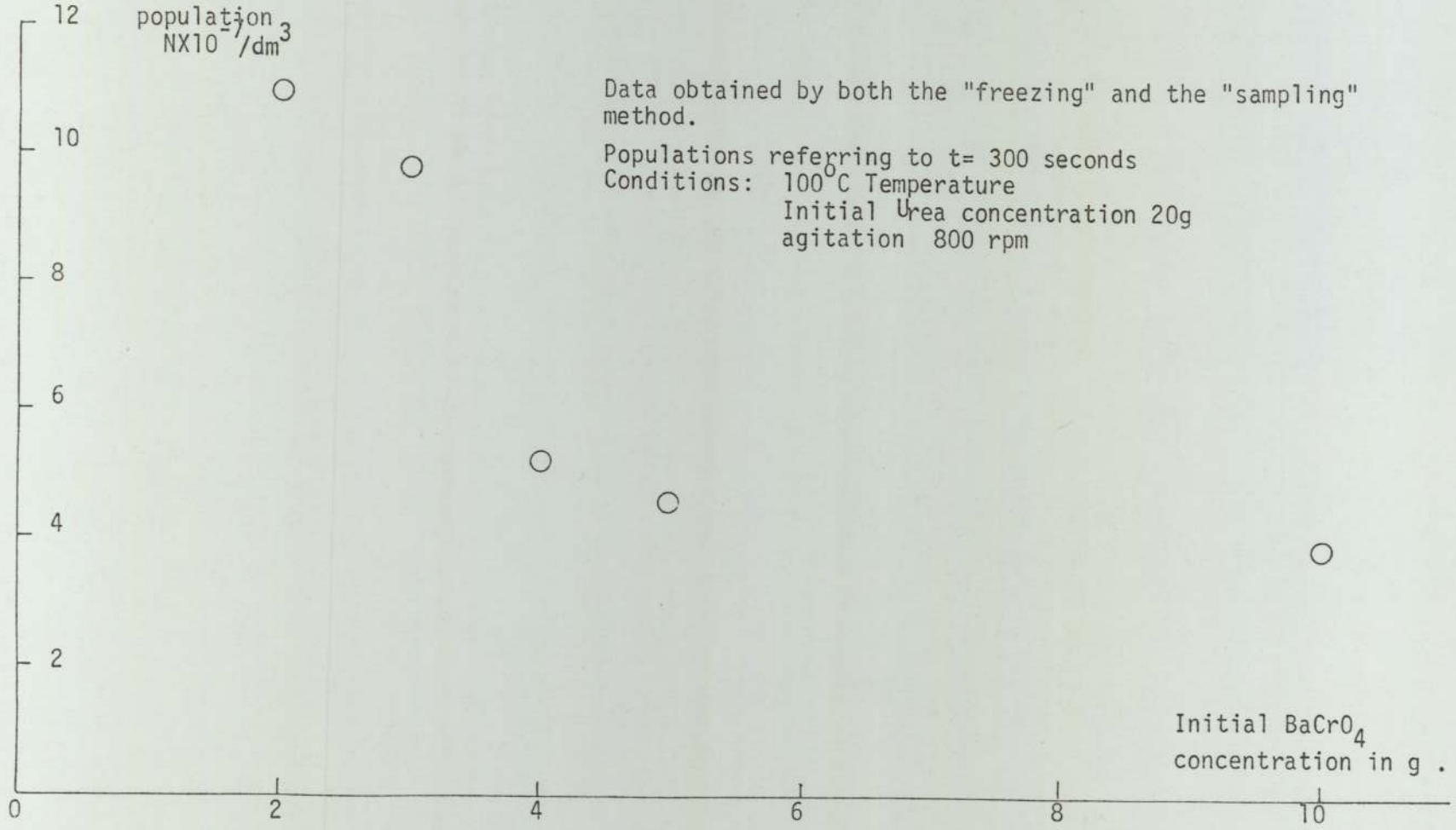

G.6.12. Graph relating the total population with the speed of agitation
(batch crystalliser No. 5.)

Data obtained by both the "freezing" and
the "sampling" methods.
Populations refer to t=300 seconds
Conditions: $100^{o}C$ temperature
Initial $BaCrO_4$ concentration $5g/dm^3$
Initial Urea concentration 20g
Initial acid concentration 0.06M HCl

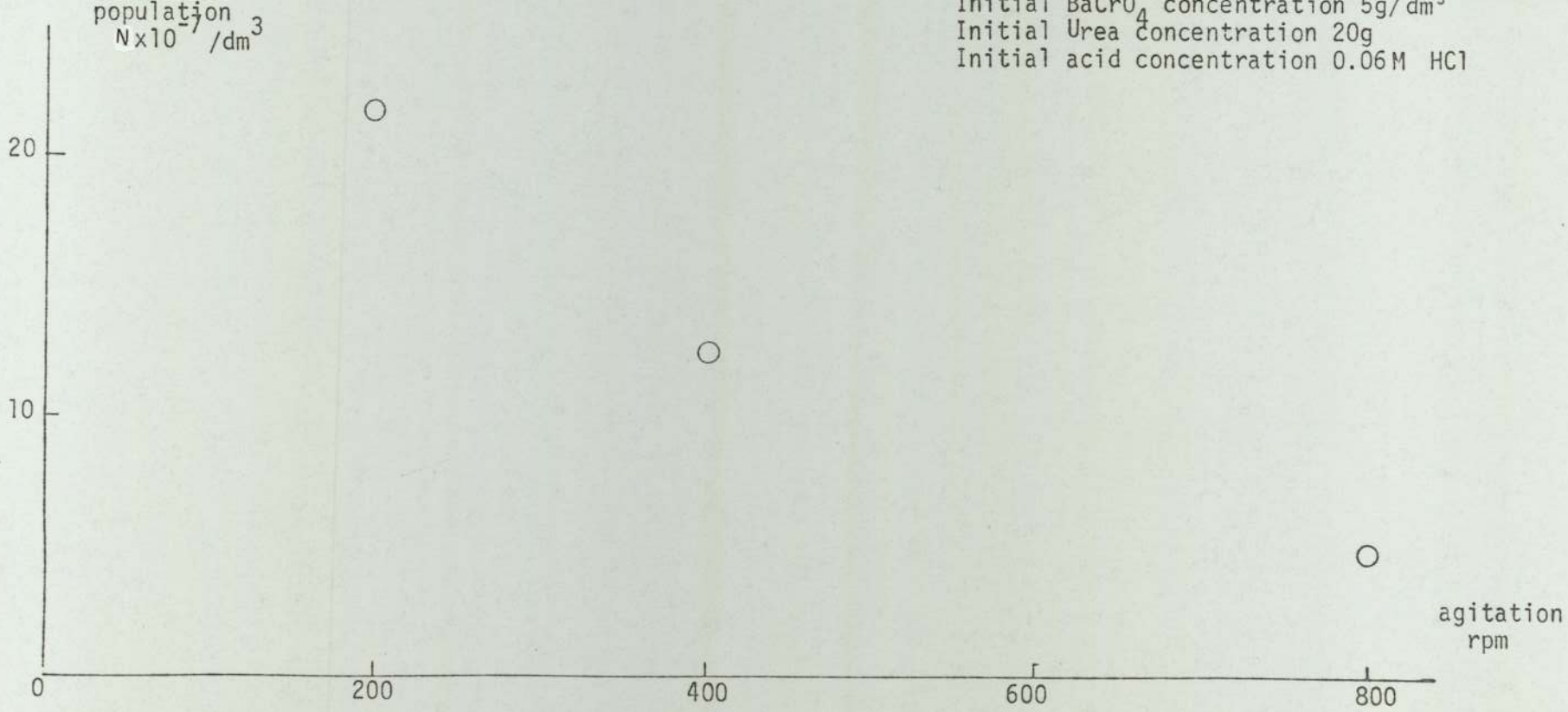

G.6.13. Graph relating the total population to time for the standard conditions (batch crystalliser No. 5.)

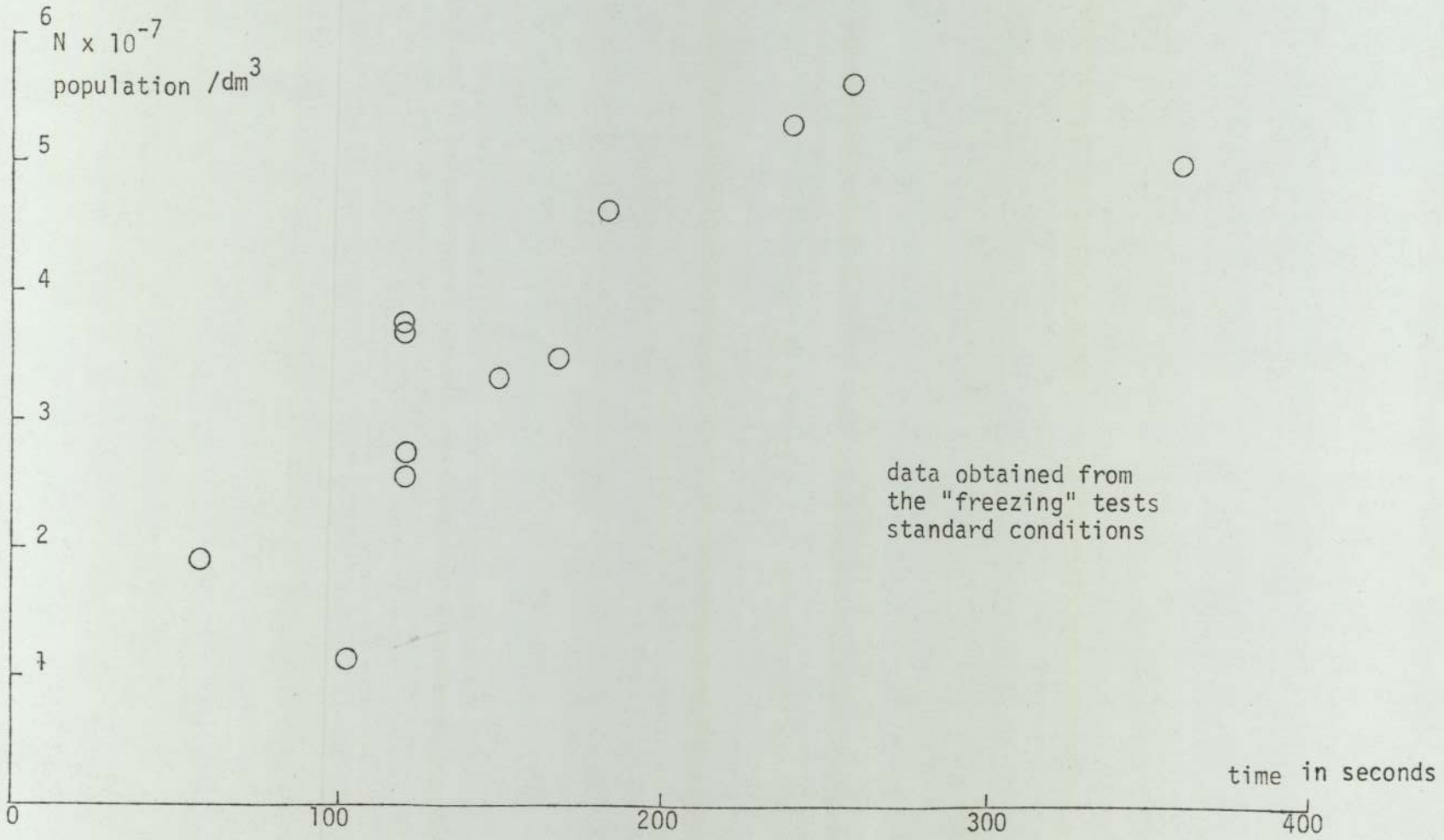

Results obtained from the fluidised bed (Reactor No.6)

Preliminary tests with the fluidised bed showed that Barium chromate can grow to about 10μm(mean mass radius) crystals. The size of the crystals is comparable to the 200 rpm agitation tests, in reactor No. 5 . However, no attempt will be made to relate the agitation of the fluidised bed to that of 200 rpm since the systems are different. Furthermore, the nucleation and possibly the growth rate were aided by the lower temperature which existed in the fluidised bed (graph G.6.15.) compared with the temperature in the reservoir. Because of this, fine precipitates were also formed in the recycles (RC1 and RC2). However, when Tungsten powder was present in the fluidised bed, preferential nucleation occurred there (Appendix 3) suggesting that a fluidised bed crystalliser is most suitable for epitaxial growth.

The operation of reactor No. 6 is somewhat difficult, requiring long heating times (graph G.6.15.) as well as fine control of recycle RC1 in order to suspend the heavy particles (chapter 4) but not to carry them over to the rest of the system.

The shape of the Barium chromate crystals growing on a Tungsten nucleus was considerably affected by the type of Tungsten used as well as by the impurities left from the metallurgical treatment of the Tungsten powder. (Photographs F.6.4. and F.6.5.).

In graph G.6.14. the expected Barium chromate to Tungsten ratio is plotted versus the actual ratio which was estimated by redissolving the crystals and reclaiming the metal (Appendix 6). It appears (graph G.6.14.) that there is a tendency to lose Tungsten, possibly the very fine particles are carried over to the recycle. The size analysis of the product proved difficult. The particles were too heavy for the Andreasen sedimentometer and the mechanical stirrer of the Coulter-Counter (Appendix 1) proved inadequate to stir a solution of Glycerol and Water sufficiently viscous to suspend the particles. A bigger four-blade stirrer was also tried. An estimation of the size can be taken from photographs F.6.4. and F.6.5. Table T.6.3. compares qualitatively the pure Barium chromate crystals with those growing on a Tungsten substrate.

Tungsten content	Colour	Free flow	shape/ photograph
None	Yellow orange	Yes	{III} habit F.6.1.
Type (I)	Green depending on the metal content	No	"Needles" "clusters" F.6.4.
Type (II)	Green depending on metal content	Yes	"equant" F.6.5.

Table T.6.3. comparing qualitatively the properties of the crystals obtained from the fluidised bed with those of the pure Barium chromate

6.6. Discussion on the fluidised bed

The fluidised bed crystalliser proved suitable for the epitaxial growth of Barium chromate crystals on a metal substrate. However, possibly because of the very small metal particles used (chapter 4), Tungsten appeared to be lost in the system (graph G.6.14.).

The treatment of the Tungsten powder, before use, appears to be essential since the impurities which are probably present greatly affect the crystal habit (photographs F.6.4. and F.6.5.).

6.7. Qualitative Analysis

The photographs shown in this section were taken by an electron microscope (available in the Metallurgy Department in Aston University).

The sample to be photographed, was coated with a resin. However, because of the very small sizes involved ($<100\mu m$) and the intense "radiation", the particles (crystals) were electrically charged and as a result no photographs could be taken. To avoid this, an extra thick coat of resin was applied under longer periods in vacuum. This however produced breakages, as can be seen in photographs F.6.1. to F.6.5..

Type II Tungsten (chapter 4) is shown in photograph F.6.6.. However, because of the limitations of the instrument, the particles photographed are out of focus. As a result no conclusions can be drawn about the porosity of the metal.

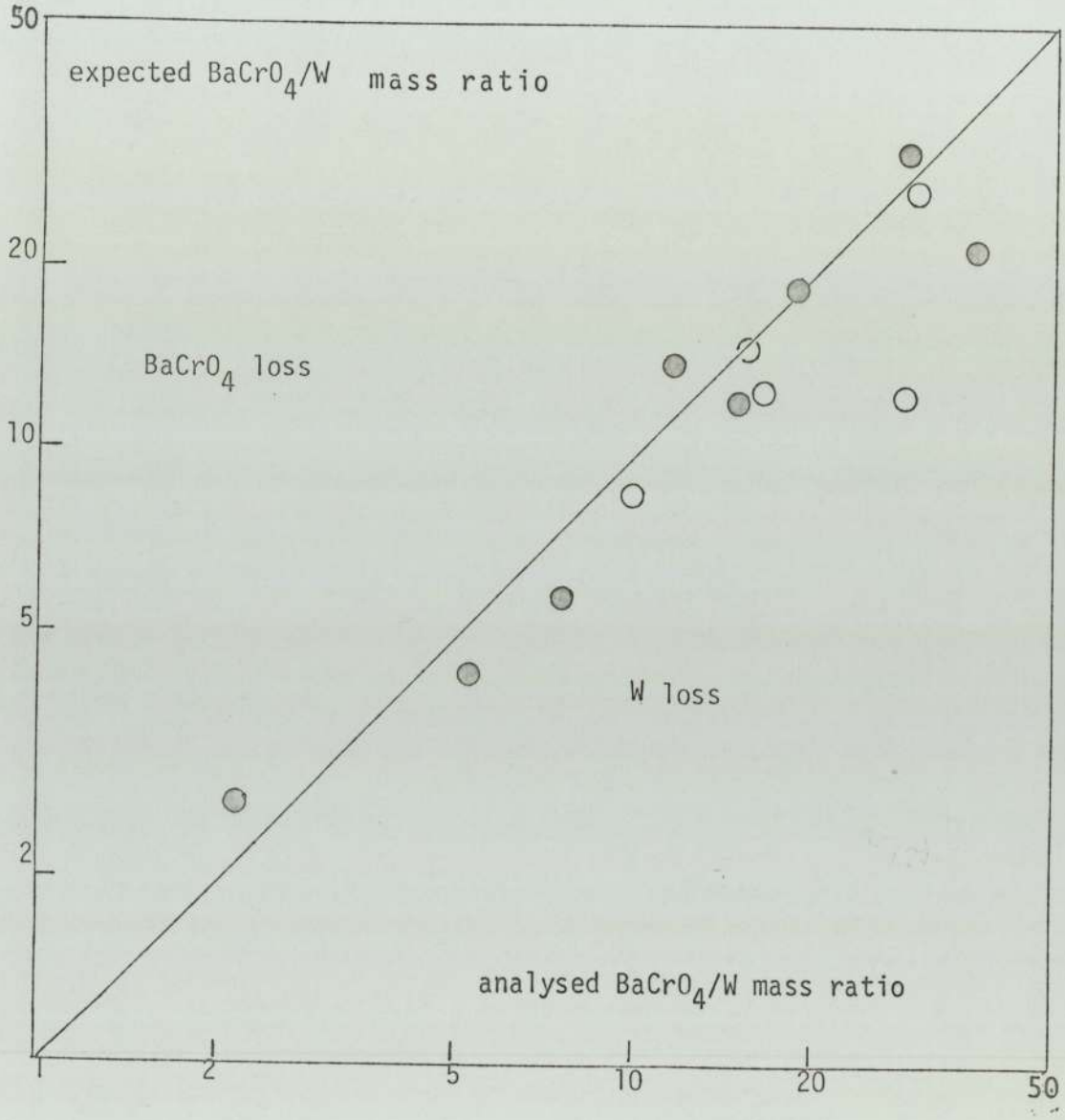

G.6.14. Analysis of products of fluidised bed tests to check mass balance

● Type II Tungsten (chapter 4)

○ Type I Tungsten

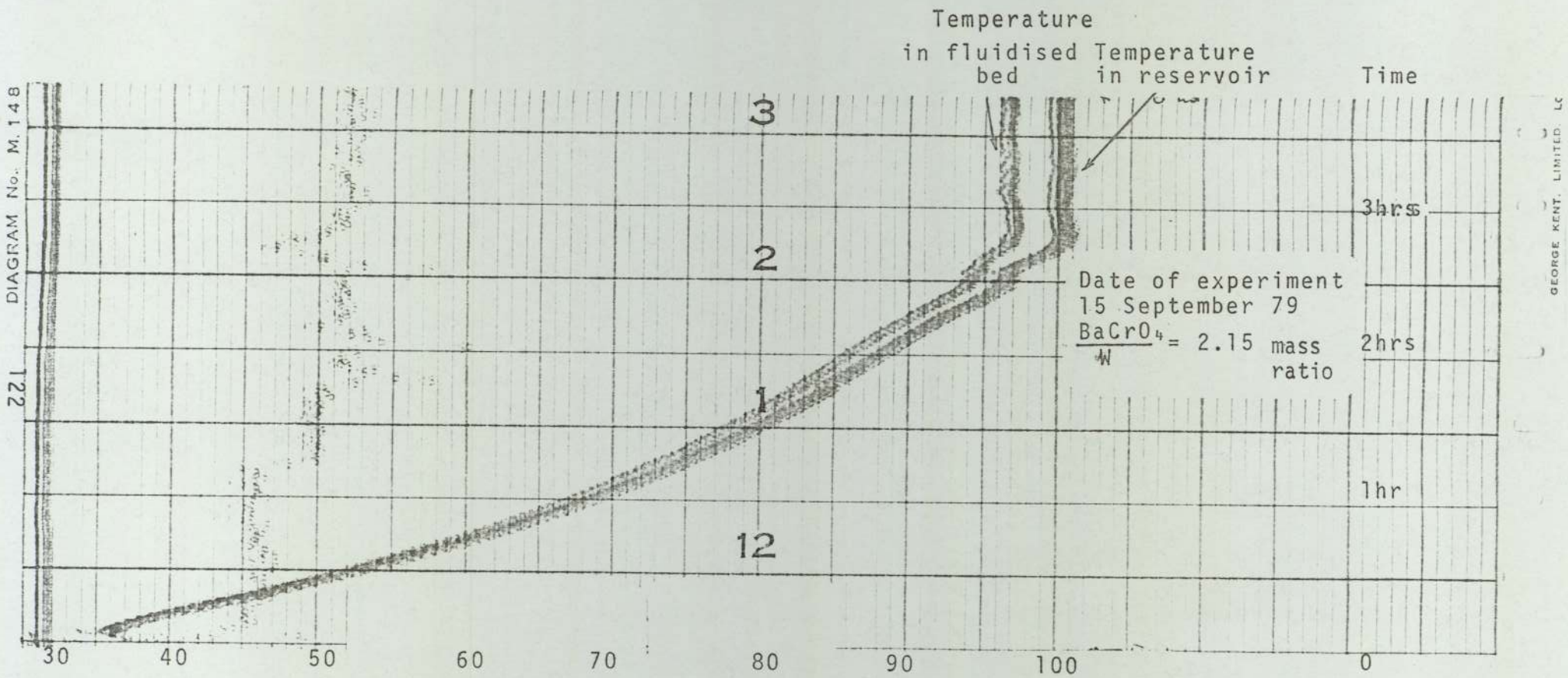

G.6.15. Graph showing temperature versus time plot for different parts of reactor No. 6. (the fluidised bed and the reservoir)

F.6.1.

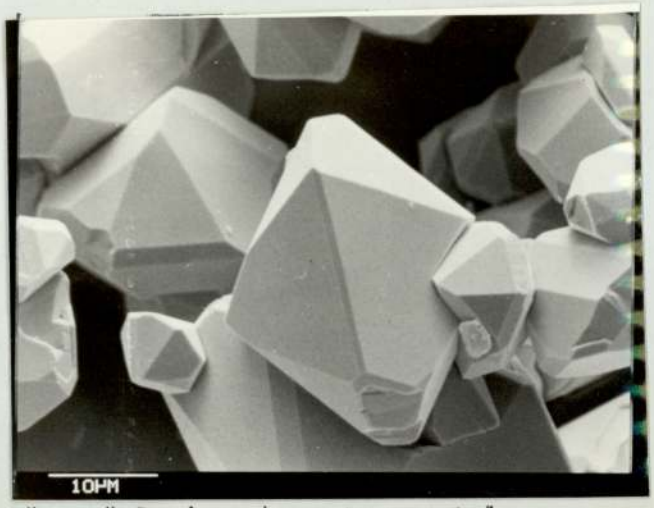

"pure" Barium chromate crystals as grown from HCl/Urea solution.

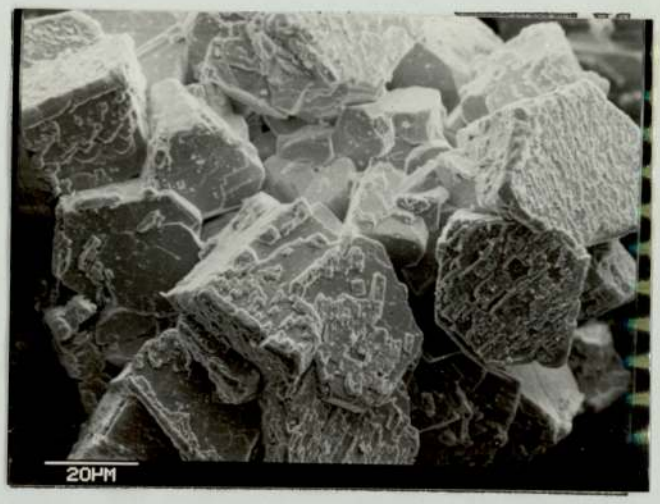

F.6.2. Barium chromate crystals as grown in the presence of Formic acid.

F.6.3. Barium chromate crystals as grown in the presence of Acetic acid.

Stereoscan pictures of Barium chromate crystals.

Stereoscan photographs of Barium chromate grown on Tungsten substrate

F.6.4. Substrate - Tungsten Type I

F.6.5. Substrate - Tungsten Type II

F.6.6. Stereoscan photograph of Tungsten Type II

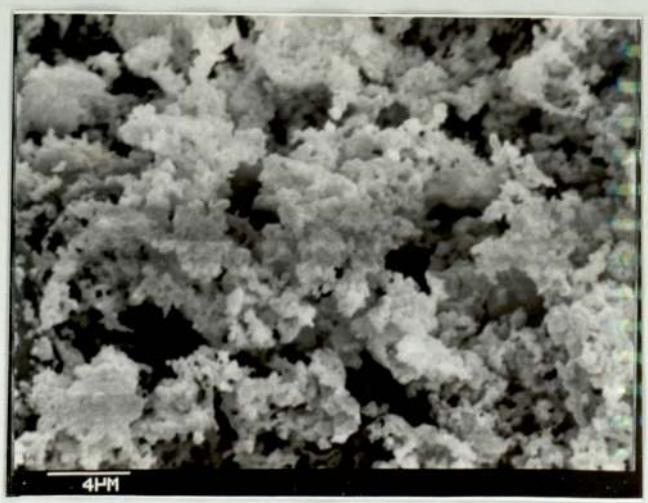

CHAPTER 7

EQUIPMENT USED

Skander (R.3.1.) has shown that the m.s.m.p.r. type crystalliser is not suitable for crystal growth measurements of Barium chromate. Furthermore, the process must be seen in the context of the coating of the Tungsten and these very dense metal particles would cause problems at various parts of the recycle system.

The jacketed vessels (reactors 1, 2 and 3) used by Skander (R.3.1.) for the determination of the solubility of Barium chromate also proved not suitable. Skander found that a stirred vessel batch crystalliser was suitable for crystal growth studies and an improved version of it constitutes reactor No. 5.

Reactor No. 6, the fluidised bed crystalliser, was designed for the purpose of increasing the capacity of the process while keeping the dense particles also gently suspended. Because of the scale, only a few experiments were carried out with it.

Finally, reactor No. 4 was hopefully an improved version of the original reactors 1, 2 and 3. Although right in its conception, it was limited by the available equipment and it was found that solubility data obtained from it were no more consistent than from reactors 1, 2 and 3.

7.1 Reactors Nos. 1, 2 and 3 (solubility measurement)

The reactors 1, 2 and 3 were used to study the solubility of the Barium chromate in acid solution.

Each consisted of

(i) A jacketed vessel (250 cm^3 capacity) stirred by magnetic stirrer

(ii) a "Churchill" thermocirculator (range 0-65^oC) with accuracy of ±0.1 ^oC,

(iii) pH probe and meter type G 1 L 7010 permitting estimation to accuracy of ±0.04 pH ,

(iv) a 10 cm^3 pipette fitted with a 0.5 μm pore size sintered glass filter and

(v) auxiliary equipment including volumetric flasks, thermometers, optical cells (Appendix 8) for use with PYE SP1800 ultra-violet spectrophotometer.

Flow diagram D.7.1. presents the three reactors. The whole apparatus is also shown in photograph F.7.4.

Reactors 1 Jacketed vessel
2 " "
3 " "

each fitted with stirrer and thermometer

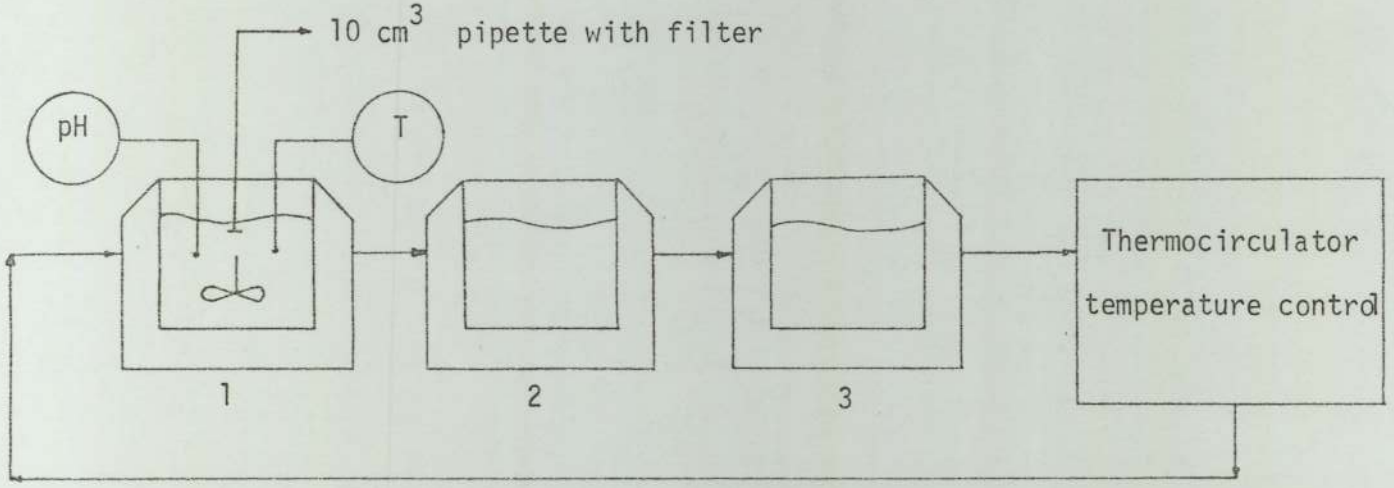

D.7.1. Diagrammatical representation of reactors 1, 2 and 3.

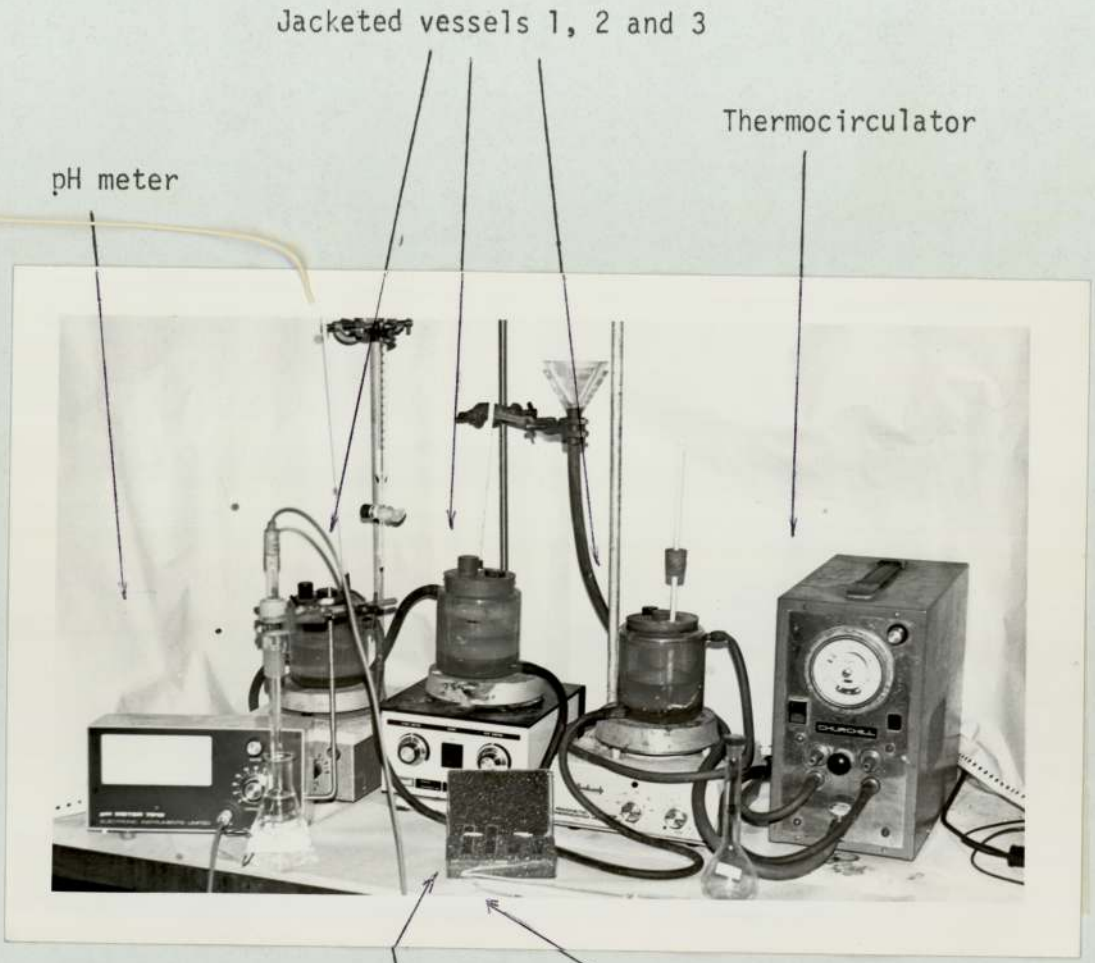

F.7.1. Reactors 1, 2 and 3 plus the auxilary equipment

7.1.1. Experimental procedure

Excess Barium chromate in acid solution was placed in the reactors and the appropriate temperature was set on the thermostat. The system was allowed to reach both thermal and physical equilibrium (R.3.1). A 10 cm^3 sample of the saturated solution was filtered off and diluted to 100cm^3 with acid (HCl or HNO_3) such that the final pH = 1 (R.3.1.). The pH and temperature of the original solution in the reactors 1, 2 and 3 were also measured. The concentrations of the samples were determined with the aid of the ultra-violet spectrophotometer which had been calibrated with samples of known concentrations.

7.1.2. Errors and limitations

The main source of error in the reactor was probably due to vapour losses (especially at higher temperatures) preventing saturation conditions. Furthermore, after removal, the sample cooled to room temperature and thus, possibly precipitation occurred. As a result, the data obtained were scattered and only a statistical correlation was possible after collecting a large number of data points. The main limitation of the apparatus was its limited temperature range. The reactor was capable of delivering hot water at no more than 65^{o}C.

7.2 Reactor No. 4. (solubility measurement)

Reactor No. 4 consisted of a 250 cm^3 spherical vessel fitted with a condenser and immersed in a water bath, controlled by a thermostat. Samples were withdrawn via a burette in which their volume was measured. The burette was also immersed in the water bath.
Auxiliary equipment required was as described in section 7.1.v..

Flow diagram D.7.2 presents reactor No. 4.

7.2.1. Experimental procedure

The experimental procedure was as described in section 7.1.1. except that the sample was held at the temperature of the operation until dilution. The minimisation of the vapour losses maintained saturated conditions while the temperature range of the operation was extended to $90^{o}C$.

7.2.2. Errors and limitations

The volume of the sample collected was less accurately measured by the burette than the pipette used in the other method. The whole apparatus was immersed in a water bath and thus the speed of the operation was limited.

A Filter

B Burette

C Condenser

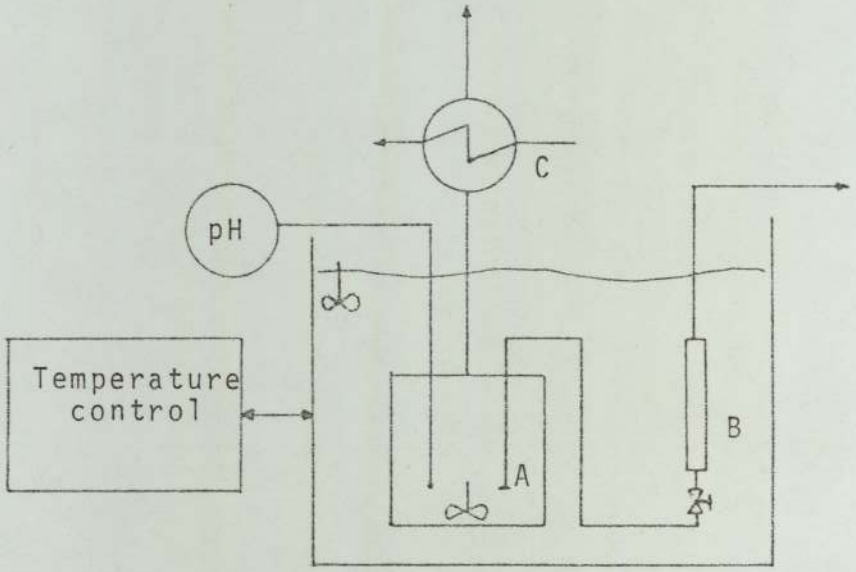

D.7.2. Diagrammatical representation of reactor No. 4.

7.3 Reactor No. 5. (crystal growth rate measurement)

Skander (R.3.1) showed that a stirred vessel batch crystallizer was suitable for studying the crystal growth. An improved version of the original design was used consisting of:

(i) a one litre spherical vessel, made from Borosilicate (with baffles or not) fitted with a five neck lid for thermometer , stirrer shaft, condenser, pH probe and sampling point,

(ii) an electrical heater ("Isomantle" type MUL/CT/1 300 watts),

(iii) a pH meter (type E I L 7010 with up to 30cm long probes)
a second pH meter (type PYE 40182) was also available for comparison,

(iv) a sampling probe and

(v) auxiliary equipment including mechanical stirrer, stroboscope , tachometer, stopclock, thermometers, etc.

Reactor No. 5 proved very versatile and it was used to measure the solubility of Barium chromate, the hydrolysis of Urea as well as the crystallisation of Barium chromate.
Flow diagram D.7.3 shows reactor No. 5, while photographs F.7.2 and F.7.3 show the apparatus assembled and "broken" respectively.
The sampling probe was the original design of Skander (R.3.1.).

7.3.1 Experimental procedure

(i) To measure the solubility of Barium chromate

The experimental procedure was as described in Section 7.1.1. except that the removed sample was kept in the reactor until

H Heater

C Condenser

O Outlet (fitted with a filter or not)

S Stirrer

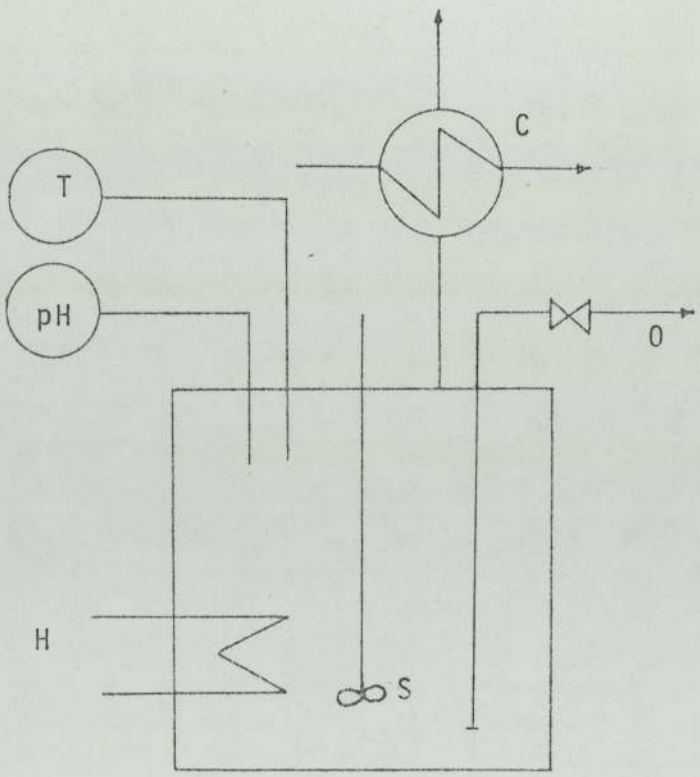

D.7.3. Diagrammatical representation of reactor No. 5.

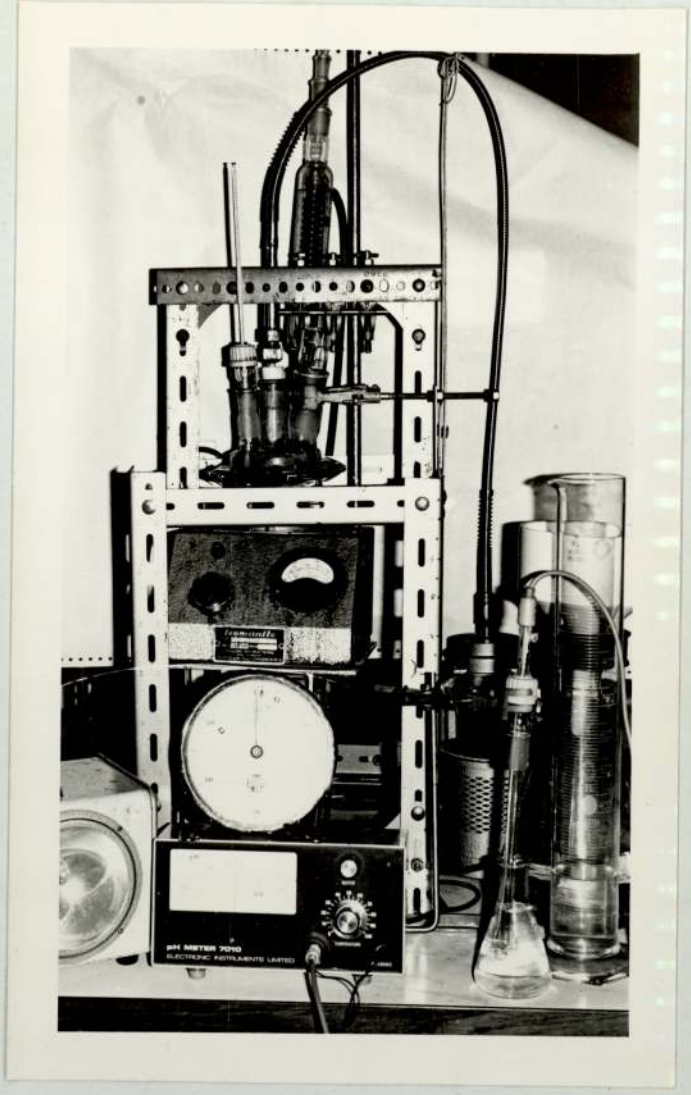

F.7.2. Reactor No. 5. plus auxiliary equipment

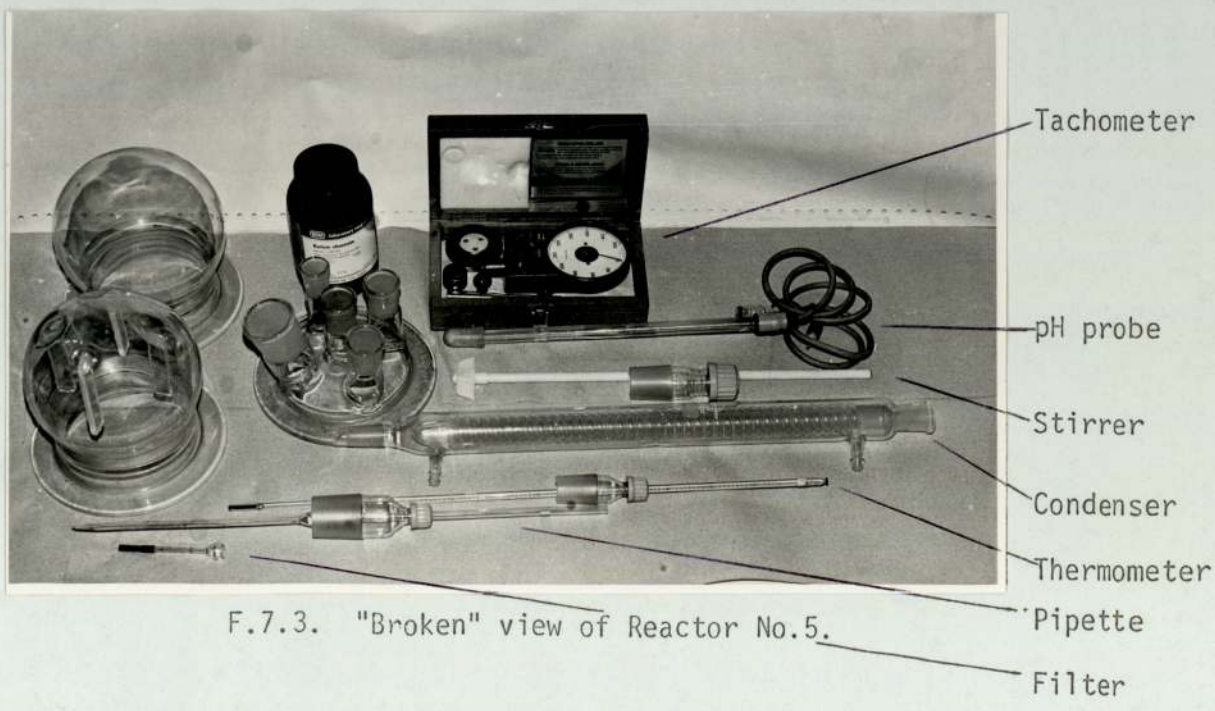

F.7.3. "Broken" view of Reactor No.5.

dilution, to reduce the risk of precipitation due to cooling.

(ii) To measure the hydrolysis of Urea in acid solutions

Predetermined amounts of Urea and acid were placed in the reactor (total volume of solution one litre).
The agitation and temperature were kept constant while the change of pH was measured against time.

(iii) To measure the crystallisation of Barium chromate

Predetermined amounts of acid (HNO_3 or HCl), Barium chromate, and Urea and Tungsten (when required) were placed in the reactor (total volume of solution one litre).
The agitation, temperature, pH and time were measured or kept constant according to the requirements.
Samples of the suspension were removed and analysed in the Coulter-Counter at regular intervals of time to follow the progress of the crystallisation. It was found that the samples were not consistent and therefore not typical of the suspension (on a mass balance basis).
The experimental technique was therefore modified by "freezing out" the reaction and filtering off all the crystal product formed to that point in time, weighing and analysing it.
The "freezing" of the process was achieved by adding cold water since the rate of hydrolysis is negligible, below $95^{o}C$ (R.3.1.)
A predetermined amount of Water was added such that the dilution would compensate the drop in solubility due to the temperature fall.

The technique was further changed, by allowing the crystals to settle, syphoning off the supernated liquid, filtering and washing the residual crystals.

7.3.2. Errors and limitations

The main errors originally associated with this reactor when used for the crystallisation of Barium chromate was the removal of the samples of suspension as already mentioned (R.3.1.).

The sample was removed with a syringe connected to a long tube. Although the tube was bent at the end to trap the particles, the sample collected was proved to be unrepresentative of the suspension (on a mass balance basis).

This error was later removed, when the "freezing out" technique was introduced. This technique suffered from the fact that it was impossible to carry it out at zero time. Furthermore, it involved dilution and thus the risk of either the smaller particles being dissolved or further precipitation occurring was increased.

These errors however, were minor and allowed a successful mass balance.

The filtering off of the solution, after allowing the particles to settle, was also proved to give reasonable mass balances (Chapter 6).

The main limitation of the apparatus was the stirrer. Skander (R.3.1) tried a number of types of stirrers, coated with acid-resistant materials.

In this work a Polypropylene propeller with two blades 15mm wide and 3mm thick was used. The shaft of the stirrer proved

too flexible at high speed (>1700 rpm) for safety and thus set a limit to the maximum agitation speed.

7.4 Reactor No. 6. (The fluidised bed crystalliser)

The need for the fluidised bed crystalliser was to increase the scale of the operation, bearing in mind the difficulty of stirring boiling Hydrochloric acid experienced on the one litre scale.

It was designed with the following considerations:

(i) the Tungsten particles should not settle anywhere,

(ii) it must provide sufficient circulation to suspend the metal particles,

(iii) it must be accessible for cleaning.

After preliminary designs, the crystalliser shown in the flow diagram D.7.4. was constructed.

Photograph F.7.1. shows the fluidised bed crystalliser (Reactor No. 6) in its development stage.

The general construction is of standard Q.V.F. glassware.

F fluidised bed 2.5 litre capacity

The outlet of the recycled RCl at the bottom of the fluidised bed suspends the metal particles (and later the crystals). The temperature of the fluidised bed is below (100^{o}C) in order to create preferential conditions of supersaturation and thus nucleation.

R reservoir, 10 litre spherical vessel

The reservoir is kept at a higher temperature ($100^{o}C$)

The hydrolysis of Urea is facilitated there.

V_1 Outlet valve for the removal of final product

V_2 Sample valve for the removal of sample of the solution during operation

V_3 Inlet valve for introducing the Tungsten particles into the system

V_4 Inlet valve for introducing the soluble compounds into the solution

V_5 Flow control valve for RC1

The flow of the recycle RC1 is critical.

The optimum flow is such that it will suspend the particles but not drive any into the reservoir or into any other part of the system.

RC2 needs no regulation. Its function is to have the system wellmixed and takes the pump's full surplus capacity.

H_1 1 Kw heaters type QUICKFIT glass jacketed EF13J

H_2, H_3 Heaters (QUICKFIT) to ensure that no nucleation occurred in the recycle RC2.

H_4 Isomantle 1 Kw heater

P Polypropylene centrifugal pump $\frac{1}{20}$ H.P."Schuco 3-MD"
Titanium shaft, magnetic coupling.

F_1 Flow meter (metric 7K "Rotometer") for recycle RC1.

F_2 Flow meter (metric 24K "Rotometer") for recycle RC2.

T Temperature measured by C/A thermocouples and recorded on Kent Mark 3 multipoint instrument.

pH pH measured by long probe (30cm) as described in section 7.1.

D.7.4. Flow diagram of reactor No. 6.

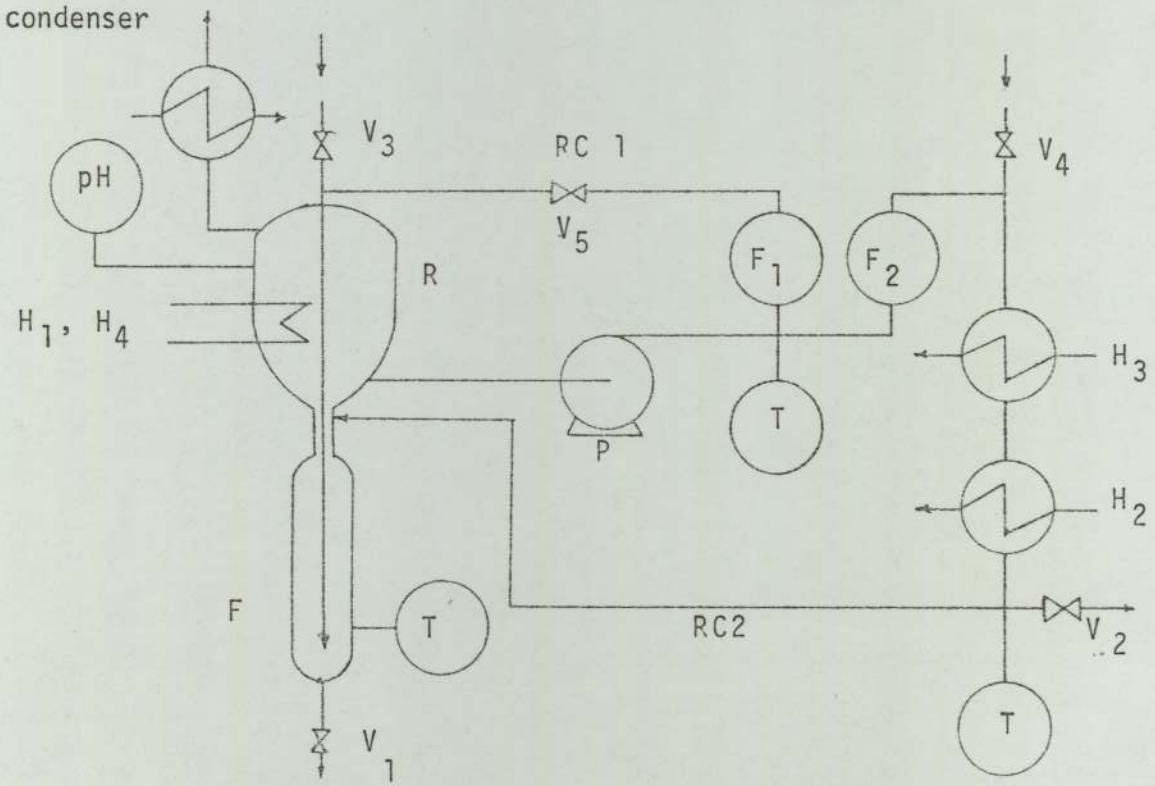

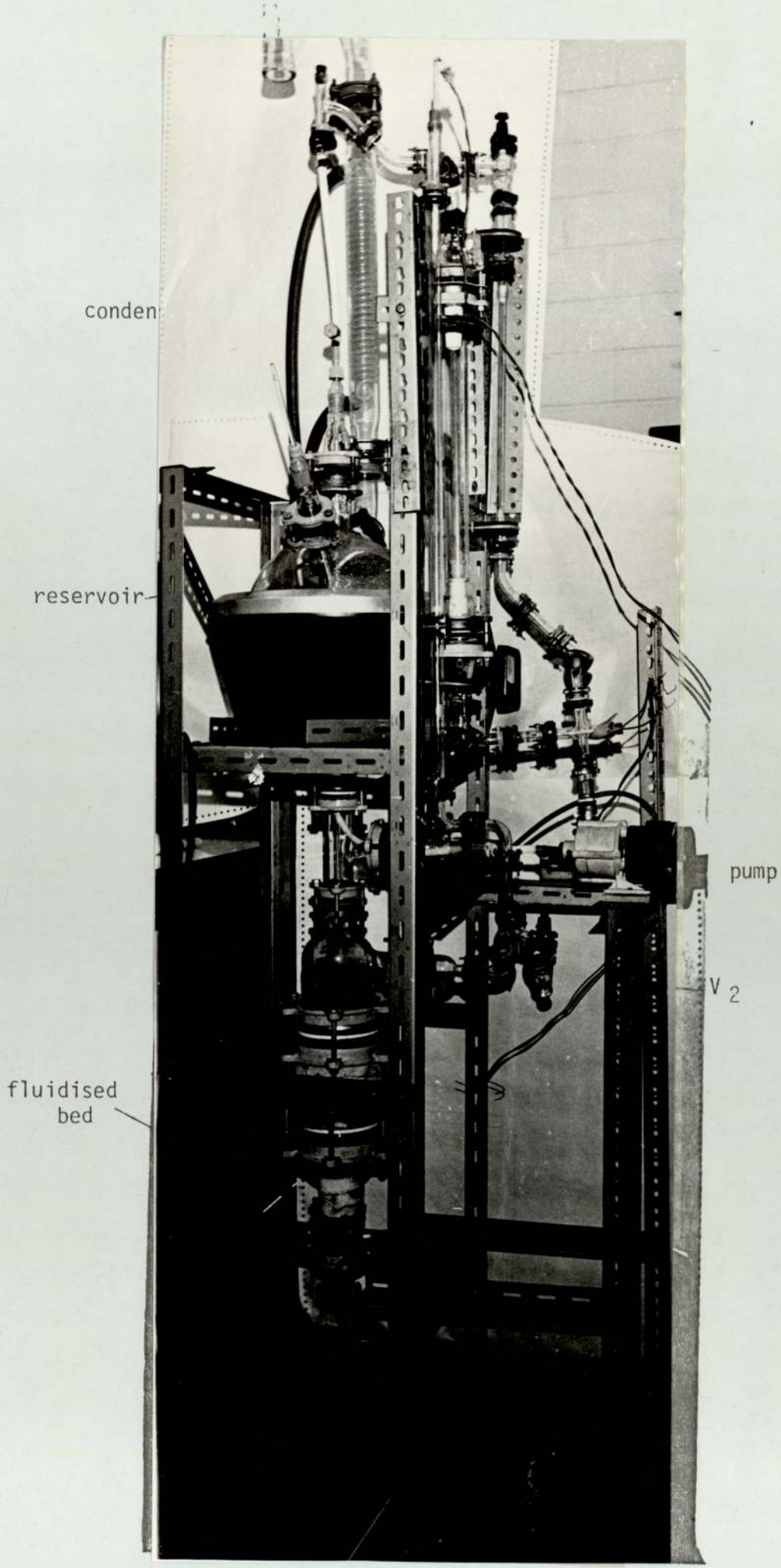

F.7.4. Reactor No. 6 (Fluidised Bed)

7.4.1 Experimental procedure

Predetermined amounts of Urea, acid (HCl) and Barium chromate are introduced into the system through the recycle RC2 at value V_4. The Tungsten particles are introduced through RC1 at value V_3, and they are taken by the flow to the fluidised bed (F). When the process is completed, value V_5 is closed and the crystals settle to the bottom of the fluidised bed.
They are then removed through value V_1.
Samples of the solution can be removed, during the process through outlet V_2. During operation V_5 is adjusted so as to maintain the flow rate through the RC1 at a value above the minimum fluidising velocity of the larger particles but below that which causes significant elutrication of the finest particles.

7.4.2. Errors and Limitations

The main limitation of the reactor No. 6 is the sensitivity of the process to the flow rate of RC1.
Other limitations are:

(i) The very high thermal capacity, causing initial start up delays. Graph G. 6. 14. presents a typical "run" and on it both the operating temperature and the starting up time may be seen.

(ii) The system can only operate when the level of the solution in the reservoir is above the pump intake.

The main source of errors originate in the indirect measurement of the controlling variables.

The pH of the solution is measured at the reservoir (not at the fluidised bed) and the supersaturation can be evaluated from a sample removed from V_2.

CHAPTER 8

CRITICAL EVALUATION OF THE PROJECT

8.1. Crystal growth models

In the previous chapters the data obtained from the crystallisation of Barium chromate were treated to a suitable form for mathematical analysis and a number of models were applied (Mc.Cabe law, bulk diffusion control using programmes EF20 and EF21). All however, failed to describe the obtained data satisfactorily, the reason being that the smaller particles appeared to grow faster contrary to the principles of the above-mentioned models. This led to the estimation of an empirical correlation (equ.E.6.2.) which did describe the data reasonably well (graphs G.6.8. and G.6.9.). The obvious advantages of such a correlation are that the units of the parameters are of no importance, since they can be accommodated in the constant (K) and that the values of the various exponents can indicate the behaviour of the process. (The negative exponent of L indicates that the smaller particles grow faster.) No population terms were included in the correlation (equation E.6.2.) since no reliable population data were available for all the conditions tested. The omission of such terms is justified in the next section (8.2) in which an alternative model is also suggested.

8.2. The stationary particle model

As it was suggested earlier, section 6.3.4., there is evidence to suggest that the smaller crystals produced by attrition or any other form of breeding grow much faster than the bigger ones and as a result the size distributions have no significant "tail" of very small particles ($L \leq 7.5\mu m$) for $t > 150$ seconds. This gave rise to the suggestion of an alternative model of growth. The model assumes the existence of one "stationary" particle inside a controlling volume of fluid (diagram D.8.1.) and considers the following steps

(i) The hydrolysis of Urea produces fresh material homogeneously which is stored as supersaturation

(ii) As the fluid moves around the particle it presents fresh material readily available for crystallisation.

(iii) The crystal incorporates the fresh material into its crystal lattice and it thus grows.

(iv) Excess fresh material which is not incorporated into the crystal creates points of local supersaturation and secondary nucleation thus

reducing the controlling volume.

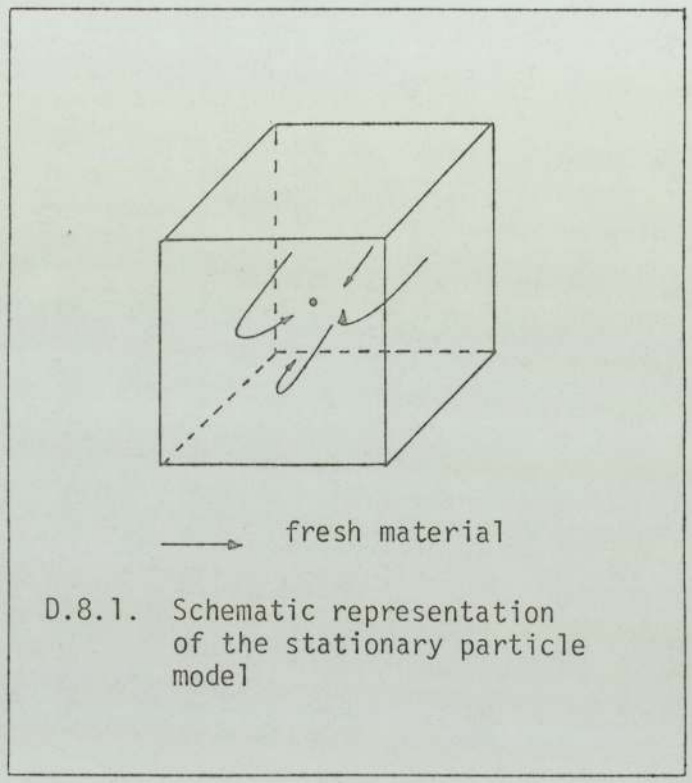

D.8.1. Schematic representation of the stationary particle model

By this model, the crystal is not competing for fresh material with the other bigger particles and it grows independently of its size (surface, velocity, etc.) Thus the smaller crystals grow faster since they have equal amount of material deposited on them.

The model is developed below.

Let dm be the mass released in a given time t=J-1 to t=J+1 and let the particles grow in size from $L_{i,J-1}$ to $L_{i\ J+1}$

$$dm = Km\left[\sum_{i=1}^{N_{J+1}} n_{i,J+1}\cdot L^3_{i,J+1} - \sum_{i=1}^{N_{J-1}} n_{i,J-1}\ Li^3,_{J-1}\right] \qquad \text{E.8.1.}$$

But
$$\sum_{i=1}^{N_{J+1}} n_{i,J+1}\ L^3_{i,J+1} = N_{J+1}L^3_{J+1} \qquad \text{E.8.2.}$$

and
$$\sum_{i=1}^{N_{J-1}} n_{i,J-1}\ L^3_{i,J-1} = N_{J-1}\ L^3{}_{J-1} \qquad \text{E.8.3.}$$

Km is constant

Li,J is the size of particles of interval i at time J

L_J is the mass mean particle of the distribution at time J

$n_{i,J}$ is the population of particles of interval i at time J

N_J is the total population of the distribution at time J.

$$\therefore\ dm = Km\left[N_{J+1}\ L^3_{J+1} - N_{J-1}\ L^3_{J-1}\right] \qquad \text{E.8.4.}$$

By changing the subscripts to differentials

$$\frac{\partial m}{\partial t} = Km\ \frac{(N+\partial N)(L+\partial L)^3 - NL^3}{\partial t} \qquad \text{E.8.5.}$$

by ignoring small terms

$$\frac{\partial m}{\partial t} = Km\left[\frac{NL^3 + 3L^2N\partial L + L^3\partial N - NL^3}{\partial t}\right] \qquad \text{E.8.6.}$$

$$\therefore \quad \frac{\partial m}{\partial t} = Km \left[3L^2 N \frac{\partial L}{\partial t} + L^3 \frac{\partial m}{\partial t} \right| \qquad \text{E.8.7.}$$

The term $\frac{\partial m}{\partial t}$ is proportional to the driving force $\frac{C-C_s}{C_s}$ and the other parameters (R.6.3.).

However, in order to test the validity of such a model the term $\frac{\partial m}{\partial t}$ is equated to the other major controlling parameters by an empirical correlation of the form :

$$\frac{\partial m}{\partial t} = Km_1 L^{\bar{a}} pH^b R^f \left(\frac{C-C_s}{C_s}\right)^n N^p \qquad \text{E.8.8.}$$

substituting E.8.7.

$$\frac{\partial L}{\partial t} + \frac{L}{3N} \frac{\partial N}{\partial t} = Km_2 L^{\bar{a}-2} pH^b R^f \left(\frac{C-C_s}{C_s}\right)^n N^{p-1} \qquad \text{E.8.9.}$$

The above equation however cannot be examined accurately since no population values are available except for the standard conditions.

Therefore the following simplification is made. The additive effect of the term $\frac{L}{3N} \frac{\partial N}{\partial t}$ on the L.H.S. of equation E.8.9. is assumed to be equal to the multiplicative effect of the term N^{p-1} on the R.H.S. Thus equation E.8.9. is simplified to :

$$\frac{dL}{dt} = Km_2 L^{\bar{a}-2} pH^b R^f \left(\frac{C-C_s}{C_s}\right)^n \qquad \text{E.8.10.}$$

which is the empirical correlation E.6.2. presented in Chapter 6 where the value of $\bar{a}$ was found to be

approximately zero and so was the value of b. The value of n can be taken as approximately equal to 1.

Therefore equation E.8.8. reverts to

$$\frac{\partial m}{\partial t} = Km_3 \cdot \frac{C-C_s}{C_s} \qquad \text{E.8.11.}$$

for a constant speed of agitation and constant population.

The above simplification can be justified if the following identity is valid :

$$\frac{\partial L}{\partial t} + \frac{L}{3N}\frac{\partial N}{\partial t} \equiv N^{p-1}\frac{\partial L}{\partial t} \qquad \text{E.8.12.}$$

or

$$\frac{\partial N}{3N(N^{p-1}-1)} = \frac{\partial L}{L} \qquad \text{E.8.13.}$$

In fact equation E.8.9. can be solved for the standard conditions and the value of p is estimated to be $p = 3.05 \pm 0.2$. However, since the application of the regression technique on one set of conditions does not necessarily produce a "fair" correlation, the solution of equation E.8.13. is presented in graph G.8.1. for selective values of P in the region 1 to ∞. (The higher the value of P the more prominent the effect of secondary nucleation).

Equation E.8.13. is integrated numerically using programme EF24.

Nm and Lm are the constants of integration and also the intersection of the solutions ($1<p<\infty$). As p approaches 1 the uncertainty in the integral form of equation E.8.13. increases (as indicated by the shaded area for p=1.5).

It should also be noted that for $p<2$ the position of the line (area) representing the solution of equation E.8.13. does not move significantly (the case of p=1.5 is chosen as a typical one to approximately indicate the position of all the solutions for $1<p<2$.

The significance of graph G.8.1. is however, the fact that equation E.8.13. can represent the experimental data within experimental error irrespective of p($1<p<\infty$). Thus it can be concluded that equation E.8.13. is valid and so is therefore the earlier made simplification that the effect of the two terms involving the population are self-compensating (equation E.8.9.).

8.3. Discussion

As it was seen in the previous section (8.2.), although there is considerable secondary nucleation, there is no need to include a population term in an empirical or theoretical correlation (equation E.6.2.). In fact, the effect of nucleation is accounted for by the length (equation E.2.6.) and this is possibly the reason for the often made assumption, that the population distributions do not change shape with time. Although these assumptions are not strictly valid, they

do not affect the treatment of the data, because the population terms are self-compensating and the effect of secondary nucleation is accounted for through the other parameters of the process.

It is also worth noting that the positive value of p ($1<p<\infty$) shows that secondary nucleation is a function of the total population as well as of the supersaturation which is in agreement with the experimental evidence (graph G.6.13.) as well as with the conclusion drawn by Strickland-Constable (R.2.30.). The integration technique used in programme EF24 yields fairly large round-off errors as the value of p decreases (graph G.8.1.). In the present work, however, no attempt is made in finding either the exact solution of equation E.8.13. for selective values of p nor evaluating the value of p, but rather to identify a general trend which would enable conclusions to be drawn about the process of crystallisation in general and that of Barium chromate in particular.

Therefore, although the position of the curves representing the solution of equation E.8.13. is not known with great certainty for low values of p (< 1.5) the overall trend indicates that equation E.8.13. is valid for $1<p<\infty$ and it can be used to describe the data of the standard conditions. Therefore the earlier made assumption about the cancelling effect of the population terms is also valid.

The difference in the values of the exponents obtained by the empirical correlation (equation E.6.16.) from the theoretical one (equation E.8.10.) can be attributed to experimental errors (chapter 9), as well as to the partial failure of the stationary particle model.

Indeed no crystallisation process obeys a single model but rather the laws and effects of one model tend to be more prominent than those of the others.

G.8.1. Graph relating the total population to the characteristic length (L) of the mean particle for the standard conditions.

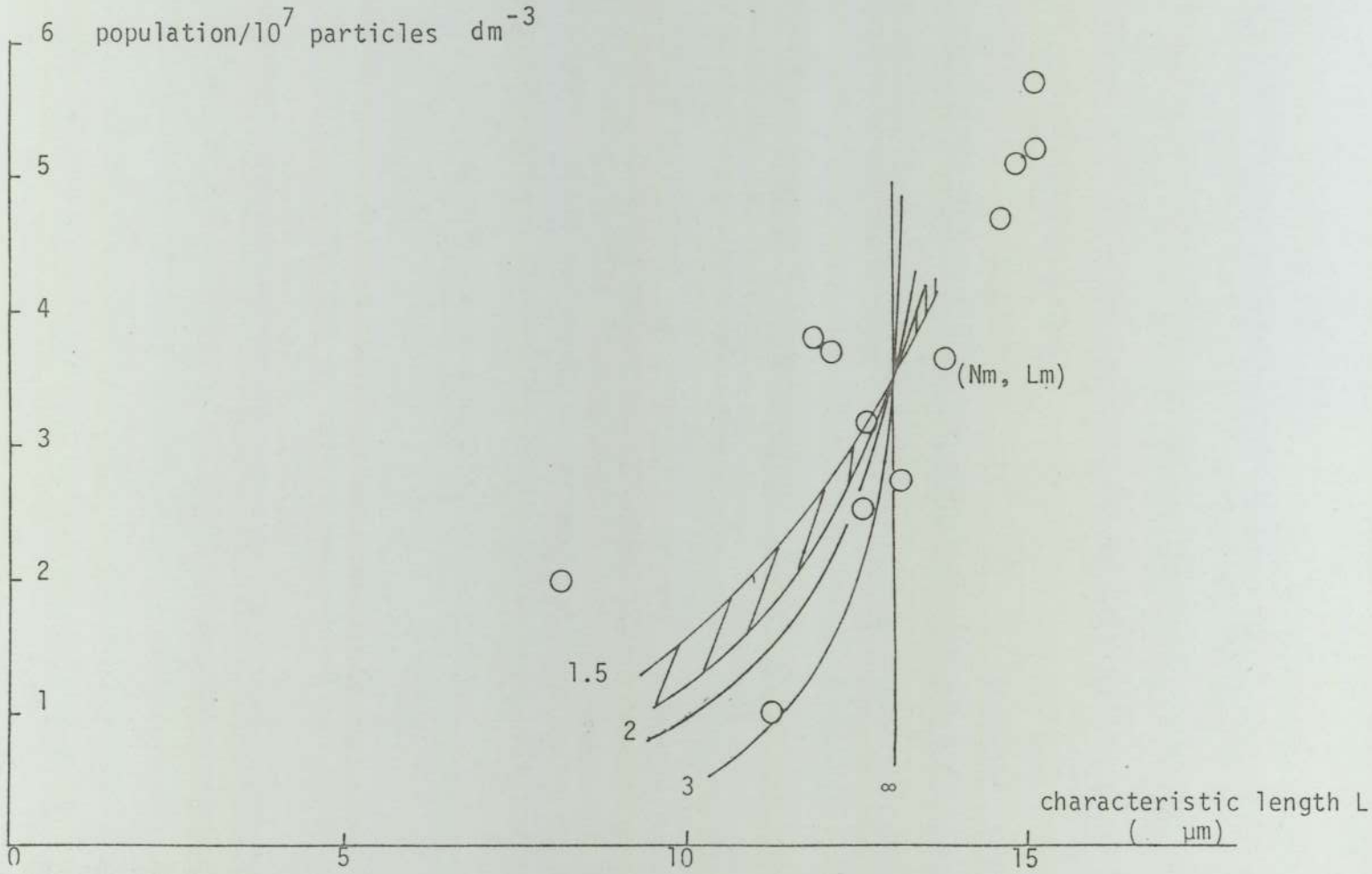

CHAPTER 9

SENSITIVITY ANALYSIS

The effect of errors on any correlation, empirical or theoretical, is important, in particular in understanding the extent to which the conclusions can be applied to similar cases.

Errors from all sources can be assumed to be of two types:

(i) Random errors, which are usually produced due to the limitations of the experimental techniques and methods.

(ii) Systematic errors, which are produced either because of the simplifications and the approximations which are assumed in the treatment of data or because of some fault in equipment, sequence of events, etc.

To study their effect, fictitious data can be used which are evaluated from the experimental ones after they have been modified by an error function.

$$X_{fi} = x_i \, f_i(e) \qquad \text{E.9.1.}$$

X_{fi} = the ith fictitious data

x_i = the ith experimental data

$f_i(e)$ = the error function at i.

For the case of $f_i(e) = 1$

$$X_{fi} = x_i \qquad \text{E.9.2.}$$

Usually $f_i(e)$ is a probability distribution of specified shape, mean value ($\bar{\mu}$) and variance (σ^2).

$$f_i(e) = \frac{1}{\sqrt{2\Pi\,\sigma^2}} \qquad \exp\left[-\frac{(f_i(e)-\bar{\mu})^2}{2\sigma^2}\right] \qquad \text{E.9.3.}$$

9.1. Random errors

The least squares method of describing experimental data by fitting an appropriate type curve greatly eliminates the random errors (R.9.1.). Random errors or scattering of the results can be achieved by setting accordingly the $\bar{\mu}$ and σ^2 of the $f_i(e)$ to:

$$\left.\begin{aligned}\bar{\mu} &= 1\\ \sigma^2 &\neq 0\end{aligned}\right\} \qquad \text{E.9.4.}$$

9.2. Systematic errors

Two types of systematic errors can be distinguished:

(i) Constant systematic errors. They can be produced by

$$\left.\begin{aligned}\bar{\mu} &= \text{constant}, \quad \bar{\mu}\neq 1\\ \sigma^2 &= 0\end{aligned}\right\} \qquad \text{E.9.5.}$$

(ii) Varied systematic errors, by which the errors introduced are different for different parts of the date range

$$\left.\begin{aligned}\bar{\mu} &= g(i) \quad \text{and} \quad \bar{\mu} \neq 1\\ \sigma^2 &= 0\end{aligned}\right. \qquad \text{E.9.6.}$$

9.3. Systematic and random errors

These are a combination of the above

$$\bar{\mu} \neq 1 \qquad \text{E.9.7.}$$
$$\sigma^2 \neq 0$$

Random probability distributions are available through the Nottingham Computer Service (R.9.2.).

9.4. Solubility of Barium chromate

In chapter 5.the solubility of Barium chromate in acid solution was examined. The data obtained were used to evaluate the saturation (equilibrium) line which was in turn used to evaluate the driving force. The date and the reactor used were also recorded and this information was placed in a two-dimension matrix (programme EF19, Appendix 10) to examine whether a particular reactor(s) or a particular date(s) gave poor results (Output OUT.A10.1. is presented in Appendix 10 as a typical one).

It was found that all three reactors (1, 2 and 3) were not very accurate (graph G.3.2.) while reactor 4 was less accurate still. Reactor 5 gave the most consistent results. Similarly, an examination of the dates showed that the data collected on certain dates were not consistent with previous results (OUT.A10.1.) A possible explanation is the electrical interference which affected the sp1800 Spectrophotometer (chapter 3) or some other failure of a part(s) of the experimental procedure.

Random errors were introduced into the data but their effect was not great, in particular for the cases shown in graphs G.3.2. to G.3.4., the reason being that due to the larger population of data the errors introduced were truly random. It is worth noting that although graphs G.3.5. to G.3.12. appear to have smaller scatter of data because of the small population involved, a true indication of the scatter can be seen when evaluating the concentration versus temperature graphs (G.3.13. to G.3.15.).

9.5. The hydrolysis of Urea

The conclusions drawn in chapter 5 about the hydrolysis of Urea suffer from relatively large experimental errors. In graph G.5.4. the natural logarithm of the slope is plotted against the natural logarithm of the concentration. The five-fold increase in the concentration is thus reduced to an 1.6 absolute increase in the $\ln \frac{dc_u}{dt}$ term. The scatter of the data suggests that the slope of the line is zero, which is however within the 1.6 increase in the $\ln \frac{dc_u}{dt}$ term.

For smaller time intervals ($t < 30$ s) the absolute value of the $\ln \frac{dc_u}{dt}$ is more accurately known and these data also suggest a horizontal line. However, for these small time intervals a more accurate method of evaluating the slope is required.

For different pH (>2.5) values the evaluated $\ln \frac{dc_u}{dt}$ terms also appear to suggest a horizontal line reducing thus the hydrolysis of Urea to a zeroth order. The scatter of the points however is increased further (Appendix 5).

The hydrolysis of Urea and the conclusions about the rate should be seen in the context of the crystallisation of Barium chromate and it appears that the growth of the crystals is not affected by the initial Urea concentration (chapter 6).

9.6. The parameters of the growth correlation

9.6.1. The characteristic length (L_c)

The characteristic length of a distribution is evaluated from counting a representative sample in the Coulter-Counter.

In the example presented in chapter 6 (Output OUT.6.1.) the total number of particles counted is ~ 1900 and the distribution has a variance of 6.8. The theoretical accuracy therefore for a 95% confidence limit (R.9.3.) is

$$L_c = \text{mean value} \pm 1.96 \times \text{standard deviation}$$

therefore $$L_c = \text{mean value} \pm 0.02\ (\mu m)$$

For smaller values of the variance the accuracy in the value of L_c is increased further while for lower populations it is reduced. For very small populations (N~ 200 particles) the accuracy in the characteristic length becomes unacceptable.

$$L_c = \text{mean value} \pm 1(\mu m)$$

For very high populations (N~5000) the accuracy suffers from high coincidence factor (Appendix 1).

The optimum count for a Coulter-Counter is $200 < N < 2000$ per sample.

The characteristic length (L_a) obtained by the Andreasen sedimentometer is significantly less accurate and based on reproduceability was estimated to be:

$$La = \text{mean value} \pm 1.5\ \mu m.$$

However, it is suspected that a greater source of error is the limitation of the instrument.

9.6.2. The linear growth rate

The linear growth term $\frac{dL}{dt}$ is evaluated by fitting a curve through the L vs. t data points.

Using the three term approximation (chapter 6) the evaluated value of $\frac{dL}{dt}$ and the experimental one differed by ~8% except immediately after nucleation when the difference is ~20%. Because the calculated length (L) at any time is evaluated by the three term approximation using the least squares method the reliability of the available data improves due to elimination of random errors and thus the term $\frac{dL}{dt}$ can be used with certainty.

For small time intervals (chapter 6) both numerical and analytical differentiation yields similar results.

9.6.3. Operating line

Although the product crystals were weighed to four decimal places the scatter of the data (graph G.6.4.) suggests that the operating line is not known with that great accuracy. However, the fitting of a four term polynomial (chapter 6) by the least square method permits the use of the operating line with greater certainty.

9.6.4. Population

Because of the small masses involved (analysed by the Coulter-Counter) the evaluation of the population appears to be the least accurately known. This is because of the

successive scalings involved in the evaluation of the total number of crystals in the crystallizer at any moment (Appendix 1).

In graph G.6.13.the population is plotted versus time and as it can be seen, the scatter is rather high, particularly at very early times (t<150s).

9.7. Sensitivity analysis performed on the overall growth correlation

In this section the empirical equation E.6.16. obtained in chapter 6 is subjected to both random and systematic errors. The resistance of the coefficients to errors will be an indication on the "fairness" of the equation. If the equation truly represents the experimental data, then it should not be affected significantly.

In Table T.9.1. the effect of random errors on the various parameters is shown. The data of the parameter to be examined are scattered and the regression analysis is performed on the modified data.

In Table T.9.2. the effect of a systematic error on the driving force is presented. The driving force is chosen as the parameter least accurately known.

In Table T.9.3. the effect of biased systematic error on the driving force is presented. The data points are modified in ascending order from 0 to 31%, 0 to 62% and 0 to 124% according to equation E.9.1.

$$\bar{\mu}_i = \bar{\mu}_{i-1} + \delta\bar{\mu} \qquad \text{E.9.1.}$$

$\delta\bar{\mu}$ takes the values of 0.005, 0.01 and 0.02 respectively.

		$\bar{\mu}=1$ $\sigma=0.15$			
	$\bar{\mu}=1$ $\sigma^2=0$	R	L	ΔC	$dL/_{dt}$
a	-1.486023±0.1336449	-1.384989±0.1493523	-1.306768±0.137929	-1.558747±0.1401836	-1.495668±0.1399727
f	1.168476±0.09952195	1.065983±0.1102176	1.063447±0.106437	1.202904±0.1054288	1.147064±0.104234
n	0.825472±0.1504978	0.8449542±0.1710879	0.9461617±0.1631324	0.6343416±0.1438849	0.8377622±0.1577625
K	-2.700060±0.2360212	-2.510251±0.2652130	-2.540137±0.2591935	-2.825549±0.2475272	-2.631297±0.2471962

Table T.9.1. Table presenting the effect of random error on the exponents of the parameters (where $K' = 10^K$ of equation E.6.16.)

	$\sigma^2=0$ $\bar{\mu}=1$	$\sigma^2=0$ $\bar{\mu}=1.2$	$\sigma^2=0$ $\bar{\mu}=1.4$	$\sigma^2=0$ $\bar{\mu}=1.6$
a	-1.486023±0.1336449	-1.486023±0.1336449	-1.486023±0.1336449	-1.486023±0.1336449
f	1.168476±0.09952195	1.168476±0.09952195	1.168476±0.09952195	1.168476±0.09959195
n	0.825472±0.1504978	0.825472±0.1504978	0.825472±0.1504978	0.825472±0.1504978
K	-2.700060±0.2360212	-2.765422±0.2329083	-2.820685±0.2307242	-2.868556±0.2291737

T.9.2. Table presenting the effect on the exponents of a systematic error in the driving force (where $K' = 10^K$ of equation E.6.16.)

		Percentage bias/$\delta\bar{\mu}$		
	$\bar{\mu}=1$ $\sigma^2=0$	31% /0.005	62%/0.01	124%/0.02
a	-1.486023±0.1336449	-1.529739±0.1333078	-1.58999±0.1327441	-1.734541±0.1327943
f	1.168476±0.09952195	1.194178±0.1006899	1.224758±0.1025655	1.28 459±0.1088592
n	0.825472±0.1504978	0.9655306±0.185978	1.067487±0.2227994	1.071565±0.2898799
K	-2.700060±0.2360212	-2.700171±0.2410697	-2.721103±0.2468998	-2.820694±0.2596505

Table T.9.3. Table presenting the effect on the exponents of a biased systematic error operating on the driving force.
(where $K' = 10^K$ of equation E.6.16.)

9.8. Discussion

Random errors (Table T.9.1.) appear to make no overall difference to the values of the exponents. A particular biased series of random numbers (Table T.9.1. column 3) might produce significant changes in the values of the coefficients (~25%) but this change is reduced significantly when the sensitivity analysis is performed with different series of random numbers. The systematic errors (Table T.9.2.) as expected, make no difference at all to the values of the exponents and only the value of the constant is changed accordingly, to accommodate the systematic error. It is worth noting however that as the absolute values of the parameters are increased, the confidence limit of the exponent becomes moderately smaller.

Biased systematic errors are the only kind of errors that appear to affect the relationship (Table T.9.3.) and perhaps they can be used to evaluate the error in the original data, assuming the value of the exponent is known. For the analysis on the driving force, which is presented as a typical one in table T.9.3., it can be seen that the value of the exponent n becomes larger as the values of the driving force become more biased towards the lower end (t>200 s).

In graph G.9.1. the magnitude of the bias is plotted versus the value of the exponent n, and for n=1 a biased error of 0 to 40% would be required (by interpolation $\delta\bar{\mu}$~0.007).

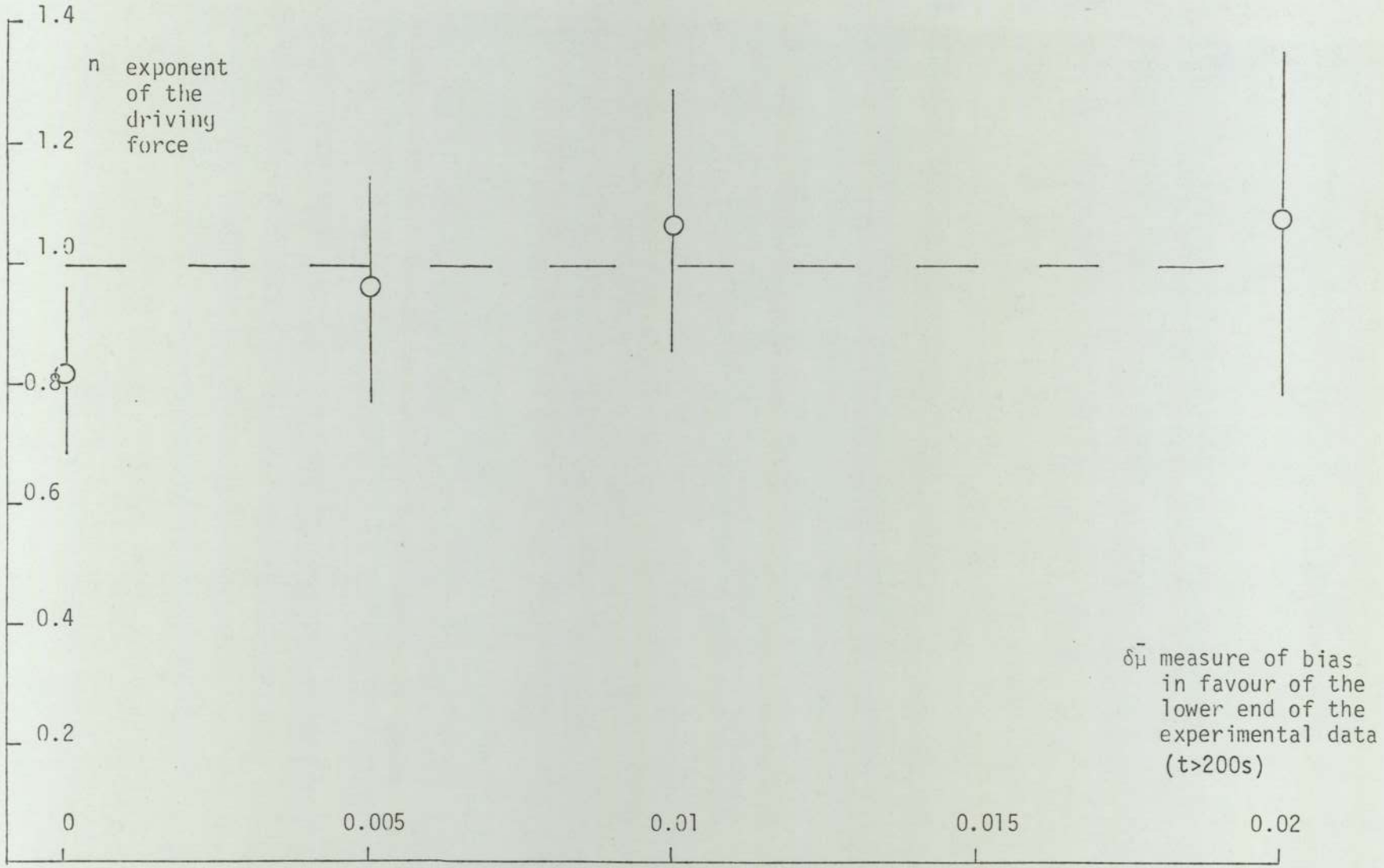

G.9.1. Graph relating the exponent n to the biased systematic error (Table T.9.3.) as the means of obtaining a possible measure of the experimental error.

CHAPTER 10

CONCLUSIONS

10.1. Conclusions

(i) The crystallisation of Barium chromate can adequately be described by an equation of the form: (chapter 6)

$$\frac{dL}{dt} = 2.1 \times 10^{-3} L^{-1.5} pH^{0.03} R^{1.2} \left(\frac{C-C_s}{C_s}\right)^{0.83} \qquad \text{E.6.16.}$$

(ii) In the crystallisation process the effect of the population terms tend to be self-compensating (section 8.2.)

(iii) Crystals of Barium chromate of shape similar to the {III} habit (photograph F.6.1.) can be produced using the Urea-hydrolysis technique (R.3.1.)

(iv) Epitaxial growth of Barium chromate crystals on a Tungsten substrate can be obtained in a system of gentle agitation (fluidised bed, chapter 7). The shape of the crystals, however, greatly depends on the type of Tungsten used (photographs F.6.4. and F.6.5.)

(v) The hydrolysis of excess Urea in acidic solution is a first order one reverting to a zeroth order as the solution is neutralized (chapter 5).

(vi) The solubility of Barium chromate is higher in HCl solution than it is in HNO_3 solution of the same strength and considerably higher when Urea is present (chapter 3).

10.2. Recommendations for future work

10.2.1. Fluidised bed studies and epitaxial growth

The fluidised bed (chapter 7) proved suitable for gentle agitation of the solution and thus suspension of the Tungsten particles. The type of epitaxial growth however was largely dependent on the type of Tungsten used and the impurities present (left from the metallurgical treatment of the metal powder). Future work should investigate the controlling parameters as well as the hydrodynamics of the fluidised bed.

10.2.2. Mathematical development of the stationary particle model with the aid of a digital computer

The partial failure of the stationary particle model, because of the competition of crystals, can be mathematically formulated into the model with the aid of a computer. The mathematical development should account for two and possibly three ways by which the model might fail, i.e. competition by the larger particles, excess fresh material resulting in secondary nucleation and a resistance in incorporating the fresh material into the crystal lattice.

APPENDIX 1.

The Coulter-Counter

Description

The instrument operates by allowing a control vacuum to draw the suspension through a Sapphire orifice and into a glass tube. Connected with it is a Mercury syphon which ensures both the constant suction and the reactivation of the electric circuit when a constant volume (0.05, 0.5, or 2 ml) has been drawn in. Immersed electrodes record the resistance as each particle passes through the orifice.

The resulting voltage is amplified and recorded. The number of all pulses greater than a certain size (threshold) is shown on an oscilloscope and on a digital counter. (R.A1.1.) and (R.A1.2.)

The manufacturer's recommended aperture size for a given particle distribution are presented in table T.A1.1. (R.A1.1.)

Largest particle (diameter in µm)	Aperture size (diameter in µm)
120	300
40	100
10	30

Table T.A1.1. presenting the recommended orifice for a given distribution

In this work, the largest particle was about 80 µm and a 280 µm orifice was used with a 2ml intake.

A 140 µm orifice was also used to check the instrument and the experimental technique.

The total volume of the suspension was 250 ml.

Calibration

A 16.6 µm diameter Sorrell Pollen standard calibration powder was used for most of the calibrations. The recommended ratio of the powder to the orifice is 5 to 20%. (R.Al.l.)

For the 280 µm orifice the 16.6 µm is 5.9%

140 " " " " 11.8%

Powders of different diameters (13.6 µm and 26.6µm) were also available. The recommended electrolyte is 1% NaCl.

In this work it was modified firstly to 1% NaCl with varied amounts of HCl and secondly, to 50/50 w/w of 2% NaCl H_2O /Glycerol. The dialectric constants of the resulting solutions were well above the limit set by the manufacturers.

The calibration performed on the 22nd February 1979 is presented as a typical one.

Current I = 6

Threshold t = 120

for the pulses to move above the 1 inch mark.

$t_{\frac{1}{2}}$ = 60 counts 9410

$t_{3/2}$ = 180 857

average 5134 t = 80 gives that count

Voltage measured at t = 10 is 25 volts

Resistance $R = \frac{65000 \times 25}{300 - 25}$ = 6 KΩ

K' = calibration factor = $\frac{16.6}{\sqrt[3]{80 \times 0.0323}}$ = 12.1

Diameters	$(d/K')^3$	I	t_1
2.5	0.0088	9	1.26
7.5	0.62	9	27.1
12.5	1.102	6	34.1
17.5	3.02	4	93.7
22.5	6.42	4	50.95
27.5	11.7	4	93.2
etc.			

T.A1.2. presenting the current and threshold setting calibrated for 5, 10, 15 µm etc.

Errors associated with the Coulter-Counter

1) Coincidence counts.

This is probably the most frequent error. It is overcome by keeping below the 10% coincidence limit and modifying the count obtained by the coincidence factor. For a 280 μm and 2 ml intake the manufacturers (R.A1.1.) recommend a 13.72 % coincidence correction.

2) Heavy particles settling inside the tube.

Although the flow is in one direction only and therefore these particles cannot cross the orifice in the reverse direction, they might become suspended by the jet action of the intake and move into the sensitive area.
This can be overcome by frequently cleaning the tube during the measurement of a sample by the procedure recommended. (R.A1.1.)

3. Oversized distributions

This is an error which many workers have identified but have explained differently.
Allen (R.A1.1.) suggests that it is due to the thin layer which surrounds each particle and increases its resistivity.
Mullin (R.A1.5) offers a similar explanation.
Rogers proposes a correction which is mainly applicable to the larger particles. (R.A1.4.).

In the present work this error is explained as the difference between an irregular particle from a spherical one. The instrument measures conductance and in effect an equivalent diameter. Particles of equal volume but of different

masses would be counted as similar and thus the resulting distribution would be oversized.

To accommodate for the error the following correction was made. The total weight of the distribution is compared with the true weight and if they differ by more than a set limit, each size increment is reduced (or increased) by a factor.

$$\text{Error} = (Mt - Me)/Mt \qquad \text{E.A1.1.}$$

Mt is the true mass

Me is the effective mass

$$Me = K.\sum_{i=1}^{N} Ni \; dij \; . \; pcj$$

i is the size increment

j is the optimizing step

Ni is the population at i

dij is the diameter at i and j

pc is the correcting factor at j

K' is a constant (density etc.)

t_L is the tolerance limit

The following flow diagram presents the optimization which is included in programme EF17.

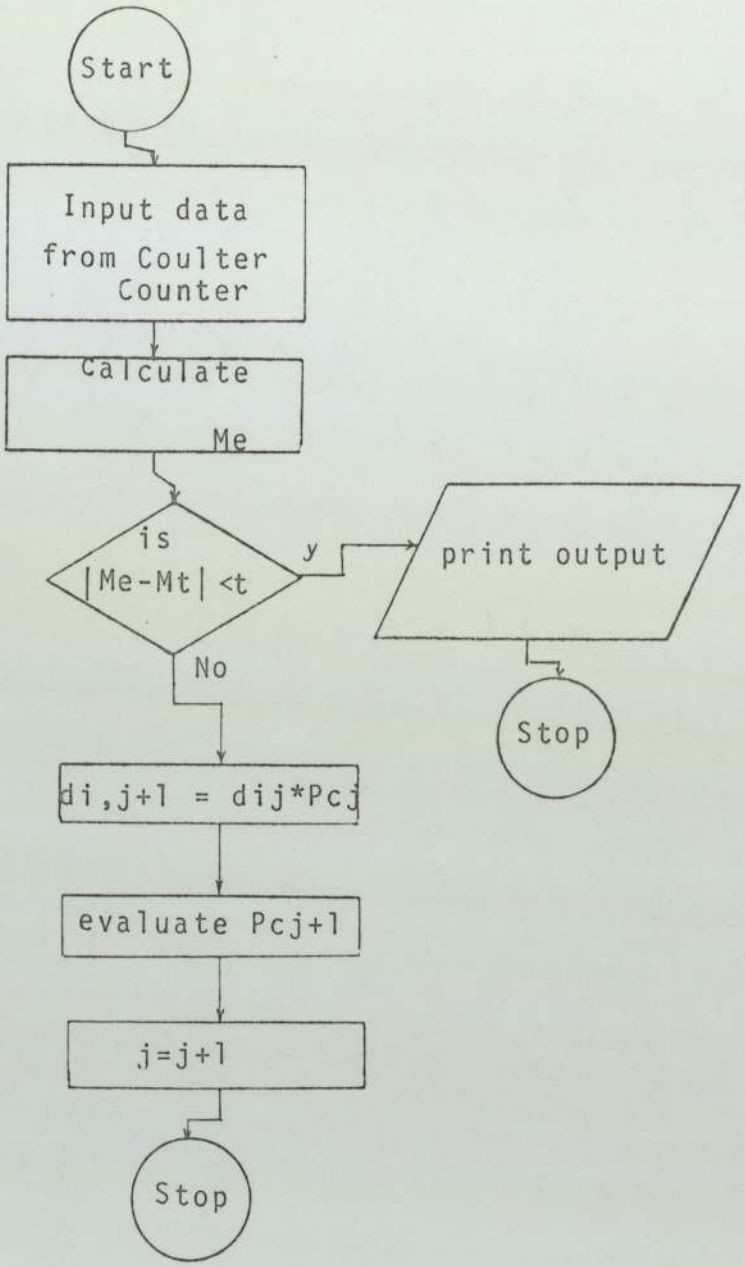

D.A1.1. Logical flow diagram of the optimisation method

The corrections obtained compare favourably with those obtained by Rogers (R.A1.4.) especially for particles below 60 μm.

The optimisation method used is the dichotomy one. This involves the discovery of an upper and a lower limit in between which the optimum exists.

This average value is calculated and one of the limits is substituted by it (depending on which side of the optimum it lies). (R.A1.6). The average of the new limits is calculated and the process is repeated until the optimum has been approached.

Measures taken for collecting accurate results

1) Following the recommended procedure R.A1.1.
2) Positioning the machine in a place free of vibration and dust and operating it when the electrical noise was minimal.
3) Keeping the time of the analysis to a minimum, due to the current passing through the temperature of the solution being increased, especially when counting the heavier particles.
4) Counting the heavier particles first.
   The fall in the level of the electrolyte in the 250 ml beaker resulted in bubble formation by the stirrer. To terminate this the speed of the stirrer was decreased which resulted in the settling of the heavier particles.
   The problem of the suspension has been encountered by many workers.
   Yarde (R.A1.7) makes use of stirrers with four blades placed in pairs. A U-shaped vessel is also suggested.
   Bugay et al (R.A1.8) recognized the harmful effect of over-stirring, and suggested that this not only creates bubbles, but also decreases the "layer" which surrounds each particle.

APPENDIX 2

The Andreasen Sedimentometer

Description

The Andreason (R.A2.1), (R.A2.2.) apparatus is a pipette sedimentometer of a vertical cylinder in which the dispersion is originally shaken up and allowed to settle. 10 ml samples of the suspension are withdrawn at different times. The water is completely removed from the samples by evaporation and the weight of the solids is measured.

Assuming that the particles fall with terminal velocity and that the interaction between them is negligible, then the diameter can be calculated from Stoke's Law. Stokes suggested that the force exerted on a particle by the viscous forces of the fluid is (R.A2.3.)

$$\text{force} = 6.\Pi.\, r.\mu V \qquad \text{E.A2.1.}$$

For a sphere falling under the influence of gravity is

$$\text{force} = \frac{4}{3}\Pi.\; r^3(\rho_{s_l}-\rho_{f_l})g \qquad \text{E.A2.2.}$$

At terminal velocity the two forces are equal

$$6.\Pi.\, r.\mu.V = \frac{4}{3}\Pi\; r^3(\rho_{s_l}-\rho_{f_l})g$$

$$\text{or} \quad d_i = \sqrt{\frac{18V}{g}\mu/(\rho_{s_l}-\rho_{f_l})} \qquad \text{E.A2.3.}$$

The velocity of the falling particle is obtained by measuring the height of the fluid and the time that has been taken from the beginning of the experiment. A plot of di against the corresponding weight of the particles collected at sample

i will give a cumulative weight distribution of the material.

Errors associated with the method

1) The analysis must be preceded by violent agitation, not by stirring since this imparts a centrifugal motion to the suspension (R.A2.4.) Zero time is when the agitation stops but the particles do not rest immediately.

2) The sample is withdrawn not instantaneously and therefore the size of the largest particle will vary throughout the sampling time.

3) The sucking action of the pipette draws small particles which are not necessarily near the intake point. Furthermore, the region immediately below the pipette is deficient in solids and the intake is not from a narrow cylindrical element but from a balloon around the entrance of the intake.

4) By far the highest source of error is the failure of the Stokes' Law. If the particles are too small they "slip" through the fluid. If they are too large, turbulence occurs (R.A2.3.)

The Reynold's number as defined below gives an indication as to whether the Stokes' Law is valid.

$$Re = (\rho_{s_l} - \rho_{f_l}) \frac{V \cdot d}{\mu} \qquad E.A2.4$$

Re must be <1 and preferably ~0.1 to ensure "creeping" flow. It was found that 50/50 w/w H_2O/ Glycerol produced Re numbers as required.

5) A small amount of liquid is retained in the pipette and this reduces the intake volume of the next sample.

6) If the particle concentration is sufficiently large, then the particles do not have a free fall. They form "clouds" which drag and are dragged by the fluid (R.A2.3.)

Evaluation of the sphericity of a particle

The Andreasen sedimentometer, which measures a diameter based on the area can be used in association with the Coulter-Counter which measures the diameter based on mass, to evaluate the sphericity of the particle.

Because the particle is not spherical, it will fall under highest drag (R.A2.7.) and thus it will give the impression of a smaller particle falling more slowly than a bigger one.

Sphericity is defined as $\left(\frac{\text{area diameter}}{\text{volume diameter}}\right)^2$ E.A2.5.

Thus, by direct comparison of the mean values the sphericity of the crystals is evaluated.

In this appendix the symbols used are

		r	radius of partical
ρ_{s_1}	density of solids	μ	viscosity
ρ_{f_1}	density of fluid	g	gravity constant
		V	terminal velocity

APPENDIX 3

Lattice Mismatch between Barium chromate and Tungsten

When epitaxial growth is attempted the lattice mismatch should be as small as possible and certainly less than 20% (R.A3.1.). The Tungsten interatomic distance for the a-form is $\alpha_o = 3.165$ Å (25^oC). The shortest interatomic distance (corner to centre atom) is $\alpha_o \frac{\sqrt{3}}{2}$ or 2.741Å and the greatest distance (face diagonal is $\alpha_o \sqrt{2}$ or 4.476 Å (Chapter 4). However, if alternate Tungsten atoms are considered then the rows through the diagonals through the body centred atoms have atomic spacings of 2 x 2.741 = 5.482Å. This is only 0.8% smaller than the Barium-chromate bo value. Similarly, the face diagonal row has alternate Tungsten atom spacings of 2X4.476 = 8.252 Å which is less than 2% than the Barium chromate a_o value. However these two rows are at 35.26^o to one another, whereas in the Barium chromate they are at right angles.

APPENDIX 4

Computational aspects for the distribution of Barium chromate crystals

Programme EF17 performs all the necessary calculation and evaluates the various statistical parameters of the distributions, as presented in OUTput OUT.6.1.

Flow diagrams D.A4.1. and D.A4.2. present the main steps of the programme and the subroutines used for processing the results from the Coulter-Counter respectively OUTput OUT.A4.1. lists programme EF17 including its subroutines.

D.A 4.1. Logical flow diagram of programme EF 17

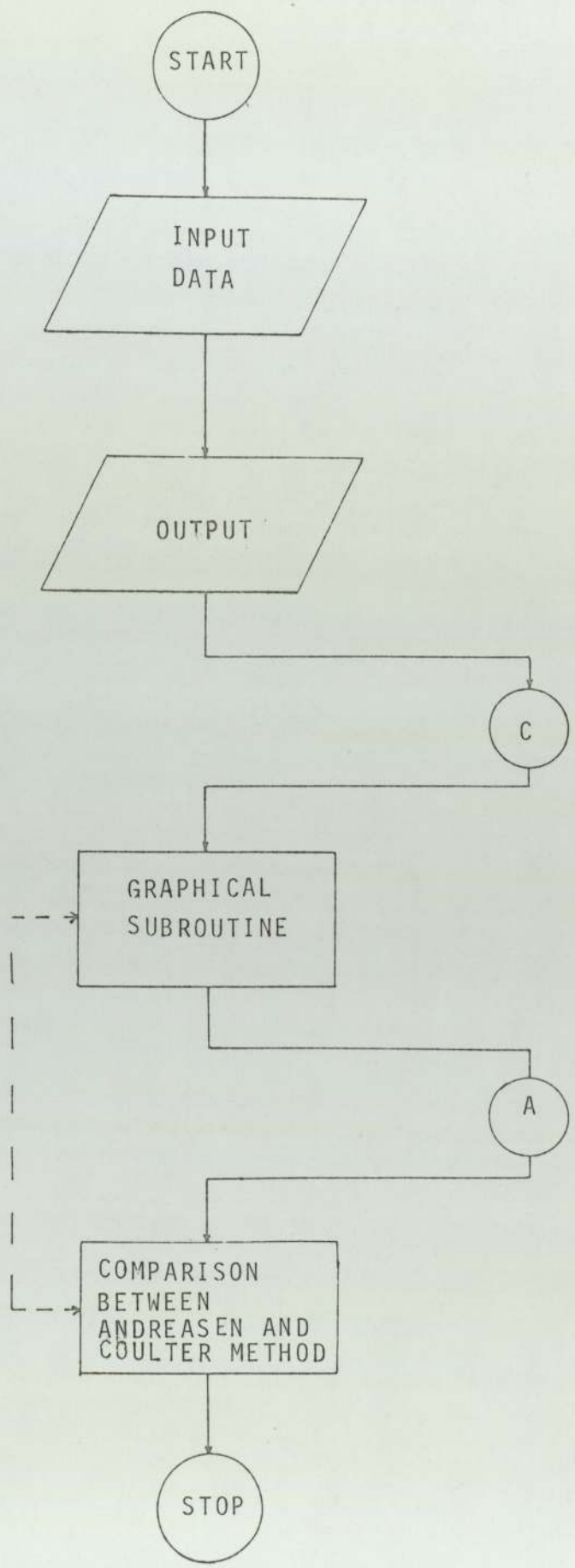

G.A.4.2. Logical flow diagram of Coulter-Counter subroutine

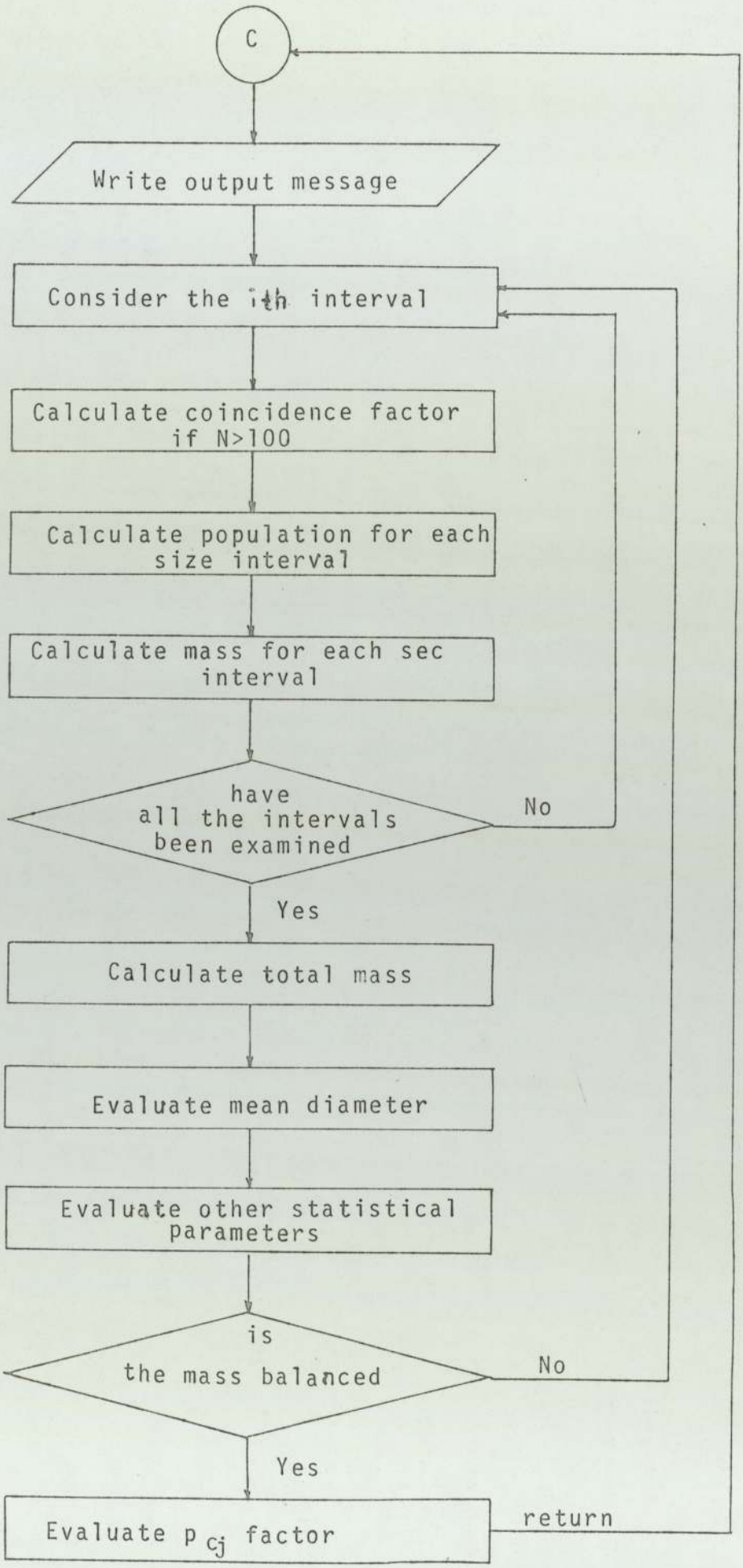

OUT A41

```
0012                TRACE 1
0000                TRACE 2
0001                MASTER EF17
0002                CALL OPENGINOGP
0003                CALL DEVPAP(1500.,720.,1)
0004                DIMENSION CUMASS(20)
0005                DIMENSION DDIAM(20)
0006                DIMENSION DDDIAM(20)
0007                DIMENSION ADIAM(20),ACUWET(20)
0008                DIMENSION CALCT(100),CALCY(100)
0009                DIMENSION DIFF(20)
0010                DIMENSION DIAM(20),AN(20,5),AV(20)
0011                DIMENSION DG(30)
0012                DIMENSION TIME(20),PH(20),VOLUME(20)
0013                DIMENSION A(10,10)
0014                DIMENSION AA(10)
0015                DIMENSION Y(30),X(30,5)
0016                DIMENSION VAR(20),SCEW(20)
0017                REAL MODE(20)
0018                REAL MASS(20),MASSFR(20),MEAN(20)
0019          C
0020          C
0021                N=10
0022                N=11
0023                N=12
0024          C
0025                XOR=100.
0026          C
0027          C
0028                READ(1, 4)NSAMPL,NDATE,MONTH
0029                READ(1,6)(TIME(I),I=1,NSAMPL)
0030                READ(1,6)(PH(I),I=1,NSAMPL)
0031             6  FORMAT(50F0.0)
0032             4  FORMAT(10I0)
0033                WRITE(2,13)       NDATE,MONTH
0034            13  FORMAT(1HO,8X,'THIS SAMPLE'
0035              1'WAS TAKEN ON THE',I3,1X,
0036              1'OF',I3,2 X,'1979')
0037            75  FORMAT(1HO,55X)
0038                WRITE(2,75)
0039                WRITE(2,75)
0040                WRITE(2,75)
0041                WRITE(2,75)
0042                WRITE(2,15)
0043            15  FORMAT(1HO,8X,'NO',15X,'TIME',18X,'PH',15X,'VOLUME')
0044                WRITE(2,75)
0045                WRITE(2,75)
0046                DO 12 I=1,NSAMPL
0047                WRITE(2,11)I,TIME(I),PH(I)
0048            11  FORMAT(1HO,I10,6F20.2)
0049            12  CONTINUE
0050                CALL MASDIA (AN,N,NSAMPL,MEAN,VOLUME,XOR,MASSFR)
0051                CALL DEVEND
0052                STOP
0053                END

ND OF SEGMENT, LENGTH   172, NAME  EF17
```

```
0054                SUBROUTINE MASDIA(AN,N,NSAMPL,MEAN,VOLUME,XOR,MASSFR)
0055                DIMENSION DIFF(20)
0056                DIMENSION DIAM(20),AN(20,5),AV(20)
0057                DIMENSION CUMASS(20)
0058                DIMENSION DDIAM(20)
0059                DIMENSION DDDIAM(20)
0060                DIMENSION ADIAM(20),ACUWET(20)
0061                DIMENSION A(10,10)
0062                DIMENSION AA(10)
0063                DIMENSION Y(30),X(30,5)
0064                DIMENSION CALCT(100),CALCY(100)
0065                DIMENSION VAR(20),SCEW(20)
0066                REAL MASS(20),MASSFR(20),MEAN(20)
0067                REAL MODE(20)
0068                DENSIT=4.492
0069                NOREAD=2
0070                NOPTUM=2
0071                NOPTUM=10
0072                TOLERO=0.00005
0073                UPPER=1.
0074                BELOW=0.
0075                CACTOR=1.
0076                READ(1,41)WEIGHT,DIA
0077                DDIA=DIA
0078                DO 10 I=1,N
0079                DIAM(I)=DDIA
0080                DDIA=DDIA+5.
0081                DDIAM(I)=DIAM(I)
0082             10 CONTINUE
0083                READ(1,41)((AN(I,J),J=1,NOREAD),I=1,N-1)
0084             41 FORMAT(50F0.0)
0085                DO 100 II=1,NOPTUM
0086                WRITE(2,73)
0087             73 FORMAT(1H1,10X,'VALUES OF N',8X,'AVERAGE',10X,'DIFFER
0088               2,09X,'MASS  ',10X,'MASSFR',08X,'DIAMETER')
0089                DO 40 I=1,N-1
0090                AV(I)=(AN(I,1)+AN(I,2))/NOREAD
0091                IF(AV(I) .GT. 100. ) AV(I)=AV(I)+(AV(I)/1000.)*13.78
0092             40 CONTINUE
0093                WRITE(2,75)
0094                WRITE(2,75)
0095                AMASST=0.
0096                DO 50 I=1,N-2
0097                DIFF(I)=-AV(I+1)+AV(I)
0098                MASS(I)=DIFF(I)*  ((DIAM(I+1)/2.*10.**(-4.))**3.) *
0099               4(250./2.)*(DENSIT*3.14*4./3.)
0100                AMASST=AMASST+MASS(I)
0101             50 CONTINUE
0102                MEAN(II)=0.
0103                DO 60 I=1,N-2
0104                MASSFR(I)=MASS(I)/AMASST
0105                MEAN(II)=MEAN(II)+MASSFR(I)*DIAM(I+1)
0106             60 CONTINUE
0107                VAR(II)=0.
0108                DO 65 I=1,N-2
0109                VAR(II)=VAR(II)+(MASSFR(I)*(DIAM(I+1)-MEAN(II))**2.)
0110             65 CONTINUE
0111                VAR(II)=VAR(II)/(N-2)
0112                MODE(II)=0.
0113                DO 68 I=2,N-2
0114                IF(MASSFR(I)-MASSFR(I-1))68,68,67
0115             67 CONTINUE
0116                MODE(II)=DIAM(I+1)
0117             63 CONTINUE
0118                SCEW(II)=(MODE(II)-MEAN(II))/(VAR(II)**0.5)
```

```
0119                  DO 70 I=1,N-1
0120                  WRITE(2,71)      AN(I,1),AN(I,2),AV(I)
0121               71 FORMAT(1HO,1X,5F12.2)
0122                  WRITE(2,72)DIFF(I),MASS(I),MASSFR(I),DIAM(I+1)
0123               72 FORMAT(1HO,40X,F15.1,F15.4,F15.3,F15.2)
0124               70 CONTINUE
0125                  WRITE(2,75)
0126                  WRITE(2,75)
0127                  WRITE(2,75)
0128                  WRITE(2,74)MEAN(II),   AMASST,II
0129               74 FORMAT(1HO, 74X,
0130                 1'THE MEAN DIAMETER IS ',
0131                 2F5.2,81X,
0132                 8'TOTAL MASS IS',F8.4 ,2X,
0133                 9'GRAMMES', 70X,'NUMBER IS',I10)
0134                  WRITE(2,76) WEIGHT,CACTOR
0135               76 FORMAT(1HO,42X,'INITIAL ',1X,
0136                 1'WEIGHT IS ',F8.4,
0137                 5 13X,'REDUCING FACTOR IS',
0138                 6F5.2)
0139                  WRITE(2,77)VAR(II)
0140                  WRITE(2,78)SCEW(II)
0141               77 FORMAT(1HO,82X,'VARIANCE IS',F10.4)
0142               78 FORMAT(1HO,82X,'SCEWNESS IS',F9.4)
0143               75 FORMAT(1HO,55X)
0144                  IF(ABS(WEIGHT-AMASST).LT. TOLERO)GO TO 110
0145                  IF(AMASST .GT. WEIGHT) GO TO 90
0146                  BELOW=CACTOR
0147                  GO TO 98
0148               90 CONTINUE
0149                  UPPER=CACTOR
0150               98 CONTINUE
0151                  CACTOR=(UPPER+BELOW)/2.
0152                  DO 99 I=1,N
0153                  DIAM(I)=DDIAM(I)*CACTOR
0154               99 CONTINUE
0155              100 CONTINUE
0156              110 CONTINUE
0157                  CALL LINDA(N,MASSFR,XOR,DIAM,DIA
0158                 9,MASS,DIFF,WEIGHT,DDIAM)
0159                  RETURN
0160                  STOP
0161                  END

ND OF SEGMENT, LENGTH   736, NAME  MASDIA
```

```
0162                SUBROUTINE  LINDA(N,MASSFR,XOR,DIAM,DIA
0163               9,MASS,DIFF,WEIGHT,DDIAM)
0164                REAL       MASSFR(20)
0165                REAL MASS(20)
0166                DIMENSION ADIAM(20),ACUWET(20)
0167                DIMENSION DDIAM(20)
0168                DIMENSION DDDIAM(20)
0169                DIMENSION CUMASS(20)
0170                DIMENSION DIFF(20)
0171                DIMENSION DIAM(20)
0172                DIMENSION AA(10)
0173                DIMENSION Y(30),X(30,5)
0174                DIMENSION A(10,10)
0175                DIMENSION CALCT(100),CALCY(100)
0176          C
0177          C  PARAMETERS FOR SCALING AND PLOTTING THE GRAPHS
0178          C
0179                CALLCHASIZ(2.6,2.302)
0180                YOR=350.
0181                CALL TETRA(YOR,XOR)
0182                AYLEN=60.
0183                YBEG=0.
0184                YEND=600.
0185                NINTY=6
0186                DO 5 I=1,N
0187                DIAM(I)=DIAM(I+1)
0188                DDIAM(I)=DDIAM(I+1)
0189              5 CONTINUE
0190                CALL AXON(YOR ,XOR,AYLEN,YBEG,
0191               6YEND,NINTY)
0192                CALL GRASYM(DIAM,DIFF,N-1,5,0)
0193                CALL GRACUR(DIAM,DIFF,N-1)
0194                CALL GRACUR(DDIAM,DIFF,N-1)
0195                YOR=YOR-99.
0196                CALL TETRA(YOR,XOR)
0197                NINTY=3
0198                YBEG=0.
0199                YEND=0.3
0200                 AYLEN=60.
0201                CALL AXON(YOR ,XOR,AYLEN,YBEG,
0202               6YEND,NINTY)
0203                DO 7 I=2,N-1
0204                DDDIAM(I)=DDIAM(I-1)
0205              7 CONTINUE
0206                CALL HISTA(MASSFR,N-1,DDDIAM)
0207                YOR=YOR-99.
0208                CALL TETRA(YOR,XOR)
0209                YBEG=0.
0210                NINTY=WEIGHT*1.05*100.
0211                YEND=NINTY
0212                YEND=YEND/100.
0213                AYLEN=YEND*3000.
0214                CALL AXON(YOR ,XOR,AYLEN,YBEG,
0215               6YEND,NINTY)
0216                CALL GRAMOV(9.,WEIGHT)
0217                CALL GRALIN(60.,WEIGHT)
0218                CM=0.
0219                DO 10 I=1,N-1
0220                CM=CM+MASS(I)
0221                CUMASS(I)=CM
0222             10 CONTINUE
0223                CALL GRASYM(DIAM,CUMASS,N-1,2,0)
0224                CALL GRACUR(DIAM,CUMASS,N-1)
0225                CALL ANDREA(DIAM,CUMASS,N
0226               6,LIMITA, ADIAM,ACUWET)
```

```
0227                    CALL GRACUR(ADIAM,ACUWET,LIMITA)
0228                    CALL GRASYM(ADIAM,ACUWET,LIMITA,4,0)
0229                    DO 70 I=1,N-1
0230                    DIAM(1)=7.5
0231                    CUMASS(I)=(1.-EXP(DIAM(I)*AA(1)
0232                   1+DIAM(I)**2*AA(2)))*WEIGHT
0233                    DIAM(I+1)=DIAM(I)+5.
0234                 70 CONTINUE
0235                    DIAM(1)=10.
0236                    DO 80 I=2,N-1
0237                    MASS(I)=CUMASS(I)-CUMASS(I-1)
0238                    MASSFR(I)=MASS(I)/WEIGHT
0239                    DIAM(I+1)=DIAM(I)+5.
0240                    WRITE(2,78)MASS(I),MASSFR(I),DIAM(I)
0241                 78 FORMAT(1HO,10F10.2)
0242                 80 CONTINUE
0243                    XOR=XOR+210.
0244                    RETURN
0245                    STOP
0246                    END

ND OF SEGMENT, LENGTH   534, NAME  LINDA
```

```
 0247                     SUBROUTINE AXON(YOR ,XOR,AYLEN,
 0248                    7YBEG,YEND,NINTY)
 0249                     IYORY=2
 0250                     IXORY=1
 0251                     IOR=1
 0252                     AXLEN=120.
 0253                     XBEG=0.
 0254                     XEND=60.
 0255                     NINTX=12
 0256                     CALL AXIPOS (IOR,XOR,YOR,AYLEN,IYORY)
 0257                     CALL AXIPOS (IOR,XOR,YOR,AXLEN,IXORY)
 0258                     CALL AXISCA(1,NINTX,XBEG,XEND,IXORY)
 0259                     CALL AXISCA(1,NINTY,YBEG,YEND,IYORY)
 0260                     CALL AXIDRA(-1,-1,IYORY)
 0261                     CALL AXIDRA(1,1,IXORY)
 0262                     RETURN
 0263                     STOP
 0264                     END

END OF SEGMENT, LENGTH   121, NAME  AXON
```

```
0265                    SUBROUTINE TETRA(YOR,XOR)
0266                    CALL MOVTO2(XOR-65.,YOR-10.)
0267                    CALL LINTO2(XOR+145.,YOR-10.)
0268                    CALL LINTO2(XOR+145.,YOR+90.)
0269                    CALL LINTO2(XOR-65.,YOR+90.)
0270                    CALL LINTO2(XOR-65.,YOR-10.)
0271                    RETURN
0272                    STOP
0273                    END

END OF SEGMENT, LENGTH     80, NAME  TETRA


0274                     SUBROUTINE ANDREA(DIAM,CUMASS,N
0275                   6,LIMITA, ADIAM,ACUWET)
0276                     DIMENSION DIAM(20)
0277                     DIMENSION CUMASS(20)
0278                     DIMENSION ADIAM(20),ACUWET(20)
0279                     READ(1,12)LIMITA
0280                  12 FORMAT(10I0)
0281                     READ(1,15)((ACUWET(I),ADIAM(I)),I=1,LIMITA)
0282                  15 FORMAT(50F0.0)
0283                     DO 18 I=1,LIMITA
0284                     WRITE(2,19)ACUWET(I),ADIAM(I),I
0285                  19 FORMAT(1H0,2F10.2,I10)
0286                  18 CONTINUE
0287                     RETURN
0288                     STOP
0289                     END

ND OF SEGMENT, LENGTH    103, NAME  ANDREA


0290                     SUBROUTINE HISTA(MASSFR,N,DDIAM)
0291                     DIMENSION DDIAM(20)
0292                     REAL      MASSFR(20)
0293                     CALL GRAMOV(DDIAM(1)+2.5,0.)
0294                     DO 99  I=1,N-1
0295                     XX=DDIAM(I+1)-2.5
0296                     CALL GRALIN(XX,MASSFR(I))
0297                     CALL GRALIN(XX+5.,MASSFR(I))
0298                     CALL GRALIN(XX+5.,0.)
0299                  99 CONTINUE
0300                     WRITE(2,132)XOR
0301                 132 FORMAT(1H0,F10.2)
0302                     RETURN
0303                     STOP
0304                     END

ND OF SEGMENT, LENGTH    102, NAME  HISTA
```

APPENDIX 5

Computational aspects for the hydrolysis of Urea

Interpolation of the data

The method used for the interpolation of the data is the "average one". By this method the independent variable, time, is divided into convenient equal intervals, minutes, and the corresponding value of the dependent variables are estimated from the experimental data. In this case, NDATA numbers of points of time are available while the whole range is divided into LIMIT intervals (LIMIT>NDATA). This method has the obvious disadvantage that no account of the slope is taken on the interpolated values. However, this error is minimised by ensuring that enough data points were collected at the points of the curve where the slope changed considerably. This can be clearly seen in graphs G.5.1., G.5.2. and G.5.5 to G.5.7. where the NDATA are represented by the symbol ▽.

Programme EF 16 is used to perform all the necessary calculations. Output OUT.A5.1. presents the programme and the graphical subroutines associated with it while OUT.A5.2. presents a set of computed data for curve 2 Graph G.5.1. for selected time intervals, as a typical one. The logical flow diagram of the programme EF 16 is presented in D.A5.1.

In graph G.A.5.1. the zero order model is tested for selected values of pH.

D.A5.1. Logical flow diagram EF16

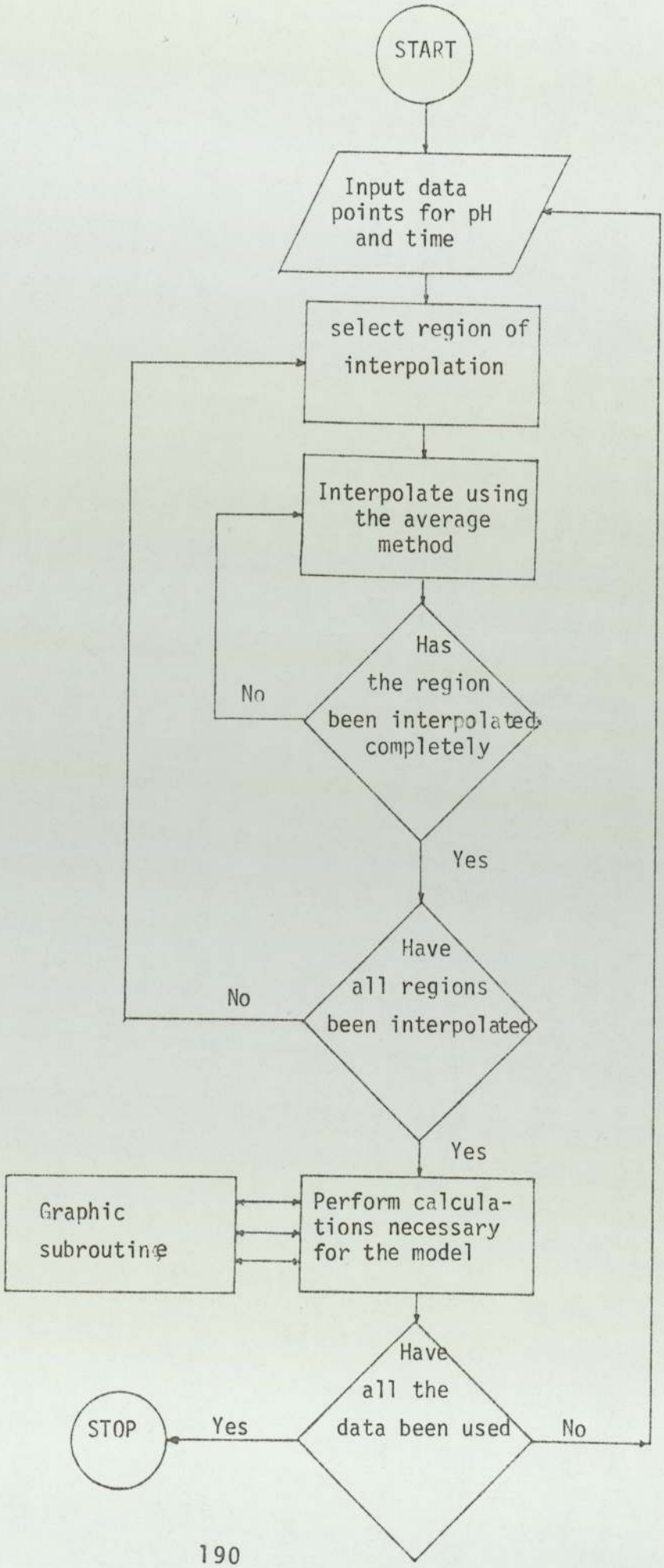

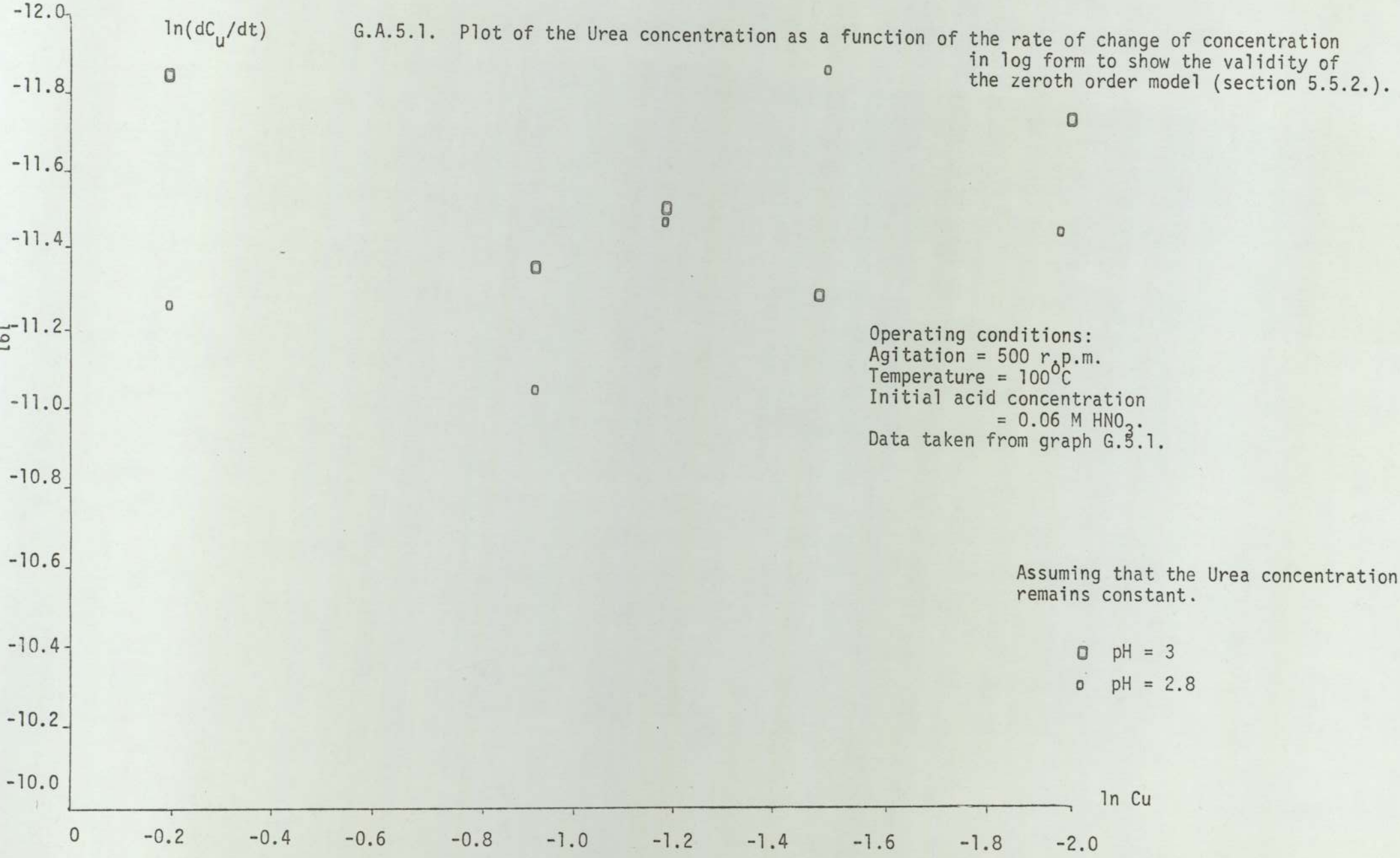

G.A.5.1. Plot of the Urea concentration as a function of the rate of change of concentration in log form to show the validity of the zeroth order model (section 5.5.2.).

```
0012                TRACE 1
0000                TRACE 2
0001                MASTER  EF16
0002                CALL OPENGINOGP
0003                CALL DEVPAP(1500.,720.,1)
0004                DIMENSION U(10),T(10)
0005                DIMENSION SLOPE(250)
0006                DIMENSION SS(250),CC(250)
0007                DIMENSION  HC(250,6),SL(250,6)
0008                DIMENSION S(250,6),C(250,6)
0009                DIMENSION UCONC(250)
0010                DIMENSION UUCONC(250)
0011                DIMENSION HCONC(250),TIME(250)
0012                DIMENSION CONST(9,150)
0013                DIMENSION HHCONC(60),TTIME(60)
0014                INTEGER LALA(10)
0015                INTEGER DATE
0016                CALL DARIA(XOR)
0017                LLL=3
0018                LLL=5
0019                YOR=200.
0020                DO 111 LL=1,LLL
0021                READ(1,2)NDATA,LIMIT ,DATE,MONTH
0022              2 FORMAT(12I0)
0023          C
0024          C     NDATA  THE NO. OF POINTS AVAILABLE FOR
0025          C            EVERY CURVE
0026          C
0027          C     LIMIT THE NO. OF POINTS NEEDED TO DRAW
0028          C           THE CURVE
0029          C
0030                READ(1,3)UREA,ACID,TEMP
0031                READ(1,3)((TTIME(J),HHCONC(J)),J=1,NDATA)
0032              3 FORMAT(5OF0.0)
0033                WRITE(2,5)
0034                WRITE(2,5)
0035                WRITE(2,5)
0036                WRITE(2,5)
0037                WRITE(2,4)DATE,MONTH
0038              4 FORMAT(1H1,35X,'THE DATE OF THE EXPERIMENT IS',
0039               4I3 ,'TH',I2,1X,'1978')
0040                WRITE(2,5)
0041                WRITE(2,5)
0042              5 FORMAT(1H0,5X)
0043                WRITE(2,6)
0044              6 FORMAT(1H0,35X,'OPERATING CONDITIONS')
0045                WRITE(2,5)
0046                UREA=UREA/60.06
0047                WRITE(2,7)UREA
0048                UREA=UREA*60.06
0049              7 FORMAT(1H0,35X,'THE CONC. OF UREA IS',F6.3,1X,'M')
0050                WRITE(2,8)ACID
0051              8 FORMAT(1H0,35X,'THE CONC. OF THE ACID IS',F6.3,1X,'M
0052                WRITE(2,9)TEMP
0053              9 FORMAT(1H0,35X,'THE TEMPERATURE IS',1X,F6.2,1X,'C')
0054                WRITE(2,5)
0055                WRITE(2,5)
0056                WRITE(2,21)
0057             21 FORMAT(1H0,36X,'TIME',11X,'PH', 9X,'UREA')
0058                DO 20 J=1,NDATA
0059                ITIME=TTIME(J)
0060                TIME(ITIME)=TTIME(J)
0061                HCONC(ITIME)=HHCONC(J)
0062                TTIME(J)=TTIME(J)*60.
0063                UUCONC(J )=UREA/60.06-(ACID-10**(-HHCONC(J)))/2.
```

```
0064              WRITE(2,46)TTIME(J),HHCONC(J),UUCONC(J)
0065              UCONC(ITIME)=UREA/60.06-(ACID-10**(-HCONC(ITIME)))/2
0066             20 CONTINUE
0067              DO 25 I=1,LIMIT
0068              TIME(I)=I
0069             25 CONTINUE
0070              DO 30 I=1,LIMIT
0071              IF(HCONC(I).GT.0.1)GO TO 30
0072              DO 35 II=I,LIMIT
0073              IF(HCONC(II).GT.0.1)GO TO 36
0074             35 CONTINUE
0075             36 CONTINUE
0076              HCONC(I)=HCONC(II)+(TIME(II)
0077            5-TIME(I))/(TIME(II)-TIME(I-1))*(
0078            UHCONC(I-1)-HCONC(II))
0079              UCONC(I)=UREA/60.06-(ACID-10**(-HCONC(I)))/2.
0080             30 CONTINUE
0081              CALL GRACUR(TTIME,HHCONC,NDATA)
0082              CALL GRASYM(TTIME,HHCONC,NDATA,2,0)
0083              WRITE(2,5)
0084              WRITE(2,5)
0085              WRITE(2,5)
0086              WRITE(2,5)
0087              WRITE(2,10)
0088             10 FORMAT(1H1,36X,'TIME',11X,'PH', 9X,'UREA',8X,
0089            6'SLOPE',10X,'K')
0090              DO 45 I=2,LIMIT   -1
0091              SLOPE(I)=(UCONC(I+1)-UCONC(I-1))/120.
0092              CONST(LL,I)=-SLOPE(I)/UCONC(I)
0093              IF(HCONC(I)-HCONC(I-1).LT.0.4)GO TO 41
0094              U(LL)=ALOG(UCONC(I))
0095              T(LL)=TIME(I)*60.
0096             41 CONTINUE
0097             45 CONTINUE
0098              DO 98 I=1,LIMIT
0099              S(I,LL)=TIME(I)*60.
0100              C(I,LL)=UCONC(I)
0101              LALA(LL)=LIMIT
0102              SL(I,LL)=SLOPE(I)
0103              HC(I,LL)=HCONC(I)
0104             98 CONTINUE
0105              DO 100 I=5,LIMIT,5
0106              WRITE(2,46)S(I,LL),HCONC(I)
0107            7,UCONC(I),SLOPE(I),CONST(LL,I)
0108             46  FORMAT(1H0,30X,9E13.3)
0109            100 CONTINUE
0110              DO 112 I=1, LIMIT
0111              HCONC(I)=0.
0112              UCONC(I)=0.
0113              TIME(I)=0.
0114            112 CONTINUE
0115            111 CONTINUE
0116        C
0117              WRITE(2,113)
0118            113 FORMAT(1H1,44X,'TIME IN SEC.',15X,'LOG C')
0119              DO 115 I=1,LLL
0120              WRITE(2,114)T(I),U(I)
0121            114 FORMAT(1H0,45X,F8.1,15X,F8.2)
0122              CALL MOVTO2(XOR+1.7*T(I)/60.,YOR+60.)
0123              CALL CHAINT(I ,3)
0124            115 CONTINUE
0125              CALL AMARA(XOR)
0126              CALL GRASYM(T,U,LLL,8,0)
0127              CALL GRACUR(T,U,LLL,8,0)
0128              AZ=2.
0129              DO 118 J=1,LLL
```

```
0130                    DO 116 I=1,LALA(J)
0131                    IF (HC(I,J).LT.AZ)GO TO 116
0132                    CC(J)=ALOG(C(I,J) )
0133                    SS(J)=S(I,J)
0134                    GO TO 118
0135                116 CONTINUE
0136                118 CONTINUE
0137                    CALL GRASYM(SS,CC,LLL,1,0)
0138                    CALL ZARA(XOR,LLL,LALA,SL,HC,C)
0139                    CALL DEVEND
0140                    STOP
0141                    END

END OF SEGMENT, LENGTH   915, NAME  EF16
```

```
0142                    SUBROUTINE DARIA(XOR)
0143                    YOR=200.
0144                    XOR=10.
0145                    IYORY=2
0146                    IXORY=1
0147                    IOR=1
0148                    AYLEN=140.
0149                    AXLEN=240.
0150                    YBEG=7.
0151                    XBEG=0.
0152                    YEND=0.
0153                    XEND=8000.
0154                    NINTY=7
0155                    NINTX=16
0156                    CALL PALOCA(XOR)
0157                    CALLCHASIZ(2.6,2.302)
0158                    CALL MOVTO2(XOR+150.,YOR-12.)
0159                    CALL CHAHOL(19HT*LIME IN SECONDS*.)
0160                    CALL MOVTO2(XOR+10.,YOR+135.)
0161                    CALL CHAHOL(6H*UPH*.)
0162                    CALL MOVTO2(XOR+10.,YOR+150.)
0163                    CALL CHAHOL(10H*UG.5.1.*.)
0164                    CALL MOVTO2(XOR+30.,YOR+150.)
0165                    CALL CHAHOL(27H H*LYDROLYSIS OF *UU*LREA*.)
0166                    CALL CHAHOL(21H *LIN ACID SOLUTION*.)
0167                    CALL MOVTO2(XOR+30.,YOR+145.)
0168                    CALL CHAHOL(25H*UC*LURVE OF *U P*LH OF*.)
0169                    CALL CHAHOL(22H *LTHE SOLUTION AS A*.)
0170                    CALL CHAHOL(21H*L FUNCTION OF TIME*.)
0171                    CALL CHAHOL(12H *LSHOWING*.)
0172                    CALL MOVTO2(XOR+30.,YOR+140.)
0173                    CALL CHAHOL(31H*LT*LHE EFFECT OF THE INITIAL*.)
0174                    CALL CHAHOL(25H *UU*LREA CONCENTRATION*.)
0175                    CALL MOVTO2(XOR+210.,YOR+137.)
0176                    CALL CHAHOL(26H*UO*LPERATING CONDITIONS*.)
0177                    CALL MOVTO2(XOR+215.,YOR+130.)
0178                    CALL CHAHOL(28H*LCURVE 1  0.83 *UM U*LREA*.)
0179                    CALL MOVTO2(XOR+215.,YOR+125.)
0180                    CALL CHAHOL(28H*L      2  0.42          *.)
0181                    CALL MOVTO2(XOR+215.,YOR+120.)
0182                    CALL CHAHOL(28H*L      3  0.35          *.)
0183                    CALL MOVTO2(XOR+215.,YOR+115.)
0184                    CALL CHAHOL(28H*L      4  0.27          *.)
0185                    CALL MOVTO2(XOR+215.,YOR+110.)
0186                    CALL CHAHOL(28H*L      5  0.19          *.)
0187                    CALL MOVTO2(XOR+210.,YOR+100.)
0188                    CALL CHAHOL(28H*UT*LEMPERATURE=100.08*U C*.)
0189                    CALL MOVTO2(XOR+227.,YOR+95.)
0190                    CALL CHAHOL(17H*LAPPR. 373 *UK*.)
0191                    CALL MOVTO2(XOR+210.,YOR+90.)
0192                    CALL CHAHOL(23H*UA*LCID 0.06 *UM HNO*.)
0193                    CALL MOVTO2(XOR+249.,YOR+89.)
0194                    CALL CHAHOL(3H3*.)
0195                    CALL AXIPOS (IOR,XOR,YOR,AYLEN,IYORY)
0196                    CALL AXIPOS (IOR,XOR,YOR,AXLEN,IXORY)
0197                    CALL AXISCA(1,NINTX,XBEG,XEND,IXORY)
0198                    CALL AXISCA(1,NINTY,YBEG,YEND,IYORY)
0199                    CALL AXIDRA(-1,-1,IYORY)
0200                    CALL AXIDRA(1,1,IXORY)
0201                    RETURN
0202                    STOP
0203                    END

END OF SEGMENT, LENGTH   384, NAME  DARIA
```

```
0204                SUBROUTINE ANARA(XOR)
0205                NINTY=10
0206                NINTX=14
0207                IOR=1
0208                YOR=200.
0209                IXORY=1
0210                IYORY=2
0211                CALL PALOCA(XOR)
0212                CALL MOVTO2(XOR+155.,YOR)
0213                CALL CHAHOL(21H*UT*LIME IN SECONDS*.)
0214                CALL MOVTO2(XOR,YOR+115.)
0215                CALL CHAHOL(8H*LLN C*.)
0216                CALL MOVTO2(XOR+14.,YOR+148.)
0217                CALL CHAHOL(10H*UG.5.3.*.)
0218                CALL MOVTO2(XOR+150.,YOR+120.)
0219                CALL CHAHOL(27H*UO*LPERATING CONDITIONS.*.)
0220                CALL MOVTO2(XOR+155.,YOR+110.)
0221                CALL CHAHOL(24H*UT*LEMPERATURE 100*UC*.)
0222                CALL MOVTO2(XOR+151.,YOR+105.)
0223                CALL CHAHOL(24H*L                373*UK*.)
0224                CALL MOVTO2(XOR+190.,YOR+70.)
0225                CALL CHAHOL(11H*UP*LH=2.*.)
0226                CALL MOVTO2(XOR+225.,YOR+70.)
0227                CALL SYMBOL(1)
0228                CALL MOVTO2(XOR+187.,YOR+65.)
0229                CALL CHAHOL(14H*U4.>P*LH>2.*.)
0230                CALL MOVTO2(XOR+225.,YOR+65.)
0231                CALL SYMBOL(8)
0232                CALL MOVTO2(XOR+185.,YOR+60.)
0233                CALL CHAHOL(31H*UT*LHE EFFECT OF THE INITIAL*.)
0234                CALL MOVTO2(XOR+185.,YOR+55.)
0235                CALL CHAHOL(26H*L ACID CONCENTRATION  O*.)
0236                CALL MOVTO2(XOR+187.,YOR+50.)
0237                CALL CHAHOL(15H*U1 0.06M HNO*.)
0238                CALL MOVTO2(XOR+187.,YOR+45.)
0239                CALL CHAHOL(11H*U2 0.09M*.)
0240                CALL MOVTO2(XOR+187.,YOR+40.)
0241                CALL CHAHOL(11H*U3 0.12M*.)
0242                CALL MOVTO2(XOR+215.,YOR+49.)
0243                CALL CHAHOL( 5H*U3*.)
0244                CALL MOVTO2(XOR+30.,YOR+148.)
0245                CALL CHAHOL(28H*UH*LYDROLYSIS OF *UU*LREA*.)
0246                CALL CHAHOL(21H *LIN ACID SOLUTION*.)
0247                CALL MOVTO2(XOR+25.,YOR+143.)
0248                CALL CHAHOL(27H*UT*LHE TIME REQUIRED FOR*.)
0249                CALL CHAHOL(25H *LA GIVEN *UU*LREA CON*.)
0250                CALL CHAHOL(23H*LCENTRATION TO       *.)
0251                CALL MOVTO2(XOR+25.,YOR+138.)
0252                CALL CHAHOL(33H*LHYDROLYSE TO A CERTAIN *UP*LH*.)
0253                CALL CHAHOL(33H*L AS A FUNCTION OF THE         *.)
0254                CALL MOVTO2(XOR+25.,YOR+133.)
0255                CALL CHAHOL(42H*LNATURAL LOGARITHM OF THE CONCENTRATI
0256                CALL MOVTO2(XOR+65.,YOR+43.)
0257                CALL CHAINT(1,3)
0258                CALL MOVTO2(XOR+96.,YOR+43.)
0259                CALL SYMBOL(7)
0260                CALL MOVTO2(XOR+ 95.,YOR+43.)
0261                CALL CHAINT(2,3)
0262                CALL MOVTO2(XOR+132.,YOR+43.)
0263                CALL SYMBOL(7)
0264                CALL MOVTO2(XOR+130.,YOR+43.)
0265                CALL CHAINT(3,3)
0266                YBEG=-2.
0267                YEND=0.
0268                XBEG=0.
```

```
0269                    XEND=7000.
0270                    AYLEN=100.
0271                    AXLEN=140.
0272                    CALL AXIPOS (IOR,XOR,YOR,AYLEN,IYORY)
0273                    CALL AXIPOS (IOR,XOR,YOR,AXLEN,IXORY)
0274                    CALL AXISCA(1,NINTX,XBEG,XEND,IXORY)
0275                    CALL AXISCA(1,NINTY,YBEG,YEND,IYORY)
0276                    CALL AXIDRA(-1,-1,IYORY)
0277                    CALL AXIDRA(1,1,IXORY)
0278                    RETURN
0279                    STOP
0280                    END

END OF SEGMENT, LENGTH   503, NAME  AMARA
```

```
0281                    SUBROUTINE PALOCA(XOR)
0282                    YOR=200.
0283                    XOR=XOR+300.
0284                    CALL MOVTO2(XOR-20.,YOR-25.)
0285                    CALL LINTO2(XOR-20.,YOR+185.)
0286                    CALL LINTO2(XOR+280.,YOR+185.)
0287                    CALL LINTO2(XOR+280.,YOR-25.)
0288                    CALL LINTO2(XOR-20.,YOR-25.)
0289                    RETURN
0290                    STOP
0291                    END

END OF SEGMENT, LENGTH    83, NAME  PALOCA
```

```
0292                    SUBROUTINE ZARA(XOR,LLL,LALA,SL,HC,C)
0293                    DIMENSION C(250,6)
0294                    DIMENSION SS(250),CC(250)
0295                    DIMENSION  HC(250,6),SL(250,6)
0296                    INTEGER LALA(10)
0297                    YOR=200.
0298                    AXLEN=240.
0299                    AXLEN=200.
0300                    XBEG=0.
0301                    NINTX=6
0302                    NINTX=10
0303                    AYLEN=160.
0304                    XEND=6.
0305                    XEND=-2.
0306                    YBEG=0.
0307                    YBEG=-10.
0308                    YEND=-0.05
0309                    YEND=-10.
0310                    YEND=-12.
0311                    NINTY=8
0312                    IYORY=2
0313                    IXORY=1
0314                    IOR=1
0315                    CALL PALOCA(XOR)
0316                    CALL AXIPOS (IOR,XOR,YOR,AYLEN,IYORY)
0317                    CALL AXIPOS (IOR,XOR,YOR,AXLEN,IXORY)
0318                    CALL AXISCA(1,NINTX,XBEG,XEND,IXORY)
0319                    CALL AXISCA(1,NINTY,YBEG,YEND,IYORY)
0320                    CALL AXIDRA(-1,-1,IYORY)
0321                    CALL AXIDRA(1,1,IXORY)
0322                    CALL MOVTO2(XOR+220.,YOR)
0323                    CALL CHAHOL(10H*LLN *UC*.)
0324                    CALL MOVTO2(XOR+10.,YOR+160.)
0325                    CALL CHAHOL(13H*LLN(DC/DT)*.)
0326                    CALL MOVTO2(XOR+45.,YOR+160.)
0327                    CALL CHAHOL(40H*UG.5.4.   P*LLOT OF THE CONCENTRATION
0328                    CALL CHAHOL(40H*L AS A FUNCTION OF THE RATE OF CHANGE
0329                    CALL MOVTO2(XOR+45.,YOR+155.)
0330                    CALL CHAHOL(40H*LOF CONCENTRATION IN LOG FORM
0331                    PHLIM=2.5
0332                    DO 10 J=1,LLL
0333                    DO 5 I=2,LALA(J)  -1
0334                    CC(J)=ALOG(C(I,J))
0335                    SS(J)=ALOG(-SL(I,J))
0336                  9 FORMAT(1H0,5E15.5)
0337                    IF(HC(I,J).GT.PHLIM)GO TO 6
0338                  5 CONTINUE
0339                  6 CONTINUE
0340                 10 CONTINUE
0341                  8 FORMAT(1H0,2E15.2,4I10,E12.2)
0342                    CALL GRASYM(CC,SS,LLL,1  ,0)
0343                    WRITE(2,9)C(I,J),SL(I,J),HC(I,J)
0344                    WRITE(2,8)CC(J),SS(J),I,LALA(J),J,LLL,PHLIM
0345                    RETURN
0346                    STOP
0347                    END

END OF SEGMENT, LENGTH    365, NAME  ZARA
```

OUT A5 2

TIME	PH	UREA	SLOPE	K
0.300E 03	0.117E 01	0.420E 00	-0.717E-05	0.171E-04
0.600E 03	0.120E 01	0.418E 00	-0.459E-05	0.110E-04
0.900E 03	0.121E 01	0.417E 00	-0.116E-04	0.279E-04
0.120E 04	0.130E 01	0.411E 00	-0.205E-04	0.499E-04
0.150E 04	0.143E 01	0.405E 00	-0.180E-04	0.445E-04
0.180E 04	0.155E 01	0.400E 00	-0.173E-04	0.432E-04
0.210E 04	0.175E 01	0.395E 00	-0.288E-04	0.729E-04
0.240E 04	0.250E 01	0.388E 00	-0.182E-04	0.469E-04
0.270E 04	0.505E 01	0.386E 00	-0.932E-08	0.241E-07
0.300E 04	0.535E 01	0.386E 00	-0.360E-08	0.931E-08
0.330E 04	0.545E 01	0.386E 00	-0.168E-08	0.436E-08
0.360E 04	0.560E 01	0.386E 00	-0.987E-09	0.255E-08
0.390E 04	0.565E 01	0.386E 00	0.000E 00	0.000E 00

APPENDIX 6

Data for the crystallisation of Barium chromate

In this appendix the data for the crystallisation of Barium chromate are presented in tabular form. (Tables T.A6.1. to T.A6.6.) Not all the data obtained by the "sampling" method are included mainly because of their bulk. They are presented, however, in graphical form (graphs G.6.5. and G.6.6.). The effect of a number of different parameters were tested (e.g. baffles, weak acid, etc.). Of these results only the conclusions are presented (chapter 6).

The crystal samples collected at the end of each experiment were numbered by the date. These samples are available for further examination.

In table T.A6.7. the treated data used for the regression analysis are presented.

In table T.A6.8. the results obtained from the fluidised bed are presented.

Table T.6.1. Results R.1.

Conditions: Agitation 800 rpm
Initial $BaCrO_4$ concentration 5 g .
Initial Urea concentration 20 g
Initial acid concentration 0.06 M HCl
Temperature 100^oC
Method "Freezing"

Date	t	L	Wt	pH
8 May 79 A	102	11.2	0.3027	2.50
8 May 79 B	158	13.8	1.6992	2.70
10 May 79 A	258	15.1	3.5845	3.08
10 May 79 B	438	18.5	4.9795	4.50
10 May 79 C	588	17.8	4.9905	5.0
4 June 79 A	720	18.83	4.8907	5.30
4 June 79 B	780	18.89	4.9768	5.50
4 June 79 C	96	7.9	4.054	2.50
5 June 79 A	150	12.6	1.2515	2.65
5 June 79 B	60	8.1	0.4222	2.44
6 June 79 A	120	11.9	1.1507	2.55
6 June 79 B	183	14.3	2.5065	2.70
13 June 79 A	57	8.6	0.2246	2.44
13 June 79 B	120	12.1	1.2571	2.55
14 June 79 A	120	12.55	1.0025	2.55
14 June 79 B	120	12.3	0.9895	2.55
14 June 79 C	360	14.45	4.9835	4.00
18 June 79 A	240	15.2	3.472	2.98
18 June 79 B	480	17.9	4.9835	4.70

Table T.6.2. Results R2

Conditions: Agitation 200/400 rpm
Initial Barium chromate concentration 5 g
Initial Urea concentration 20 g
Initial acid concentration 0.06 M HCl
Temperature 100°C
Method "freezing"

Date	t	L	Wt	pH	R
28 June 79	90	13	0.7632	2.5	200
3 July 79 A	162	19	1.9527	2.67	200
3 July 79 B	204	19	2.6635	2.82	200
20 July 79 A	126	20.5	1.4328	2.55	400
20 July 79 B	168	21	1.5095	2.7	400
21 July 79 A	140	21	1.2565	2.61	400
21 July 79 B	300	24	4.3115	3.5	400

Table T.6.3. Results R3

Conditions: Initial $BaCrO_4$ concentration 5 g
Initial Urea concentration 20 g
Initial acid concentration 0.006 M HCl
Temperature 100°C
Method "sampling"

Date	R	Annealing time hours	No. of samples	
28 Nov 78	800	-	3	
29 Nov 78	200	-	37	)Presented
				)graphically
17 Jan 79	400	-	45	)in graph G.6
22 Jan 79	1600	-	10	
24 Jan 79	1300	-	9	
26 Jan 79	1500	-	8	
15 Feb 79	800	6	8	
19 Feb 79	800	3	18	
22 Feb 79	800	2	16	
23 Feb 79	800	12	16	
26 Feb 79	800	15	8	
6 Feb 79 *	800	-	8	
5 Feb 79 *	800	-	8	

* Reactor using baffles

Table T.6.4. Results R.4.

Conditions: Agitation 800 rpm
Initial Urea concentration 20 g
Initial acid concentration 0.12/0.06 m HCl
Temperature 100°C
Method "freezing"

Date	t	L	Wt	pH	Initial $BaCrO_4$ weight/acid strength
25 June 79 A	120	18.8	6.2137	2.55	10.0/0.12
25 June 79 B	180	19.7	7.3875	2.74	10.0/0.12
27 June 79 A	240	10.2	3.6655	2.98	4.0/0.06
27 June 79 B	400	13.5	3.9950	4.90	4.0/0.06
2 July 79 A	400	12.75	2.9875	4.10	3.0/0.06
2 July 79 B	460	12.8	2.9895	4.60	3.0/0.06
4 July 79 A	415	10.7	1.9776	4.60	2.0/0.06
4 July 79 B	440	11.31	1.9871	4.70	2.0/0.06
5 July 79	480	11.12	1.9875	4.75	2.0/0.06

Table T.6.5. Results R5

Conditions: Agitation 800 rpm
Temperature 100°C
Method "sampling"

Date	Urea concentration in gr	Initial $BaCrO_4$ concentration	No. of samples
24 Nov 78	20	10	16
1 Feb 79	20	4	16
1 Mar 79	20	3	16
2 Mar 79	20	2	12
2 Feb 79	15	5	16
26 Feb 79	25	5	16

Table T.6.6. Results R6.

Conditions: Agitation 800 rpm
Initial $BaCrO_4$ concentration 5g
Initial rea concentration 20 g
Initial acid concentration 0.06 M HCl
Temperature 100°C

Date	Concentration of weak acid		$BaCrO_4$ to Tungsten mass ratio	No. of samples
18 Nov 78	A	0.006	-	1
19 Nov 78	A	0.012	-	2
20 Nov 78	F	0.006	-	1
21 Nov 78	F	0.009	-	3
22 Nov 78	F	0.012	-	1
27 Nov 78	F	0.018	-	1
7 Dec 78	F	0.02	-	10
18 Jan 79	F	0.025	10.1	1
28 Jan 79	C	0.25	-	1
29 Jan 79	C	0.5	-	1
16 Nov 78		-	10.1	1
17 Nov 78		-	9.6	1
1 Dec 78		-	9.3	1
4 Dec 78		-	9.0	1
6 Dec 78		-	11.7	1
14 Dec 78 A		-	12.1	1
14 Dec 78 B		-	20.3	1
15 Jan 79 A		-	25.1	1
15 Jan 79 B		-	26.8	1
29 Jan 79 B		-	37.28	8

C Citric acid
F Formic acid
A Acetic acid

Table T.A6.7. presenting the treated data used for the regression analysis (Chapter 6.)

L	dL/dt	pH	$\frac{C-C_s}{C_s}$	dL/dt evaluated	%fit	R
.19	0.14250E 00	2.40	0.43	0.43661E 00	-2.06	800.0
.72	0.11380E 00	2.42	0.39	0.16802E 00	-0.48	800.0
.74	0.91600E-01	2.44	0.35	0.99806E-01	-0.09	800.0
.38	0.74500E-01	2.47	0.33	0.71319E-01	0.04	800.0
.72	0.61000E-01	2.50	0.32	0.56153E-01	0.08	800.0
.83	0.50400E-01	2.55	0.31	0.47112E-01	0.07	800.0
.74	0.42000E-01	2.61	0.30	0.41172E-01	0.02	800.0
.51	0.35300E-01	2.67	0.29	0.36682E-01	-0.04	800.0
.15	0.29900E-01	2.74	0.27	0.32958E-01	-0.10	800.0
.70	0.25500E-01	2.82	0.26	0.29538E-01	-0.16	800.0
.17	0.21900E-01	2.90	0.23	0.25905E-01	-0.18	800.0
.58	0.18900E-01	2.98	0.20	0.21937E-01	-0.16	800.0
.93	0.16500E-01	3.08	0.16	0.17360E-01	-0.05	800.0
.24	0.14500E-01	3.20	0.10	0.11687E-01	0.19	800.0
.31	0.37100E-01	2.40	0.43	0.38637E-01	-0.04	800.0
.01	0.33000E-01	2.42	0.39	0.33267E-01	-0.01	800.0
.63	0.29500E-01	2.44	0.35	0.29369E-01	0.00	800.0
.19	0.26500E-01	2.47	0.33	0.26655E-01	-0.01	800.0
.69	0.23900E-01	2.50	0.32	0.24583E-01	-0.03	800.0
.15	0.21700E-01	2.55	0.31	0.23029E-01	-0.06	800.0
.56	0.19800E-01	2.61	0.30	0.21772E-01	-0.10	800.0
.94	0.18100E-01	2.67	0.29	0.20569E-01	-0.14	800.0
.28	0.16600E-01	2.74	0.27	0.19072E-01	-0.15	800.0
.60	0.15300E-01	2.82	0.26	0.17890E-01	-0.17	800.0
.90	0.14200E-01	2.90	0.23	0.16091E-01	-0.13	800.0
.17	0.13100E-01	2.98	0.20	0.13909E-01	-0.06	800.0
.42	0.12200E-01	3.08	0.16	0.11180E-01	0.08	800.0
.66	0.11300E-01	3.20	0.10	0.76180E-02	0.33	800.0

6.30	0.24000E 00	2.74	0.27	0.10969E 00	0.54	800.0
9.61	0.12900E 00	2.82	0.26	0.55552E-01	0.57	800.0
1.46	0.73600E-01	2.90	0.23	0.39299E-01	0.47	800.0
2.56	0.44300E-01	2.98	0.20	0.30216E-01	0.32	800.0
3.23	0.27900E-01	3.38	0.16	0.22878E-01	0.18	800.0
3.67	0.18300E-01	3.20	0.10	0.15097E-01	0.18	800.0
4.90	0.92000E-01	2.42	0.39	0.94076E-01	-0.02	400.0
2.84	0.12000E 00	2.40	0.43	0.23086E 00	-0.92	400.0
6.48	0.69800E-01	2.44	0.35	0.57820E-01	0.17	400.0
7.69	0.53800E-01	2.47	0.33	0.42625E-01	0.21	400.0
8.64	0.42000E-01	2.50	0.32	0.34423E-01	0.18	400.0
9.38	0.33200E-01	2.55	0.31	0.29590E-01	0.11	400.0
9.97	0.26600E-01	2.61	0.30	0.26368E-01	0.01	400.0
0.44	0.21500E-01	2.67	0.29	0.23937E-01	-0.11	400.0
0.83	0.17600E-01	2.74	0.27	0.21816E-01	-0.24	400.0
1.14	0.14500E-01	2.82	0.26	0.19843E-01	-0.37	400.0
1.41	0.12200E-01	2.90	0.23	0.17598E-01	-0.44	400.0
1.63	0.10300E-01	2.98	0.20	0.15071E-01	-0.46	400.0
1.82	0.88000E-02	3.08	0.16	0.12034E-01	-0.37	400.0
1.98	0.75900E-02	3.20	0.10	0.81715E-02	-0.08	400.0
3.01	0.12400E 00	2.40	0.43	0.94207E-01	0.24	200.0
4.99	0.82950E-01	2.42	0.39	0.40737E-01	0.51	200.0
6.33	0.56900E-01	2.44	0.35	0.26635E-01	0.53	200.0
7.27	0.40130E-01	2.47	0.33	0.20614E-01	0.49	200.0
7.94	0.28900E-01	2.50	0.32	0.17363E-01	0.40	200.0
8.43	0.21400E-01	2.55	0.31	0.15428E-01	0.28	200.0
8.79	0.16200E-01	2.61	0.30	0.14146E-01	0.13	200.0
9.07	0.12500E-01	2.67	0.29	0.13125E-01	-0.05	200.0
9.29	0.99180E-02	2.74	0.27	0.12191E-01	-0.23	200.0
9.47	0.80200E-02	2.82	0.26	0.11238E-01	-0.40	200.0
9.61	0.66300E-02	2.90	0.23	0.10105E-01	-0.52	200.0
9.74	0.55990E-02	2.98	0.20	0.87265E-02	-0.56	200.0
9.84	0.48200E-02	3.08	0.16	0.70303E-02	-0.46	200.0
9.93	0.42400E-02	3.20	0.20	0.85147E-02	-1.01	200.0

Table T.A6.8. Results R7

Test No.	Tungsten Type	$BaCrO_4$/W mass ratio	
		analysed	expected
SF.10.8.79.	I	18.2	18.1
SF.13.8.79.	I	14.7	11.8
SF.22.8.79.A	I	28.1	30.2
SF.22.8.79.B	I	11.4	13.7
SF.23.8.79.	I	7.4	5.6
SF.24.8.79.	I	5.2	4.3
SF. 6.9.79.	I	36.6	21.2
SF.15.9.79.	I	2.2	2.6
SF.18.9.79.A	II	28.1	12.4
SF.18.9.79.B	II	29.8	26.7
SF.18.9.79.C	II	16.3	12.5
SF.19.9.79.A	II	25.2	24.7
SF.19.9.79.B	II	9.9	8.3

Results obtained from the fluidised bed.

APPENDIX 7

Computation of the parameters used in the overall growth correlation

The driving force, growth rise, length, etc. are calculated at specific time intervals using programme EF20 and its modified version EF21. Output OUT.A7.1. lists programme EF20. A simplified flow diagram of the programme is presented in D.A7.1.

In graphs G.A7.1. and G.A7.2. the Bulk Diffusion Control model is tested.

G.A7.1. Graph testing the Bulk Diffusion Control model for selected speeds of agitation

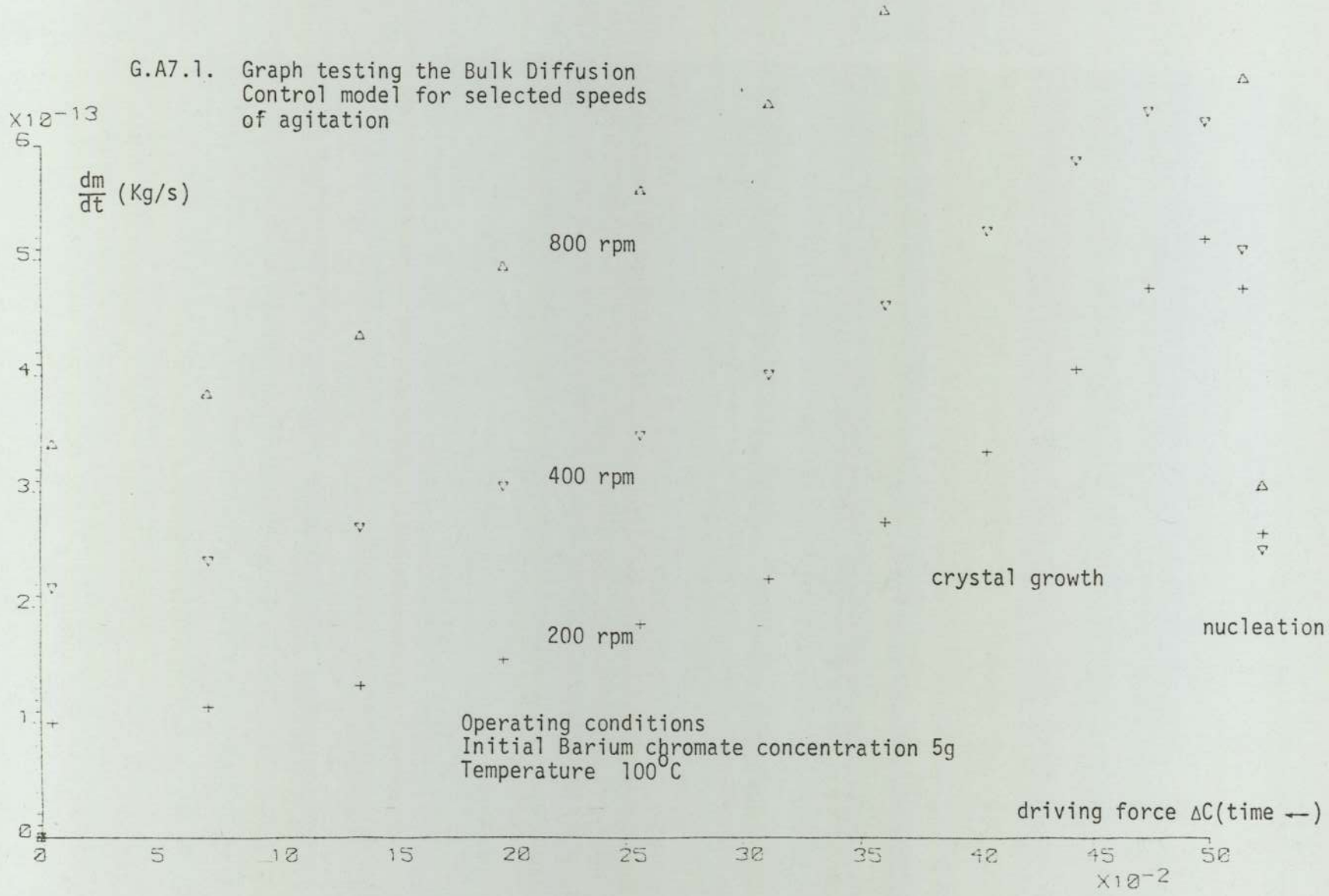

G.A7.2. Graph testing the Bulk Diffusion Control model for selective initial Barium chromate concentration

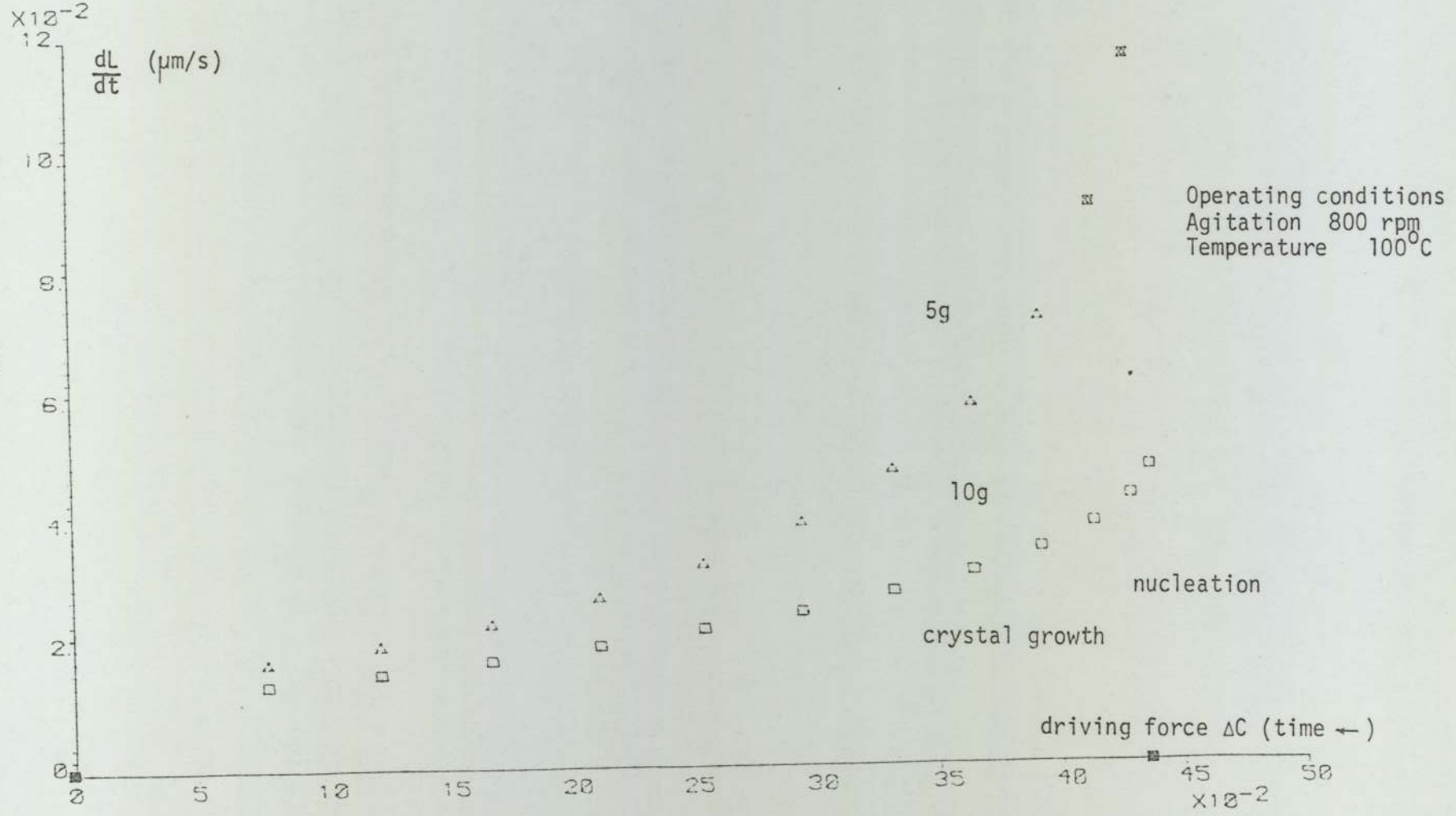

D.A 7.1. Logical flow diagram of programmes EF20 and EF21

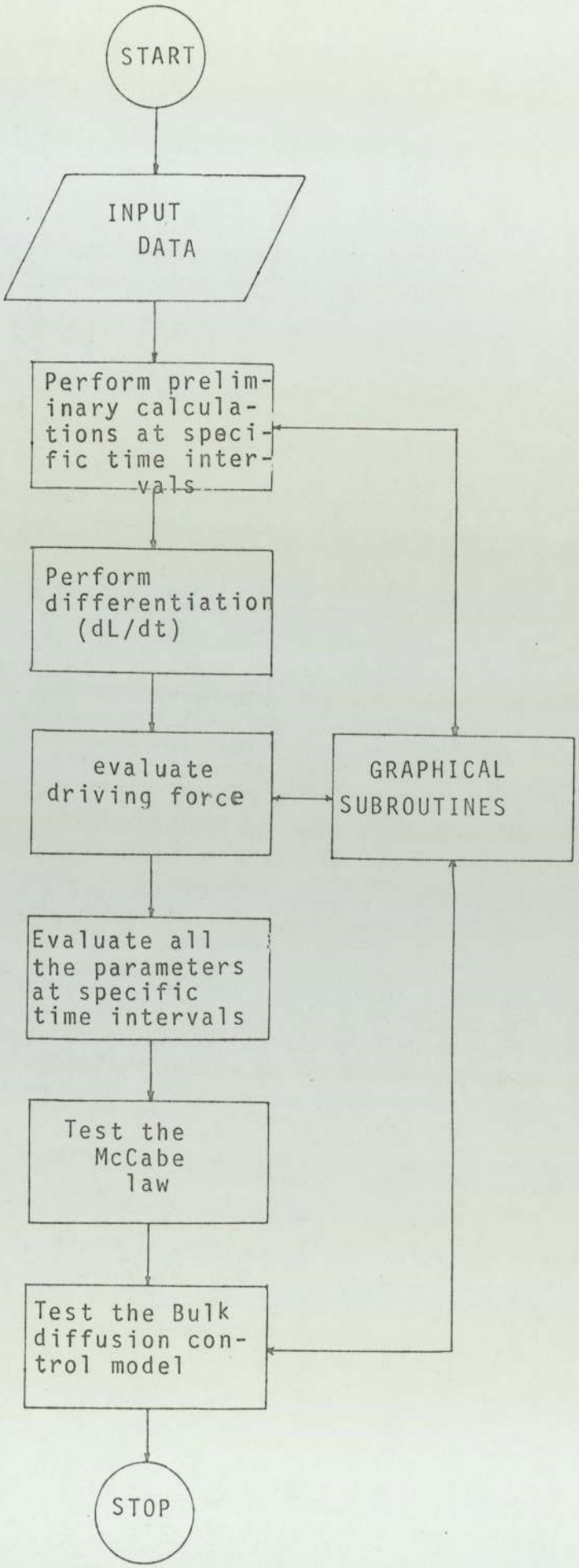

OUT A7 1

```
0012          TRACE 1
0000          TRACE 2
0001          MASTER EF20
0002          DIMENSION CALCY(100),CALCT(100)
0003          DIMENSION A(10,10)
0004          DIMENSION AA(10)
0005          DIMENSION APC(5,5)
0006          DIMENSION RPM(10)
0007          DIMENSION GROWTH(100),DRIVNG(100)
0008          DIMENSION Y(30),X(30,5)
0009          DIMENSION PC(20),SPC(20),PCT(20),SPCT(20)
0010          DIMENSION TTIME(100)
0011          DIMENSION DG(100,5),DDG(100,5)
0012          DIMENSION TIME(40)
0013          DIMENSION PH(40)
0014          DIMENSION XX(50)
0015          REAL MEAN(40)
0016          REAL LENGTH(100)
0017          CALL OPENGINOGP
0018          XOR=100.
0019          YOR=40.
0020          CALL TETRA(YOR,XOR)
0021          CALL CHASIZ(2.6,2.302)
0022          AYLEN=120.
0023          YEND=20.
0024          NINTY=4
0025          IYORY=2
0026          IXORY=1
0027          IOR=1
0028          XBEG=0.
0029          YBEG=0.
0030          AXLEN=180.
0031          XEND=900.
0032          NINTX=9
0033          CALL AXIPOS (IOR,XOR,YOR,AYLEN,IYORY)
0034          CALL AXIPOS (IOR,XOR,YOR,AXLEN,IXORY)
0035          CALL AXISCA(1,NINTX,XBEG,XEND,IXORY)
0036          CALL AXISCA(1,NINTY,YBEG,YEND,IYORY)
0037          CALL AXIDRA(1,1,IXORY)
0038          CALL AXIDRA(-2,-1,IYORY)
0039          MASTRA=1
0040          MASTRA=3
0041          DO  150 MM=1,MASTRA
0042          READ(1,9)NPOINT,NORDER, NINT, RADINF,RPM(MM)
0043        9 FORMAT(3I0,2F0.0)
0044          WRITE(2,12)NPOINT,NORDER,NINT,RADINF,RPM(MM)
0045       12 FORMAT(1H0,12X,3I10,2F12.2)
0046          READ(1,10)((MEAN(I),TIME(I),PH(I)),I=1,NPOINT)
0047       10 FORMAT(90F0.0)
0048          DO 25 I=1,NPOINT
0049          TIME(I)=TIME(I) *60.
0050          WRITE(2,20)MEAN(I),TIME(I),PH(I)
0051       20 FORMAT(1H0,20X,10F10.2)
0052       25 CONTINUE
0053          CALL GRASYM(TIME,MEAN,NPOINT,MM,0)
0054          DO 20 I=1,NPOINT
0055          Y(I)=ALOG(1.-MEAN(I)/RADINF)
0056          DO 20 J=1,NORDER
0057          AJ=J
0058          X(I,J)=TIME(I)**AJ
0059       20 CONTINUE
0060          CALL MARGOT(X,Y,NORDER,NPOINT,A)
0061          CALL SUSSAN(A,NORDER,AA)
0062          VIN=20.
0063          CALCT(1)=0.1
```

```
0064                DO  60 I=1,NINT
0065                ANA=0.
0066                DO 55 M=1,NORDER
0067                AM=M
0068                ANA=ANA+AA(M)* CALCT(I)**(AM)
0069             55 CONTINUE
0070                CALCY(I)=(1.-EXP(ANA))*RADINF
0071                CALCT(I+1)=CALCT(I)+VIN
0072             60 CONTINUE
0073                CALL GRACUR(CALCT,CALCY,NINT)
0074                DO 70 I=2,NINT-1
0075                LENGTH(I)=CALCY(I)
0076                DG(I,MM)=(CALCY(I+1)-CALCY(I-1))/(VIN*2.)
0077             70 CONTINUE
0078                DO 80 I=3,NINT-2
0079                DDG(I,MM)=(DG(I+1,MM)-DG(I-1,MM))/(VIN*2.)
0080             80 CONTINUE
0081                DO 84 I=1,NINT
0082                WRITE(2,75)CALCT(I),CALCY(I),DG(I,MM),DDG(I,MM),I,
0083               1LENGTH(I)
0084             75 FORMAT(1HO,2F10.2,2E20.5,I10,F10.2)
0085             84 CONTINUE
0086            150 CONTINUE
0087                AYLEN=120.
0088                AXLEN=160.
0089                NINTX=4
0090                XEND=400.
0091                YBEG=1.6
0092                YEND=2.5
0093                NINTY=8
0094                YOR=YOR+300.
0095                CALL AXIPOS (IOR,XOR,YOR,AYLEN,IYORY)
0096                CALL AXIPOS (IOR,XOR,YOR,AXLEN,IXORY)
0097                CALL AXISCA(1,NINTY,YBEG,YEND,IYORY)
0098                CALL AXISCA(1,NINTX,XBEG,XEND,IXORY)
0099                CALL AXIDRA(1,1,IXORY)
0100                CALL AXIDRA(-2,-1,IYORY)
0101                CALL TETRA(YOR,XOR)
0102                READ(1,86)KPOINT
0103             86 FORMAT(10I0)
0104                READ(1,90)(PC(I),PCT(I),I=1,KPOINT)
0105                NINTO=15
0106                NINTO=16
0107                READ(1,86)LPOINT
0108                READ(1,90)(SPCT(I),SPC(I),I=1,LPOINT)
0109             90 FORMAT(50F0.0)
0110                DO 95 I=1,KPOINT
0111                WRITE(2,97)PC(I),PCT(I)
0112             95 CONTINUE
0113             97 FORMAT(1HO,13X,2F21.3)
0114                DO 96 I=1,KPOINT
0115                Y(I)=PC(I)
0116                X(I,1)=PCT(I)
0117                X(I,2)=1.
0118                X(I,3)=PCT(I)**2.
0119             96 CONTINUE
0120                NA=3
0121                CALL MARGOT(X,Y,NA,KPOINT,A)
0122                CALL SUSSAN(A,NA,AA)
0123                APC(1,1)=AA(1)
0124                APC(1,2)=AA(2)
0125                APC(1,3)=AA(3)
0126                DO 98 I=1,NINTO
0127                CALCY(I)=AA(1)*CALCT(I)+AA(2)+AA(3)*CALCT(I)**2.
0128                CALCT(I+1)=CALCT(I)+VIN
0129             98 CONTINUE
```

```
0130              CALL GRASYM(PCT,PC,KPOINT,3,0)
0131              CALL GRACUR(CALCT,CALCY,NINTO)
0132              DO 105 I=1,LPOINT
0133              WRITE(2,97)SPC(I),SPCT(I)
0134          105 CONTINUE
0135              NO=3
0136              DO 107 I=1,LPOINT
0137              Y(I)=SPC(I)
0138              X(I,1)=SPCT(I)
0139              X(I,2)=1.
0140              X(I,3)=SPCT(I)**2.
0141          107 CONTINUE
0142              CALL MARGOT(X,Y,NO,I-1    ,A)
0143              CALL SUSSAN(A,NO,AA)
0144              APC(2,1)=AA(1)
0145              APC(2,2)=AA(2)
0146              APC(2,3)=AA(3)
0147              DO 108 I=1,NINTO
0148              CALCY(I)=AA(1)*CALCT(I)+AA(2)+AA(3)*CALCT(I)**2.
0149              CALCT(I+1)=CALCT(I)+VIN
0150          108 CONTINUE
0151              CALL GRASYM (SPCT,SPC,LPOINT,4,0)
0152              CALL GRACUR(CALCT,CALCY,NINTO)
0153              TTIME(2)=20.1
0154              IEND=15
0155              DO 112 I=2,IEND
0156              TTIME(I+1)=TTIME(I)+VIN
0157          112 CONTINUE
0158              DO 123 I=2,IEND
0159              BAP =APC(1,1)*TTIME(I)+APC(1,2)+APC(1,3)*TTIME(I)**2.
0160              BASP=    APC(2,1)*TTIME(I)+APC(2,2)+APC(2,3)*TTIME(I)*
0161              DRIVNG(I)=(10.**(-BASP)-10.**(-BAP))/(10.**(-BAP))
0162          123 CONTINUE
0163              XOR=XOR+300.
0164              YBEG=0.
0165              XBEG=0.
0166              AYLEN=120.
0167              AXLEN=200.
0168              XEND=0.5
0169              YEND=0.6*10.**(-12.)
0170              NINTY=6
0171              NINTX=8
0172              CALL TETRA(YOR,XOR)
0173              CALL AXIPOS (IOR,XOR,YOR,AYLEN,IYORY)
0174              CALL AXIPOS (IOR,XOR,YOR,AXLEN,IXORY)
0175              CALL AXISCA(1,NINTX,XBEG,XEND,IXORY)
0176              CALL AXISCA(1,NINTY,YBEG,YEND,IYORY)
0177              CALL AXIDRA(1,1,IXORY)
0178              CALL AXIDRA(-2,-1,IYORY)
0179              DENSIT=4.45
0180              DO 200 MM=1,MASTRA
0181              DO 126 I=2,IEND
0182              GROWTH(I)=DG(I,MM)*(DENSIT*4.*3.14*LENGTH(I)**2.)
0183             1*10.**(-12.)/252.
0184              AKKA=GROWTH(I)/DRIVNG(I)
0185              WRITE(2,127)GROWTH(I),DRIVNG(I),TTIME(I),  I   ,AKKA
0186          127 FORMAT(1HO,10X,3E11.3, I5,E11.3)
0187          126 CONTINUE
0188              NANT=IEND-1
0189              CALL GRASYM(DRIVNG,GROWTH,NANT,MM,0)
0190          200 CONTINUE
0191              YOR=YOR-300.
0192              XBEG=0.
0193              XEND=-1.2
0194              YBEG=-11.
0195              YEND=-13.
```

```
0196                    AXLEN=180.
0197                    AYLEN=120.
0198                    NINTX=6
0199                    NINTY=6
0200                    CALL TETRA(YOR,XOR)
0201                    CALL AXIPOS (IOR,XOR,YOR,AYLEN,IYORY)
0202                    CALL AXIPOS (IOR,XOR,YOR,AXLEN,IXORY)
0203                    CALL AXISCA(1,NINTX,XBEG,XEND,IXORY)
0204                    CALL AXISCA(1,NINTY,YBEG,YEND,IYORY)
0205                    CALL AXIDRA(1,1,IXORY)
0206                    CALL AXIDRA(-2,-1,IYORY)
0207                    DO 280 MM=1,MASTRA
0208                    DO 226 I=2,IEND
0209                    Y(I-1)=ALOG10(DG(I,MM)
0210                   1*(DENSIT*4.*3.14*LENGTH(I)**2.*10.**(-12.))/252.)
0211                    X(I-1,1)=ALOG10(DRIVNG(I))
0212                    X(I-1,2)=1.
0213                    XX(I-1)=X(I-1,1)
0214                    WRITE(2,127)Y(I-1),X(I-1,1),TTIME(I)
0215                226 CONTINUE
0216                    CALL GRASYM(XX,Y,NANT,MM,0)
0217                280 CONTINUE
0218                    CALL DEVEND
0219                    STOP
0220                    END

END OF SEGMENT, LENGTH  1676, NAME  EF20
```

APPENDIX 8

Measurement of $BaCrO_4$ concentration in acid solution by ultraviolet absorption

The ultraviolet spectrophotometer used is type PYE Sp. 1800 connected to a "graph plotter", with TSL optical cells of 2,5 and 10mm.

Calibration of the instrument

A wavelength is selected at which the solute absorbs ultra-violet radiation while the solvent does not. Barium chromate has two strong absorbing peaks at 258nm and 352 nm. The 352nm wavelength was chosen because of the light absorbing predominance of the $HCrO_4^-$ ion (R.3.1.) and (R.3.7.). In fact, the absorbance recorded is the sum of the absorbances of the ions in equilibrium and thus it was found that the peaks move slightly across the spectrum since at different total Cr(VT) concentrations different ions become prominant (graph G.A8.1.) The machine was then zeroed, which was done when neither the sample nor the reference cell were absorbing light. (filled with dionised water) (R.3.12.) A calibration curve relating the total absorbance to the $BaCrO_4$ concentration was obtained by plotting the absorbance of samples for various $BaCrO_4$ concentrations for the range 250-400 nm. (Graph G.A8.1.) and G.A8.2.).

Experimental procedure

A 10 cm^3 sample of saturated Barium chromate solution was collected as described in Chapter 7 and diluted to 100cm^3

Either HNO_3 or HCl was added in such quantities and strength as to make the final strength of the diluted solution equal to 0.1 N. (R.3.1.). The "sample" cell was filled with this solution while the "reference" one with O.I.N. acid and both were placed in the instrument. The amount of light absorbed was recorded and compared with the calibration curve.

Errors associated with ultraviolet spectrophotometry

(i) Electrical noise, especially at very low concentrations of solute.

(ii) Stray light.

(iii) Validity of the absorption laws.

Of these three, the first was overcome by using samples of fairly high concentrations of Barium chromate (>0.05g/ℓ). Stray light is greatest at the ends of the wavelength range and at the short wavelength end of the Tungsten lamp region (R.3.12.). At most a ±12% error is produced and at λ=352nm this error can be neglected. The validity of the absorption laws is tested by examining the calibration curve. A straight line indicated that the laws are valid for that particular concentration range G.A8.2.

Other measures taken for collecting accurate data were

(i) Careful cleaning and handling of the optical cells(R.3.12.)

(ii) Fairly slow scanning speed, to allow the mechanical graph-plotter to follow the electronic register of the ultraviolet spectrophotometer.

(iii) Alternating the cells. The exchange should produce identical results because the cells are optically matched. In practice a small difference was found to exist (~2%).

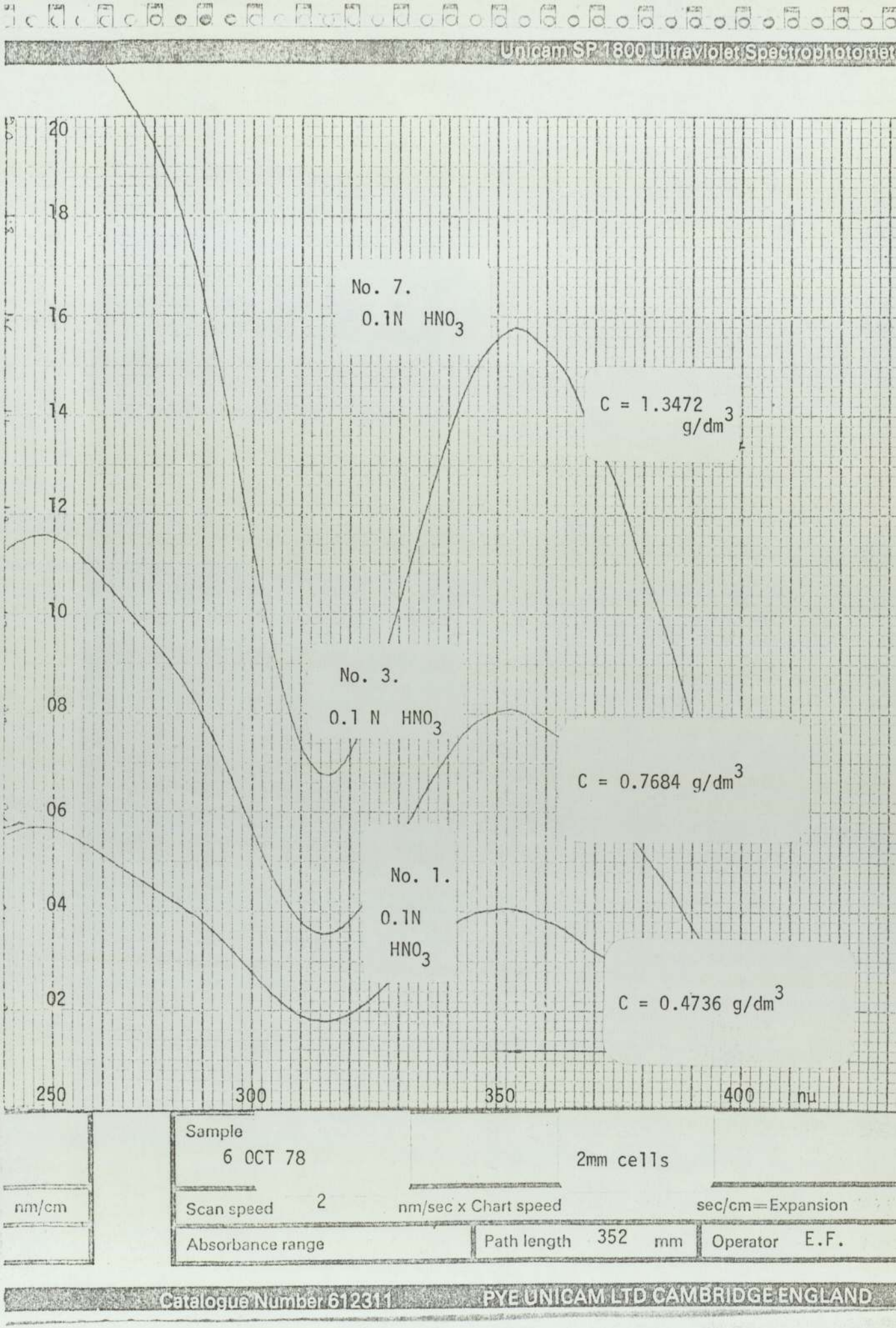

G. A8.1 Graph of absorbance of $BaCrO_4$ solutions of various strengths for the range 260-400 nm

Conditions: $BaCrO_4$ in 0.1 N HNO_3

2mm optical cells
wavelength measured at 352 nm
"Reference" cell 0.1N HNO_3

Date: 6 October 1978

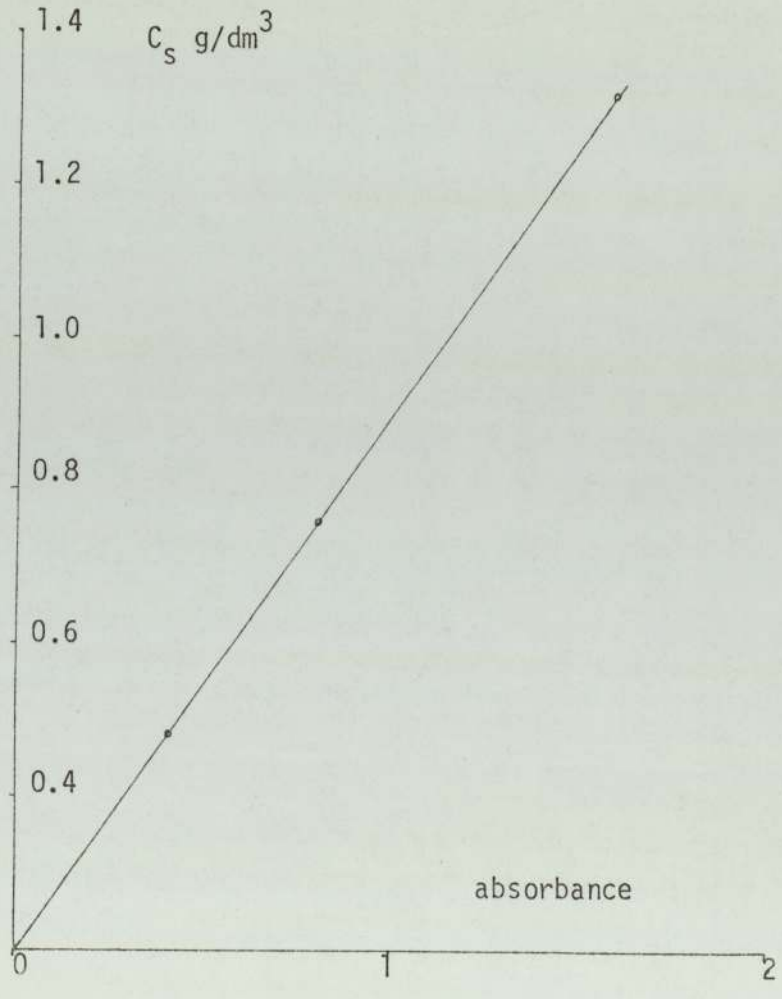

G.A8.2. Calibration curve relating absorbance to concentration

APPENDIX 9

Measurement of $BaCrO_4$ concentration in acid solution by atomic absorption

The atomic absorption spectrophotometer used was an I.L. 151 type with N_2O or air as oxidants.

The theory of the method is well presented in (R.3.17) the atomic absorption manual. Knowledge of the materials to be examined is needed so that the appropriate lamp and burners may be used. In using the instrument properly, experience is essential since the accuracy of the results is very sensitive to the "nature" of the flame.

In Graph D.A9.1. a calibration curve is presented relating concentration of $[Ba]^{++}$ to some convenient scale of measurement. The scatter of the results however indicates that the instrument was probably not functioning properly and thus the results obtained by this method were abandoned.

G.A9.1. Calibration curve of atomic absorption for $[Ba]^{++}$

- ● acidic $BaCrO_4$ solution
- o acidic $BaCrO_4$ solution + 1% Sodium chloride to ensure full ionisation

acidity 0.1 N HCl

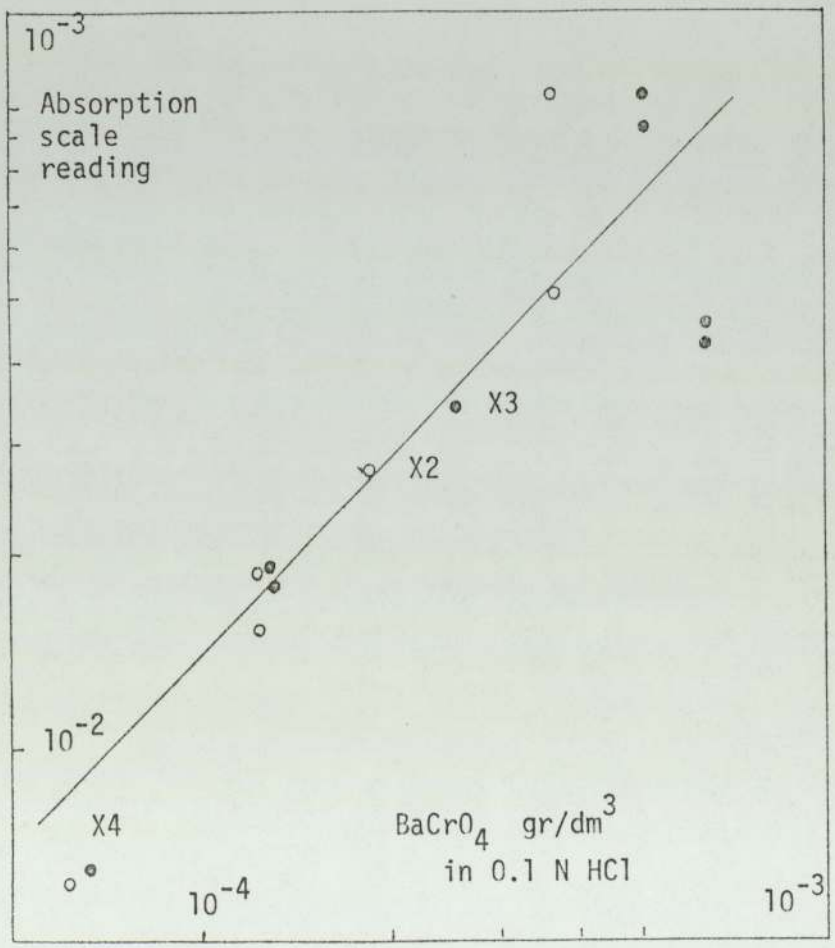

APPENDIX 10

Computational aspects of the solubility of $BaCrO_4$ in acidic solutions

Programme EF19 was used to process the data collected for the solubility of $BaCrO_4$. The programme had access to the "graphical" and "regression" subroutine and thus the relationships between pC_s and pH or $\frac{1}{T}$ were evaluated.

Output OUT.A10.1 presents a typical listing of the results while OUT.A10.2 presents the programme EF19.
A logical flow diagram is presented in D.A10.1.

The results (OUT.A10.1) are placed in a two-dimensional matrix (Reactor vs. data) to facilitate the sensitivity analysis by examining whether one or more of the reactors gave consistently "low" results or by how many standard derivations the data collected on a particular date are distanted. (Chapter 9).

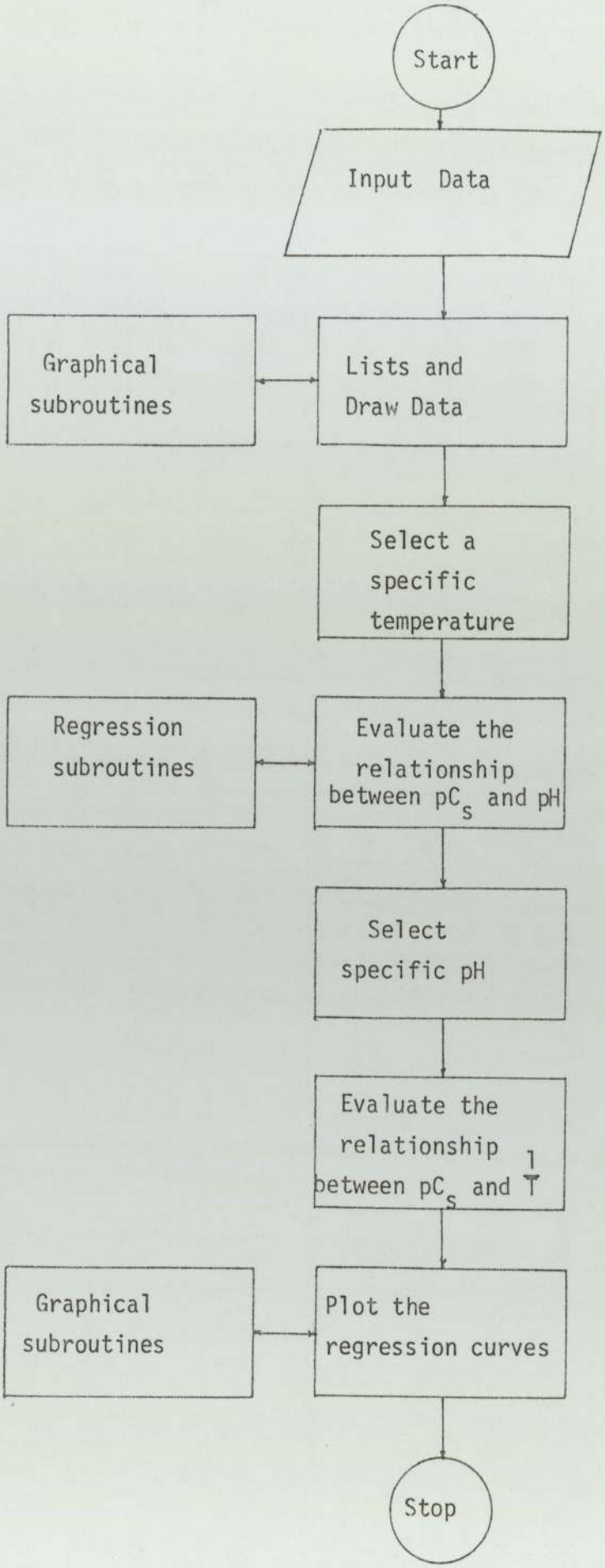

D. A10.1. Simplified logical flow diagram for programme EF19

OUT A10 1

PH	CONC	PC	TEMP.	REACTOR	NO.
1.77	0.584E-02	2.2	35.0	1.0	1.0
2.42	0.245E-02	2.6	35.0	2.0	1.0
1.72	0.679E-02	2.2	35.0	3.0	1.0
2.26	0.316E-02	2.5	35.0	4.0	1.0
2.25	0.271E-02	2.6	35.0	1.0	2.0
2.69	0.163E-02	2.8	35.0	2.0	2.0
2.45	0.193E-02	2.7	35.0	3.0	2.0
3.00	0.928E-03	3.0	35.0	4.0	2.0
2.92	0.147E-02	2.8	35.0	1.0	3.0
2.89	0.116E-02	2.9	35.0	2.0	3.0
3.14	0.658E-03	3.2	35.0	3.0	3.0
3.46	0.829E-03	3.1	35.0	4.0	3.0
4.20	0.231E-03	3.6	35.0	1.0	4.0
4.40	0.166E-03	3.8	35.0	2.0	4.0
5.08	0.462E-04	4.3	35.0	3.0	4.0
3.75	0.341E-03	3.5	35.0	4.0	4.0
5.25	0.194E-03	3.7	35.0	4.0	4.0
1.00	0.173E-01	1.8	35.0	1.0	5.0
1.44	0.920E-02	2.0	35.0	2.0	5.0
0.77	0.291E-01	1.5	35.0	3.0	5.0
5.81	0.158E-04	4.8	35.0	1.0	7.0
5.10	0.711E-04	4.1	34.1	2.0	7.0
5.52	0.324E-04	4.5	35.0	3.0	7.0
2.19	0.316E-02	2.5	35.0	1.0	8.0
2.00	0.316E-02	2.5	35.0	2.0	8.0
2.22	0.316E-02	2.5	35.0	3.0	8.0
2.55	0.237E-02	2.6	35.0	4.0	8.0
2.61	0.217E-02	2.7	35.0	1.0	9.0
2.90	0.126E-02	2.9	33.9	4.0	9.0
3.15	0.126E-02	2.9	34.5	1.0	10.0
2.80	0.131E-02	2.9	34.7	4.0	10.0

OUT A10 2

```
0012                  TRACE 1
0000                  TRACE 2
0001                  MASTER EF19
0002                  CALL OPENGINOGP
0003                  CALL DEVPAP(2000.,720.,1)
0004                  DIMENSION AAA(5,3)
0005                  DIMENSION CALCPC(100),CALCK(100)
0006                  DIMENSION CALCPH(100)
0007                  DIMENSION CRSIX(100)
0008                  DIMENSION PH(100)
0009                  DIMENSION PCRSIX(100)
0010                  DIMENSION          A(10,10),AA (10)
0011                  DIMENSION        X(90,10),Y(90)
0012                  DIMENSION TEMP(100)
0013                  REAL      DATANO(100)
0014                  DIMENSION REACT(100)
0015                  CALLCHASIZ(2.5,2.3)
0016                  XOR=100.
0017                  YOR=350.
0018                  AXLEN=240.
0019                  XBEG=0.
0020                  XEND=6.
0021                  NINTX=6
0022                  IYORY=2
0023                  IXORY=1
0024                  IOR=1
0025                  AYLEN=140.
0026                  YBEG=0.5
0027                  YEND=4.
0028                  NINTY=7
0029                  III=2
0030                  III=3
0031                  III=4
0032                  DO 100 II=1,III
0033                  CALL TETRA(YOR,XOR)
0034                  CALL AXIPOS (IOR,XOR,YOR,AYLEN,IYORY)
0035                  CALL AXIPOS (IOR,XOR,YOR,AXLEN,IXORY)
0036                  CALL AXISCA(1,NINTX,XBEG,XEND,IXORY)
0037                  CALL AXISCA(1,NINTY,YBEG,YEND,IYORY)
0038                  CALL AXIDRA(-1,-1,IYORY)
0039                  CALL AXIDRA(1,1,IXORY)
0040                  READ(1,9)MAX,NR,NN ,N
0041                9 FORMAT(12I0 )
0042                  WRITE(2,12)MAX,NR,NN,N
0043               12 FORMAT(1H0,5I20)
0044                  WRITE(2,13)
0045               13 FORMAT(1H1,33X,'PH' ,8X,'CONC', 8X,
0046                 1'PC',  7X,'TEMP.',4X,'REACTOR',5X,'NO.')
0047                  DO 24 I=1,N
0048                  READ(1,10)PH(I),CRSIX(I),TEMP(I),REACT(I),
0049                 1DATANO(I)
0050               10 FORMAT(2D0.0,3F0.0)
0051                  CRSIX(I)=CRSIX(I)/253.33
0052                  PCRSIX(I)=-ALOG10(CRSIX(I))
0053                  WRITE(2,11)PH(I),CRSIX(I),PCRSIX(I)
0054                 1,TEMP(I),REACT(I),DATANO(I)
0055               11 FORMAT(1H0,30X,F6.2,E12.3,5F10.1)
0056               24 CONTINUE
0057                  DO 23 J=1,N
0058               23 CONTINUE
0059                  CALL GRASYM(PH,PCRSIX,N,1    ,0)
0060                  DO 20 I=1,N
0061                  Y(I)=PCRSIX(I)
0062          227     DO  22 J=1,NR
```

```
0063                AJ=J-1.
0064                X(I,J)=PH(I)**AJ
0065             22 CONTINUE
0066             20 CONTINUE
0067                CALL MARGOT(X,Y,NR,N,A)
0068                CALL SUSSAN(A,NR,AA)
0069                CALCPH(1)=0.5
0070                CALCPH(1)=0.1
0071                NL=6
0072                NL=11
0073                NL=4
0074                NL=12
0075                NL=13
0076                DO 3 I=1,NL
0077                CALCPC(I)=AA(1)+AA(2)*CALCPH(I)
0078                CALCPH(I+1)=CALCPH(I)+0.5
0079             3  CONTINUE
0080                CALL GRACUR(CALCPH,CALCPC,NL)
0081                XOR=XOR+310.
0082                AAA(II,1)=AA(1)
0083                AAA(II,2)=AA(2)
0084            100 CONTINUE
0085                XBEG=0.002
0086                XEND=0.004
0087                AXLEN=200.
0088                NINTX=8
0089                CALL TETRA(YOR,XOR)
0090                CALL AXIPOS (IOR,XOR,YOR,AYLEN,IYORY)
0091                CALL AXIPOS (IOR,XOR,YOR,AXLEN,IXORY)
0092                CALL AXISCA(1,NINTX,XBEG,XEND,IXORY)
0093                CALL AXISCA(1,NINTY,YBEG,YEND,IYORY)
0094                CALL AXIDRA(-1,-1,IYORY)
0095                CALL AXIDRA(1,1,IXORY)
0096                TEMP(1)=35.
0097                TEMP(1)=21.
0098                TEMP(2)=52.
0099                TEMP(3)=65.
0100                TEMP(4)=100.
0101                TEMP(4)=90.
0102                DO 113 K=1,III
0103                TEMP(K)=1./(273.+TEMP(K))
0104            113 CONTINUE
0105                DO 120 IPH=2,4
0106                PHI=IPH
0107                DO 110 K=1,III
0108                Y(K)=AAA(K,2)*PHI+AAA(K,1)
0109                X(K,1)=TEMP(K)
0110                X(K,2)=1.
0111                WRITE(2,108) TEMP(K),Y(K)
0112            108 FORMAT(1H0,2F20.5)
0113            110 CONTINUE
0114                CALL GRASYM(TEMP,Y,III,2,0)
0115                CALL MARGOT(X,Y,2,III,A)
0116                CALL SUSSAN(A,2,AA)
0117                CALCK(1)=0.00268
0118                NL=10
0119                DO 103 I=1,NL
0120                CALCPC(I)=AA(2)+AA(1)*CALCK(I)
0121                CALCK(I+1)=CALCK(I)+0.0001
0122            103 CONTINUE
0123                CALL GRACUR(CALCK,CALCPC,NL)
0124                CALL GRAMOV(0.00268,0.5)
0125                CALL GRALIN(0.00268,3.5)
0126            120 CONTINUE
0127                CALL DEVEND
0128            228 STOP
```

APPENDIX 11

Computational aspects and background information on the relationship between CrO_4^{--} and Cr(VT)

The total solubility of Cr(VT) and $BaCrO_4$ is the sum of the concentrations of the various species present (Chapter 3).

By arranging equations E.3.10. and E.3.11. the concentration of the CrO_4^{--} ion can be related to the concentration of the(CrVT) as a function involving the rate constants.

Skander (R.3.1.) suggested such a rearrangement which included the following ions and the following rate constants:

$[H_2CrO_4]$	Ka_1 ~1 X 10^{-4}
$[HCrO_4^-]$	Ka ~2 X 10^{-1}
$[Cr_2O_7^{--}]$	Kd ~4 X 10^{1}
$[CrO_3Cl^-]$	Kc$_\iota$ ~1 X 10^{-3}
$[HCr_2O_7^-]$	Kd_1 ~1 X 10^{0}
$[H_2Cr_2O_7]$	Kd_2 ~1 X 10^{1}
$[CrO_4^{--}]$	Kc ~3 X 10^{-7}

Furthermore, the following assumptions were made

(i) The rate constants did not change significantly with temperature

(ii) The $[Cl^-]$ concentration was equal to the $[H^+]$ concentration.

From the above ,graph G.3.1.at specific pH values was plotted. Programme EF.18 was used to compute an arithmetic relationship between pC_s and $p[CrO_4^{2-}]$ at specific pH values. Programme EF.18 is presented in output OUT.A11.1 and in output OUT.A11.2, the coefficients of the arithmetic relationships are presented.

Their form is:

$$p[CrO_4^{--}] = e^{f(pC_s)}$$

where $f(pC_s) = A_1 + A_2\ pC_s + A_3 pC_s^{\ 2}$

However, it should be stressed that the purpose of graph G.3.1. is to give an indication on whether $p[CrO_4^{--}]$ is proportional to C_s for small supersaturations ($S<1.5$) and not to compute an accurate relationship between the two.

OUT A111

```
0012                TRACE 1
0000                TRACE 2
0001                MASTER  EF18
0002                CALL OPENGINOGP
0003                DIMENSION PCRSIX(10,10)
0004                DIMENSION PCRATE(10,10)
0005                DIMENSION SCRATE(10)
0006                DIMENSION SCRSIX(10)
0007                DIMENSION COEF(10,10)
0008                DIMENSION PH(10)
0009                DIMENSION Y(30),X(30,5)
0010                DIMENSION YY(10),XX(10)
0011                DIMENSION AA(10)
0012                DIMENSION CALCX(100),CALCY(100)
0013                DIMENSION A(10,10)
0014                READ(1,10)NODATA,NCOEF
0015              10 FORMAT(10I0)
0016                LM=3
0017                DO 30 J=1,LM
0018                READ(1,20)PH(J),(PCRSIX(I,J),
0019               1PCRATE(I,J),I=1,NODATA)
0020              20 FORMAT(20F0.0)
0021              30 CONTINUE
0022                XOR=100.
0023                CALL PALOCA(XOR)
0024                YOR=200.
0025                AXLEN=200.
0026                XBEG=0.
0027                XEND=5.
0028                NINTX=5
0029                AYLEN=160.
0030                YBEG=5.
0031                YEND=9.
0032                NINTY=4
0033                IYORY=2
0034                IXORY=1
0035                IOR=1
0036                CALLCHASIZ(2.5,2.3)
0037                CALL AXIPOS (IOR,XOR,YOR,AYLEN,IYORY)
0038                CALL AXIPOS (IOR,XOR,YOR,AXLEN,IXORY)
0039                CALL AXISCA(1,NINTX,XBEG,XEND,IXORY)
0040                CALL AXISCA(1,NINTY,YBEG,YEND,IYORY)
0041                CALL AXIDRA(-1,-1,IYORY)
0042                CALL AXIDRA(1,1,IXORY)
0043                CALL MOVTO2(XOR+205.,YOR+5.)
0044                CALL CHAHOL(17H*LP*U(C*LR*UVI)*.)
0045                CALL MOVTO2(XOR+ 10,YOR+155.)
0046                CALL CHAHOL(18H*LP*U(C*LR*UO  )*.)
0047                CALL MOVTO2(XOR+ 23.,YOR+153.)
0048                CALL CHAHOL(5H*L4*.)
0049                CALL MOVTO2(XOR+ 23.,YOR+156.)
0050                CALL CHAHOL(6H*L--*.)
0051                CALL MOVTO2(XOR+170.,YOR+150.)
0052                CALL CHAHOL(10H*LP*UH=2*.)
0053                CALL MOVTO2(XOR+170.,YOR+100.)
0054                CALL CHAHOL(10H*LP*UH=3*.)
0055                CALL MOVTO2(XOR+170.,YOR+65.)
0056                CALL CHAHOL(10H*LP*UH=4*.)
0057                CALL MOVTO2(XOR+165.,YOR+50.)
0058                CALL CHAHOL(16H*US*LOLUBILITY*.)
0059                CALL MOVTO2(XOR+165.,YOR+47.)
0060                CALL CHAHOL(9H*LCURVE*.)
0061                DO 40 J=1,LM
0062                WRITE(2,49)
```

```
0063                49 FORMAT(1HO,10X)
0064                   WRITE(2,49)
0065                   WRITE(2,32)PH(J)
0066                32 FORMAT(1HO,50X,'PH VALUE IS',
0067                  2F5.2)
0068                   WRITE(2,49)
0069                   WRITE(2,49)
0070                   WRITE(2,33)
0071                33 FORMAT(1HO,45X,'PCRSIX',4X,'PCRATE')
0072                   WRITE(2,49)
0073                   DO 38 I=1,NODATA
0074                   WRITE(2,35)PCRSIX(I,J),PCRATE(I,J)
0075                35 FORMAT(1HO,40X,5F10.2)
0076                   XX(I)=PCRSIX(I,J)
0077                   YY(I)=PCRATE(I,J)
0078                38 CONTINUE
0079                   CALL GRASYM(XX,YY,NODATA
0080                  3,8,0)
0081                   CALL NORMA(YY,XX,NODATA,NCOEF,Y,X)
0082                   CALL MARGOT(X,Y,NCOEF,NODATA,A)
0083                   CALL SUSSAN(A,NCOEF,AA)
0084                   CALL PLOCA(AA)
0085                40 CONTINUE
0086                   READ(1,45)(SCRSIX(J),SCRATE(J),J=1,LM)
0087                   READ(1,45)(PH(J),J=1,LM)
0088                45 FORMAT(20F0.0)
0089                   CALL GRACUR(SCRSIX,SCRATE,LM)
0090                   CALL GRASYM(SCRSIX,SCRATE,LM,2,0)
0091                   DO 48 I=1,LM
0092                   XX(I)=PH(I)
0093                   YY(I)=SCRATE(I)
0094                48 CONTINUE
0095                   WRITE(2,49)
0096                   WRITE(2,49)
0097                   WRITE(2,49)
0098                   CALL NORMA(YY,XX,LM,NCOEF,Y,X)
0099                   CALL MARGOT(X,Y,NCOEF,LM,A)
0100                   CALL SUSSAN(A,NCOEF,AA)
0101                   B=1.5
0102                   DO 80 I=1,4
0103                   B=B+0.5
0104                   PH(I)=B
0105                   SCRSIX(I)=3.5
0106                   IF(PH(I)-3.)50 ,60,60
0107                50 CONTINUE
0108                   SCRATE(I)=EXP(1.72+0.06957*SCRSIX(I)
0109                  7+0.009819*SCRSIX(I)**2.)-(PH(I)-2.)*1.05
0110                   GO TO 70
0111                60 CONTINUE
0112                   SCRATE(I)=EXP(1.5085+0.0928*
0113                  8SCRSIX(I)+0.008812*SCRSIX(I)**2.)
0114                  9-(PH(I)-3.)*1.15
0115                   GO TO 70
0116                70 CONTINUE
0117                80 CONTINUE
0118                   CALL DEVEND
0119                   STOP
0120                   END

END OF SEGMENT, LENGTH   703, NAME  EF18
```

```
0147                    SUBROUTINE NORMA(YY,XX,NR,N,Y,X)
0148                    DIMENSION YY(10),XX(10)
0149                    DIMENSION Y(30),X(30,5)
0150                    DO 20 I=1,NR
0151                    Y(I)=YY(I)
0152                    Y(I)=ALOG(YY(I) )
0153                    DO 20 J=1,N
0154                    AJ=J
0155                    AJ=J-1
0156                    X(I,J)=XX(I)**(AJ)
0157                 20 CONTINUE
0158                    RETURN
0159                    STOP
0160                    END
```

END OF SEGMENT, LENGTH 121, NAME NORMA

```
0210                    SUBROUTINE PLOCA(AA)
0211                    DIMENSION AA(10)
0212                    DIMENSION CALCX(100),CALCY(100)
0213                    NINT=60
0214                    NINT=40
0215                    CALCX(1)=4.15
0216                    DO 10 I=1,NINT
0217                    CALCY(I)=EXP(AA(1)
0218                   1+AA(2)*CALCX(I)
0219                   2+AA(3)*CALCX(I)**2.)
0220                    CALCX(I+1)=CALCX(I)-0.1
0221                    IF(CALCY(I).LE. 5.00)GO TO 12
0222                 10 CONTINUE
0223                 12 CONTINUE
0224                    CALL GRAPOL(CALCX,CALCY,I-1)
0225                    RETURN
0226                    STOP
0227                    END
```

END OF SEGMENT, LENGTH 124, NAME PLOCA

OUT A11 2

PH VALUE IS 2.00

PCRSIX	PCRATE
1.00	6.05
2.00	6.70
3.00	7.51
4.00	8.65

A 1= 0.172143E 01

A 2= 0.695699E-01

A 3= 0.981865E-02

PH VALUE IS 3.00

PCRSIX	PCRATE
1.00	5.00
2.00	5.65
3.00	6.45
4.00	7.55

A 1= 0.150855E 01

A 2= 0.928131E-01

A 3= 0.881245E-02

APPENDIX 12

Computational aspects relating to the overall growth equation

Programmes EF22 and EF23 evaluate the coefficients of the empirical correlation (equation E.6.2.) by repression analysis and by optimisation respectively.

Output OUT.A12.1. lists programme EF22 and a simplified flow diagram is presented in diagrams D.A12.1 and D.A12.2 for programmes EF22 and EF23 respectively.

Included in programme EF22 is the CALL to the RANDOM NUMBER SUBROUTINE used for the sensitivity analysis.

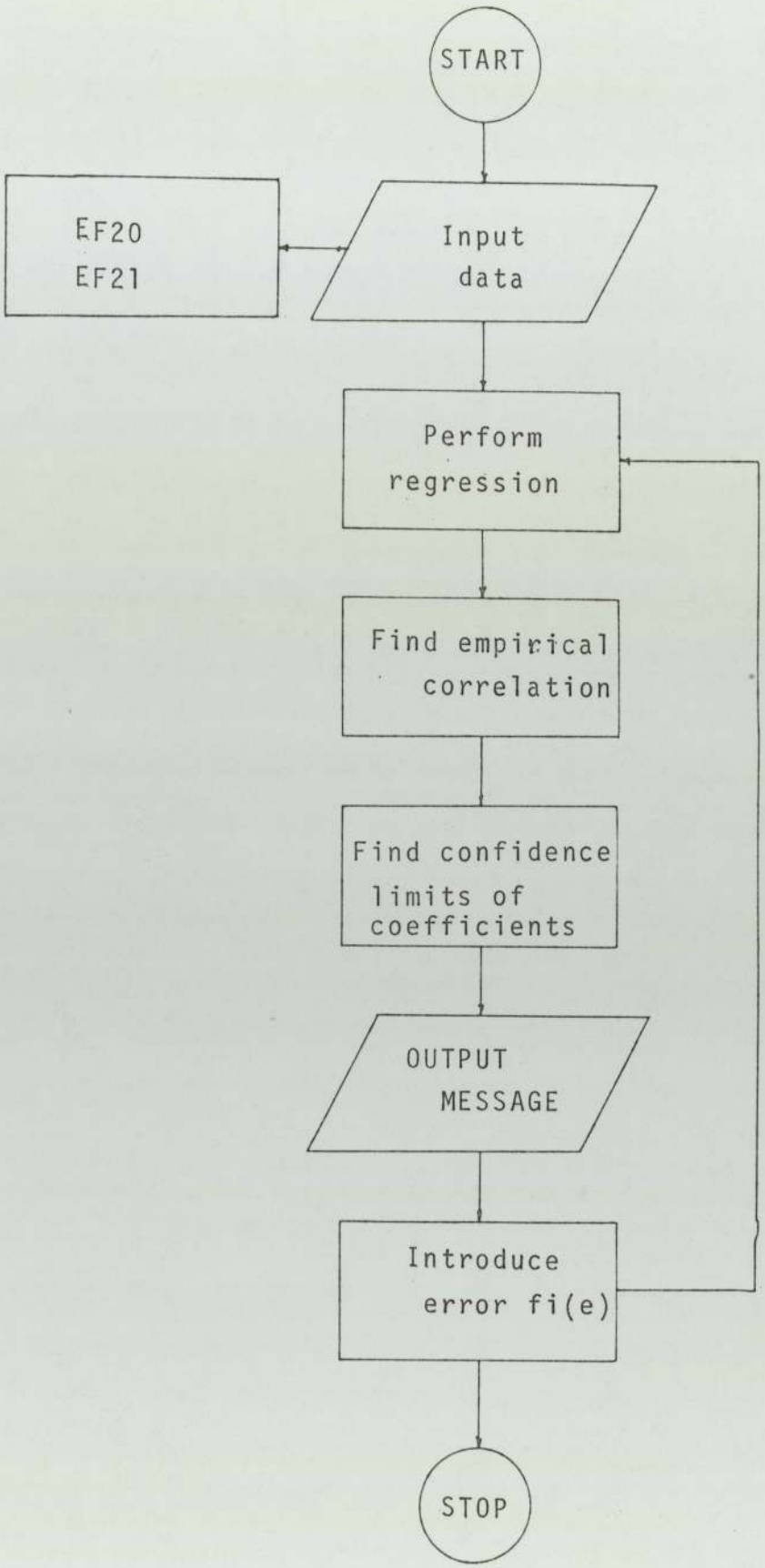

D.A12.1. Simplified logical flow diagram of programme EF22

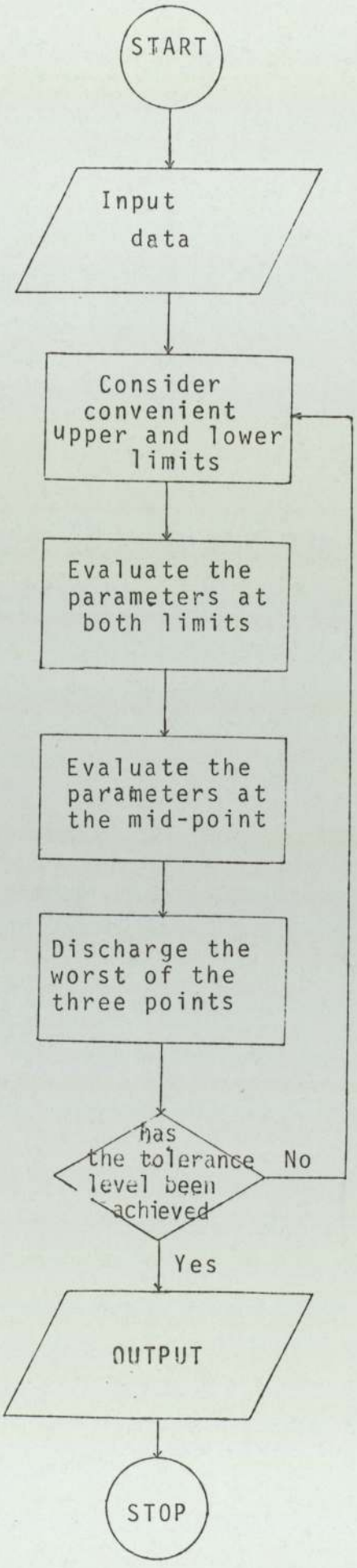

D.A12.2. Logical flow diagram of programme EF23.

OUT A121

```
0012          TRACE 1
0000          TRACE 2
0001          MASTER EF22
0002          REAL       LENGTH(100),NOPART(100)
0003          DIMENSION CALCY(100),CALCT(100)
0004          DIMENSION GROWTH(100),DRIVNG(100)
0005          DIMENSION DG(100,5),DDG(100,5)
0006          DIMENSION RPM(100)
0007          DIMENSION PH(100)
0008          DIMENSION Y(100),X(100,5)
0009          DOUBLE PRECISION    A( 10,10),AA(10)
0010          DIMENSION XX(100,10)
0011          DIMENSION XBAR(10),STD(10),SSP(10,10)
0012          DIMENSION WKZ(10,10)
0013          DIMENSION  CONST(4)
0014          DIMENSION COEFF(10,10), C(10,10)
0015          REAL RESULT(14),RINV (10,10)
0016          REAL R(10,10)
0017          DENSIT=4.45
0018          NORDER=3
0019          NORDER=5
0020          NORDER=4
0021          ENXP=1.
0022          MASTRA=1
0023          DO 200 M=1,MASTRA
0024          READ(1,5)NPOINT
0025        5 FORMAT(I0)
0026          DO 15 I=1,NPOINT
0027          READ(1,10)  DG(I,M),LENGTH(I),PH(I),
0028         1DRIVNG(I),RPM(I)
0029       10 FORMAT(5OF0.0)
0030       15 CONTINUE
0031          CALL G05CBF(1)
0032          ADM=1.2
0033          ADM=1.4
0034          ADM=1.
0035          ADM=1.6
0036          ADM=0.8
0037          ADS=0.6
0038          ADS=.2
0039          ADS=0.5
0040          ADS=0.4
0041          ADS=0.
0042          DO 17 I=1,NPOINT
0043          AD=G05DDF(ADM,ADS)
0044          DRIVNG(I)=DRIVNG(I)*AD
0045       17 CONTINUE
0046          DO 20 I=1,NPOINT
0047          Y(I)=ALOG10(DG(I,M))
0048          X(I,1)=1.
0049          X(I,2)=ALOG10(LENGTH(I))
0050          X(I,3)=ALOG10(RPM(I))
0051          X(I,4)=ALOG10(DRIVNG(I))
0052       20 CONTINUE
0053          CALL MARGOT(X,Y,NORDER,NPOINT,A)
0054          CALL SUSSAN(A,NORDER,AA)
0055          PERCET=0.
0056          ACCUM=0.
0057          DO 25 I=1,NPOINT
0058          CALCY(I)=10.**AA(1)*LENGTH(I)**AA(2)*RPM(I)**AA(3)
0059         1*DRIVNG(I)**AA(4)
0060          PERCET=    (DG(I,M)-CALCY(I))/DG(I,M)
0061          WRITE(2,26)LENGTH(I),DG(I,M),PH(I),DRIVNG(I)
0062         1 CALCY(I),PERCET   ,RPM(I)
```

```
0063                26 FORMAT(1HO,10X,F10.2,E15.5,2F10.2,E15.5,4F10.2)
0064                   PERCET=ABS(DG(I,M)-CALCY(I))/DG(I,M)
0065                   ACCUM=ACCUM+PERCET
0066                25 CONTINUE
0067                   ACCUM=ACCUM/NPOINT
0068                   WRITE(2,26)ACCUM
0069                   NARDER=NORDER-1
0070                   DO 195 I=1,NPOINT
0071                   XX(I,1)=ALOG10(LENGTH(I))
0072                   XX(I,2)=ALOG10(RPM(I))
0073                   XX(I,3)=ALOG10(DRIVNG(I))
0074                   XX(I,4)=ALOG10(DG(I,M))
0075               185 CONTINUE
0076                   IXX=100
0077                   ISSP=10
0078                   IR=10
0079                   IRINV=10
0080                   IC=10
0081                   ICOEFF=10
0082                   IWKZ=10
0083                   IFAIL=0
0084                   CALL G02BAF(NPOINT,NORDER,XX,IXX,XBAR,STD,SSP,ISSP,R,I
0085                   WRITE(2,190)(XBAR(I),I=1,NORDER)
0086                   WRITE(2,190)(STD (I),I=1,NORDER)
0087               190 FORMAT(1HO,20X,10F12.2)
0088                   CALL G02CGF(NPOINT,NORDER,NARDER,XBAR,SSP,ISSP,R,IR,
0089                  1RESULT,COEFF,ICOEFF,CONST,RINV,IRINV,C,IC,WKZ,IWKZ,IFA
0090                   DO  195 I=1,4
0091                   WRITE(2,197)(COEFF(I,J),J=1,4)
0092               197 FORMAT(1HO,20E15.7)
0093               195 CONTINUE
0094                   WRITE(2,197)(CONST(J),J=1,3)
0095               200 CONTINUE
0096                   STOP
0097                   END

ND OF SEGMENT, LENGTH   670, NAME  EF22
```

APPENDIX 13

General Computation

In this appendix some general purpose subroutines are presented OUT.A13.1. and OUT.A13.2. as well as a simplified flow diagram of them. A simplified logical flow diagram of programme EF24 is also presented.

The obvious advantage of the Simpson's method of integration is the relative simplicity combined with accuracy. Integration techniques, however, tend to fail to produce accurate results throughout the examined range and thus a more powerful technique would be required to evaluate the integral of equation E.8.13. for values of $P < 2$.

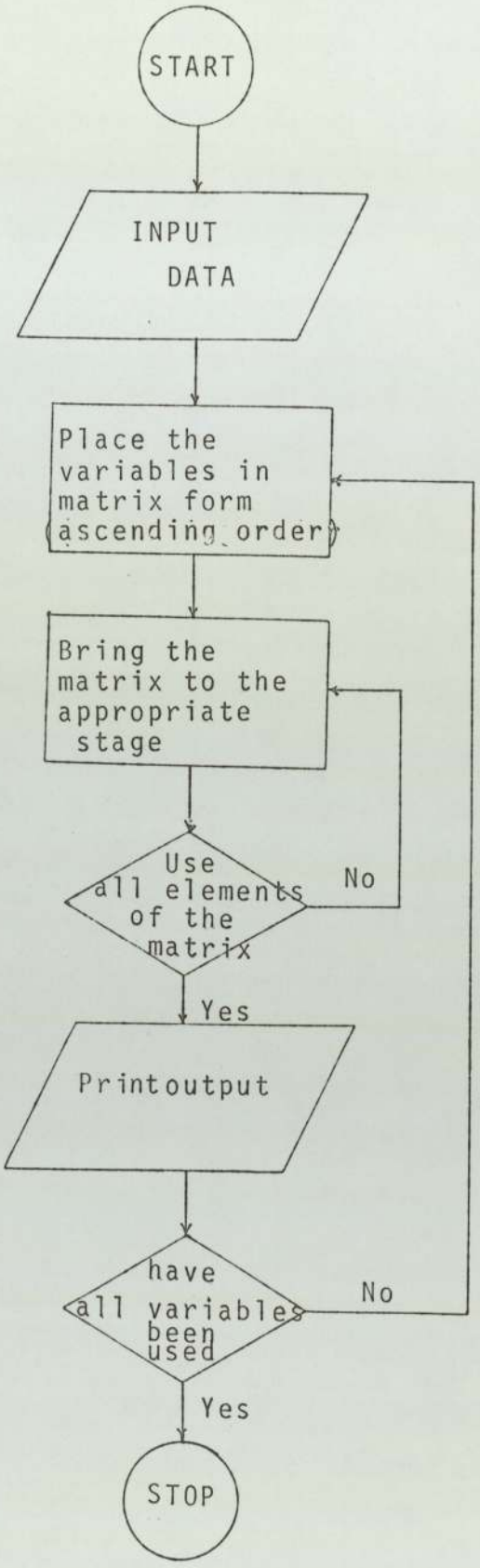

D.A13.1. Simplified flow diagram of subroutines SUSSAN and MARGOT

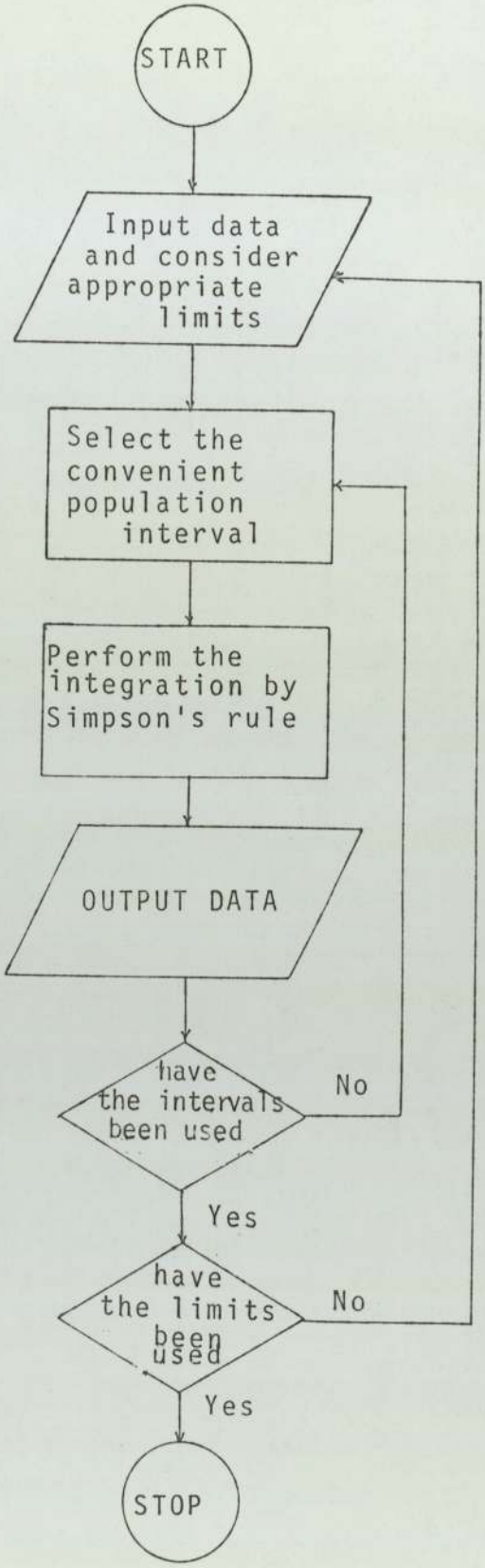

D.A13.2. Simplified logical flow diagram for the integration using the Simpson's rule EF24.

```
0161                  SUBROUTINE SUSSAN(A,NAROWS,AA)
0162                  DIMENSION A(10,10)
0163                  DIMENSION AA(10)
0164                   NCOLMN=NAROWS+1
0165            CSIZE CONSTRAIN
0166                   NCOLMN=NAROWS+1
0167                   NAR=NAROWS-1
0168                   DO 10 I=1,NAR
0169                   NARTWO=I+1
0170                   LEMAX=I
0171                   C=ABS(A(I,I))
0172                   DO 20 J=NARTWO,NAROWS
0173                   IF (C-ABS(A(J,I))) 30,20,20
0174              30   C=ABS(A(J,I))
0175                   LEMAX=J
0176              20   CONTINUE
0177                   DO 40 K=I,NCOLMN
0178                   B=A(I,K)
0179                   A(I,K)=A(LEMAX,K)
0180              40    A(LEMAX,K)=B
0181                   DO 10 J=NARTWO,NAROWS
0182                   B=A(J,I)/A(I,I)
0183                   DO 10 K=I,NCOLMN
0184               10   A(J,K)=A( J,K)-A(I,K)*B
0185                   DO50 J=1,NAR
0186                   N=NCOLMN-J
0187                   B=A(N,NCOLMN)/A(N,N)
0188                   L=J+1
0189                   DO 60 K=L,NAROWS
0190                   I=NCOLMN-K
0191              60    A(I,NCOLMN)=A(I,NCOLMN)-A(I,N)*B
0192                   A(N,N)=1.
0193              50   A(N,NCOLMN)=B
0194                   A(1,NCOLMN)=A(1,NCOLMN)/A(1,1)
0195                   A(1,1)=1.
0196                   DO 72 M= 1,NAROWS
0197                   WRITE(2,71 )M,A(M,NCOLMN)
0198             71    FORMAT(1HO,35X,'A',I2,'=',E20.6)
0199             72     CONTINUE
0200                  DO 78 I=1,NAROWS
0201                  AA(I)=A(I,NCOLMN)
0202              78  CONTINUE
0203                  DO 80 I=1,NAROWS
0204                  DO 80 J=1,NCOLMN
0205                  A(I,J)=0.
0206               80 CONTINUE
0207                  RETURN
0208                  STOP
0209                  END

END OF SEGMENT, LENGTH   395, NAME  SUSSAN
```

```
0121                    SUBROUTINE PALOCA(XOR)
0122                    YOR=200.
0123                    XOR=XOR+300.
0124                    CALL MOVTO2(XOR-20.,YOR-25.)
0125                    CALL LINTO2(XOR-20.,YOR+185.)
0126                    CALL LINTO2(XOR+280.,YOR+185.)
0127                    CALL LINTO2(XOR+280.,YOR-25.)
0128                    CALL LINTO2(XOR-20.,YOR-25.)
0129                    RETURN
0130                    STOP
0131                    END
```

END OF SEGMENT, LENGTH   83, NAME PALOCA

```
0132                    SUBROUTINE MARGOT(X,Y,N,NR,A)
0133                    DIMENSION A(10,10)
0134                    DIMENSION Y(30),X(30,5)
0135                    DO 50 I=1,N
0136                    DO 50 K=1,N
0137                    DO 50 J=1,NR
0138                    A(I,K)=A(I,K)+X(J,I)*X(J,K)
0139                 50 CONTINUE
0140                    DO 60 I=1,N
0141                    DO 60 J=1,NR
0142                     A(I,N+1)=A(I,N+1)+X(J,I)*Y(J)
0143                 60 CONTINUE
0144                    RETURN
0145                     STOP
0146                     END
```

END OF SEGMENT, LENGTH   145, NAME MARGOT

NOMENCLATURE

Symbol	Meaning
A	Surface area of the crystal $\mu m^2 (m^2)$
A_i	Coefficient of an algebraic equation
a_i	Shape factor of the crystal
a $\bar{a}$	Constant
AB	Absorbance
B_i	Coefficient of an algebraic equation
b	Constant
C	Concentration of Barium chromate, and also of total $Cr(\underline{VI})$ (mol/dm^3)
C_c	Concentration of the chromate ion (mol/dm^3)
C_i	Concentration of the impurity (mol/dm^3)
C_j (C_j')	Concentration at the crystal surface (mol/dm^3)
C_u	Concentration of Urea (mol/dm^3)
C_o	Initial Urea concentration (mol/dm^3)
C_{ol}	Constant of solubility
C_i	Coefficient of an algebraic equation
C_s	Concentration of Barium chromate at saturated conditions (mol/dm^3)
C_u^*	Active Urea concentration (mol/dm^3)
D	Diffusivity $(\mu m^2/s)$ (section 2.2.2.1.)
D_i	Coefficients of an algebraic equation
d_c	Critical diameter of a nucleus (equation E.2.6.)

$\bar{d}$, d	Mean diameter of a crystal
Eg	Activation energy of the growth process
f	Constant
f_1 (e)	Error function (sensitivity analysis)
ΔG	Energy of formation of a critical nucleus
ΔG^*	Energy of a critical nucleus for heterogeneous nucleation
ΔG^*_H	Energy of a critical nucleus for homogeneous nucleation
dG/dt	Growth rate of a crystal (kg/s)
I	Current (Amps)
i	Computer variable (suffix)
J	Computer variable (suffix)
K (K´)	Constant of crystal growth ($K' = 10^K$)
K_{N1}, K_{N2}	Constants of nucleation (section 2.2.1.1.)
K_g .$K_{m's}$	Constants of crystal growth (section 2.2.2.1.)
K_s	Constant of crystal growth rate
K_{c_1}	Equilibrium constant of the CrO_3Cl^- ion
K_a	Equilibrium constant of the $HCrO_4^-$ ion
K_d	Equilibrium constant of the $Cr_2O_7^{--}$ ion
K_c	Equilibrium constant of the CrO_4^{--} ion
K_T K_{To}	Constants of solubility (section 2.2.1.1.)
$K_1, K_2, K_3 . K_m$,	Equilibrium constants for the hydrolysis of Urea
K_P, K_N	Constant of nucleation
K^1	Constant in Coulter-Counter calculations
K_H	Constant of angle in heterogeneous nucleation (section 2.2.1.1.)

L	Characteristic length of crystal (radius) (μm)
L_{a_t}	Arithmetic mean radius (μm)
L_{ar}	Area mean radius (μm)
L_m	Mass mean radius (μm)
L_a	Andreasen mean radius (μm)
L_c	Coulter-Counter mean radius (μm)
L_∞	Value of L at infinite time (μm)
$\bar{L}, L_j$	Mass mean radius (μm)
L_i	Characteristic radial length of crystals at size interval i (μm)
M_t	True mass (g.), in Coulter-Counter calculations
M_e	Effective mass (g), in Coulter-Counter calculations
M_j	Total mass (g.), at time j
m	Mass (g, moles)
m_1	Constant
N	Population
n, n_u	Constants (exponents)
n_i, n_T	No of ions
p	Prefix indicating $-\log_{10}$ (pH, pC, pC_s etc.)
p	Constant (section 8.1.)
p_{cj}	Correction factor in Coulter-Counter calculations
R_1	Resistance (Ω)
R	Agitation speed (rpm)
R_d	Radius of curvature (um)(section 2.2.2.2.)

R_d^*	Radius of curvature of a critical two dimensional nucleus (um)(section 2.2.2.2.)
R	Boltzman's constant
r	Radius of a crystal (μm)
S	Supersaturation ratio (C/C_s)
Sk	Skewness of a population distribution
t	Time (s)
t_o	Time at which nucleation occurs(s)
t_1	Threshold for the Coulter-Counter
T	Temperature (K, ^oC)
U	Calibration factor for the Coulter-Counter
V	Relative velocity between the crystal and the fluid (m/s)
V_{Rd}	Velocity of growth of a crystal(um/s) (curved step of radius R_d)
V_∞	Velocity of growth of a crystal (straight step) (um/s)
W	Weight (g, moles)
W_t	Weight of crystals (g, mol)
X	Correction factor for the driving force, relative to the standard conditions
X,Y	Independent variables/functions
x,y,z	Three dimensional axes

Greek Symbols	Meaning
α	Proportionality constant
α_0	Interatomic distance of a crystal lattice
α_x, α_y, α_z	Coefficients of thermal expansion for the lattice of a crystal K^{-1}
δ	Thickness of stagnant film surrounding a crystal (μm)
ΔC	Driving force $(\frac{C-C_s}{C_s})$
$\Delta C'$	Concentration difference $(C-C_s)$
ε	Molar absorptivity
θ	Angle of contact between crystal and impurity
Λ	Enthalpy
λ	Wavelength
μ	Viscosity (Kg/ms)
ρ ($'s_l/'s_f$)	Density (g/cm^3) (solid/fluid)
σ	Variance
$\bar{\mu}$	Mean value of error

Subscript

s	saturation
i, j	computer variables

REFERENCES

R.1.1. MILLER C.H.
Proceedings of the 3rd Symposium on Chemical problems connected with stability of explosives 1973.

R.2.1. COULSON J.M. and RICHARDSON J.F.
Chemical Engineering, Vol. II, Pergamon Press.

R.2.2. PERRY R.H. ed.
Handbook of Chemical Engineering, 4th edition, McGraw Hill 1963.

R.2.3. MULLIN J.W.
Crystallisation, Butterworth, London

R.2.4. BECKER R.R. and DÖRING W.
Ann. Physik 24, 719,(1935).

R.2.5. CETTINI G. and RICCA F.
Chemical abstracts 55:2260 b.

R.2.6. ADAMSKI T.
Chemical abstracts 58:1321 e.

R.2.7. GORDON L. and FIRSCHING F.H.
Analytical Chemistry, 26 ,4,759,(1954).

R.2.8. PETROV T.G. et al.
Growing Crystals from solution, Consultants Bureau N.Y. 1969.

R.2.9. NYVLT J.
Industrial crystallisation from solutions Butterworth, 1971.

R.2.10. OHARA M. and REID R.C.
Modelling Crystal Growth, Prentice Hall 1973.

R.2.11. NIELSEN A.E.
Kinetics of Precipitation, Pergamon 1964.

R.2.12. MULLIN J.W. ed.
Industrial Crystallisation, Plenum Press, N.Y. 1976.

R.2.13. KONAK A.R.
Chem. Eng. Sci. 29, 1537 and 1785 (1974).

R.2.14. SÖHNEL O. et al.
J. Crystal Growth 39, 307 (1977).

R.2.15. RANZ W.E. and MARSHALL W.R.
Chem. Eng. Progr. 48(3), 141 (1952).

R.2.16. ROGERS J.F.
PhD. Thesis, Aston University 1969.

R.2.17. STRICKLAND-CONSTABLE R.F. and MASON R.E.A.
Nature, London 197, 897, (1963).

R.2.18. NIENOW A.W.
Trans. Inst. of Chem. Eng., 54, 205, (1976).

R.2.19. RAMSHAW C.
The Chemical Engineer, (London)
July/August 446, (1974)

R.2.20. BUJAC P.D.B.
Industrial Crystallisation, ed. by MULLIN J.W.
Butterworths 1976.

R.2.21. SRIKANTAN B.S.
J. Ind. Chem. Soc. 29, 674 (1952).

R.2.22. BURTON W.K., CABRERA N., FRANK F.C.
Phil. Trans. Roy. Soc. A243, 299-358 (1951).

R.2.23. JACKSON K.A.
J. Cryst. Growth 5, 13 (1969).

R.2.24. MULLIN J.W. and JANCIC S.J.
Trans. I. Chem. Eng. Vol. 57. 188, (1979).

R.2.25. MULLIN J.W. and SÖHNEL
Chem. Eng. Sci., 32, 683 (1977)

R.2.26. SÖHNEL O. et al
J. Cryst. Growth 39, 307, (1977)

R.2.27. SÖHNEL O. and MULLIN J.W.
Chem. Eng. Sci. 33, 1935, (1978)

R.2.28. CREASY D.E. (ASTON U.)
Private communications.

R.2.29. MELIA J.K. and MOFFITT J.W.
I and E.C. Fundamentals
3, (4.), 313, (1964).

R.2.30. STRICKLAND-CONSTABLE R.F.
Kinetics and Mechanism of
Crystallisation
Academic Press, London
and N.Y. 1968.

R.2.31. BUCKLEY H.E.
Crystal Growth p.350, 405-408
J. Wiley & Sons N.Y.

R.2.32. ALLEN T.
Particle Size Measurement
Chapman and Hall, 1968.

R.2.33. RANDOLPH A.D. and LARSON M.A.
Theory of Particulate Processes
Academic Press, N.Y. 1971.

R.2.34. JONSHON N.L. and KOTZ S.
Continuous Univariate Distributions
Parts 1 and 2, vol. 2.
J. Wiley & Sons, N.Y. 1970.

R.2.35. FREUND J.E.
Mathematical statistics
Prentice Hall

R.3.1. SKANDER J.L.
Ph.D. Thesis, Aston University, 1979.

R.3.2. WYCKOFF R.W.G.
Crystal Structure, vol. 3.
Wiley, N.Y. 1966.

R.3.3. SHIDLOWSKI A.A. et al.
U.S.S.R. J. Phys. Chem., 1067, (1971).

R.3.4. PISTORIUS C.W.F.T. and PISTORIUS M.C.
Z. Krist., 117, 2522, (1962).

R.3.5. WEAST R.G.
Handbook of Chemistry and Physics
57th edition Chem. Rubber

R.3.6. COTTON F.A. and WILKINSON G.
Advanced Inorganic Chemistry
J. Wiley, N.Y. 1960.

R.3.7. HAIGHT G.P. et al.
J. Inorg. Chem. , 3, 1777, (1964).

R.3.8. TONG J.Y.
J. Inorg. Chem., 3, 1804, (1964).

R.3.9. JELLINECK F.
J. Inorg. and Nuclear Chem. 13, 329 , (1960).

R.3.10. GETTINI G. and RICCA F.
Ricera Sci. 30, 994, (1960).

R.3.11. HUEPER W.C. and PAYNE W.W.
Proc. Intern. Corp. of Occupational
Health, 13, N.Y. 1260 pub. 1961,
473-86.

R.3.12. Sp1800 manual P.Y.E. (section 3.3.2.).

R.3.13. LUKKARI O.
Annales Universitatio Turkuensis, series (A) No. 100 p. 57 (1967).

R.3.14. LEWIS J. and WILKINS R.G. ed.
Modern Co-ordination Chemistry, Principles and Methods.
Wiley, Interscience N.Y. 1960. Ch. 1.

R.3.15. KIRK R.E. ed.
Encyclopaedia of Chemical Technology
2nd ed. Vol.6. p. 1-24.

R.3.16. ROSSOTTI F.T.C. and ROSSOTTI H.
The Determination of Stability Constants.
McGraw-Hill N.Y. 1960.

R.3.17. I.L. 151/251 AA/AE Spectrophotometer Manual

R.3.18. U.S. Patent 3434668

R.3.19. LINGE H.G. and JONES A.L.
Aust. J. Chem. 21 , 2189, (1968).

R.3.20. GABA J. and HALADJIAN J.
Rev. de Chimie Minerale 7, 3, (1970)

R.3.21. GABA J. and ANTONETTI G. et al
Rev. de Chimie Minerale 10, 3, 475, (1973).

R.3.22. ARNEK K.R. and JOHANSON S.R.
Acta. Che. Scand. 26, 2903, (1972).

R.3.23 JAIN D.V.S. and JAIN C.M.
J. Chem. Soc. (A), 1541, (1967).

R.3.24. NEUSS J.D. and RIEMAN W.
J. Am. Chem. Soc. 52, 2238 (1934)

R.3.25. ALBERT A. and SERGEANT E.P.
Ionisation constants of acids and bases
Methuen, London 1962.

R.3.26. PAMPLIS B.R. ed., B. LEWIS
International series of Morphologyin the Science of the Solid State No. C. p.12.
Pergamon 1975.

R.4.1. KIRK R.E. ed.
Encyclopaedia of Chemical Technology
2nd ed. Vol. 22, p.234.

R.4.2. RIECK G.D.
Tungsten and its Components
Pergamon Press, Oxford 1967.

R.4.3. Li K.C. and WANG C.Y.
Tungsten its History, Reinholds Publ. N.Y. (1955).

R.4.4. PARISH W.
Acta Cryst. 13, 838, (1960).

R.4.5. HEYWOOD H.
Proc. I. Mech. Eng. 140, 280, (1938).

R.4.6. WALTON A.G.
The Formation and Properties of Precipitates
Wiley, Interscience N.Y. p.100, (1967).

R.4.7. YIH S.W.H. and WANG C.T.
Tungsten, Plenum Press N.Y. 1979.

R.5.1. WARNER R.C.
J. Bio. Chem. 142, 705, (1942)

R.5.2. KUCHERYAVYI V.I. et al.
Soviet J. Appl. Chem. 42, 502, (1909)

R.5.3. WELLES H.L. et al.
J. Pharmaceutical Science 75, 1812,(1971)

R.5.4. SHAW W.H.R. and BORDEAUX
J. Am. Chem. Soc. 77 ,729,(1955)

R.6.1. NIENOW A.W.
Trans. Instn. Chem. Engrs. 54, (1976).

R.6.2. NIENOW A.W., BUJAC P.D.B., MULLIN J.W.
J. Crystal Growth, 13/14, 488, (1972).

R.7.1. B.S. 1553 Part 1. 1977.

R.9.1. FALANGAS E.
M.Sc. Thesis 1977, Aston University.

R.9.2. NAG MIN MANUAL
Aston University Computer Library.

R.A1.1. Coulter Counter Manual, Model A.(Appendix 1).

R.A1.2. U.K. Patent 22418 or U.S. Patent 265 6508.

R.A1.3. ALLEN T., (p.143-153).
Particle Size Measurements, Chapman & Hall, 1968.

R.A1.4. ROGERS J.F. Ph.D. thesis,
Aston University (1969)

R.A1.5. MULLIN J.W., ANG H.M.
Powder Technology, 10, 153, (1974).

R.A1.6. ADBY P.R., DEMPSTER M.A.H.
Introduction to optimization Methods
Chapman and Hall 1974.

R.A1.7. YARDE H.R.
J. Sci. Instr. ,9, 42, (1971).

R.A1.8. BUNGAY H.R., KREBS R.D.
J. Sci. Instr. 9, 42, 891, (1971).

R.A2.1. B.S. 3406 Part 2.

R.A2.2. HEYWOOD H.
Process J. Mech. Eng., 140, 277, (1938).

R.A2.3. CADLE R.D.
Particle size.
Reinheld Publ. Co. N.Y. 1965.

R.A2.4. ALLEN T. (84-86).
Particle size measurement, Chapman & Hall, 1968.

R.A2.5. BIRD R.B., STEWARD W.E., LIGHTFOOT E.N.
Transport Phenomena, Wiley N.Y. 1960.

R.A2.6. PERRY R.H. ed.
Chemical Engineering handbook, 4th ed. 1963

R.A2.7. HEISS J.F., COULL J.
Chem. Eng., 48, 3, 133, (1952).

R.A3.1. WALTON A.G.
The formation and properties of precipitates
Wiley, Interscience, N.Y. 1967.